

Part I: Catalytic Direct C-H Arylation of Pyrazoles

Part II: Toward Modulation of Neuroplasticity with Small Molecules

Teresa L. Jacques

Submitted in partial fulfillment of the
requirements for the degree of
Doctor of Philosophy
in the Graduate School of Arts and Sciences

COLUMBIA UNIVERSITY

2013

ABSTRACT

Part I: Catalytic Direct C-H Arylation of Pyrazoles

Part II: Toward Modulation of Neuroplasticity with Small Molecules

Teresa L. Jacques

Part I of this thesis (Chapter 1) describes the development of the first synthetic method for intermolecular palladium-catalyzed direct C-H arylation of *N*-substituted pyrazole compounds. The scope of the reaction and the ability to sequentially and selectively arylate specific positions on the azole core to rapidly access highly substituted pyrazoles will be discussed.

Part II of this thesis addresses two separate targets to modulate neuroplasticity. In Chapter 2, the TrkB receptor as a potential target for pharmacological modulation is examined. Its signaling, role in brain disease, and reported agonists and antagonists are reviewed. In addition, our attempts at establishing an assay to assess TrkB activation, as well as our results using the reported agonists and an antagonist in several model cell lines, are discussed. The third chapter of this work features the development of rationally-designed isoquinuclidines that induce GDNF production by brain cell models. In addition to examining the mechanism of action of an isoquinuclidine (XL-026) using pharmacological inhibition, the mapping of GDNF production and release by C6 rat glioma cells is described and a mechanistic model based on our results is presented.

Table of Contents

Chapter 1.	Palladium-Catalyzed Direct C-H Arylation of Pyrazoles.....	1
I.	Introduction.....	1
II.	Results and Discussion.....	5
II.1	Development of C-H Arylation Protocol for SEM-Protected Pyrazoles....	5
II.2	Regioselectivity of C-Arylation of SEM-Protected Pyrazoles.....	7
II.3	Rationale for the Observed Regioselectivity.....	8
II.4	Arene Donor Substrate Scope.....	10
II.5	Pyrazole Substrate Scope.....	11
II.6	SEM-Group Transposition (SEM-group switch)	12
II.7	The Second C-Arylation and Preparation of 3,4,5-Triarylpyrazoles.....	14
II.8	Deprotection of SEM-Pyrazoles.....	16
II.9	Regioselective N-Alkylation/C-Arylation Sequence Enabled by the SEM Group.....	17
III.	Conclusions.....	20
IV.	Experimental Section.....	22
IV.1	General Information.....	22
IV.2	Synthesis of Starting Materials.....	23
IV.3	Procedure for Pyrazole Arylation.....	27
IV.4	Triarylated Pyrazoles.....	34
IV.5	Procedure for SEM-switch.....	37
IV.6	General Procedure for Formation of Pyrazolium Salts.....	40

IV.7	Determination of the Tautomer Ratio for Selected Free (NH)-Pyrazoles in DMSO- <i>d</i> ₆	41
IV.8	¹ H and ¹³ C NMR Spectra.....	45

Chapter 2.	Toward Pharmacological Modulation of Neuroplasticity: The Neurotrophin Receptor TrkB as a Potential Target.....	136
I.1	Introduction.....	136
I.2	BDNF/TrkB Signaling.....	138
I.3	BDNF/TrkB in Psychiatric and Neurodegenerative Disease.....	141
I.4	TrkB Agonism.....	142
I.4.1	Amitriptyline.....	144
I.4.2	LM22A-4.....	145
I.4.3	7,8-Dihydroxyflavone.....	146
I.4.4	Deoxygedunin.....	148
I.4.5	<i>N</i> -Acetylserotonin.....	149
I.4.6	L-783,281.....	151
I.4.7	Transactivation.....	152
I.5	TrkB Antagonism.....	153
I.5.1	Cyclotraxin B.....	154
I.5.2	ANA-12.....	155
II.	Establishing an Assay for Assessment of TrkB Activation.....	157
II.1	NIH-3T3-Trk and HEK-TrkB Cells.....	158

II.2	Efforts to Establish Small Molecule Controls: HEK-TrkB.....	161
II.3	Efforts to Establish Small Molecule Controls: SH-SY5Y.....	163
II.4	Development of High-Throughput Screening Assays for TrkB Agonists.....	165
III.	Conclusions and Future Directions.....	167
IV.	Experimental.....	169
V.	References.....	172
Chapter 3.	Isoquinuclidine-Induced GDNF Release in C6 Glioma Cells: Studies Toward the Mechanism of Action.....	182
I.	Introduction.....	182
I.1	GDNF in the CNS.....	182
I.2	GDNF/Ret Signaling.....	183
I.3	Ibogaine and GDNF.....	184
II.	Development & Pharmacological Profiling of Isoquinuclidine Ibogaine Analog.....	188
II.1	Development of GDNF Release Assay & Identification of Lead Compounds.....	188
II.2	Structural Design.....	190
III.	Hypotheses for the Mechanism of Action of Isoquinuclidines.....	197
III.1	Transactivation or Direct Signaling Through Receptor Tyrosine Kinase(s)	199
III.2	Sigma Receptor Involvement.....	200

III.3	GDNF Release as a Response to Stress.....	203
III.4	GDNF Release as a Secondary Effect.....	204
IV.	Results & Discussion.....	205
IV.1	Ret Activation.....	207
IV.2	ERK1/2 Involvement.....	209
IV.3	GPCR Involvement.....	211
IV.3.1	Serotonin Receptors.....	211
IV.3.2	Opioid Receptors.....	213
IV.3.3	Adenosine Receptors.....	214
IV.3.4	Adrenergic Receptors.....	215
IV.3.5	Angiotensin Receptors.....	217
IV.3.6	Endothelin Receptors.....	218
IV.3.7	GABA _A Receptors.....	219
IV.3.8	Histamine Receptors.....	220
IV.3.9	Glutamate Receptors.....	222
IV.3.10	Melatonin Receptors.....	223
IV.3.11	Muscarinic Receptors.....	224
IV.3.12	Prostanoid Receptors.....	225
IV.3.13	Sphingosine-1-phosphate Receptors.....	226
IV.3.14	PTX-Sensitive Receptors.....	227
IV.3.15	Adenylate Cyclase Involvement.....	228
IV.4	RTK and Other Growth Factor Receptor Involvement.....	228
IV.4.1	Ret.....	229

IV.4.2	FGFR.....	233
IV.4.3	Trk Receptors.....	236
IV.4.4	PDGFR.....	237
IV.4.5	VEGFR.....	242
IV.4.6	EGFR.....	244
IV.4.7	TGF β -R.....	245
IV.4.8	Other Growth Factor and Cytokine Receptors	247
IV.5	Nuclear and Cytokine Receptor Involvement.....	248
IV.5.1	Glucocorticoid Receptors.....	248
IV.5.2	Estrogen Receptors.....	249
IV.5.3	TNF- α Receptors.....	250
IV.6	Sigma Receptor Involvement.....	253
V.	Potential of Growth Factor-Induced GDNF Release.....	260
V.1	FGFR-Induced GDNF Release is Potentiated by XL-026.....	260
V.2	PDGFR-Induced GDNF Release is Potentiated by XL-026.....	262
V.3	TNF- α -R-Induced GDNF Release is Potentiated by XL-026.....	263
V.4	Other RTKs Are Not Potentiated by Co-treatment With XL-026.....	264
V.5	RTK Signaling Potentiation: Precedent.....	265
VI.	Conclusions and Mechanistic Models.....	267
VI.1	Mechanistic Model for Potentiation of FGF- β and PDGF-Induced GDNF Release.....	268

VI.2	Mechanistic Model for XL-026-Induced GDNF Release: σ Rs as Key Players.....	269
VI.3	Alternate Mechanistic Models: Stress-Induced GDNF Release.....	270
VII.	Future Studies.....	270
VIII.	Experimental.....	273
IX.	References.....	278

Table of Abbreviations

18-MC	18-Methoxycoronaridine
5-HT	5-Hydroxytryptamine, serotonin
7,8-DHF	7,8-Dihydroxyflavone
Akt	Protein kinase B/PKB
ART	Artemin
ATP	Adenosine triphosphate
BDNF	Brain-derived neurotrophic factor
CNS	Central nervous system
DAT	Dopamine transporter
ECD	Extracellular domain
EDTA	Ethylenediamine tetraacetic acid
EGF	Epidermal growth factor
EGFR	Epidermal growth factor receptor
ER	Endoplasmic reticulum
ERK	Extracellular-regulated kinase
ET-1	Endothelin 1
FGF- β	Basic fibroblast growth factor (FGF-2)
FGFR	Fibroblast growth factor receptor
GDNF	Glial cell-derived neurotrophic factor
GFL	GDNF-family ligand
GFR α	GDNF-family receptor alpha
GPCR	G protein-coupled receptor
GPI	Glycophosphatidylinositol
HEK	Human embryonic kidney cell line
Her	Heregulin
HGF	Hepatocyte growth factor
ICD	Intracellular domain
IGF	Insulin-like growth factor
c-Kit	Stem cell factor (SCF) receptor
LIF	Leukemia inhibitory factor
MAPK	Mitogen activated protein kinase
MEK	Mitogen activated protein kinase kinase
c-Met	Hepatocyte growth factor (HGF) receptor
nAChR	Nicotinic acetylcholine receptor
NAS	N-Acetyl serotonin
NGF	Nerve growth factor
NT	Neurotrophin
NTN	Neurturin

OR	Opioid receptor
p75NTR	p75 neurotrophin receptor
PDGF	Platelet-derived growth factor
PDGFR	Platelet-derived growth factor receptor
Pgrmc1	Progesterone membrane component 1 receptor; σ 2R
PKC	Protein kinase C
PI3K	Phosphoinositide 3 kinase
PLC γ	Phospholipase C-gamma
PR	Progesterone receptor
PSN	Persephin
Ras	'Rat sarcoma' enzyme
Ret	Rearranged during transfection receptor
RTK	Receptor tyrosine kinase
SCF	Stem cell factor
SEM	Standard error of the mean
SERT	Serotonin transporter
S1P	Sphingosine-1-phosphate
σ R	Sigma receptor
TGF- β	Transforming growth factor β
TNF- α	Tumor necrosis factor α
Trk	Tropomyosin receptor kinase
VEGF	Vascular endothelial growth factor
VEGFR	Vascular endothelial growth factor receptor
VMAT	Vesicular monoamine transporter
Y	Tyrosine

Acknowledgements

First and foremost, I am greatly indebted to my research advisor, Prof. Dalibor Sames. My journey through this program has been an unusually long and difficult one, and without Dali's faith and continued support, I would not be where I am today. I also thank my thesis committee for their time, support, and insight: Professor Ronald Breslow, Professor Tristan Lambert, Professor Ruben Gonzalez, and Professor Milan Stojanovic. Studying at Columbia in the presence of these faculty members has been an amazing privilege.

I also owe thanks to the faculty at Smith College that encouraged me to pursue graduate study in the first place. My research advisor and mentor, Dr. Maureen Fagan, was responsible for sparking my interest in organometallic chemistry and continues to be helpful and supportive in my endeavors. Professor Kevin Shea has also continued mentoring me during my time at Columbia and I am grateful for his support and advice. My academic advisor Professor Shizuka Hsieh continues to inspire me with her relentless energy and enthusiasm for chemistry.

The staff in the chemistry department at Columbia also deserves a great deal of thanks; in particular, Anel Cortez and Dani Farrell have been wonderful friends, and Alix Lamia has provided support beyond the call of duty. These are only several of many, many supportive members of the department that enable us to do our work, and deserve a great deal of credit.

The Sames group has changed over the years, and just when I think it cannot get better, its new members continue to surprise me. I can only hope that I'll again have the pleasure of working with so many fun, talented, creative, and driven scientists in one place. One colleague in particular, Rich Karpowicz, has had a hand in my progress in more ways than I can count. Without his friendship, I am very sure I would be nowhere near the person and scientist that I am today. When it comes to science, I have not met a more energetic and passionate individual who

is absolutely *compelled* to both seek knowledge and share his knowledge with those around him; when it comes to ‘real life,’ he is truly the most loyal and selfless friend one can have. A better labmate does not exist. He’s been a wonderful co-pilot in our work and I have learned a great deal from him, and he continues to be incredibly motivating. I know that he is going to make an amazing professor someday.

Other former and current group members that deserve many thanks are those that are not only my colleagues, but also my friends. Dr. Rachel Tundel, Dr. Yves Meyer, Madalee Gassaway, Paolomi Merchant, Dr. Adam Henke, and Dr. Julien Massue have been so much fun to work and learn with and I know I will continue to be in touch with them for many years to come. So many others were also like family, instrumental in providing the supportive environment necessary to thrive, and I am grateful for everyone in the group. It has truly been an honor.

Friends made along the way have also been an essential component of my support system, and I owe special thanks to Dr. Michelle Hall, Dr. Ethan Fisher, and Tania Cabrera. Adam Gil has been there for me since I began high school, and he more than any other friend has played a vital role in keeping me grounded, seeing me through high school, college, and the latter end of graduate school. Kate Rieppel has been the best friend anyone could ask for. Dr. Brad Conrad gave me the final push I needed to finish writing this dissertation, at the very moment when I needed someone the most, and I will always be so, so grateful. I cannot even begin to list the countless others who have been in my life and contributed to the person I am today.

Last, but not least, my family deserves more credit than I can possibly ever give. My mother, father, and sister Heather especially, have collectively been the rock that I so very much

needed these past several years, not to mention the unconditional encouragement during my entire education. I continue to credit my amazing mother especially for instilling in me a thirst for knowledge and a desire to discover the truth in nature, and my incredible father for encouraging my inquisitiveness but also reminding me to maintain a sense of balance in my life. Both my parents are self-made in many ways, and they both have strengths I can only hope I've inherited. My grandmother, grandfather, Nana, and aunts Tracy and Melissa have been encouraging and endlessly supportive, and I am so grateful for their love. I must also thank Marcia Szkolka, since sometimes we chose our family; she has been a wonderful mother to me for the past four and a half years and I am so grateful for her presence in my life.

Chapter 1

Palladium-Catalyzed Direct C-H Arylation of Pyrazoles

I. Introduction

Nitrogen-containing heteroarenes are frequently found in biologically active compounds, including natural products, protein ligands, and pharmaceuticals.¹ These azoles constitute crucial components of the contemporary medicinal chemistry repertoire.² Though pyrazoles are rarely found in nature, they serve as important core motifs of many pharmaceuticals and pharmaceutical leads with a wide range of biological activities^{2b} (e.g., cholesterol lowering,³ anti-inflammatory,⁴ anticancer,⁵ antidepressant, and antipsychotic agents⁶; see Figure 1). They are also used in polymer chemistry,⁷ as ligands for catalysis and coordination chemistry,⁸ and as agrochemicals.⁹ As a result, there continues to be great interest in the development of versatile methods to access highly substituted, complex pyrazoles. Traditionally, pyrazoles have been synthesized via condensation reactions of 1,3-dicarbonyls and hydrazines or by cycloadditions of diazoalkanes and alkynes.¹⁰ Although recent advances have greatly expanded the generality and specificity of *de novo* approaches, each method inevitably has its scope and efficiency limitations.¹¹

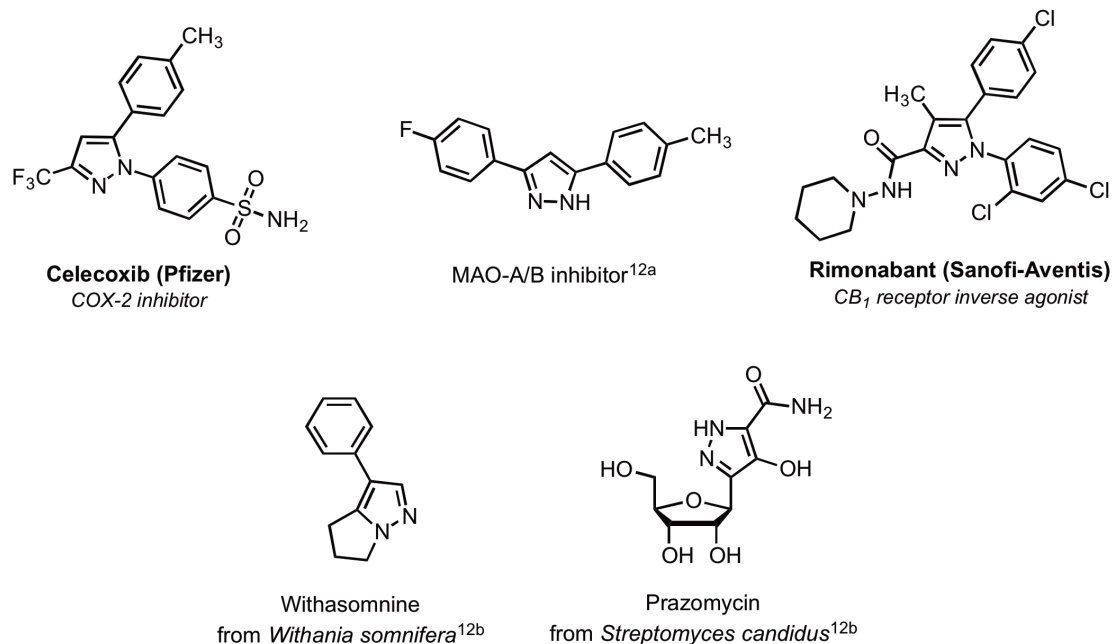


Figure 1. Examples of biologically active pyrazoles.

We envisioned a conceptually different and modular approach to the construction of arylated pyrazoles based on direct C-H bond arylation (Figure 2). Our strategy was to directly attach new aromatic rings to the existing pyrazole core at desirable positions (“*topologically obvious synthesis*”),¹³ which would allow rapid assembly of highly functionalized heterocycles via an efficient approach to synthesize a diverse series of pyrazole analogs and regioisomers.

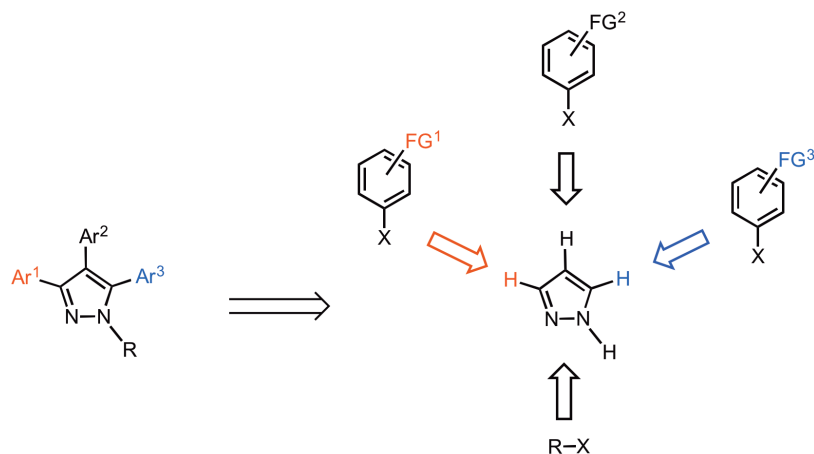


Figure 2. A new approach to synthesis of complex pyrazoles via direct C-H arylation.

Direct functionalization of C-H bonds is a highly desirable approach to rapid functionalization and generation of complex structures in modern organic chemistry, as it circumvents the need to pre-install required coupling components in order to form the bond of interest (Figure 3). This approach also avoids the use of metals like tin or zinc, reducing potentially toxic by-products of the reaction. Aryl halides and triflates, while ubiquitously used in cross-coupling chemistry, are also utilized as aryl donors in direct C-H arylation reactions. This approach is valuable to the field, as it enables chemists to quickly generate diverse libraries of compounds from more readily accessible reagents, reducing the time, cost, and loss of material associated with additional synthetic steps in a sequence. The past decade has seen tremendous advances in the field, particularly in transition metal-catalyzed direct functionalization and arylation of arenes.¹⁴

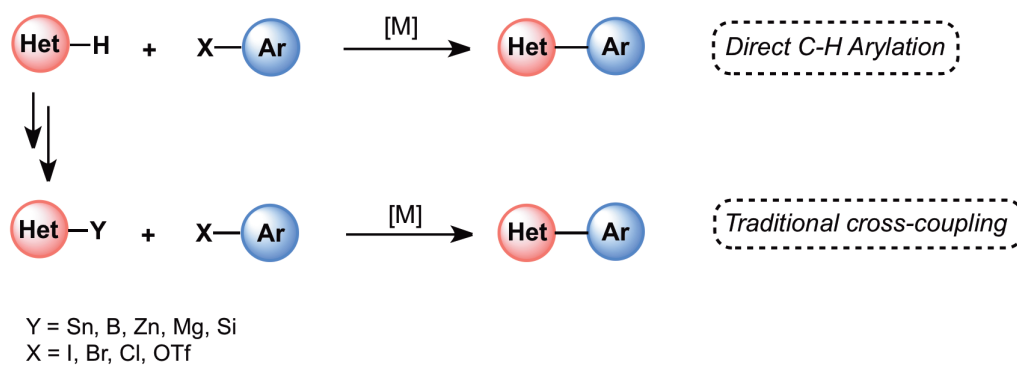
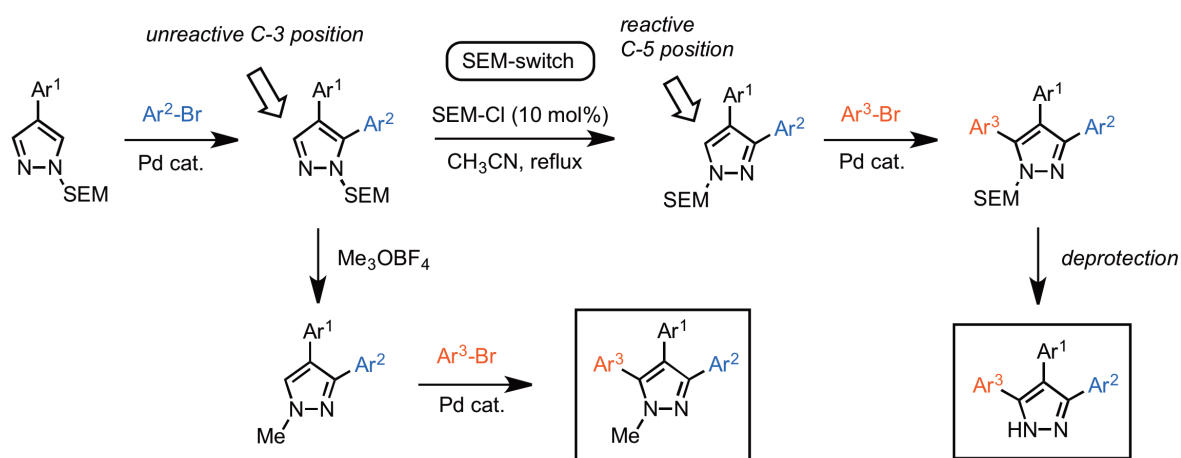


Figure 3. Comparison of direct functionalization with traditional cross-coupling approaches.

When we considered applying this approach to the pyrazole core, careful inspection of the literature yielded no existing intermolecular, catalytic C-arylation of pyrazoles, so our first task was to develop the first catalytic method and explore its regioselectivity. Preliminary results allowed us to devise a general approach for the synthesis of mono-, di-, and triarylpyrazoles (Scheme 1). The first aryl group can be installed regioselectively in the 4-position of pyrazole by bromination followed by Suzuki coupling; other substituents can also be introduced at this position due to its high nucleophilicity. The first direct C-H arylation takes place with good selectivity at the 5-position, which provides a method to obtain unsymmetrical diarylpyrazoles, overcoming a significant drawback of cyclization-condensation approaches. However, due to the low reactivity of the 3-position, arylation only occurs there minimally. To address this problem, we developed a simple one-step protocol to transfer the SEM group from one nitrogen to the other. This converts the unreactive position 3 to the reactive position 5, which enables the second C-H arylation to proceed efficiently, generating a protected, trisubstituted pyrazole. Subsequent SEM-deprotection produces free *N*-H triarylpyrazoles¹⁵ and the utility of the method is increased by regioselective introduction of a nitrogen substituent by the *N*-alkylation of unsymmetrical SEM-pyrazoles (Scheme 1). Thus, this strategy allows for rapid assembly of fully

substituted pyrazoles with complete regio-control of all C- and N-substituents. Complex pyrazoles with different numbers and positions of aryl rings can be readily synthesized from common precursors by choosing the desirable haloarene donor and the order of the arylation and alkylation reactions.

Scheme 1. Sequential C-arylation enabled by SEM group switch provides a rapid access to triarylpyrazoles with complete control of regioselectivity.



II. Results & Discussion

II.1 Development of C-H Arylation Protocol for SEM-Protected Pyrazoles

As of the time of this work, we had previously reported catalytic protocols for the direct C-arylation of indoles, pyrroles, and imidazoles using palladium¹⁶ and rhodium¹⁷ catalysts and carboxylate bases. Unfortunately, these methods were inefficient for arylation of pyrazoles, calling for the development of new conditions.^{18,19,20} We rationalized the low reactivity of pyrazoles in terms of the relatively high Lewis basicity of these compounds and their ability to deactivate the catalyst. We chose to examine SEM-protected pyrazoles as the substrates [SEM =

2-(trimethylsilyl)ethoxymethyl] for two reasons: first, due to the stability of this protecting group under the catalytic arylation conditions^{16c,21} and second, the ability of SEM group to be transposed from one nitrogen to another, enabling sequential arylations as outlined above. Rigorous and systematic optimization of the reaction parameters (metal catalyst, ligand, base, and solvent) for the coupling of 1*N*-SEM-4-phenylpyrazole (as to avoid potential side reaction at the 4-position) and bromobenzene led to a robust method which uses the following conditions: 5 mol % Pd(OAc)₂, 7.5 mol % P(*n*-Bu)Ad₂, and 3 equiv. KOPiv, in DMA as the solvent and heating at 140°C under inert atmosphere (**Figure 4**; this work was performed in collaboration with postdoctoral colleague Dr. Roman Goikhman). Consistent with previous results in our group, an objective search for catalytic C-H arylation conditions identified a carboxylate salt as the optimal base, validating the importance of carboxylate base in the metalation step of heteroarenes.^{16,17} It is also worth noting that these conditions are very similar to those developed independently by other laboratories, including Fagnou and colleagues', for arylation of benzene aromatics.²² The latter team also showed that potassium pivalate can be generated *in situ* from potassium carbonate and a substoichiometric amount of pivalic acid. Therefore, we replaced potassium pivalate with potassium carbonate and a substoichiometric amount of pivalic acid, resulting in a more practical procedure; both versions of this protocol (PivOK or PivOH/K₂CO₃) provided comparable yields of arylated SEM-pyrazoles.

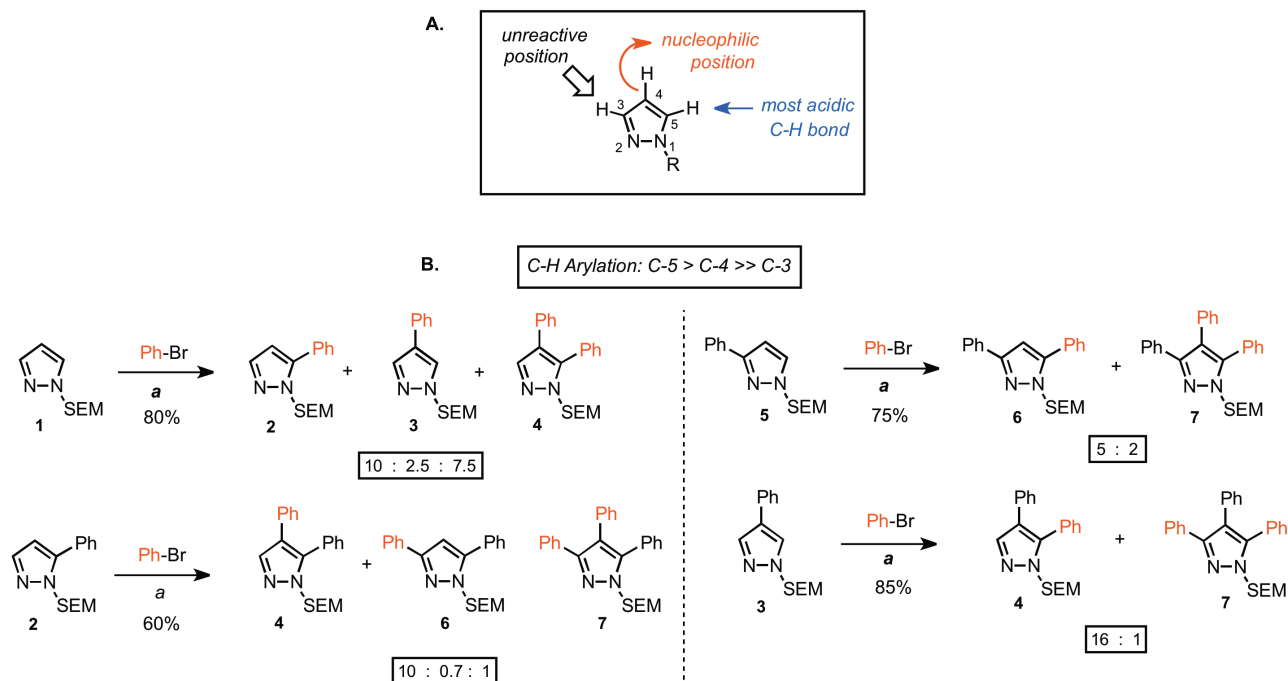


Figure 4. (A) General reactivity properties of pyrazole. (B) Reactivity profile of pyrazoles toward palladium-catalyzed C-H arylation. The C-5 position exhibits the highest reactivity. (a) Reaction conditions: Pyrazole, PhBr (1.5 equiv.), Pd(OAc)₂ (5 mol %), P(*n*-Bu)Ad₂ (7.5 mol %), K₂CO₃ (3 equiv.), HOPIv (25 mol %), 2.5 M DMA, 140°C for 12 h. Isolated yields are shown except for substrate 1, where the substrate conversion and the product ratio was determined by ¹H NMR of the crude mixture. All product ratios were confirmed by ¹H NMR of crude mixtures.

II.2 Regioselectivity of C-Arylation of SEM-Protected Pyrazoles

With optimized reaction conditions in hand, our next task was to determine the regioselectivity of the method (**Figure 4**). When the simple parent SEM-pyrazole **1** was subjected to the catalytic conditions, the resulting mixture of arylated products indicated higher reactivity of the 5-position relative to the 4-position and very low to no reactivity at the 3-position (**Figure 4B**). In addition to the monoarylated products, the bis-arylation product **4** was also formed in a significant amount. This trend was confirmed by examining the reaction of 1*N*-SEM-3-phenylpyrazole **5**, which gave a 5:2 ratio of bisarylated **6** and triarylated **7**. In contrast,

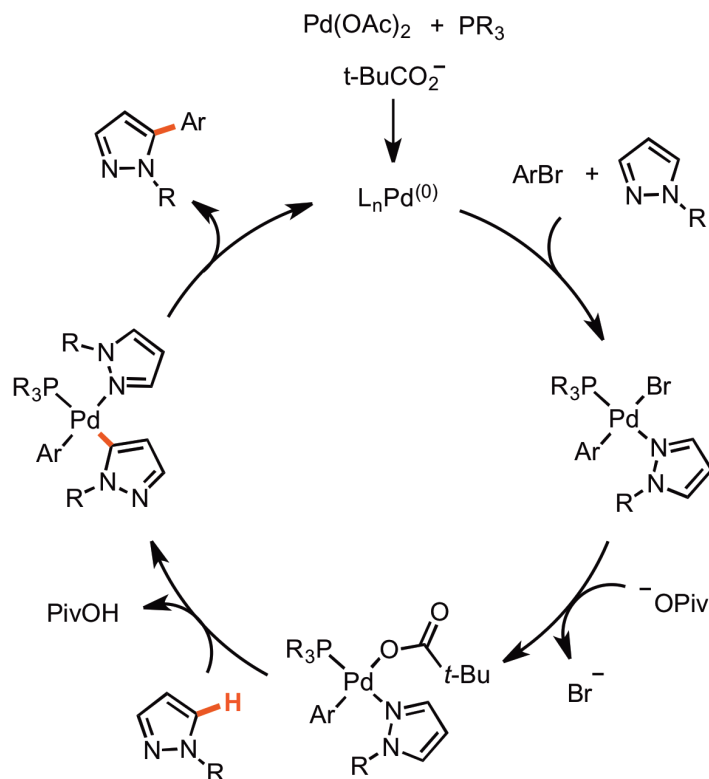
compound **3**, with the 4-position blocked, was arylated at the 5-position with high selectivity to provide compound **4** in 80% yield; the regioisomer stemming from arylation at the 3-position was not detected, and only a small amount of the bis-arylation product **7** was formed (16:1 ratio, 4:7). Arylation of compound **2** was also selective, taking place at the 4-position to afford product **4** as the major product; however, the yield was lower compared to arylation of the 5-position. These experiments pointed to inefficient C-arylation at the 3-position, which is consistent with the low reactivity of this site (to both electrophiles and strong bases), while arylation was achieved at both C-4 and C-5 positions with preference for the latter. These reactivity trends were the basis for the general synthetic strategy shown in Scheme 1, where almost any substituted, protected pyrazole may be arylated at desired positions according to their relative reactivities.

II.3 Rationale for the Observed Regioselectivity

We hoped to gain insight into the mechanism of the reaction through the regioselectivities discussed above so that we could use the information to either improve the method or apply comparable methods to other azole substrates our laboratory was investigating. It is well known that the 4-position of pyrazole is the most nucleophilic and readily undergoes electrophilic substitution, while the 5-position possesses the most acidic C-H bond, which can be selectively deprotonated by strong bases (e.g., lithiation).²³ Our previous results suggest that both our palladium-acetate^{16b} and the rhodium-pivalate¹⁷ catalytic systems, as well as related systems developed by others,²⁴ proceed via an electrophilic-like mechanism (or EMD, electrophilic metalation-deprotonation mechanism)²⁵, in the context of indoles, pyrroles, and imidazoles, where the metal acts as an electrophile, breaking the aromaticity, and the carboxylate ligand as the base, removing the proton. However, Fagnou's laboratory generated evidence indicating that

the palladium-pivalate system, in the context of benzene arenes, selectively targets acidic C-H bonds via a “ σ -deprotonation mechanism”, or a concerted metalation-deprotonation (CMD) mechanism, where the metal-carboxylate complex directly engages the C-H bond.^{22,26} The preference of the catalytic system for the acidic C-H bonds explains the C-5 selectivity observed in our current case. It is also reasonable, however, that an electrophilic-like mechanism occurs, with the migration of palladium from the most electrophilic site (C-4) to the position adjacent to the nitrogen (C-5), analogous to the rationale proposed for C-2 arylations of indoles.^{16b} Considering all of the systems mentioned (our previous and current systems combined with those of Fagnou), the successful reaction of both electron-deficient benzenes and electron-rich heteroarenes suggests substantial plasticity of the palladium-pivalate catalytic system, which may also account for the ability to arylate both C-5 and C-4 positions of the pyrazole system. The phosphine ligand modulates the reactivity of this catalytic system; in the context of pyrazoles, strong σ -donor phosphines also protect the catalyst against the inhibition by the basic sp^2 nitrogen of the substrate (results not shown). In order to address these mechanistic questions, a colleague in our laboratory, Dr. Rachel Tundel, extensively examined the palladium-carboxylate catalytic system with a variety of heteroarenes.²⁷ Her experiments support the conclusion that the carboxylate co-catalyst is required to provide the carboxylate ligand, which plays two crucial roles: 1) It facilitates the C-H activation most likely via the CMD mechanism, and 2) it stabilizes the catalyst resting state from decomposition (Scheme 2).

Scheme 2. Proposed catalytic cycle on the basis of mechanistic studies performed in the Sames group.



II.4 Arene Donor Substrate Scope

Compound **3**, 4-phenyl-1*N*-SEM-pyrazole, was used to examine the reaction scope of the arylation method; it is rapidly accessible by bromination of free (NH)-pyrazole at the 4-position,²⁸ *N*-alkylation with SEM-Cl, and a Suzuki reaction with phenylboronic acid (see Experimental). The arylation reactions may be performed on the benchtop under argon, and the conditions tolerate a wide variety of functional groups on the bromoarene donor, including ketone, ester, nitro, dimethylamino, and pyridyl groups (Table 1). Electron-deficient and electron-neutral bromoarenes perform best in the reaction, whereas bromoarenes with electron-donating substituents in the para-position (entry 7, Table 1) or steric bulk in the ortho-position give lower yields of desired products.

Table 1. Arylation Substrate Scope.^a

3: R = Ph

Entry	R	Product	Isolated Yield, %	Entry	R	Product	Isolated Yield, %
1	Ph		4 80% (5% bis)	7	Ph		13 35%
2	Ph		8 65% (15% bis)	8	Ph		14 74%
3	Ph		9 82%	9	Ph		15 58%
4	Ph		10 74% (13% bis)	10	o-tol		16 79%
5	Ph		11 58%	11			17 69% (8% bis)
6	Ph		12 76%	12	COOEt		18 75%

^a Reaction conditions: Pyrazole, ArBr (1.5 equiv.), Pd(OAc)₂ (5 mol %), P(*n*-Bu)Ad₂ (7.5 mol %), K₂CO₃ (3 equiv.), HOPiv (25 mol %), 2.5M DMA, 140°C for 12 h. Isolated yields are an average of at least two separate reactions.

II.5 Pyrazole Substrate Scope

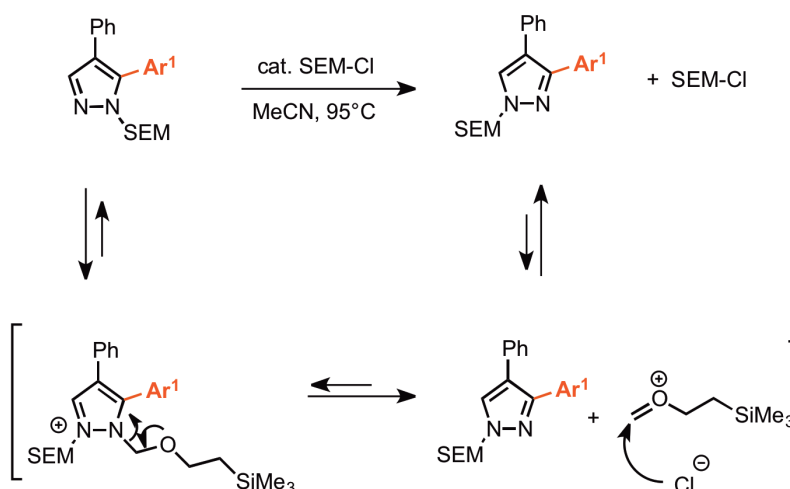
Substitution on the phenyl ring in the 4-position of the pyrazole is also tolerated as illustrated by the ortho-tolyl- and para-trifluoromethylphenyl-substrates, which give the corresponding products **16** and **17**, respectively, in good yields (Table 1, entries 10 and 11). The

conditions are also compatible with functionality beyond aryl groups as demonstrated by efficient arylation of the substrate containing an electron-withdrawing ester directly attached to the pyrazole in the 4-position, affording product **18** in 75% isolated yield (Table 1, entry 12). Thus, this method allows for synthesis of 4,5-diaryl-SEM-pyrazoles in one step from readily available 4-aryl-SEM-pyrazoles.

II.6 SEM-Group Transposition (SEM-group switch)

After the installment of the second arene ring at C-5, the subsequent arylation would have to take place at the 3-position, which bears the last available C-H bond. However, as shown in **Figure 4** and discussed previously, the arylation of this site is not feasible due to its low reactivity; no reaction or very low yields of the desired product were obtained. To solve this problem, we considered switching the SEM group from one nitrogen atom to another, which would transform the unreactive position 3 to the reactive position 5 (Scheme 3).

Scheme 3. SEM group transposition (SEM switch).



It has been reported that a mixture of unsymmetrical N-protected imidazoles could be equilibrated by heating in the presence of certain alkylating agents, leading to formation of the thermodynamic product.²⁹ Applying this approach to SEM-pyrazoles, we were able to achieve the SEM switch by heating the starting material with 10 mol % of SEM-Cl in acetonitrile. Alkylation of the pyrazole nitrogen by SEM-Cl forms a pyrazolium salt, which facilitates the equilibration of the two regioisomers, ultimately yielding the less hindered, thermodynamically favored product (Scheme 3). The SEM-switch produces an average of ~90% conversion, as demonstrated with four different substrates (Table 2), with the ~10% accounting for the pyrazolium salt remaining from the 10 mol % SEM-Cl in the reaction mixture. Due to the extremely close polarity of the regioisomers, they were frequently difficult to separate via flash chromatography; in these cases, reverse-phase HPLC was used to separate and purify these compounds. Separating the two isomers is not necessary when triarylpyrazoles are desired, as the “unswitched material” may readily be removed after the subsequent arylation. In one step, the SEM-group switch transforms an unreactive compound to a reactive substrate, avoiding the need for deprotection and reprotection, and enables the two consecutive C-H arylations.

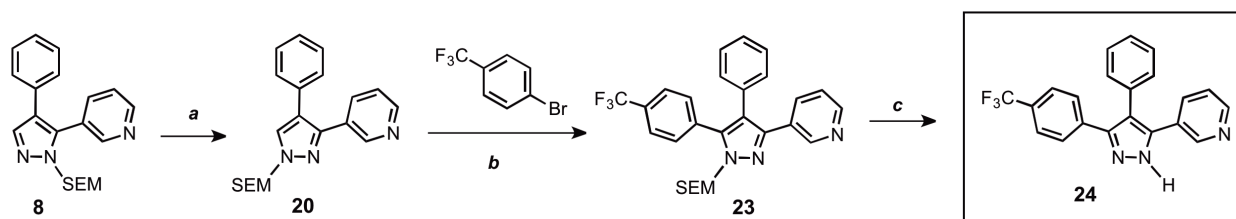
Table 2. SEM switch scope.

Entry	Aryl Group	Product	% Conversion ^a
1		19	85%
2		20	90% (84%) ^b
3		21	91% (80%) ^c
4		22	90%

^a Determined by ¹H NMR. ^b Isolated yield (flash chromatography). ^c Isolated yield (HPLC).

II.7 The Second C-Arylation and Preparation of 3,4,5-Triarylpyrazoles

Scheme 4 illustrates the brevity of the sequential arylation scheme for preparation of 3,4,5-triarylpyrazoles. The SEM-group transposition was applied to compound **8**, which is available in one arylation step from starting material **3**, to provide compound **20**. The second arylation with 4-bromotrifluoromethylbenzene proceeded in high yield under the standard catalytic conditions to construct SEM-protected triarylpyrazole **23**, which after deprotection furnished triarylpyrazole **24**. Thus, all three arene rings are introduced to the pyrazole core with complete regiochemical control; two of the rings are attached directly via C-H bond functionalization.

Scheme 4. Synthesis of triarylpyrazoles via sequential C-arylation.^a

^a Conditions: (a) Pyrazole, SEMCl (10 mol %), MeCN, 95°C, 24 h; 84% yield. (b) Pyrazole, ArBr (1.5 equiv.), Pd(OAc)₂ (5 mol %), P(*n*-Bu)Ad₂ (7.5 mol %), K₂CO₃ (3 equiv.), HOPiv (25 mol %), 2.5 M DMA, 140°C, 12 h; 77% yield. (c) 3N HCl, EtOH, reflux, 3 h, 75% yield. In DMSO-*d*₆, compound **24** exists as a mixture of tautomers. Yields are an average of at least two separate isolated yields.

The scope of the arylation catalytic method was further examined in bisarylated, 1-SEM-3,4-diarylpyrazole substrates (Table 3). Good to excellent yields of SEM-protected triarylpyrazoles were obtained with a variety of functional groups on both the pyrazole substrate and the bromoarene donor.

Table 3. C-Arylation of diarylpyrazoles, substrate scope.^a

Reaction scheme: A pyrazole derivative with a phenyl group at position 3, an Ar¹ group at position 5, and an R group on the nitrogen at position 1 reacts with Ar²-Br in the presence of a [Pd] catalyst to form a product with an additional Ar² group at position 4.

Entry	Product	Isolated Yield	Entry	Product	Isolated Yield
1	23	77%	5	28	67%
2	25	88%	6	29	53%
3	26	64%	7	30	54%
4	27	70%	8	31	43%

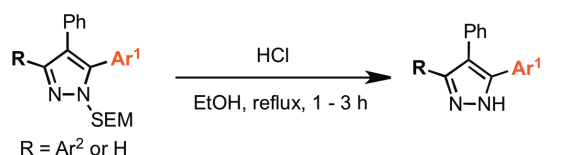
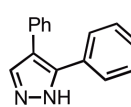
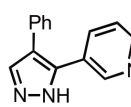
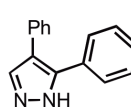
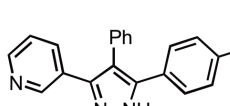
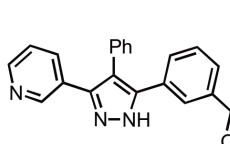
^a Reaction conditions: Pyrazole, ArBr (1.5 equiv.), Pd(OAc)₂ (5 mol %), P(*n*-Bu)Ad₂ (7.5 mol %), K₂CO₃ (3 equiv.), HOPiv (25 mol %), 2.5 M DMA, 140°C, 12 h. Yields are an average of at least two separate isolated yields.

II.8 Deprotection of SEM-Pyrazoles

Free (NH)-pyrazoles are readily accessible by the deprotection of the SEM group, which is accomplished by the action of hydrochloric acid in ethanol.³⁰ To confirm the generality of this protocol in the context of complex pyrazoles, triarylpyrazoles **23** and **25** (Table 3) as well as diarylpyrazoles **4**, **8**, and **10** (Table 1) were deprotected to afford high yields of the corresponding free pyrazoles (Table 4). It is well known that free pyrazoles exist as a mixture of tautomers,^{31,32} which is consistent with ¹H NMR observations; while the signal for the NH

proton is broad in CDCl₃, the two peaks are resolved in DMSO-*d*₆ (δ 13-14.5 ppm); in the case of compound **24**, both tautomers are present in a 56:44 ratio (see Experimental).

Table 4. Deprotection of complex pyrazoles.

 <p style="text-align: center;">R = Ar² or H</p>			
Entry	Product		Isolated Yield
1		32	90%
2		33	99%
3		34	72%
4		24	75%
5		35	75%

II.9 Regioselective *N*-Alkylation/*C*-Arylation Sequence Enabled by the SEM Group

The sequential arylation mediated by the SEM-group switch, described above, provides a rapid access to protected and free triarylpyrazoles and offers an attractive alternative to the *de novo* approaches. However, when *N*-alkylated products are desired, the *N*-alkylation of free *N*-H pyrazoles that lack sufficient steric bias to encourage selective alkylation result in a mixture of two regioisomers. Triarylpyrazole **24** (Scheme 4) is an example substrate that would suffer from

this problem. To address this concern, we considered the idea of using the SEM group to selectively introduce the alkyl group at the desired nitrogen of the pyrazole by blocking the undesired position. We tested a number of methylating reagents (dimethyl sulfate, methyl iodide, and trimethyloxonium tetrafluoroborate), of which $\text{Me}_3\text{O}^+\text{BF}_4^-$ gave best results, yielding *N*-methylated pyrazolium salts at room temperature in dry dichloromethane; facile deprotection of the SEM group in acidic conditions yields *N*-methylated products as a single isomer (Table 5).

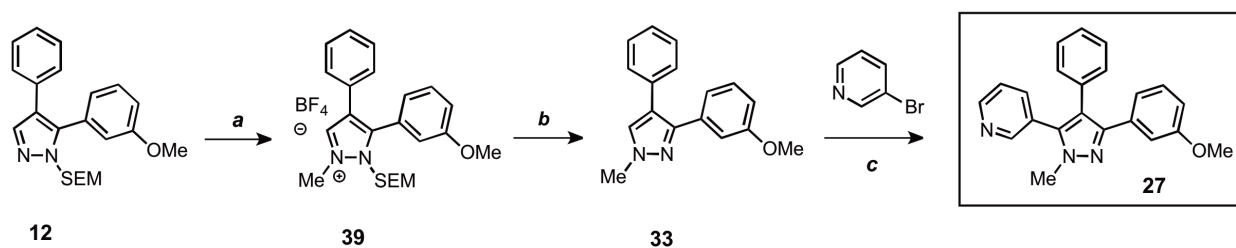
Table 5. *N*-Methylation of bisarylated, SEM-protected pyrazoles.

Entry	Product	Isolated Yield (2 steps)
1		70%
2		82%
3		66%
4		77%

For example, compound **12** was methylated and deprotected to produce the single desired isomer of the alkylated pyrazole **33** (Scheme 5). This two-step procedure not only selectively alkylates the nitrogen of choice, but simultaneously serves to change the unreactive 3-position of the pyrazole to the reactive 5-position in a similar fashion as the SEM group switch. The *N*-

methylpyrazole **33** was then arylated with 3-bromopyridine to afford the highly functionalized pyrazole **27**. Consequently, the regioselective *N*-alkylation was incorporated into the sequential arylation scheme to provide the fully substituted pyrazole as a single regioisomer.

Scheme 5. Sequential *C*-arylation and *N*-methylation provides a rapid access to 1-methyl-3,4,5-triarylpyrazoles with complete regioselectivity control.^a



^a Conditions: (a) Pyrazole, $\text{Me}_3\text{O-BF}_4$ (1.2 equiv.), CH_2Cl_2 , RT, 1 h. (b) 3N HCl, EtOH, reflux, 1 h; 70% yield over 2 steps. (c) Pyrazole, ArBr (1.5 equiv.), $\text{Pd}(\text{OAc})_2$ (5 mol %), $\text{P}(n\text{-Bu})\text{Ad}_2$ (7.5 mol %), K_2CO_3 (3 equiv.), HOPiv (25 mol %), 2.5 M DMA, 140°C for 12 h; 70% yield. Yields are an average of at least two separate isolated yields.

One obvious limitation of this approach is that other nucleophilic functions present in the substrate would also undergo methylation; namely, the pyridyl and dimethylamino groups we encountered were not compatible with the methylation reaction conditions. To introduce *N*-alkylation into product that also contains an aniline, this problem can be solved by introducing the nitrophenyl ring (Table 1 and Table 3), and reducing the nitro group after the alkylation step. Another solution is to perform the alkylation earlier in the sequence and thus introduce the alkylation-prone groups by *C*-arylation after the *N*-alkylation step as illustrated in Scheme 5. The pyridine ring would be attached in the last step of the sequence, combining the utility of the regioselective *N*-alkylation with direct C-H arylation while bypassing substituent incompatibility.

III. Conclusions

Pyrazoles are an important class of heteroarenes frequently found in pharmaceuticals and protein ligands, and there has been a growing interest in new synthetic methods for their preparation. We have developed a strategically new approach based on the synthetic logic enabled by direct C-H bond functionalization, where new substituents are directly attached to predetermined positions of the heteroarene nucleus.¹³ This approach permits functionalization of all five pyrazole positions with complete regiocontrol and allows for the efficient synthesis of analog and regioisomeric series from common precursors. The particular strength of this strategy is the ability to utilize the synthesis from either the parent pyrazole or practically any pyrazole intermediate. Due to the inherent reactivity preferences of pyrazole in this palladium-catalyzed system, the sequential *C*-arylation of free N-H pyrazoles or N-alkylated pyrazoles was not possible, and therefore we conceived an innovative strategy based on the SEM-protecting group and its transposition. The SEM group fulfills three major roles: first, it protects the pyrazole amine group and thus enables the *C*-arylation, as free pyrazoles are not good substrates; second, it facilitates the regioselective sequential C-H arylation via the SEM group switch; and third, it allows for regioselective N-methylation which can be coupled to subsequent *C*-arylation.

In summary, the catalytic C-H arylation combined with the protecting group transposition and *N*-alkylation provides a rapid route to fully substituted pyrazoles with complete regiocontrol of all substituents. Significant advances have recently been reported for the *de novo* synthesis of pyrazoles, both in terms of regiocontrol and scope.¹¹ Also, major improvements have been achieved in the area of Suzuki coupling of pyrazoles; many of the problems associated with inefficient preparation of azolyl boronate esters and the low yielding coupling process have recently been addressed.^{15,33} Our approach is complementary to these methods, and together they

enable the design and synthesis of a wide variety of complex pyrazole compounds. This work was successfully published³⁴ and has been a significant contribution to the field, evidenced by its citation in 50 unique papers as of this writing (not including those from our laboratory), several of which are comprehensive reviews of recent advances in pyrazole synthesis (both de novo and more modular, direct functionalizations related to those presented here).³⁵ Our group has successfully extended this catalytic palladium-carboxylate C-H arylation system to further heteroarenes, namely imidazoles,^{25a} electron-deficient pyridines,^{25b} and even 1,2,4-triazoles.³⁶ The SEM group switch approach established in this work was successfully applied to the imidazole and triazole methods. These extensions of the methods presented here testify to the generality of the palladium-carboxylate catalytic system for direct C-H arylation of heteroarenes and the practicality of the SEM switch approach to selectively functionalize specific positions on these pharmacologically relevant heteroarene rings.

IV. Experimental Section

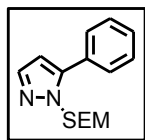
IV.1 General Information

All manipulations of air and/or water sensitive compounds were performed using standard Schlenk techniques under an atmosphere of argon passed through Drierite. Arylation reactions were carried out in capped glass vials (VWR, 8 mL) equipped with a magnetic stir bar and Teflon-lined cap and heated in a 34-well reaction block (Chemglass). All solvents were passed through a column of alumina under an argon atmosphere and used without further purification, with the exception of 1,4-dioxane, which was used as received (Aldrich, anhydrous). All chemicals were purchased from Sigma-Aldrich, Acros, or Strem (palladium complexes and phosphines) and used as received unless otherwise noted. Phosphines were stored under Ar in a glovebox between uses. Flash chromatography was carried out on SILICYCLE silica gel (230-400 mesh). Nuclear Magnetic Resonance spectra were recorded at 300 K on Bruker Advance DPX 300 or 400 Fourier transform NMR spectrometers in CDCl_3 and proton spectra referenced to TMS or the solvent residual peak (δ 7.26) and the solvent residual peak (δ 77.0) in ^{13}C NMR. Some spectra were recorded in DMSO-d_6 and were referenced to the solvent residual peak (δ 2.50) in proton spectra. Mass spectra were recorded on a JEOL LCmate (Ionization mode: APCI+). HPLC was performed on a Waters Millennium32 Analytical system with a 996 photodiode array detector using an Xterra RP₁₈ 5 μm column (4.6 x 150mm) with a Waters 600 Controller; fractions were detected at 254 nm with a Waters 2487 Dual λ Absorbance Detector and data was analyzed using OpenLynx software. All HPLC methods were conducted using 80% acetonitrile / water (with 0.1% trifluoroacetic acid) for 35 minutes, unless otherwise noted.

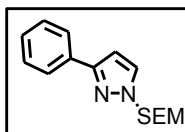
IV.2 Synthesis of Starting Materials

1-((2-(trimethylsilyl)ethoxy)methyl)-1*H*-pyrazole (1) was synthesized from the commercially available pyrazole (Aldrich) according to literature procedure.³⁷

3-Phenyl-1-((2-(trimethylsilyl)ethoxy)methyl)-1*H*-pyrazole (5) and 5-Phenyl-1-((2-(trimethylsilyl)ethoxy)methyl)-1*H*-pyrazole (2): 3-Phenylpyrazole was used as purchased from Acros Organics. The compound (2.88 g, 20 mmol) was dissolved in 30 mL THF and cooled to 0 °C under an argon atmosphere. NaH (0.72 g, 30 mmol, 1.5 eq.) was added slowly at 0 °C and the resulting mixture was allowed to stir for 30 minutes, or until hydrogen evolution was complete. SEMCl (3.7 mL, 3.5 g, 21 mmol, 1.05 eq.) was added slowly and the reaction allowed to warm to room temperature and stirred for an additional 12 hours. The reaction was quenched with 5 mL deionized water, extracted with ether, washed with brine, dried with MgSO₄ and the solvent removed. After workup, the resulting crude mixture was separated via column chromatography with 10% diethyl ether in hexanes, to produce 1.92 g (35%) of **5**, and 3.12 g (57%) of **2**.

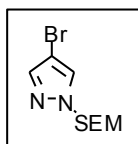


5-Phenyl-1-((2-(trimethylsilyl)ethoxy)methyl)-1*H*-pyrazole (2): ¹H NMR (400 MHz, CDCl₃): 7.62 (m, 2H), 7.56 (d, *J* = 1.8 Hz, 1H), 7.37 – 7.48 (m, 3H), 6.40 (d, *J* = 1.8 Hz, 1H), 5.43 (s, 2H), 3.74 (t, *J* = 8.2 Hz, 2H), 0.95 (t, *J* = 8.2 Hz, 2H), -0.01 (s, 9H). ¹³C NMR (75 MHz, CDCl₃): δ 144.4, 139.3, 130.3, 128.9, 128.8, 128.5, 106.7, 77.9, 66.7, 17.9, -1.45. MS (LR-APCI): calculated for C₁₅H₂₂N₂OSi: 274.2, measured 275.5 (M+H)⁺.



3-Phenyl-1-((2-(trimethylsilyl)ethoxy)methyl)-1H-pyrazole (5): ^1H NMR

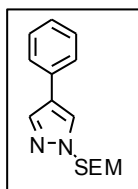
(400 MHz, CDCl_3): 7.83 (m, 2H), 7.59 (d, $J = 2.4$ Hz, 1H), 7.41 (m, 2H), 7.31 (m, 1H), 6.64 (d, $J = 2.4$ Hz, 1H), 5.47 (s, 2H), 3.64 (t, $J = 8.2$ Hz, 2H), 0.94 (t, $J = 8.2$ Hz, 2H), -0.01 (s, 9H). ^{13}C NMR (75 MHz, CDCl_3): δ 152.0, 133.3, 130.8, 128.6, 127.7, 125.8, 104.1, 80.2, 66.7, 17.7, -1.45. MS (LR-APCI): calculated for $\text{C}_{15}\text{H}_{22}\text{N}_2\text{OSi}$: 274.2, measured 275.6 ($\text{M}+\text{H}$) $^+$.



4-Bromo-1-((2-(trimethylsilyl)ethoxy)methyl)-1H-pyrazole: 4-Bromopyrazole

was used as purchased or synthesized according to the literature.³⁸ 4-

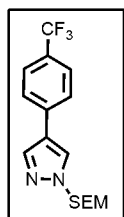
Bromopyrazole (5.50 g, 37.4 mmol) was dissolved in 50 mL THF and cooled to 0 °C under an argon atmosphere. NaH (1.35 g, 56.3 mmol, 1.5 eq.) was added slowly at 0 °C and the resulting mixture was allowed to stir for 30 minutes, or until hydrogen evolution was complete. SEMCl (6.93 mL, 6.55 g, 39.3 mmol, 1.05 eq.) was added slowly and the reaction allowed to warm to room temperature and stirred for an additional 12 hours. The reaction was quenched with 10 mL deionized water, extracted with ether, washed with brine, dried with MgSO_4 and the solvent removed. After workup, the resulting crude mixture was distilled under high vacuum to produce a colorless, clear liquid (9.30 g, 90%). Characterization of this compound was identical to that found in the literature.³⁸



4-Phenyl-1-((2-(trimethylsilyl)ethoxy)methyl)-1H-pyrazole (3): 4-Bromo-1-((2-

trimethylsilyl)ethoxy)methyl-1H-pyrazole (3.39 g, 12.2 mmol), phenylboronic acid (2.00 g, 16.5 mmol, 1.35 eq.), palladium (II) acetate (0.137 g, 0.61 mmol, 5 mol %), tricyclohexylphosphine (0.340 g, 1.2 mmol, 10 mol %), and cesium carbonate (7.76 g, 23.8

mmol, 2 eq.) were weighed in air and added to a round-bottom flask, evacuated and backfilled with Ar three times. Dioxane (70 mL) was added via syringe and the reaction mixture refluxed at an oil bath temperature of 105 °C for 6-12 hours. Deionized water (10 mL) and ethyl acetate (100 mL) were added to the reaction mixture and separated, the aqueous fraction extracted with ethyl acetate, the organic fractions combined, dried over MgSO₄, and the solvent removed. The crude, brown, viscous material was purified via column chromatography with a 100% hexanes to 10% EtOAc:hexanes gradient, after which it was necessary to distill the remaining starting material out of the column purified product under vacuum to produce 2.72 g (81% isolated, 90% by ¹H NMR of the crude product) of viscous, yellow oil. ¹H NMR (400 MHz, CDCl₃): δ 7.83 (s, 1H), 7.82 (s, 1H), 7.50 (d, *J* = 7.8 Hz, 2H), 7.38 (t, *J* = 7.8 Hz, 2H), 7.26 (m, 1H), 5.46 (s, 2H), 3.60 (t, *J* = 8.2 Hz, 2H), 0.93 (t, *J* = 8.2 Hz, 2H), -0.02 (s, 9H). ¹³C NMR (75 MHz, CDCl₃): δ 137.5, 132.4, 129.0, 126.7, 126.2, 125.7, 124.3, 80.5, 66.9, 17.9, -1.4. MS (LR-APCI): calculated for C₁₅H₂₂N₂OSi: 274.2, measured 275.3 (M+H)⁺.

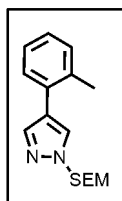


4-(4-(Trifluoromethyl)phenyl)-1-((2-(trimethylsilyl)ethoxy)methyl)-1H-

pyrazole: 4-Bromo-1-SEM-1H-pyrazole (1.4 g, 5 mmol), 4-(trifluoromethyl)phenylboronic acid (1.3 g, 6.8 mmol, 1.35 eq.), Pd(PPh₃)₄ (0.29 g, 0.25 mmol, 5 mol%), cesium carbonate (2.8 g, 8.5 mmol, 1.7 eq.) and dioxane (10 mL) were added

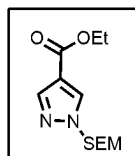
to a 20 mL vial under an argon atmosphere, and the reaction mixture was heated at 105°C for 12 hours. Deionized water (10 mL) and ethyl acetate (100 mL) were added to the reaction mixture, the product extracted with ethyl acetate, the organic fractions dried with MgSO₄, and the solvent removed. The crude, brown, viscous material was purified via column chromatography with 10% EtOAc in hexanes to produce 1.25 g (73%) of colorless liquid. Alternatively, 5 mol%

$\text{Pd}(\text{OAc})_2$ and 10% PCy_3 may be used as the catalyst system to afford a 78% yield. ^1H NMR (400 MHz, CDCl_3): δ 7.87 (s, 1H), 7.86 (s, 1H), 7.60 (AB q, J = 8.8 Hz, 4H), 5.47 (s, 2H), 3.62 (t, J = 8.2 Hz, 2H), 0.94 (t, J = 8.2 Hz, 2H), -0.02 (s, 9H). ^{13}C NMR (75 MHz, CDCl_3): δ 137.5, 135.9, 128.8, 126.7, 125.9, 125.85, 125.6, 123.0, 80.5, 67.0, 17.8, -1.46. MS (LR-APCI): calculated for $\text{C}_{16}\text{H}_{21}\text{F}_3\text{N}_2\text{OSi}$: 342.1, measured 343.3 ($\text{M}+\text{H}$) $^+$.



4-*o*-Tolyl-1-((2-(trimethylsilyl)ethoxy)methyl)-1H-pyrazole: 4-Bromo-1-SEM-

1H-pyrazole (0.7 g, 2.5 mmol), 2-methylphenylboronic acid (0.46 g, 3.4 mmol, 1.35 eq.), $\text{Pd}(\text{PPh}_3)_4$ (0.145 g, 0.125 mmol, 5 mol%), cesium carbonate (1.4 g, 4.25 mmol, 1.7 eq.) and 1,4-dioxane (10 mL) were added to a 20 mL vial under an argon atmosphere, and the reaction mixture was heated at 105°C for 12 hours. Deionized water (10 mL) and ethyl acetate (100 mL) were added to the reaction mixture, the product extracted with ethyl acetate, dried over MgSO_4 , and the solvent removed. The crude, viscous material was purified via column chromatography with 5% EtOAc in hexanes to product 0.4 g (55%) of colorless oil. ^1H NMR (400 MHz, CDCl_3): δ 7.68 (s, 1H), 7.66 (s, 1H), 7.33 – 7.35 (m, 1H), 7.20 – 7.27 (m, 3H), 5.47 (s, 2H), 3.62 (t, J = 8.2 Hz, 2H), 2.40 (s, 3H), 0.93 (t, J = 8.2 Hz, 2H), -0.02 (s, 9H). ^{13}C NMR (75 MHz, CDCl_3): δ 139.6, 135.3, 131.9, 130.6, 129.1, 128.1, 126.9, 126.0, 123.2, 80.3, 66.7, 21.2, 17.8, -1.49. MS (LR-APCI): calculated for $\text{C}_{16}\text{H}_{24}\text{N}_2\text{OSi}$: 288.2, measured 289.4 ($\text{M}+\text{H}$) $^+$.



4-Ethoxycarbonyl-1-((2-(trimethylsilyl)ethoxy)methyl)-1H-pyrazole:

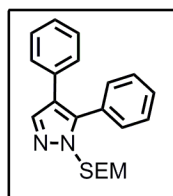
4-Ethoxycarbonyl-1H-pyrazole (1 g, 7.1 mmol) was dissolved in 20 mL THF. NaH (0.25 g, 10.4 mmol, 1.5 eq.) was added to the solution, and the resulting mixture

was allowed to stir for 30 min. at room temperature. SEMCl (1.4 mL, 1.3 g, 7.8 mmol, 1.1 eq.) was added slowly and the reaction stirred for an additional 12 hours. The reaction was quenched with 10 mL dionized water, extracted with ether, dried with MgSO_4 and the solvent removed. After workup, the resulting crude mixture was purified via column chromatography with 10% EtOAc in hexanes to produce a colorless, clear liquid (1.6 g, 83%). ^1H NMR (300 MHz, CDCl_3): δ 8.05 (s, 1H), 7.93 (s, 1H), 5.43 (s, 2H), 4.30 (q, $J = 7.2$ Hz, 2H), 3.57 (t, $J = 8.2$ Hz, 2H), 1.35 (t, $J = 7.2$ Hz, 3H), 0.91 (t, $J = 8.2$ Hz, 2H), -0.01 (s, 9H). ^{13}C NMR (75 MHz, CDCl_3): δ 162.9, 141.2, 132.8, 116.3, 80.6, 67.2, 60.3, 17.7, 14.3, -1.50. (LR-APCI): calculated for $\text{C}_{12}\text{H}_{22}\text{N}_2\text{O}_3\text{Si}$: 270.1, measured 271.4 ($\text{M}+\text{H}$) $^+$.

IV.3 Procedure for Pyrazole Arylation

These reactions were performed from 0.25 to 3 mmol scales. To a vial equipped with a stir bar, the substrate (1 equiv.), $\text{Pd}(\text{OAc})_2$ (5 mol%), $\text{P}(\text{tBu})\text{Ad}_2$ (7.5 mol%), K_2CO_3 (3 equiv.) and pivalic acid (25 mol%) were added. Reagents were weighed in air, and all were stored on the benchtop with the exception of the phosphine, which was stored under Ar in a glovebox between uses, and $\text{Pd}(\text{OAc})_2$, which was either stored in the glovebox or in a desiccator. The vial was sealed with a Teflon-capped septum and evacuated and backfilled with Ar three times. DMA (2.5M) and the aryl bromide (1.5 equiv.) were added via syringe. (If solid, the aryl bromide was added with the solids.) The septum was quickly replaced with a Teflon-lined cap under an Ar stream and the reaction mixture heated to 140 °C for 12 hours. After cooling to room temperature, the dark brown mixture was diluted with 10 mL water and 100 mL ethyl acetate, the layers separated, and the aqueous fraction back-extracted with EtOAc (30 mL x 3). The organic

fractions were combined and dried with MgSO_4 , the solvent removed, and the material purified via flash chromatography using the eluents specified.



4,5-Diphenyl-1-((2-(trimethylsilyl)ethoxy)methyl)-1H-pyrazole (4):

Procedure described above. Produced a yellow, dense oil in 80% yield, 5%

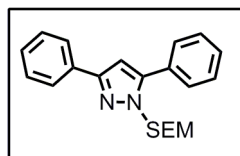
compound 7. ^1H NMR (400 MHz, CDCl_3): δ 7.78 (s, 1H), 7.42 (m, 5H), 7.19 –

7.23 (m, 5H), 5.34 (s, 2H), 3.69 (t, $J = 8.2$ Hz, 2H), 0.93 (t, $J = 8.2$ Hz, 2H), -0.01 (s, 9H). ^{13}C

NMR (75 MHz, CDCl_3): δ 140.5, 138.7, 132.4, 130.5, 129.9, 128.8, 128.7, 128.4, 127.7, 126.3,

121.8, 77.9, 67.1, 18.0, -1.1. MS (LR-APCI): calculated for $\text{C}_{21}\text{H}_{26}\text{N}_2\text{OSi}$: 350.2, measured

351.5 ($\text{M}+\text{H}$) $^+$.



3,5-Diphenyl-1-((2-(trimethylsilyl)ethoxy)methyl)-1H-pyrazole (6):

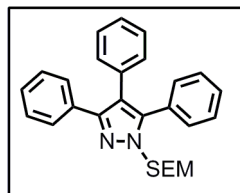
^1H NMR (400 MHz, CDCl_3): δ 7.87 (m, 2H), 7.68 (m, 2H), 7.40 – 7.50

(m, 5H), 7.34 (m, 1H), 6.72 (s, 1H), 5.48 (s, 2H), 3.82 (t, $J = 8.2$ Hz, 2H),

0.98 (t, $J = 8.2$ Hz, 2H), 0.01 (s, 9H). ^{13}C NMR (75 MHz, CDCl_3): δ 151.1, 145.9, 133.3, 130.3,

128.9, 128.7, 128.6, 128.6, 127.8, 125.8, 104.1, 77.8, 66.7, 17.9, -1.41. MS (LR-APCI):

calculated for $\text{C}_{21}\text{H}_{26}\text{N}_2\text{OSi}$: 350.2, measured 351.4 ($\text{M}+\text{H}$) $^+$.

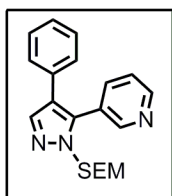


3,4,5-Triphenyl-1-((2-(trimethylsilyl)ethoxy)methyl)-1H-pyrazole (7):

^1H NMR (400 MHz, CDCl_3): δ 7.49 (m, 2H), 7.36 (m, 5H), 7.28 (m, 3H),

7.19 (m, 3H), 7.07 (m, 2H), 5.43 (s, 2H), 3.77 (t, $J = 8.2$ Hz, 2H), 0.96 (t, J

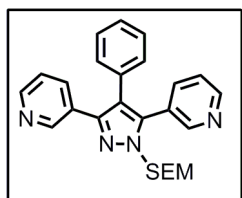
= 8.2 Hz, 2H), 0.0 (s, 9H). ^{13}C NMR (75 MHz, CDCl_3): δ 149.4, 142.7, 133.3, 133.2, 130.5, 130.4, 129.6, 128.5 (br.), 128.3 (br.), 128.1, 127.5, 126.5, 120.1, 77.9, 66.8, 17.9, -1.40. MS (LR-APCI): calculated for $\text{C}_{27}\text{H}_{30}\text{N}_2\text{OSi}$: 426.3, measured 427.1 ($\text{M}+\text{H}$) $^+$.



4-Phenyl-5-(3-pyridyl)-1-((2-(trimethylsilyl)ethoxy)methyl)-1H-pyrazole

(8): Pale yellow, dense oil; 65% yield (15% 4-phenyl-3,5-di-(3-pyridyl)-1-(SEM)-1H-pyrazole, **8b**), isolated via flash chromatography with a gradient from

100% hexanes, to 1:3 EtOAc:hexanes, to 2:3 EtOAc:hexanes as the eluent. ^1H NMR (400 MHz, CDCl_3): 8.66 (d, $J = 2.0$ Hz, 1H), 8.65 (bs, 1H), 7.81 (dt, $J_1 = 7.6$ Hz, $J_2 = 2.0$ Hz, 1H), 7.78 (s, 1H), 7.37 (ddd, $J_1 = 13.2$ Hz, $J_2 = 5.0$ Hz, $J_3 = 1.0$ Hz, 1H), 7.15-7.28 (overlapped m, 5H), 5.34 (s, 2H), 3.71 (t, $J = 8.4$ Hz, 2H), 0.94 (t, $J = 8.4$ Hz, 2H), 0.0 (s, 9H). Aromatic protons on the pyridine ring assigned with COSY 2-D NMR. ^{13}C NMR (75 MHz, CDCl_3): δ 151.0, 149.9, 138.9, 137.8, 136.9, 132.2, 128.7, 127.8, 126.7, 126.1, 123.4, 123.1, 78.1, 66.9, 17.9, -1.5. MS (LR-APCI): calculated for $\text{C}_{20}\text{H}_{25}\text{N}_3\text{OSi}$: 351.2, measured 352.5 ($\text{M}+\text{H}$) $^+$.



4-Phenyl-3,5-di-(3-pyridyl)-1-((2-(trimethylsilyl)ethoxy)methyl)-1H-

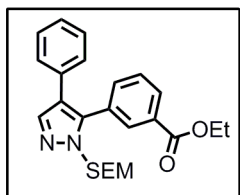
pyrazole (8b): White solid, 15% yield under arylation and isolation

conditions. ^1H NMR (400 MHz, CDCl_3): δ 8.74 (m, 1H), 8.59 (m, 2H),

8.50 (dd, $J_1 = 4.8$ Hz, $J_2 = 1.6$ Hz, 1H), 7.73 (dm, $J = 8.0$ Hz, 2H), 7.28 (ddd, $J_1 = 8.0$ Hz, $J_2 = 6.4$ Hz, $J_3 = 0.8$ Hz, 1H), 7.17 – 7.20 (m, 3H), 7.18 (ddd, $J_1 = 8.0$ Hz, $J_2 = 6.4$ Hz, $J_3 = 0.8$ Hz, 1H), 7.05 (m, 2H), 5.42 (s, 2H), 3.79 (t, $J = 8.4$ Hz, 2H), 0.97 (t, $J = 8.4$ Hz, 2H), -0.01 (s, 9H).

^{13}C NMR (75 MHz, CDCl_3): δ 150.8, 149.7, 149.2, 148.7, 146.5, 139.5, 137.6, 135.2, 131.9,

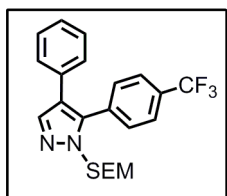
130.3, 128.9, 128.7, 127.4, 125.5, 123.2, 123.0, 121.6, 78.2, 67.1, 17.9, -1.4. MS (LR-APCI): calculated for $C_{25}H_{28}N_4OSi$: 428.2, measured 429.2 ($M+H$)⁺.



5-(3-Ethoxycarbonylphenyl)-4-phenyl-1-((2-(trimethylsilyl)ethoxy)

methyl)-1H-pyrazole (9): Yellow, viscous oil; 82% yield, isolated with flash chromatography with a gradient of 0% to 10% EtOAc in hexanes. ¹H

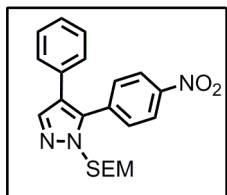
NMR (300 MHz, CDCl₃): δ 8.16 (t, *J* = 1.5 Hz, 1H), 8.10 (dt, *J*₁ = 7.8 Hz, *J*₂ = 1.5 Hz, 1H), 7.79 (s, 1H), 7.57 (dt, *J*₁ = 7.8 Hz, *J*₂ = 1.5 Hz, 1H), 7.48 (td, *J*₁ = 7.5 Hz, *J*₂ = 0.3 Hz, 1H), 7.15 – 7.23 (m, 5 H), 5.33 (s, 2H), 4.36 (q, *J* = 7.0 Hz, 2H), 3.67 (t, *J* = 8.2 Hz, 2H), 1.36 (t, *J* = 7.0 Hz, 3H), 0.94 (t, *J* = 8.2 Hz, 2H), -0.01 (s, 9H). ¹³C NMR (75 MHz, CDCl₃): δ 166.0, 139.4, 138.7, 134.8, 132.5, 131.5, 131.1, 130.2, 130.0, 128.5, 127.7, 126.5, 122.3, 78.0, 66.7, 61.2, 17.9, 14.2, -1.5. MS (LR-APCI): calculated for $C_{24}H_{30}N_2O_3Si$: 422.2, measured 423.6 ($M+H$)⁺.



4-Phenyl-5-(4-(trifluoromethyl)phenyl)-1-((2-(trimethylsilyl)ethoxy)

methyl)-1H-pyrazole (10): Pale yellow, viscous oil; 74 % yield, isolated via flash chromatography with a gradient from 100% hexanes to 10% EtOAc

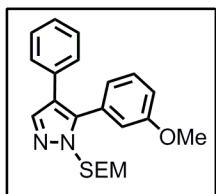
in hexanes as the eluent. ¹H NMR (400 MHz, CDCl₃): δ 7.77 (s, 1H), 7.66 (d, *J* = 8.2 Hz, 2H), 7.58 (d, *J* = 8.2 Hz, 2H), 7.16 – 7.26 (m, 5H), 5.34 (s, 2H), 3.74 (t, *J* = 8.2 Hz, 2H), 0.95 (t, *J* = 8.2 Hz, 2H), 0.00 (s, 9H). ¹³C NMR (75 MHz, CDCl₃): δ 138.9, 133.5, 132.3, 130.8, 128.6, 127.9, 126.7, 125.7, 125.6, 122.7, 78.1, 67.0, 18.0, -1.4. MS (LR-APCI): calculated for $C_{22}H_{25}F_3N_2OSi$: 418.2, measured 419.7 ($M+H$)⁺.



5-(4-Nitrophenyl)-4-phenyl-1-((2-(trimethylsilyl)ethoxy)methyl)-1H-

pyrazole (11): Dense, yellow oil; 58% yield. Flash chromatography on silica with 10% EtOAc in hexanes as the eluent provided material of 60-90%

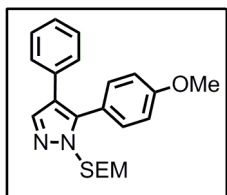
purity. For characterization, this material was further purified by preparative RP-HPLC using the conditions previously described, retention time 13.12 min. ^1H NMR (400 MHz, CDCl_3): δ 8.26 (d, $J = 9.0$ Hz, 2H), 7.76 (s, 1H), 7.66 (d, $J = 9.0$ Hz, 2H), 7.23 – 7.27 (m, 3H), 7.14 – 7.17 (m, 2H), 5.36 (s, 2H), 3.77 (t, $J = 8.3$ Hz, 2H), 0.97 (t, $J = 8.3$ Hz, 2H), 0.01 (s, 9H). ^{13}C NMR (75 MHz, CDCl_3): δ 147.8, 139.0, 138.0, 136.3, 132.0, 131.4, 128.7, 128.0, 127.0, 123.9, 123.4, 78.2, 67.2, 18.0, -1.4. MS (LR-APCI): calculated for $\text{C}_{21}\text{H}_{25}\text{N}_3\text{O}_3\text{Si}$: 395.2, measured 396.4 ($\text{M}+\text{H}$) $^+$.



5-(3-Methoxyphenyl)-4-phenyl-1-((2-(trimethylsilyl)ethoxy)methyl)-1H-

pyrazole (12): Yellow, viscous oil; 76% yield. Isolated via flash chromatography with 5% EtOAc in hexanes as the eluent. ^1H NMR (400

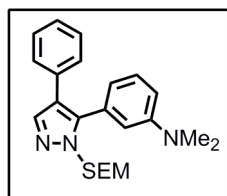
MHz, CDCl_3): δ 7.81 (s, 1H), 7.33 (m, 2H), 7.29 (m, 1H), 7.22 – 7.26 (m, 3H), 6.98 – 7.05 (m, 3H), 5.39 (s, 2H), 3.78 (s, 3H), 3.72 (t, $J = 8.3$ Hz, 2H), 0.98 (t, $J = 8.3$ Hz, 2H), 0.03 (s, 9H). ^{13}C NMR (75 MHz, CDCl_3): δ 159.6, 140.2, 138.6, 132.7, 130.9, 129.7, 128.4, 127.6, 126.3, 122.7, 121.7, 115.6, 114.7, 77.8, 66.7, 55.1, 17.9, -1.5. MS (LR-APCI): calculated for $\text{C}_{22}\text{H}_{28}\text{N}_2\text{O}_2\text{Si}$: 380.2, measured 381.2 ($\text{M}+\text{H}$) $^+$.



5-(4-Methoxyphenyl)-4-phenyl-1-((2-(trimethylsilyl)ethoxy)methyl)-1H-

pyrazole (13): 35% yield. Flash chromatography on silica with 5% EtOAc in hexanes as the eluent provided material of ~80% purity. For

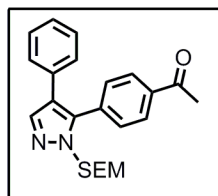
characterization, this material was further purified by RP-HPLC using conditions previously described. ^1H NMR (400 MHz, CDCl_3): δ 7.76 (s, 1H), 7.35 (d, J = 8.8 Hz, 2H), 7.22 – 7.34 (m, 5H), 6.94 (d, J = 8.8 Hz, 2H), 5.32 (s, 2H), 3.85 (s, 3H), 3.70 (t, J = 8.2 Hz, 2H), 0.94 (t, J = 8.2 Hz, 2H), 0.00 (s, 9H). ^{13}C NMR (75 MHz, CDCl_3): δ 159.9, 140.3, 138.6, 133.0, 131.7, 128.4, 127.6, 126.2, 121.9, 121.5, 114.2, 77.8, 66.7, 55.3, 18.0, -1.4. MS (LR-APCI): calculated for $\text{C}_{22}\text{H}_{28}\text{N}_2\text{O}_2\text{Si}$: 380.2, measured 381.2 ($\text{M}+\text{H}$) $^+$.



5-(3-Dimethylaminophenyl)-4-phenyl-1-((2-(trimethylsilyl)ethoxy)methyl)-1H-pyrazole (14):

Light yellow, viscous oil; 74% yield, isolated via flash chromatography with a gradient from 50:50 hexanes: CH_2Cl_2 to

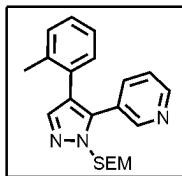
100% CH_2Cl_2 to 1% MeOH in CH_2Cl_2 as the eluent. ^1H NMR (400 MHz, CDCl_3): δ 7.79 (s, 1H), 7.16 – 7.28 (m, 6H), 6.73 – 6.78 (m, 3H), 5.36 (s, 2H), 3.69 (t, J = 8.4 Hz, 2H), 2.90 (s, 6H), 0.93 (t, J = 8.4 Hz, 2H), 0.00 (s, 9H). ^{13}C NMR (75 MHz, CDCl_3): δ 150.4, 141.4, 138.6, 133.0, 130.3, 129.3, 128.3, 127.6, 126.1, 121.3, 118.3, 114.4, 112.6, 77.8, 66.7, 40.4, 18.0, -1.5. MS (LR-APCI): calculated for $\text{C}_{23}\text{H}_{31}\text{N}_3\text{OSi}$: 393.2, measured 394.4 ($\text{M}+\text{H}$) $^+$.



4-Phenyl-5-(4-phenyl ethanone)-1-((2-(trimethylsilyl)ethoxy)methyl)-1H-pyrazole (15):

58% yield; isolated via flash chromatography with 10% EtOAc in hexanes as the eluent. ^1H NMR (400 MHz, CDCl_3): δ 7.99 (d, J =

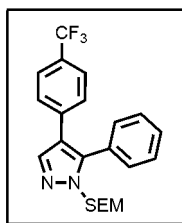
8.4 Hz, 2H), 7.77 (s, 1H), 7.55 (d, J = 8.4 Hz, 2H), 7.16 – 7.26 (m, 5H), 5.34 (s, 2H), 3.73 (t, J = 8.4 Hz, 2H), 2.63 (s, 3H), 0.95 (t, J = 8.4 Hz, 2H), -0.00 (s, 9H). ^{13}C NMR (75 MHz, CDCl_3): δ 197.5, 139.2, 138.9, 137.0, 134.5, 132.4, 130.7, 128.6, 127.8, 126.6, 122.6, 78.1, 67.0, 26.6, 17.9, -1.43.



5-(3-pyridyl)-4-(o-tolyl)-1-((2-(trimethylsilyl)ethoxy)methyl)-1H-pyrazole

(16): 79% colorless oil; isolated by flash chromatography with 4% EtOAc in hexanes as the eluent. ^1H NMR (400 MHz, CDCl_3): δ 8.54 (d, J = Hz, 2H),

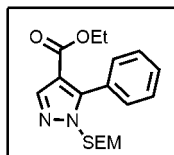
7.71 (dt, J_1 = 8.0 Hz, J_2 = 1.8 Hz, 1H), 7.26 (s, 1H), 7.24 (dd, J_1 = 7.8 Hz, J_2 = 5.0 Hz, 1H), 7.14 – 7.15 (m, 2H), 7.04 – 7.10 (m, 2H), 5.40 (s, 2H), 3.76 (t, J = 8.2 Hz, 2H), 2.03 (s, 3H), 0.95 (t, J = 8.2 Hz, 2H), -0.01 (s, 9H). ^{13}C NMR (100 MHz, CDCl_3): δ 150.2, 149.3, 139.9, 137.8, 136.8, 136.5, 131.6, 130.8, 130.2, 127.5, 126.0, 125.7, 123.2, 122.4, 78.2, 66.9, 20.2, 17.8, -1.51. MS (LR-APCI): calculated for $\text{C}_{22}\text{H}_{28}\text{N}_2\text{OSi}$: 365.2, measured 366.0 ($\text{M}+\text{H}$) $^+$.



5-Phenyl-4-(4-(trifluoromethyl)phenyl)-1-((2-

(trimethylsilyl)ethoxy)methyl)-1H-pyrazole (17): 69 % yield. Isolated by flash chromatography using 5% EtOAc:hexanes as the eluent. ^1H NMR (400 MHz, CDCl_3): δ 7.81 (s, 1H), 7.38 – 7.46 (m, 7H), 7.27 (d, J = 8.1 Hz, 2H),

5.33 (s, 2H), 3.69 (t, J = 8.4 Hz, 2H), 0.93 (t, J = 8.4 Hz, 2H), -0.01 (s, 9H). ^{13}C NMR (75 MHz, CDCl_3): δ 141.1, 138.6, 136.6, 130.4, 128.3, 129.2, 128.9, 127.6, 125.4, 125.36, 120.5, 77.9, 66.9, 17.9, -1.44. MS (LR-APCI): calculated for $\text{C}_{22}\text{H}_{25}\text{F}_3\text{N}_2\text{OSi}$: 418.2, measured 419.5 ($\text{M}+\text{H}$) $^+$.



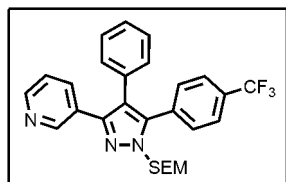
4-Ethoxycarbonyl-5-phenyl-1-((2-(trimethylsilyl)ethoxy)methyl)-1H-

pyrazole (18): 75% yield of colorless oil; isolated by flash chromatography with 10% EtOAc in hexanes as the eluent. ^1H NMR (400 MHz, CDCl_3):

δ 8.03 (s, 1H), 7.44 – 7.52 (m, 5H), 5.27 (s, 2H), 4.17 (q, J = 7.2 Hz, 2H), 3.65 (t, J = 8.2 Hz,

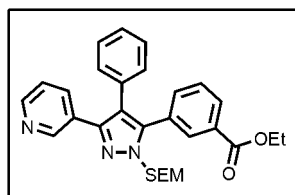
2H), 1.18 (t, $J = 7.2$ Hz, 3H), 0.89 (t, $J = 8.2$ Hz, 2H), -0.02 (s, 9H). ^{13}C NMR (75 MHz, CDCl_3): δ 162.9, 147.0, 141.7, 130.4, 129.5, 128.3, 128.0, 113.5, 77.9, 67.2, 60.0, 17.9, 14.1, -1.46. MS (LR-APCI): calculated for $\text{C}_{18}\text{H}_{26}\text{N}_2\text{O}_3\text{Si}$: 346.2, measured 347.4 ($\text{M}+\text{H}$) $^+$.

IV.4 Triarylated Pyrazoles



5-(4-(Trifluoromethyl)phenyl)-4-phenyl-3-(3-pyridyl)-1-((2-(trimethylsilyl)ethoxy)methyl)-1H-pyrazole (23): White solid, 77% yield, isolated via flash chromatography with a gradient of 10% to 25%

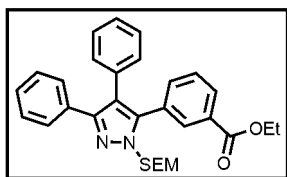
EtOAc in hexanes. ^1H NMR (400 MHz, CDCl_3): δ 8.75 (m, 1H), 8.50 (m, 1H), 7.73 (dt, $J_1 = 8.0$ Hz, $J_2 = 1.8$ Hz, 1H), 7.60 (d, $J = 8.4$ Hz, 2H), 7.51 (d, $J = 8.4$ Hz, 2H), 7.23 (m, 3H), 7.19 (dd, $J_1 = 7.6$ Hz, $J_2 = 5.2$ Hz, 1H), 7.05 (m, 2H), 5.42 (s, 2H), 3.82 (t, $J = 8.4$ Hz, 2H), 0.98 (t, $J = 8.4$ Hz, 2H), -0.01 (s, 9H). ^{13}C NMR: δ 149.2, 148.7, 146.5, 141.4, 135.2, 132.9, 132.0, 130.6, 130.6 (q, $J = 32.5$ Hz), 130.3, 129.0, 128.7, 127.3, 125.4, 123.0, 121.1, 78.2, 67.2, 17.9, -1.5. MS (LR-APCI): calculated for $\text{C}_{27}\text{H}_{28}\text{F}_3\text{N}_3\text{OSi}$: 495.2, measured 496.2 ($\text{M}+\text{H}$) $^+$.



5-(3-Ethoxycarbonylphenyl)-3-(3-pyridyl)-4-phenyl-1-((2-(trimethylsilyl)ethoxy)methyl)-1H-pyrazole (25): 88% yield. ^1H NMR (400 MHz, CDCl_3): δ 8.75 (m, 1H), 8.50 (m, 1H), 8.11 (s, 1H),

8.03 (d, $J = 8.0$ Hz, 1H), 7.75 (d, $J = 8.0$ Hz, 1H), 7.50 (d, $J = 8.0$ Hz, 1H), 7.41 (t, $J = 8.0$ Hz, 1H), 7.19 (m, 4H), 7.05 (m, 2H), 5.42 (s, 2H), 4.34 (q, $J = 7.2$ Hz, 2H), 3.76 (t, $J = 8.2$ Hz, 2H), 1.35 (t, $J = 7.2$ Hz, 3H), 0.98 (t, $J = 8.2$ Hz, 2H), -0.01 (s, 9H).

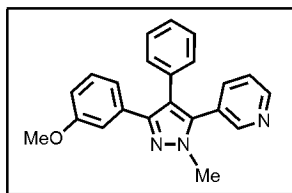
^{13}C NMR: δ 165.9, 149.3, 148.6, 146.4, 142.0, 135.3, 134.6, 132.2, 131.4, 130.9, 130.4, 129.8, 129.6, 129.1, 128.5, 127.1, 123.0, 121.0, 78.2, 77.0, 61.1, 17.9, 14.2, -1.45. MS (LR-APCI): calculated for $\text{C}_{29}\text{H}_{33}\text{N}_3\text{O}_3\text{Si}$: 498.2, measured 499.4 ($\text{M}+\text{H}$) $^+$.



5-(3-Ethoxycarbonylphenyl)-3,4-di-phenyl-1-((2-trimethylsilyl)

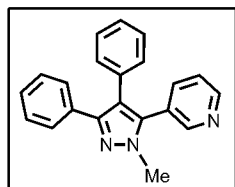
ethoxy) methyl)-1H-pyrazole (26): Yellow-white solid; 64% yield, isolated via flash chromatography with 20% EtOAc in hexanes as the

eluent. ^1H NMR (400 MHz, CDCl_3): δ 8.11 (t, $J = 1.6$ Hz, 1H), 8.01 (dt, $J_1 = 8.0$ Hz, $J_2 = 1.6$ Hz, 1H), 7.37 – 7.49 (m, 5H), 7.26 (m, 2H), 7.18 (m, 3H), 7.05 (m, 2H), 5.41 (s, 2H), 4.33 (q, $J = 7.2$ Hz, 2H), 3.74 (t, $J = 8.4$ Hz, 2H), 1.36 (t, $J = 7.2$ Hz, 3H), 0.96 (t, $J = 8.4$ Hz, 2H), -0.01 (s, 9H). ^{13}C NMR (75 MHz, CDCl_3): δ 166.0, 149.4, 141.7, 134.7, 133.2, 132.9, 131.5, 130.8, 130.5, 130.0, 129.6, 128.5, 128.3, 128.2, 128.1, 127.6, 126.7, 120.6, 78.1, 66.8, 61.1, 17.9, 14.3, -1.4. MS (LR-APCI): calculated for $\text{C}_{30}\text{H}_{34}\text{N}_2\text{O}_3\text{Si}$: 497.2, measured 498.4 ($\text{M}+\text{H}$) $^+$.



3-(3-Methoxyphenyl)-1-methyl-4-phenyl-1H-pyrazole (27): White solid; 75% yield, isolated via flash chromatography with a gradient of 0% to 1% MeOH: CH_2Cl_2 , and further purified by recrystallization from

methanol. ^1H NMR (400 MHz, CDCl_3): δ 8.59 (dd, $J_1 = 3.3$ Hz, $J_2 = 1.5$ Hz, 1H), 8.56 (d, $J = 1.5$, 1H), 7.52 (dt, $J_1 = 7.8$ Hz, $J_2 = 1.8$ Hz, 1H), 7.27 (m, 1H), 7.17 (m, 1H), 7.03 (m, 3H), 6.99 (s, 1H), 6.79 (d, $J = 8.1$ Hz, 1H), 3.90 (s, 3H), 3.64 (s, 3H). ^{13}C NMR (75 MHz, CDCl_3): δ 159.4, 150.6, 149.6, 148.5, 138.8, 137.4, 134.3, 132.8, 130.5, 129.2, 128.4, 126.9, 126.3, 123.3, 120.4, 120.3, 114.1, 112.7, 55.0, 37.5. MS (LR-APCI): calculated for $\text{C}_{22}\text{H}_{19}\text{N}_3\text{O}$: 341.2, measured 342.2 ($\text{M}+\text{H}$) $^+$.



1-Methyl-3,4-di-phenyl-5-(3-pyridyl)-1H-pyrazole (28): 67% yield,

isolated via flash chromatography with a gradient from 5% to 20% EtOAc

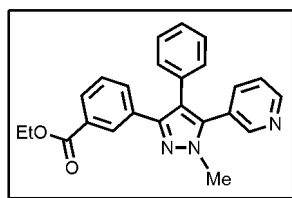
in hexanes as the eluent. ^1H NMR (300 MHz, CDCl_3): δ 8.58 (d, $J = 9.3$

Hz, 2H), 7.53 (dt, $J = 7.8$ Hz, 1H), 7.45 – 7.48 (m, 2H), 7.26 – 7.29 (m, 4H), 7.18 – 7.20 (m,

3H), 7.03 – 7.06 (m, 2H), 3.91 (s, 3H). ^{13}C NMR (75 MHz, CDCl_3): δ 150.6, 149.6, 148.7,

138.8, 137.4, 133.0, 132.7, 130.4, 128.4, 128.2, 128.0, 127.5, 126.8, 126.4, 123.3, 120.2, 37.5.

MS (LR-APCI): calculated for $\text{C}_{21}\text{H}_{17}\text{N}_3$: 310.2, measured 311.7 ($\text{M}+\text{H}$) $^+$.



3-(3-Ethoxycarbonylphenyl)-1-methyl-4-phenyl-5-(3-pyridyl)-1H-

pyrazole (29): 53 % yield, isolated via flash chromatography with a

gradient from 10% to 80% EtOAc in hexanes as the eluent. ^1H NMR

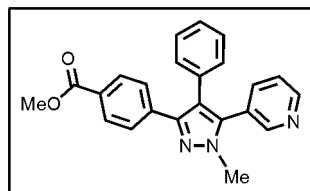
(400 MHz, CDCl_3): δ 8.60 (d, $J = 8.0$ Hz, 1H), 8.18 (s, 1H), 7.93 (d, $J = 8.0$ Hz, 1H), 7.59 (d, J

= Hz, 1H), 4.29 (q, $J = 7.0$ Hz, 2H), 3.90 (s, 3H), 1.30 (t, $J = 7.0$ Hz, 3H). ^{13}C NMR (75 MHz,

CDCl_3): δ 166.4, 150.6, 149.7, 147.8, 139.0, 137.4, 133.4, 132.4, 132.2, 130.7, 130.4, 129.0,

128.6, 128.5, 128.2, 127.0, 123.4, 120.5, 60.8, 37.6, 14.2. MS (LR-APCI): calculated for

$\text{C}_{24}\text{H}_{21}\text{N}_3\text{O}_2$: 383.2, measured 384.3 ($\text{M}+\text{H}$) $^+$.



1-Methyl-3-(4-methoxycarbonylphenyl)-4-phenyl-5-(3-pyridyl)-

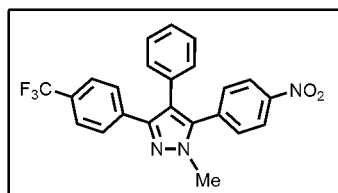
1H-pyrazole (30): 54% yield, isolated via flash chromatography

with a gradient from 100% hexanes to 30% EtOAc:hexanes to remove

impurities, then a gradient from 50% to 100% EtOAc:hexanes to elute the compound. ^1H NMR

(400 MHz, CDCl_3): δ 8.62 (d, $J = 3.6$ Hz, 1H), 8.56 (s, 1H), 8.56 (d, $J = 6.8$ Hz, 2H), 7.53 (m,

3H), 7.31 (dd, $J_1 = 8.0$ Hz, $J_2 = 5.2$ Hz, 1H), 7.21 (m, 3H), 7.02 (m 2H), 3.93 (s, 3H), 3.89 (t, 3H). ^{13}C NMR (75 MHz, CDCl_3): δ 167.0, 150.6, 149.8, 147.6, 139.2, 137.6, 137.5, 132.4, 130.3, 129.6, 129.0, 128.6, 127.8, 127.1, 126.1, 123.4, 120.8, 52.0, 37.7. MS (LR-APCI): calculated for $\text{C}_{23}\text{H}_{19}\text{N}_3\text{O}_2$: 369.2, measured 370.3 ($\text{M}+\text{H}$) $^+$.



1-Methyl-5-(4-nitrophenyl)-4-phenyl-3-(4-

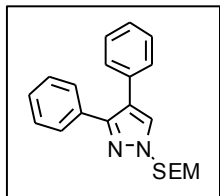
(trifluoromethyl)phenyl)-1H-pyrazole (31): Pale yellow-white solid; 43% yield, isolated via flash chromatography with 10%

EtOAc in hexanes as the eluent. ^1H NMR (400 MHz, CDCl_3): δ 8.24 (d, $J = 7.0$ Hz, 2H), 7.57 (d, $J = 8.4$ Hz, 2H), 7.52 (d, $J = 8.4$ Hz, 2H), 7.41 (d, $J = 7.0$ Hz, 2H), 7.24 – 7.26 (m, 3H), 7.01 – 7.04 (m, 2H), 3.94 (s, 3H). ^{13}C NMR (75 MHz, CDCl_3): δ 147.7, 147.3, 140.2, 136.4, 136.2, 132.1, 131.0, 130.3, 128.7, 128.0, 127.4, 125.2, 125.18, 123.8, 120.7, 115.6, 37.8. MS (LR-APCI): calculated for $\text{C}_{23}\text{H}_{16}\text{F}_3\text{N}_3\text{O}_2$: 423.1, measured 423.7 ($\text{M}+\text{H}$) $^+$.

IV.5 Procedure for SEM-switch

The substrate (**17**, 69.3 mg, 0.20 mmol) was weighed into an oven-dried vial and placed under argon, capped with a Teflon septum cap, and dissolved by stirring in 0.15 mL acetonitrile (approximately 100 μL per 50 mg) injected through the septum. SEMCl (3.5 μL , 10 mol%) was added via syringe and the mixture stirred under Ar for 5 minutes before sealing the vial with a Teflon coated cap and heating to 95 $^\circ\text{C}$ for 24 hours. After 24 hours, the solvent was removed *in vacuo* and the crude material analyzed by ^1H NMR, which showed a 90% conversion between the starting material and the SEM-switched material. Flash chromatography of this mixture with

20% EtOAc:hexanes, with 2-3 times the amount of silica normally used for flash chromatography,³⁹ produced a pale yellow, viscous oil (58.2 mg, 84%).

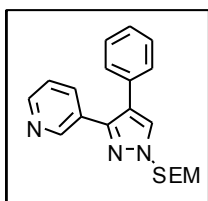


3,4-Diphenyl-1-((2-(trimethylsilyl)ethoxy)methyl)-1H-pyrazole (19):

85% conversion by ¹H NMR. Inseparable by flash chromatography and

HPLC. ¹H NMR (400 MHz, CDCl₃): δ 7.68 (s, 1H), 7.49 – 7.52 (m, 2H),

7.42 (s, 1H), 7.29 – 7.35 (m, 7H), 5.49 (s, 2H), 3.70 (t, *J* = 8.2 Hz, 2H), 0.96 (t, *J* = 8.2 Hz, 2H), - 0.00 (s, 9H).



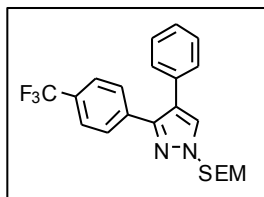
4-Phenyl-3-(3-pyridyl)-1-((2-(trimethylsilyl)ethoxy)methyl)-1H-pyrazole

(20): Synthesis and isolation described above, 84% yield. ¹H NMR (400

MHz, CDCl₃): δ 8.76 (d, *J* = 1.6 Hz, 1H), 8.53 (dd, *J*₁ = 4.8 Hz, *J*₂ = 1.6 Hz,

1H), 7.79 (dt, *J*₁ = 8.0 Hz, *J*₂ = 2 Hz, 1H), 7.69 (s, 1H), 7.21 – 7.35 (m, 6H), 5.50 (s, 2H), 3.71 (t, *J* = 8.2 Hz, 2H), 0.97 (t, *J* = 8.2 Hz, 2H), 0.01 (s, 9H). ¹³C NMR (75 MHz, CDCl₃): δ 149.3,

148.7, 146.3, 135.4, 132.4, 129.7, 129.3, 128.7, 128.6, 127.1, 123.1, 122.5, 80.5, 67.1, 17.8, - 1.43. MS (LR-APCI): calculated for C₂₀H₂₅N₃OSi: 351.2, measured 352.8 (M+H)⁺.



4-phenyl-3-(4-(trifluoromethyl)phenyl)-1-((2-(trimethylsilyl)

ethoxy)methyl)-1*H*-pyrazole (21): 91% conversion by ^1H NMR,

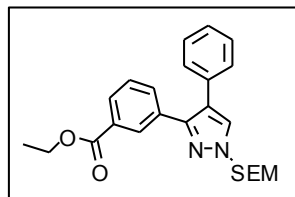
isolated 80%. ^1H NMR (400 MHz, CDCl_3): δ 7.68 (s, 1H), 7.63 (d, J =

8.2 Hz, 2H), 7.55 (d, J = 8.2 Hz, 2H), 7.26 - 7.34 (m, 5H), 5.50 (s, 2H), 3.71 (t, J = 8.2 Hz, 2H),

0.97 (t, J = 8.2 Hz, 2H), 0.01 (s, 9H). ^{13}C NMR (75 MHz, CDCl_3): δ 147.8, 136.9, 132.6,

129.8, 128.7, 128.6, 128.4, 127.1, 125.2, 125.16, 122.4, 80.5, 67.1, 17.8, -1.4. MS (LR-APCI):

calculated for $\text{C}_{22}\text{H}_{25}\text{F}_3\text{N}_2\text{OSi}$: 418.2, measured 419.3 ($\text{M}+\text{H}$) $^+$.



3-(3-Ethoxycarbonylphenyl)-4-phenyl-1-((2-(trimethylsilyl)ethoxy)

methyl)-1*H*-pyrazole (22): 90% conversion by ^1H NMR. Inseparable

by several attempts using flash chromatography and HPLC. ^1H NMR

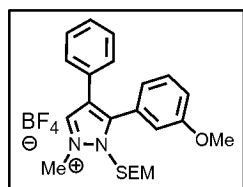
(400 MHz, CDCl_3): δ 8.23 (s, 1H), 7.96 (d, J = 8.0 Hz, 1H), 7.66 (s, 1H), 7.62 (d, J = 7.6 Hz,

1H), 7.34 (t, J = 7.6 Hz, 1H), 7.27 - 7.35 (m, 5H), 5.48 (s, 2H), 4.31 (q, J = 7.2 Hz, 2H), 3.69 (t,

J = 8.2 Hz, 2H), 1.32 (t, J = 7.2 Hz, 3H), 0.96 (t, J = 8.2 Hz, 2H), -0.01 (s, 9H).

IV.6 General Procedure for Formation of Pyrazolium Salts⁴⁰

The pyrazole (0.2 to 2 mmol) was weighed into an oven-dried flask or vial, a stir bar added, and then evacuated and flushed with Ar three times before dissolving in dry CH₂Cl₂ (0.25M), added via syringe. To this solution, trimethyloxonium tetrafluoroborate (1.2 equivalents) was rapidly added under an Ar stream after weighing in air, and the reaction mixture stirred for at least 1 hour. The solvent was removed and the crude material dried via high vacuum before verifying the presence of the product with ¹H NMR. Several of the salts are fluorescent under UV and are relatively unstable if not used within a day; store under vacuum or Ar at -2 to -8 °C if unable to proceed with the deprotection immediately.



3-(3-Methoxyphenyl)-1-methyl-4-phenyl-2-((2-(trimethylsilyl)ethoxy)

methyl)-1H-pyrazolium tetrafluoroborate (39): crude ¹H NMR (400

MHz, CDCl₃): δ 8.57 (s, 1H), 7.46 (t, *J* = 8.0 Hz, 1H), 7.26 – 7.29 (m,

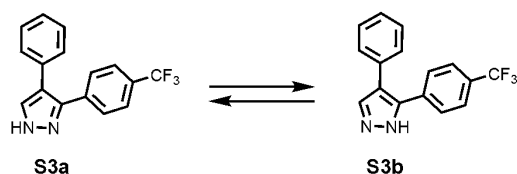
3H), 7.17 (dd, *J*₁ = 8.4 Hz, *J*₂ = 1.8 Hz, 1H), 7.01 - 7.03 (m, 3H), 5.71 (s, 2H), 4.37 (s, 3H), 3.85 (s, 3H), 3.37 (t, *J* = 8.2 Hz, 2H), 0.82 (t, *J* = 8.2 Hz, 2H), -0.02 (s, 9H).

Deprotection of SEM group from SEM-protected pyrazoles and pyrazolium salts⁴¹

The pyrazole, **23**, (30.7 mg, 0.062 mmol) was dissolved in 95% ethanol (4 mL) and 3 N HCl (1 mL) was added. The reaction mixture was refluxed for 3 hours. To quench, 10% aqueous (by weight) NaOH solution was added until the mixture was neutralized as measured with pH paper, 5 mL deionized water and 50 mL ethyl acetate added, and the layers were separated. (Alternatively, a basic work-up with saturated aqueous sodium bicarbonate added until pH is

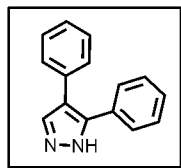
neutral is also sufficient.) After back-extraction from the aqueous layer with EtOAc (15 mL x 3), the organic fractions were combined, dried with Na₂SO₄, and the solvent removed. The crude material was purified via flash chromatography on silica gel with a gradient from 100% hexanes to 50:50 EtOAc:hexanes to produce a pale white solid (17.0 mg, 75%).

Scheme S1. Free (NH)-pyrazole tautomerism

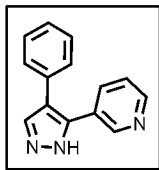


IV.7 Determination of the Tautomer Ratio for Selected Free (NH)-Pyrazoles in DMSO-*d*₆

Free (NH)-pyrazoles exist in solution as mixtures of tautomers (Scheme S1). In DMSO-*d*₆ the two NH signals are resolved in ¹H NMR (δ 13-14.5), enabling determination of the tautomer ratio. The assignment of these peaks to individual tautomers has not been carried out here. However, according to literature,⁴² the major tautomer for the diarylpyrazoles is 3,4-diaryl-1*H*-pyrazole (e.g., **S3a**)



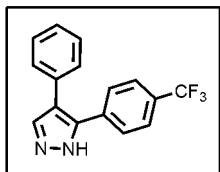
4,5-Diphenyl-1*H*-pyrazole (32): ¹H NMR (400 MHz, CDCl₃): δ 11.52 (bs, 1H), 7.63 (s, 1H), 7.46 – 7.48 (m, 2H), 7.24 – 7.34 (m, 8H). ¹H NMR (400 MHz, DMSO-*d*₆ at 298 K): δ 13.19 (bs, ~40% Pz N-H tautomer), 13.05 (bs, ~60% Pz N-H tautomer), 7.40 (bm, 3H), 7.22 – 7.33 (m, 7H). ¹³C NMR (75MHz, CDCl₃): δ 135.1, 133.1, 131.3, 128.6, 128.5, 128.4, 128.2, 128.0, 127.9, 126.6. MS (LR-APCI): calculated for C₁₅H₁₂N₂: 220.1, measured 221.0 (M+H)⁺.



4-Phenyl-5-(3-pyridyl)-1H-pyrazole (33): ^1H NMR (400 MHz, CDCl_3):

δ 12.93 (bs, 1H), 8.80 (bs, 1H), 8.56 (bs, 1H), 7.71 (d, $J = 8.1$ Hz, 1H), 7.68 (s, 1H), 7.21 – 7.34 (m, 5H). ^{13}C NMR (75 MHz, CDCl_3): δ 148.9, 148.8, 143.0,

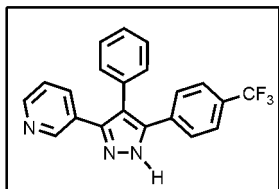
135.6, 132.5, 132.3, 128.7, 128.5, 127.0, 123.3, 120.9. MS (LR-APCI): calculated for $\text{C}_{14}\text{H}_{11}\text{N}_3$: 221.1, measured 222.1 ($\text{M}+\text{H}$) $^+$.



4-Phenyl-5-(4-(trifluoromethyl)phenyl)-1H-pyrazole (34):

^1H NMR (400 MHz, CDCl_3): δ 12.2 (s, 1H), 7.65 (s, 1H), 7.56 (d, $J = 8.7$ Hz, 2H), 7.52 (d, $J = 8.7$ Hz, 2H), 7.24 – 7.35 (m, 5H). ^1H NMR (400 MHz,

$\text{DMSO}-d_6$ at 298 K): δ 13.43 (bs, 29% Pz N-H tautomer), 13.26 (71% Pz N-H tautomer), 8.01 (s, 1H), 7.69 (d, $J = 8.0$ Hz, 2H), 7.63 (d, $J = 8.0$ Hz, 2H), 7.33 – 7.37 (m, 2H), 7.26 – 7.29 (m, 3H). ^{13}C NMR (75 MHz, CDCl_3): δ 135.6, 132.5, 130.1, 129.8, 128.7, 128.6, 128.3, 127.1, 125.5, 125.46, 122.7, 120.9. MS (LR-APCI): calculated for $\text{C}_{16}\text{H}_{11}\text{F}_3\text{N}_2$: 288.1, measured 288.8 ($\text{M}+\text{H}$) $^+$.

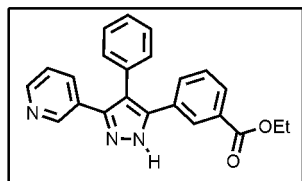


4-Phenyl-5-(4-(trifluoromethyl)phenyl)-3-(3-pyridyl)-1H-pyrazole

(24): 75% yield. ^1H NMR (400 MHz, CDCl_3): δ 8.70 (bs, 1H), 8.52 (bs, 1H), 7.61 (d, $J = 8.4$ Hz, 1H), 7.52 (d, $J = 8.4$ Hz, 2H), 7.45 (d, $J =$

8.4, 2H), 7.31 (d, $J = 3.0$ Hz, 4H), 7.11 – 7.21 (m, 5H). ^1H NMR (500 MHz, $\text{DMSO}-d_6$): δ 13.82 (bs, ~56% Pz N-H tautomer), 13.80 (~44% Pz N-H tautomer), 8.45 – 8.52 (m, 2H), 7.64 – 7.45 (m, 3H), 7.52 – 7.59 (m, 2H), 7.33 – 7.47 (m, 4H), 7.21 – 7.25 (m, 2H). ^{13}C NMR (75 MHz, CDCl_3): δ 149.0, 148.6, 135.1, 134.4, 132.1, 130.5, 129.0, 128.8, 128.6, 127.9, 127.8,

125.8, 125.6, 125.5, 123.4, 119.0. MS (LR-APCI): calculated for $C_{21}H_{14}F_3N_3$: 365.1, measured 366.4 (M+H)⁺.



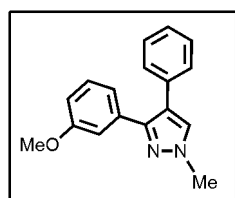
5-(3-Ethoxycarbonylphenyl)-4-phenyl-5-(3-pyridyl)-1H-pyrazole

(35): ¹H NMR (300 MHz, CDCl₃): δ 8.72 (s, 1H), 8.51 (d, *J* = 3.3 Hz, 1H), 8.12 (s, 1H), 7.95 (d, *J* = 7.5 Hz, 1H), 7.65 (d, *J* = 7.8 Hz, 1H),

7.45 (d, *J* = 7.8 Hz, 1H), 7.30 – 7.32 (m, 4H), 7.16 – 7.20 (m, 3H), 4.31 (q, *J* = 7.2 Hz, 2H), 1.32 (t, *J* = 7.2 Hz, 3H). No Pz N-H visible in CDCl₃. ¹H NMR (400 MHz, DMSO-d₆ at 298 K):

δ 14.25 (bs, ~61% N-H Pz tautomer), 14.03 (bs, ~39% N-H Pz tautomer), 8.93 – 8.95 (d, *J* = 2.0 Hz, 1H), 8.86 – 8.89 (d, *J* = 4.0 Hz, 1H), 8.40 – 8.70 (bs, 1H), 8.21 – 8.28 (d, *J* = 7.6 Hz, 1H), 8.13 (d, *J* = 8.0 Hz, 1H), 8.05 (d, *J* = 8.0 Hz, 1H), 7.23 – 7.82 (m, 4H), 7.58 – 7.65 (m, 3H), 4.65 (q, *J* = 7.2 Hz, 2H), 1.67 (t, *J* = 7.2 Hz, 3H). ¹³C NMR (75 MHz, CDCl₃): δ 166.1, 148.9, 148.7,

135.1, 132.3, 131.9, 131.2, 130.7, 130.5, 129.3, 128.9, 128.8, 128.5, 127.6, 61.2, 14.3. MS (LR-APCI): calculated for $C_{23}H_{19}N_3O_2$: 369.2, measured 370.4 (M+H)⁺.

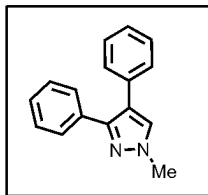


3-(3-Methoxyphenyl)-1-methyl-4-phenyl-1H-pyrazole (33): Synthesized using the procedure described above, only at room temperature in 1 hour.

75% yield over 2 steps, isolated with a gradient from 100% CH₂Cl₂ to 1%

MeOH:CH₂Cl₂. ¹H NMR (300 MHz, CDCl₃): δ 7.44 (s, 1H), 7.16 – 7.29 (m, 6H), 7.04 – 7.08 (m, 2H), 6.80 – 6.84 (ddd, *J*₁ = 8.1 Hz, *J*₂ = 2.7 Hz, *J*₃ = 0.9 Hz, 1H), 3.96 (s, 3H), 3.68 (s, 3H).

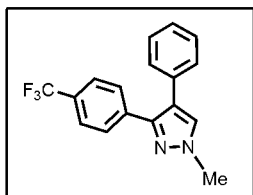
¹³C NMR (75 MHz, CDCl₃): δ 159.4, 148.6, 134.8, 133.3, 130.2, 129.2, 128.7, 128.4, 126.5, 120.9, 120.7, 113.9, 113.0, 55.1, 39.0. MS (LR-APCI): calculated for $C_{17}H_{16}N_2O$: 264.1, measured 265.3 (M+H)⁺.



1-Methyl-3,4-diphenyl-1H-pyrazole (36): Same procedure as **33**; 82% yield

over two steps. ^1H NMR (300 MHz, CDCl_3): δ 7.48 - 7.50 (m, 2H), 7.47 (s, 1H), 7.26 - 7.30 (m, 8H), 3.98 (s, 3H). ^{13}C NMR (75 MHz, CDCl_3): δ

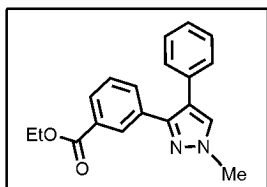
133.5, 133.3, 130.9, 130.2, 128.5, 128.4, 128.2, 127.5, 126.5, 39.0. MS (LR-APCI): calculated for $\text{C}_{16}\text{H}_{14}\text{N}_2$: 234.1, measured 234.8 (M+1).



1-Methyl-4-phenyl-3-(4-(trifluoromethyl)phenyl)-1H-pyrazole (37):

^1H NMR (400 MHz, CDCl_3): δ 7.61 (d, $J = 8.0$ Hz, 2H), 7.54 (d, $J = 8.4$ Hz, 2H), 7.48 (s, 1H), 7.24 - 7.33 (m, 5H), 4.00 (s, 3H). ^{13}C NMR (75

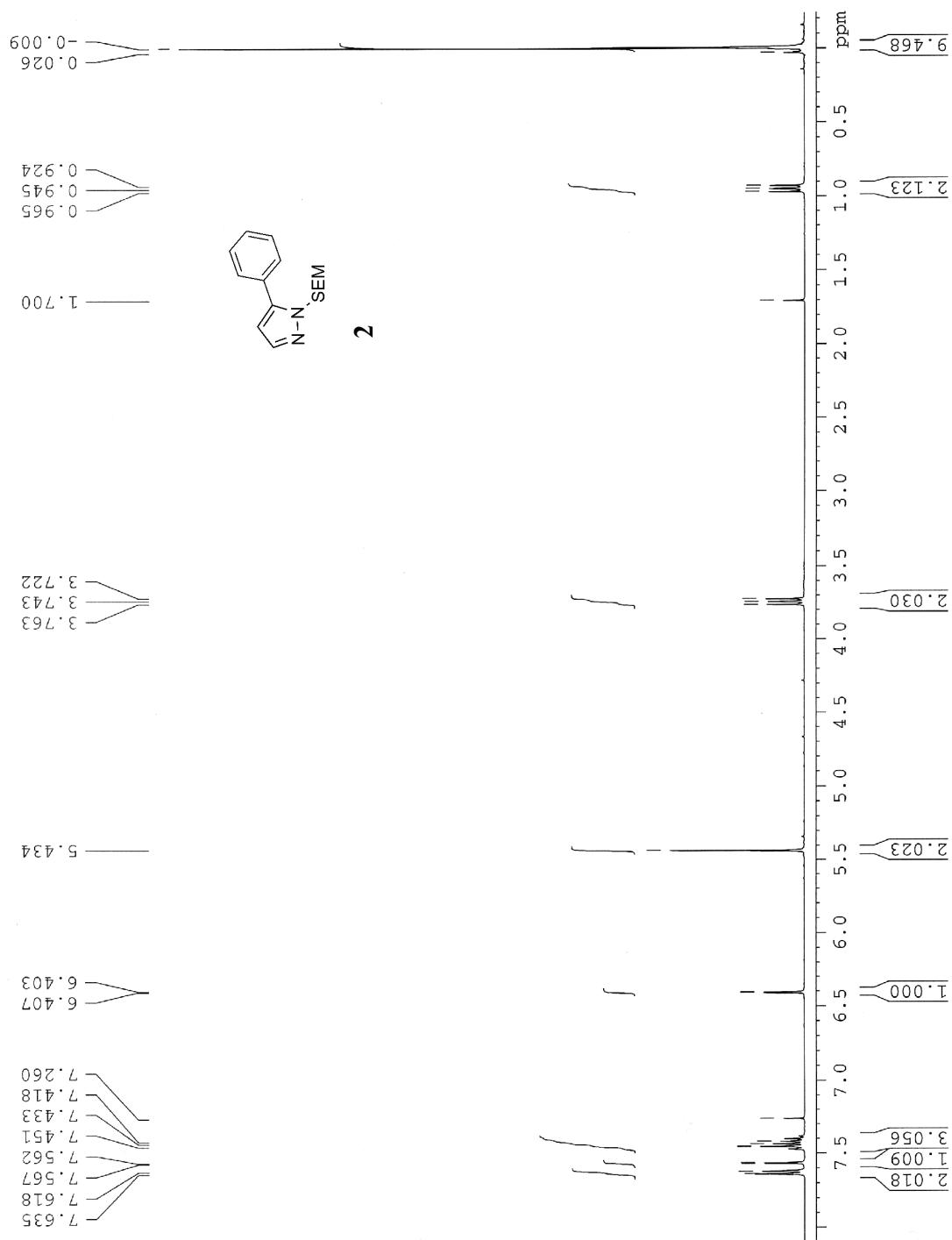
MHz, CDCl_3): δ 147.2, 137.1, 132.8, 130.6, 128.7, 128.6, 128.2, 126.9, 125.2, 125.16, 122.5, 121.4, 39.1. MS (LR-APCI): calculated for $\text{C}_{17}\text{H}_{13}\text{F}_3\text{N}_2$: 302.1, measured 302.9 (M+H) $^+$.

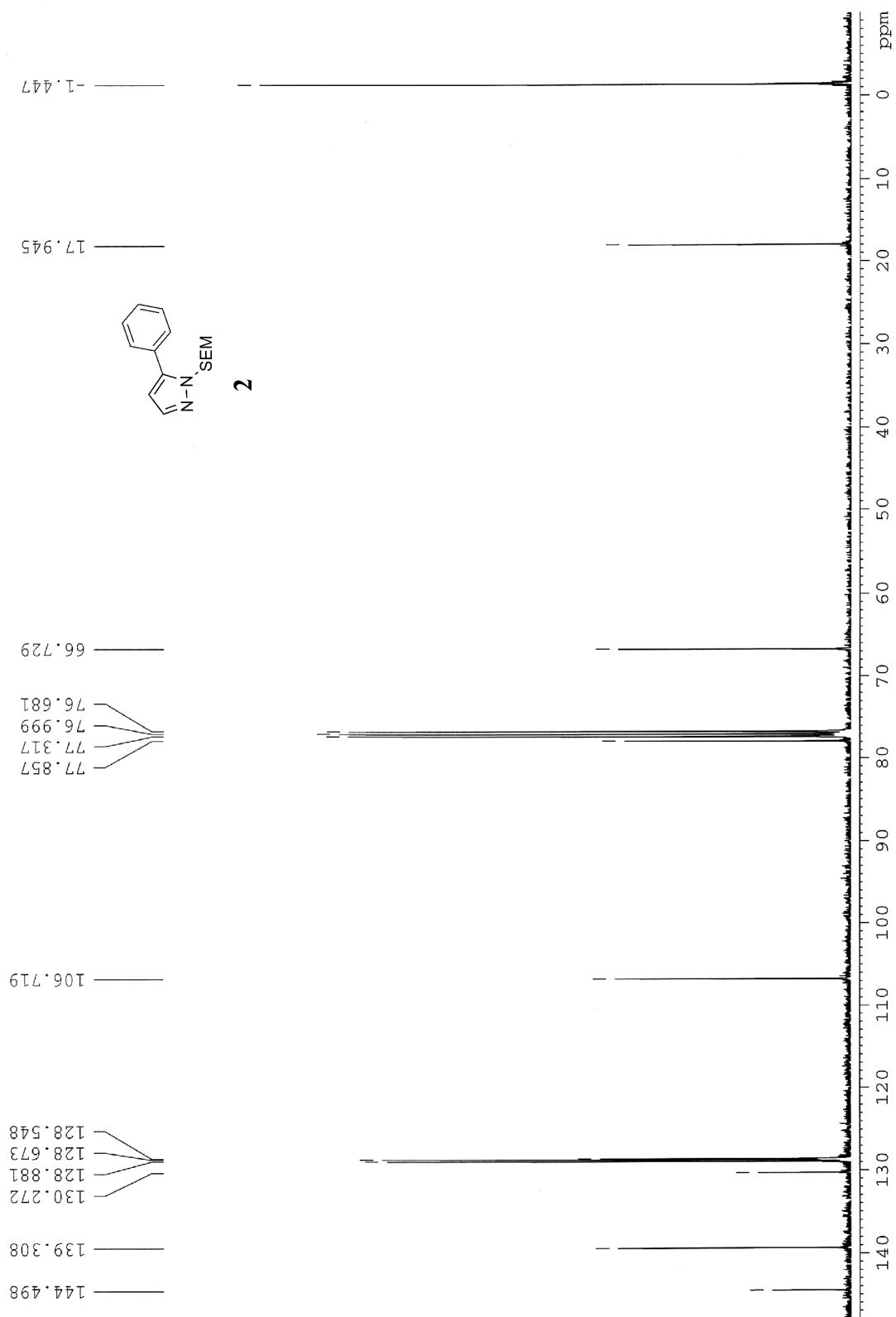


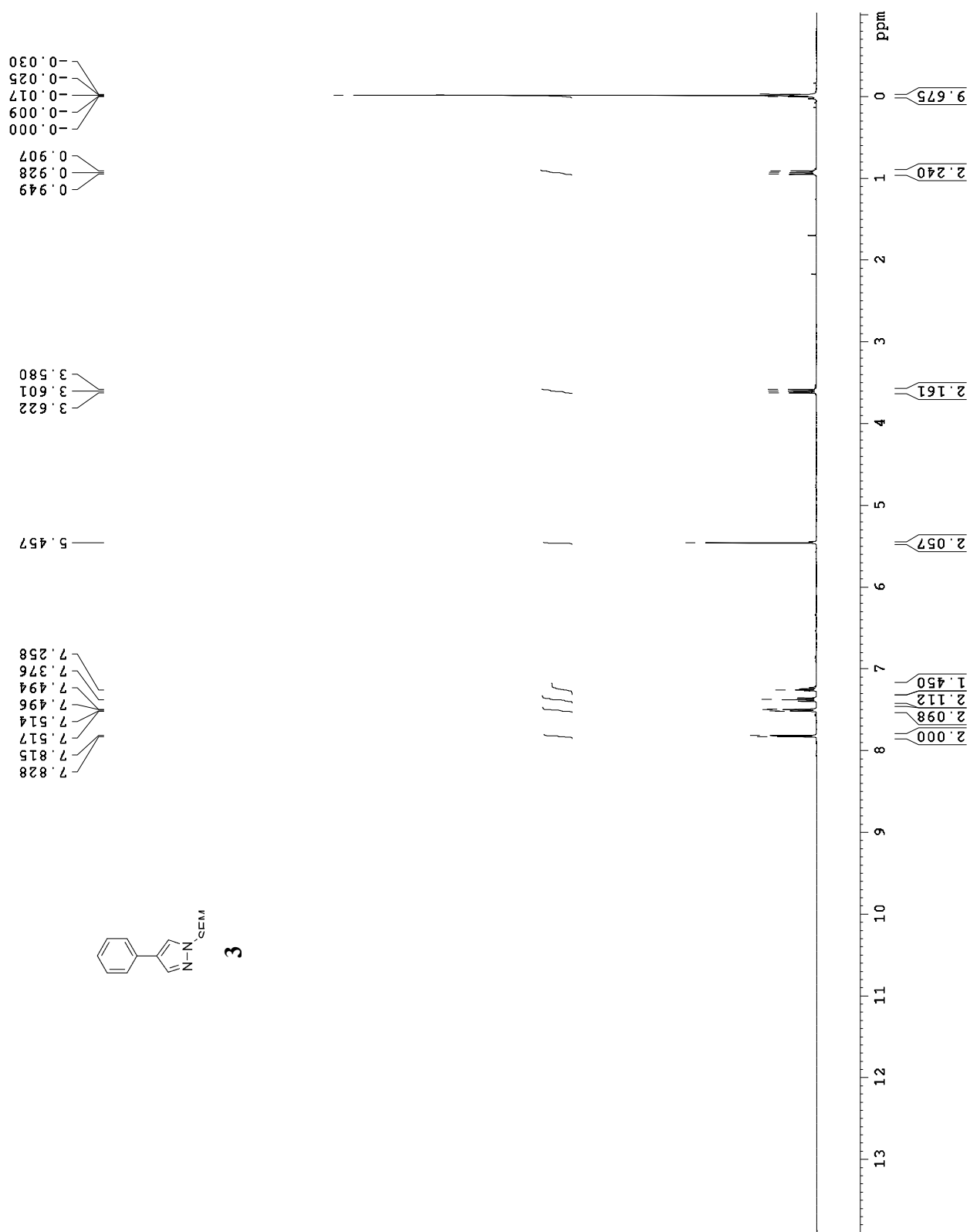
1-Methyl-3-(3-ethoxycarbonylphenyl)-4-phenyl-1H-pyrazole (38):

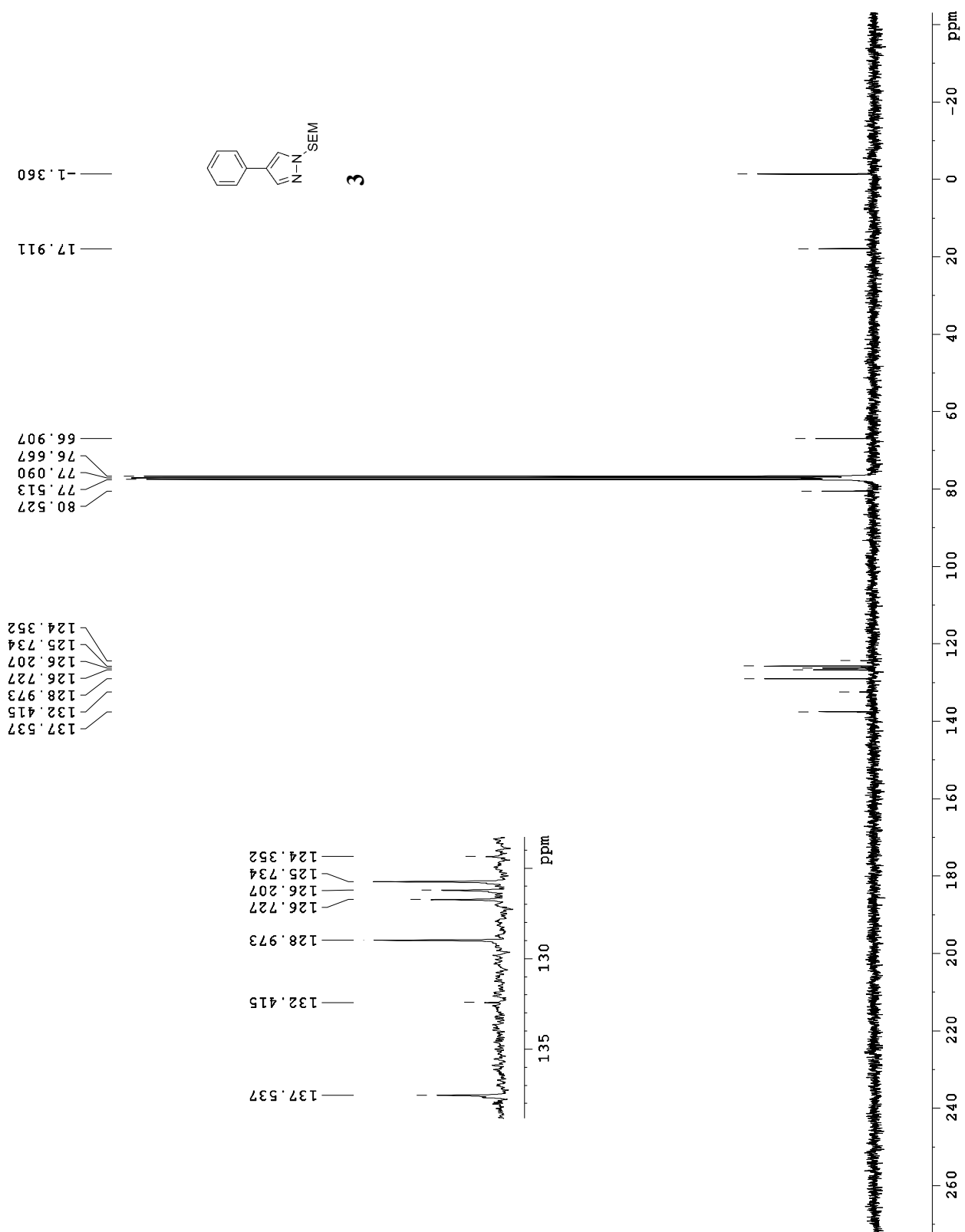
^1H NMR (400 MHz, CDCl_3): δ 8.21 (s, 1H), 7.95 (dt, $J_1 = 7.8$ Hz, $J_2 =$ 1.3 Hz, 1H), 7.62 (dt, $J_1 = 7.8$ Hz, $J_2 = 1.3$ Hz, 1H), 7.46 (s, 1H), 7.33 (t,

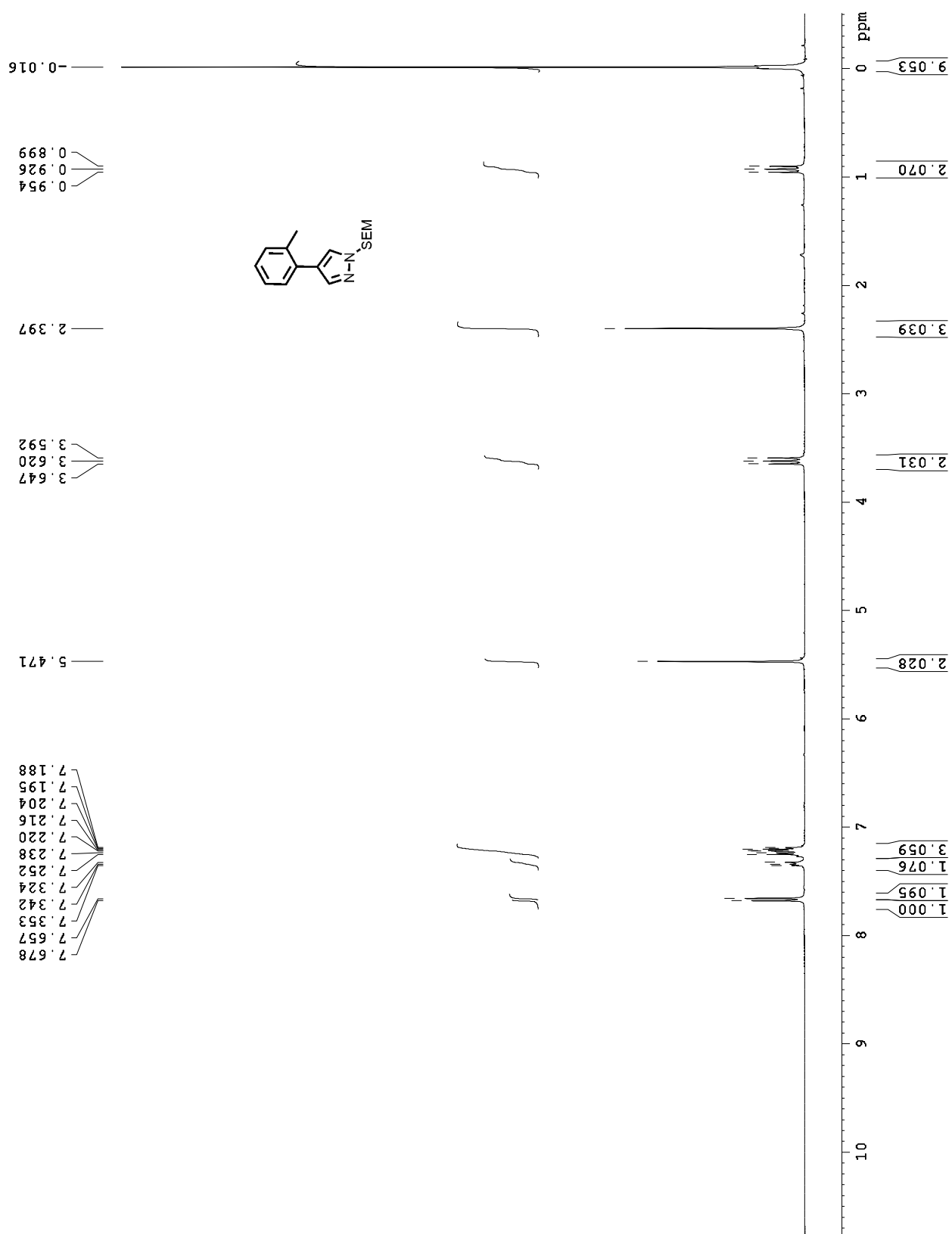
$J = 7.8$ Hz, 1H), 7.24 - 7.30 (m, 5H), 4.31 (q, $J = 7.2$ Hz, 2H), 3.98 (s, 3H), 1.32 (t, $J = 7.2$ Hz, 3H). ^{13}C NMR (75 MHz, CDCl_3): δ 166.7, 147.8, 133.8, 133.0, 132.5, 130.7, 130.3, 129.2, 128.6, 128.5, 128.2, 126.7, 121.1, 60.8, 39.1, 14.3, -0.018. MS (LR-APCI): calculated for $\text{C}_{17}\text{H}_{13}\text{F}_3\text{N}_2$: 306.1, measured 307.3 (M+H) $^+$.

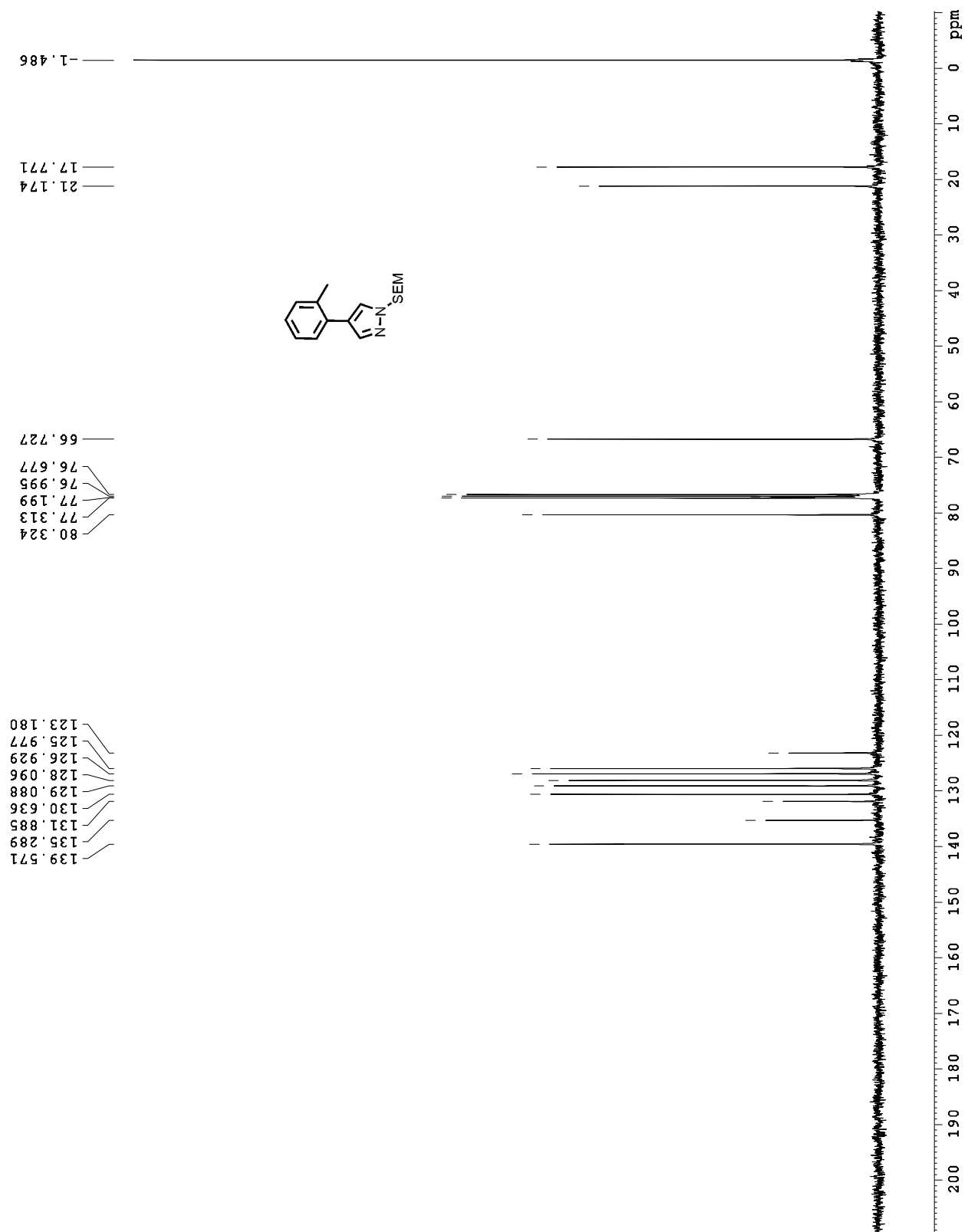


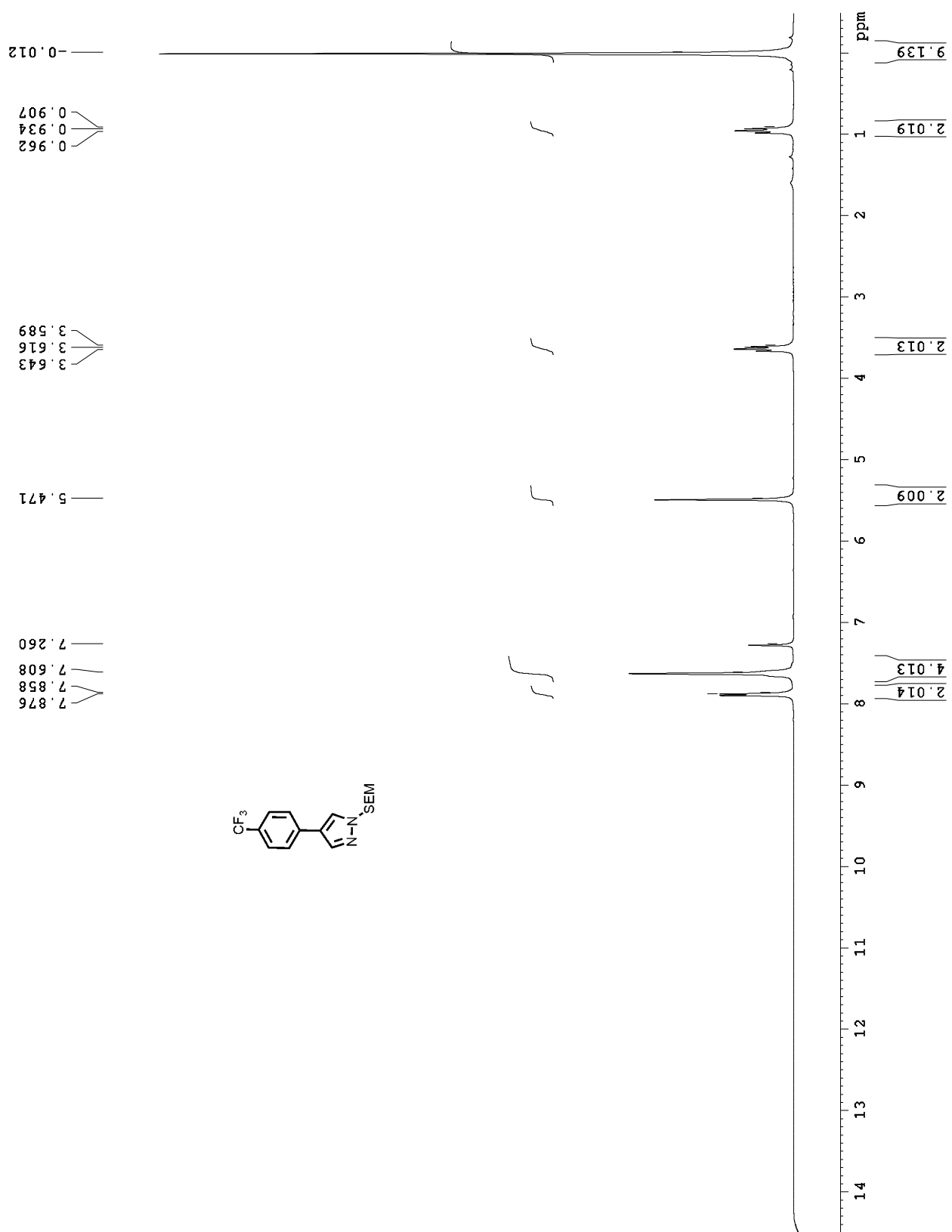


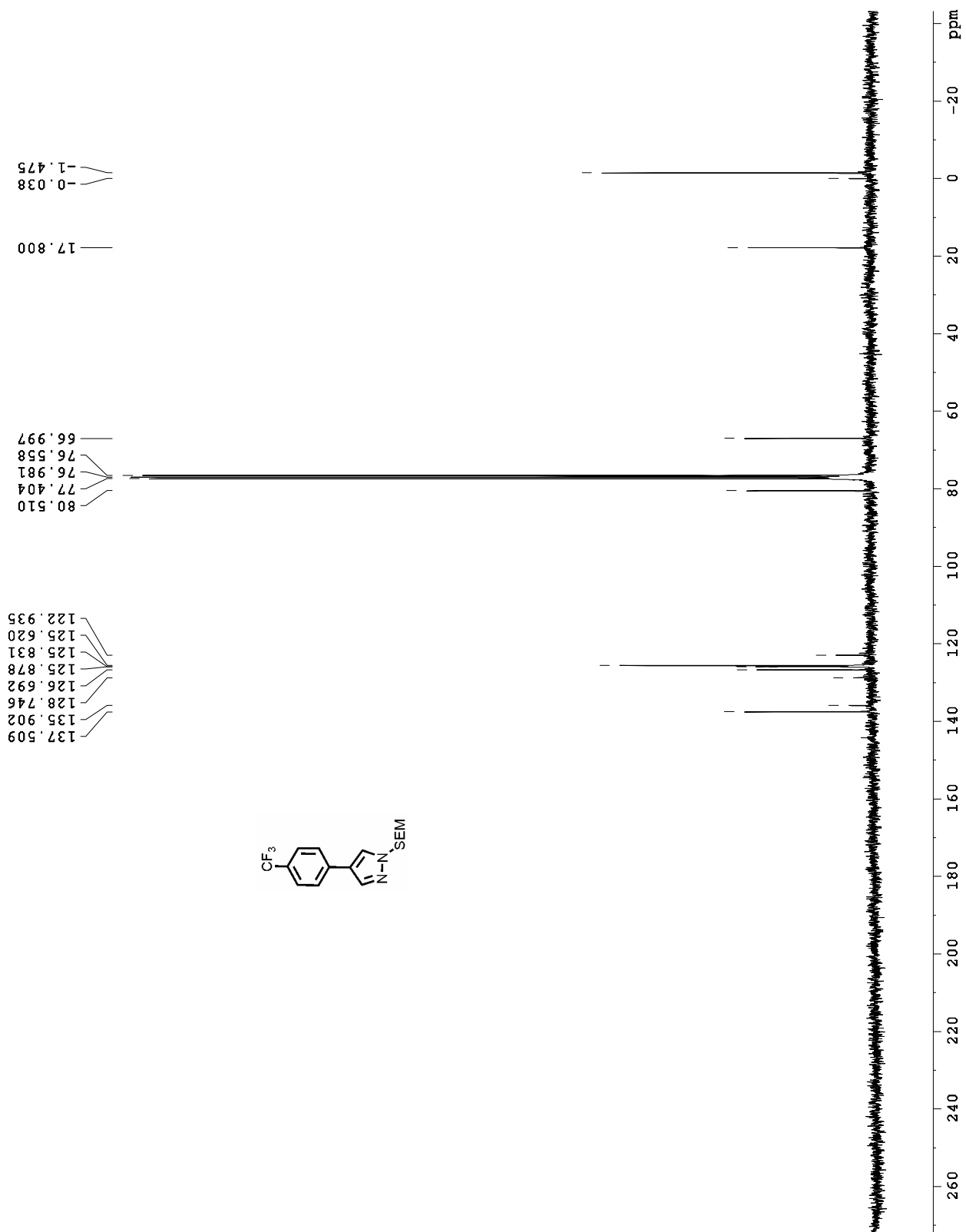


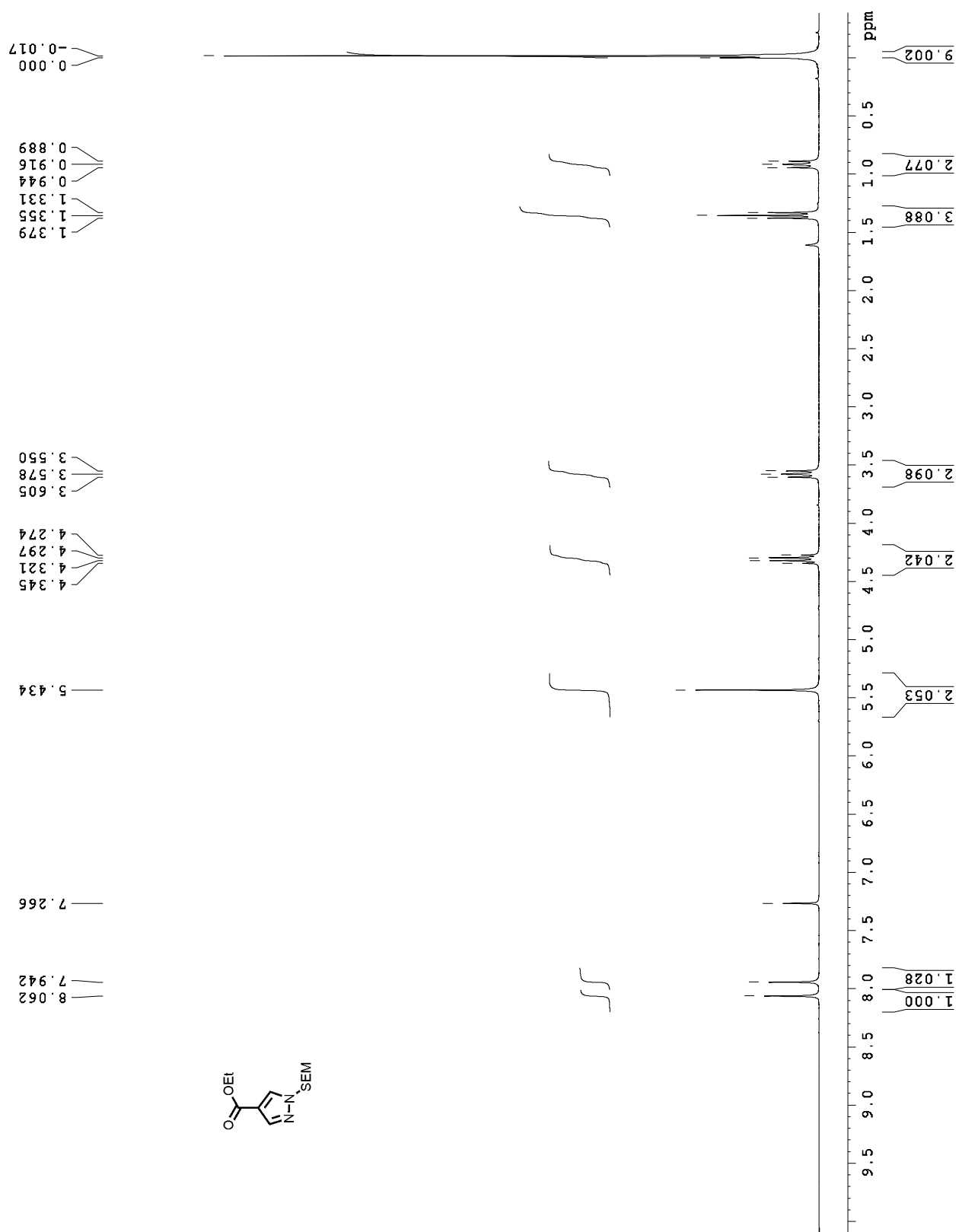


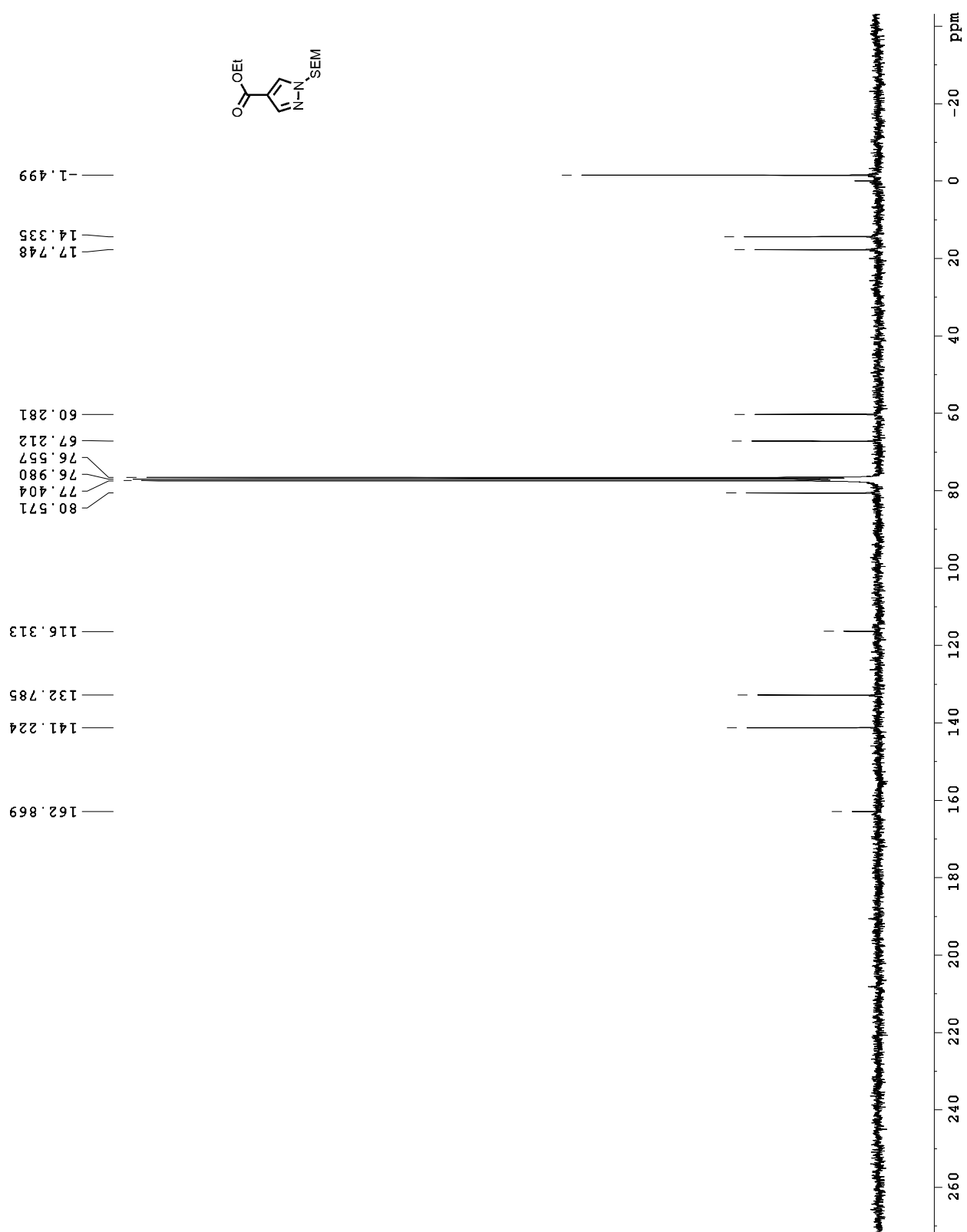


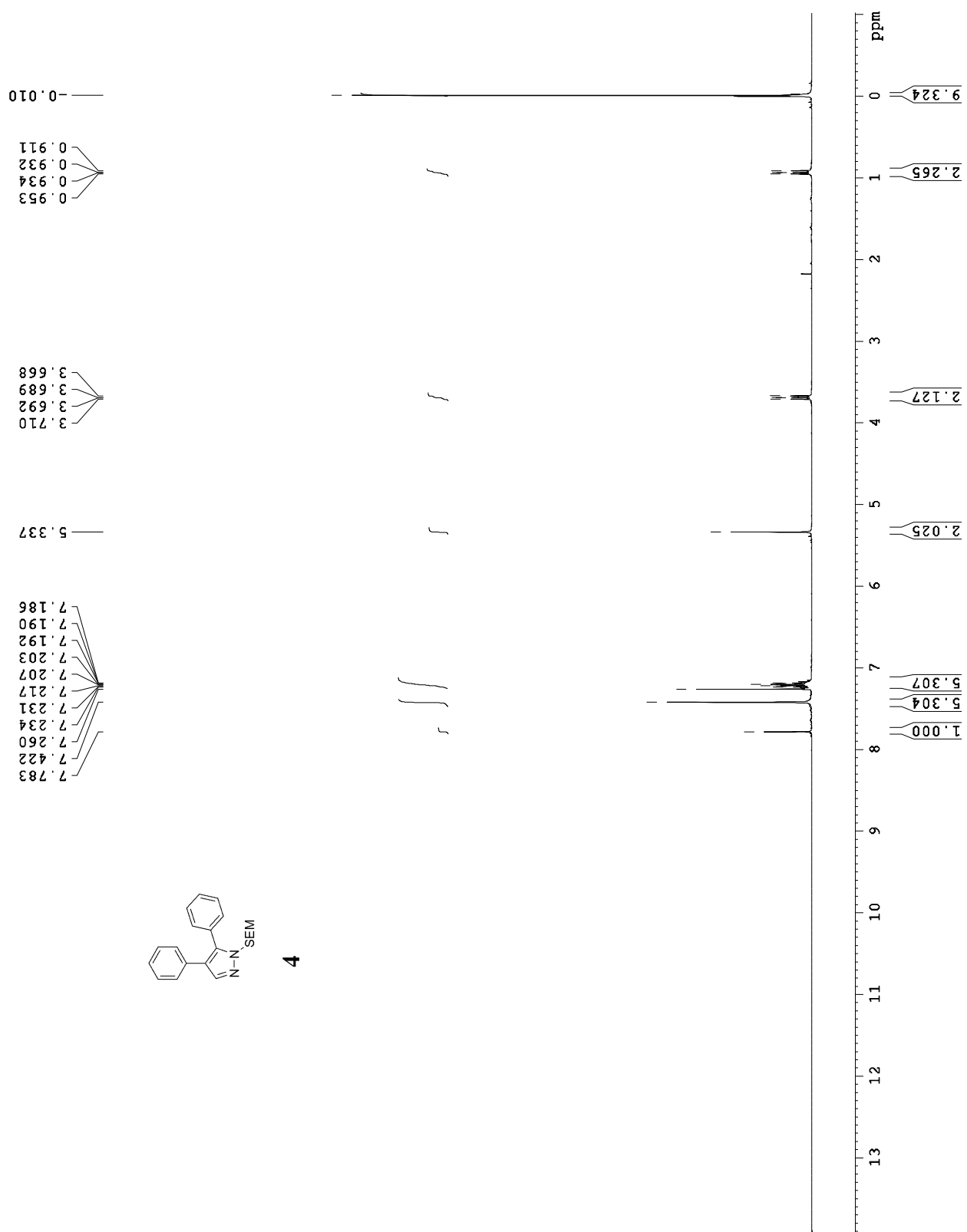


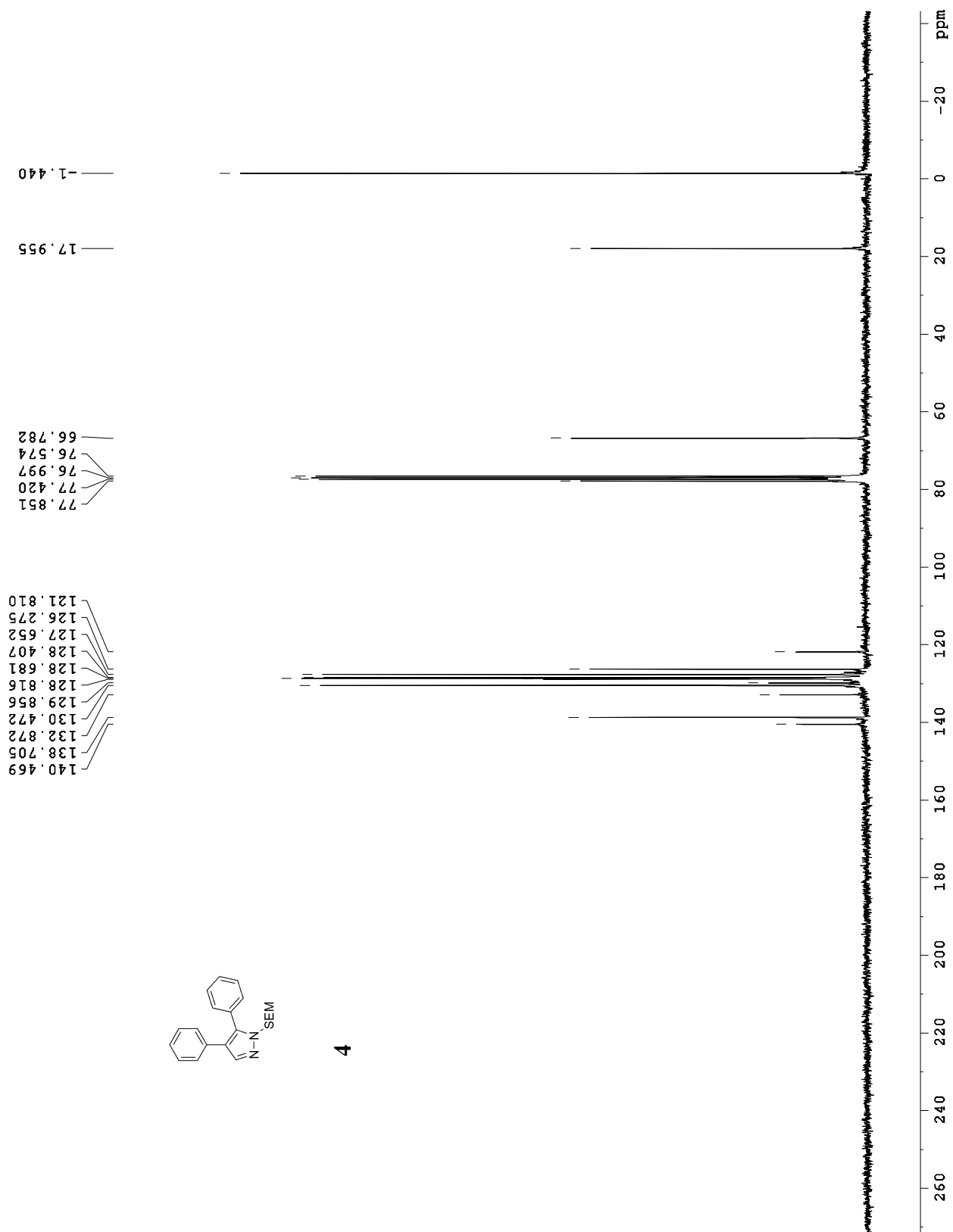


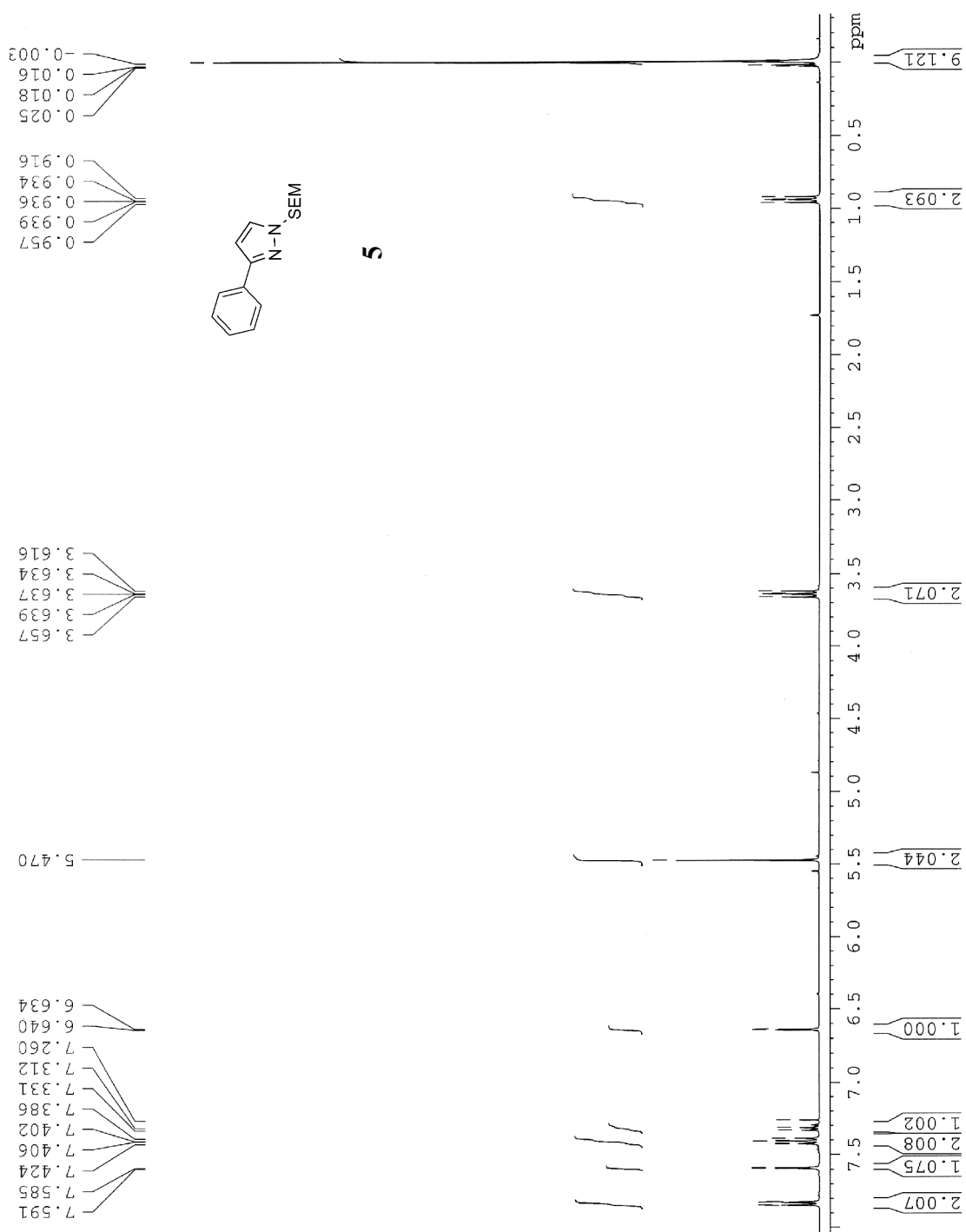


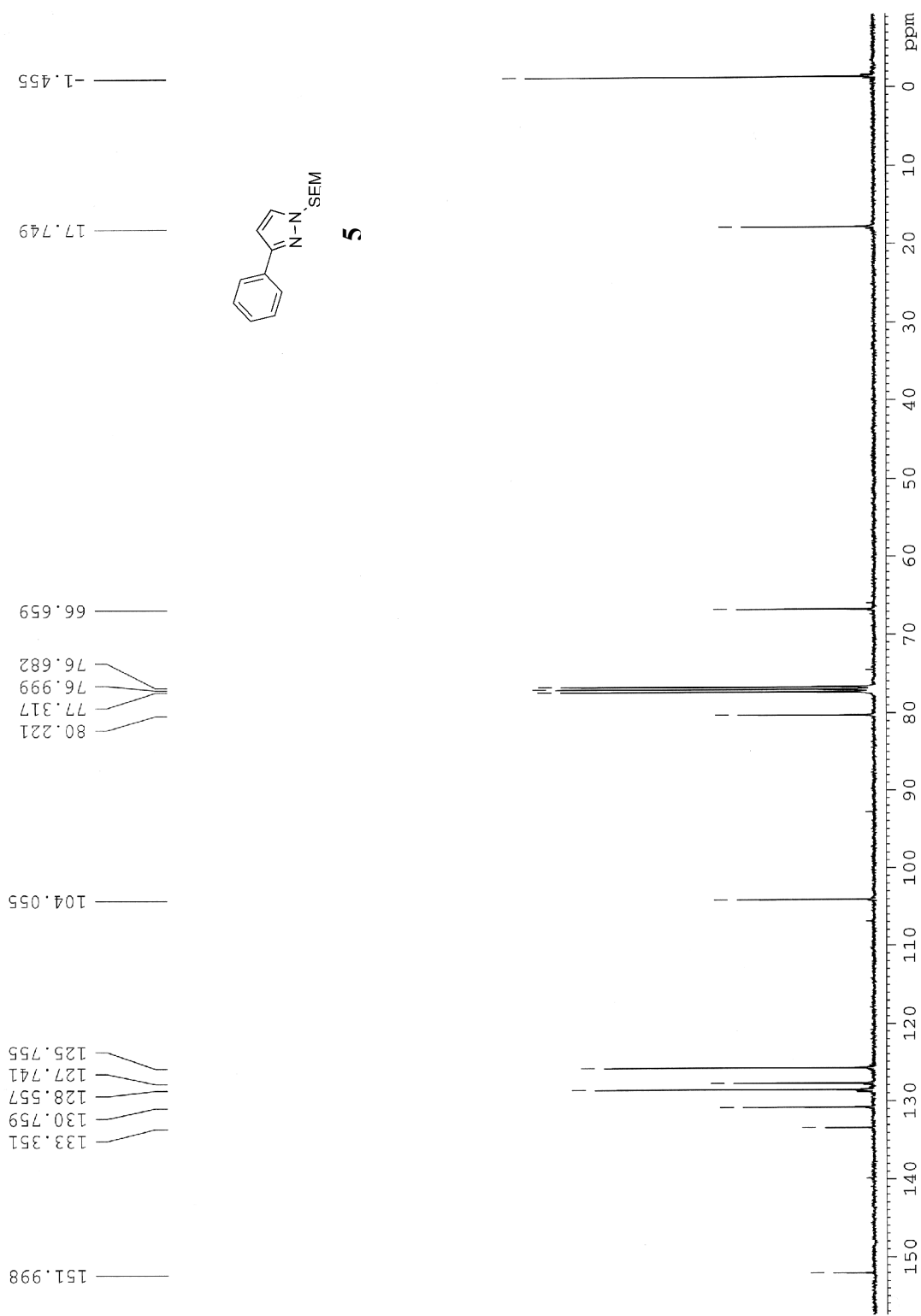


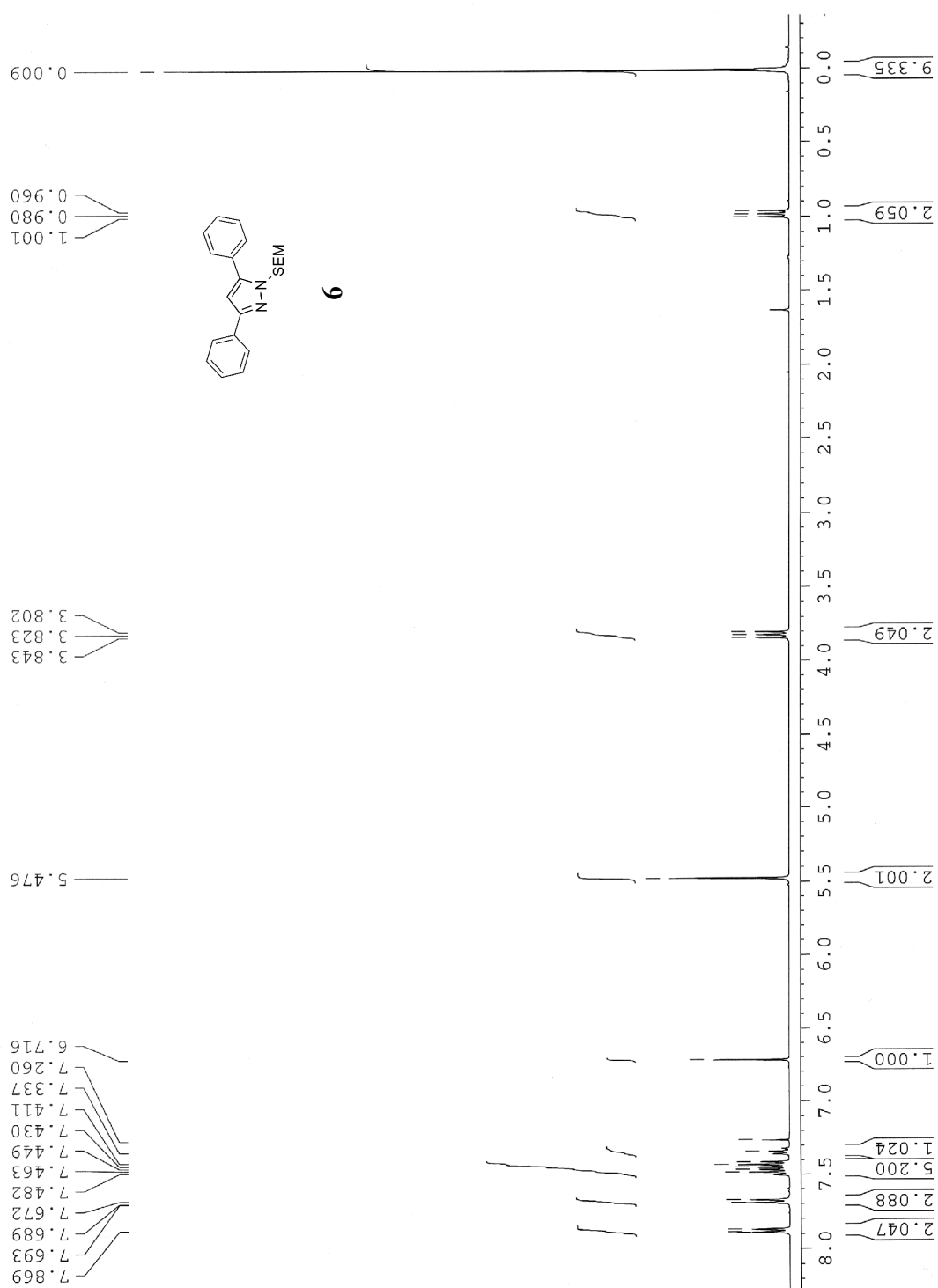


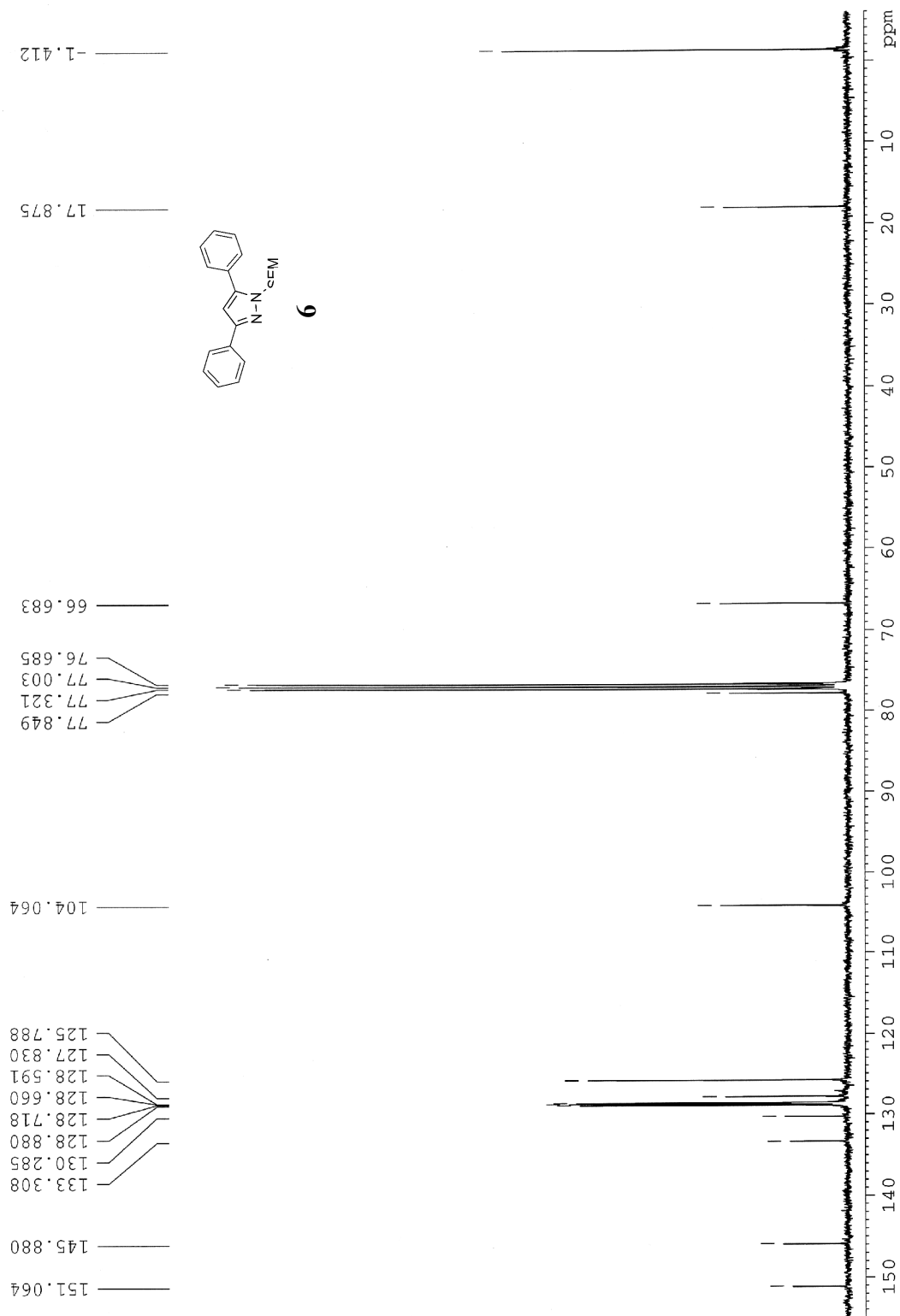


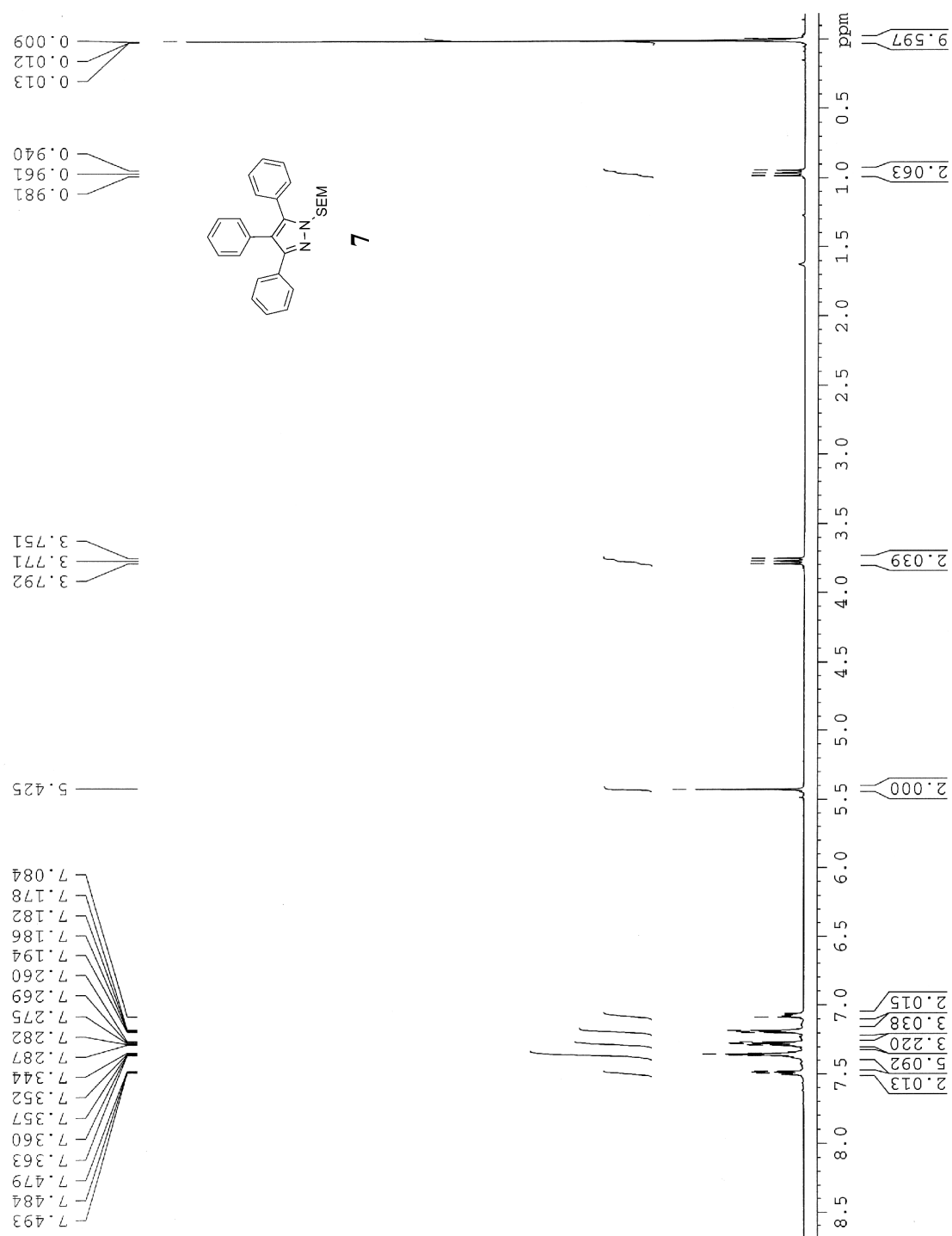


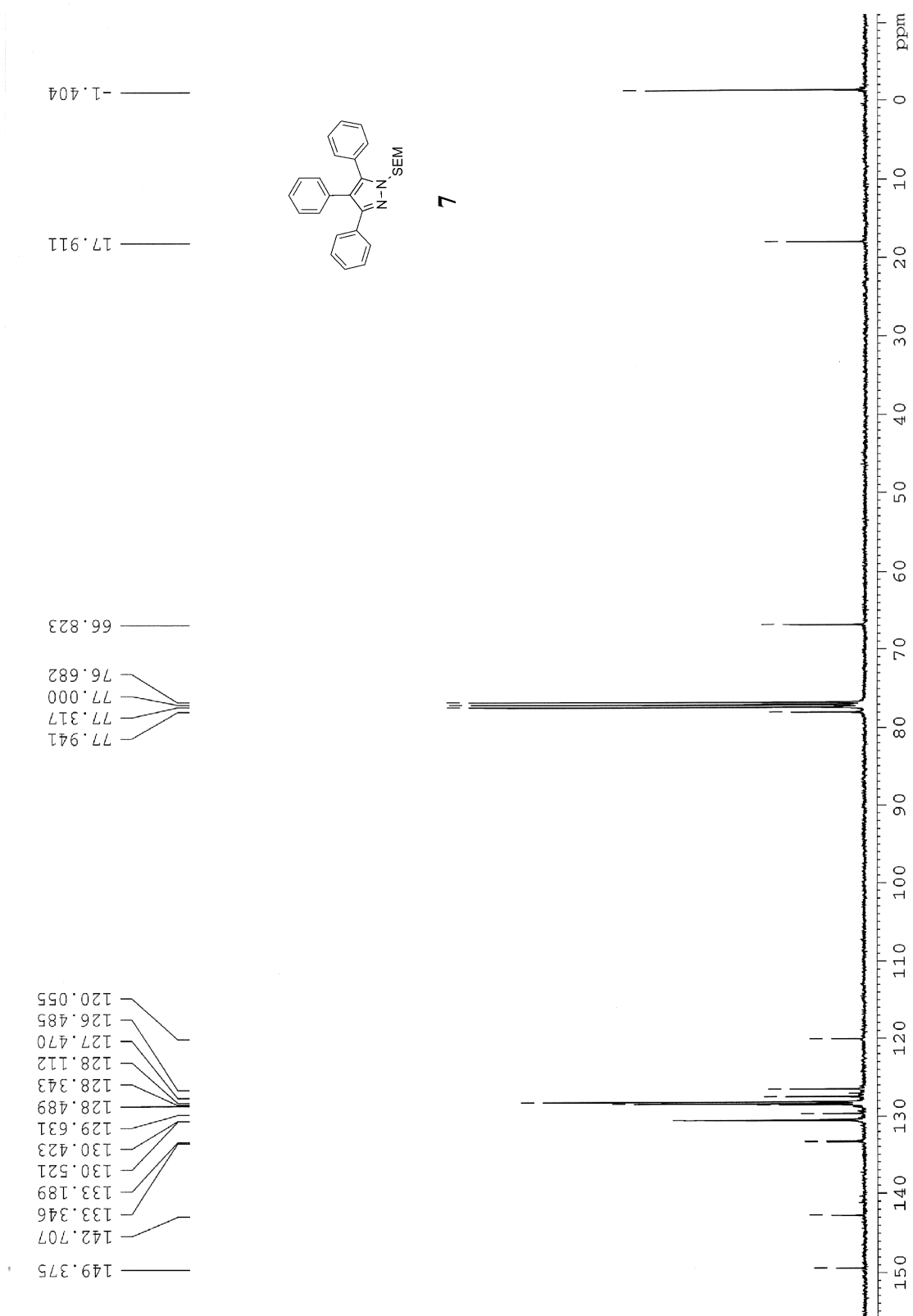


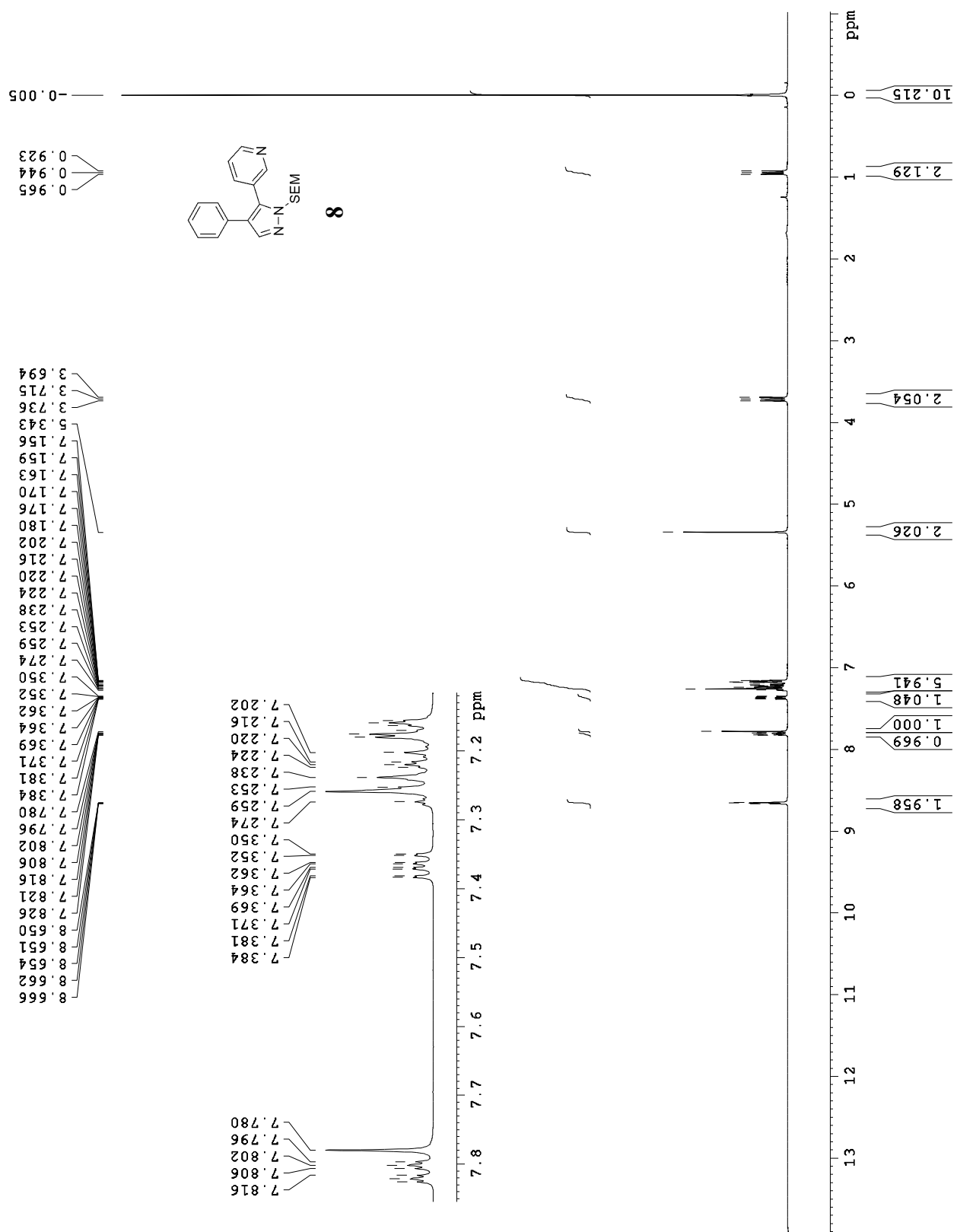


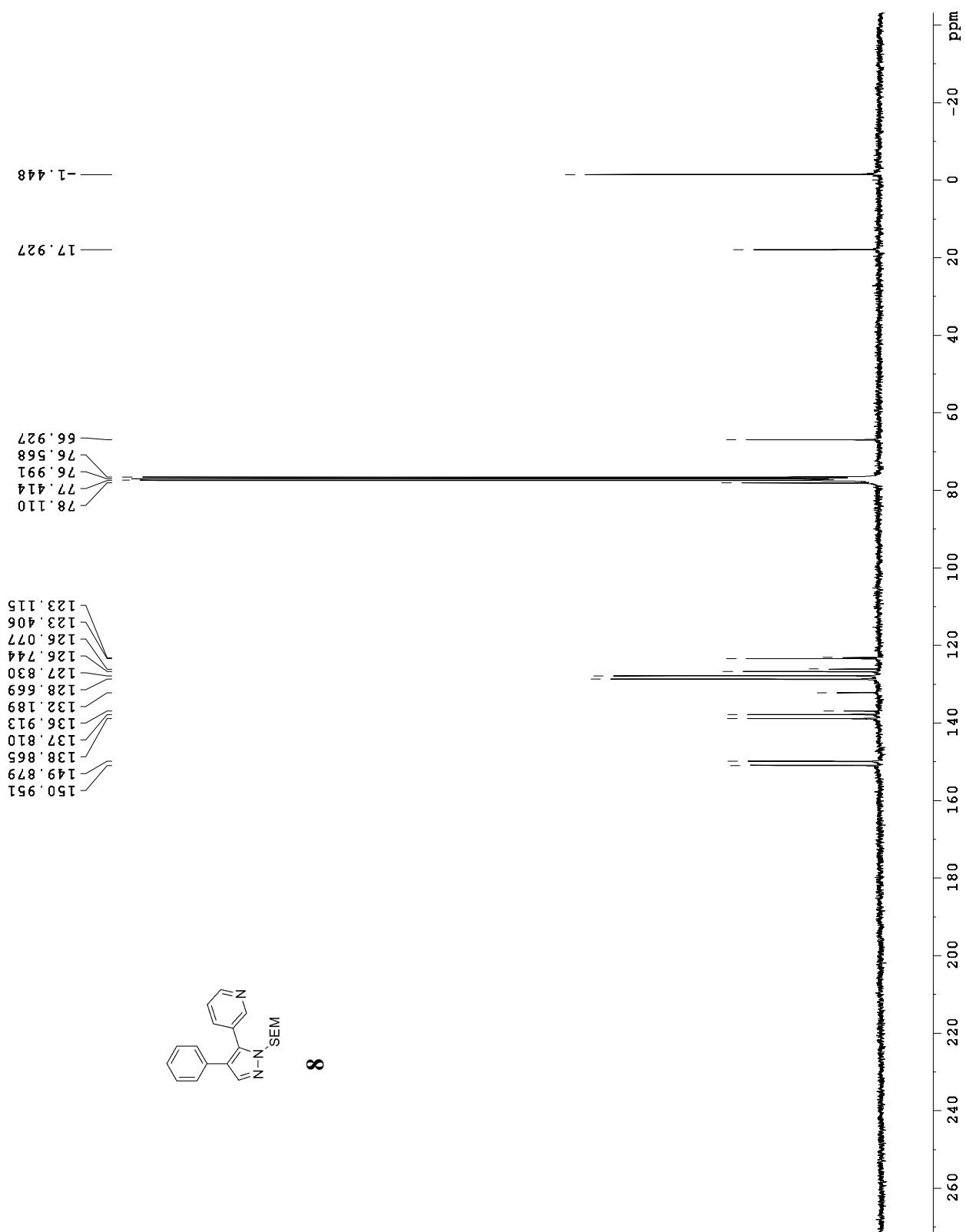


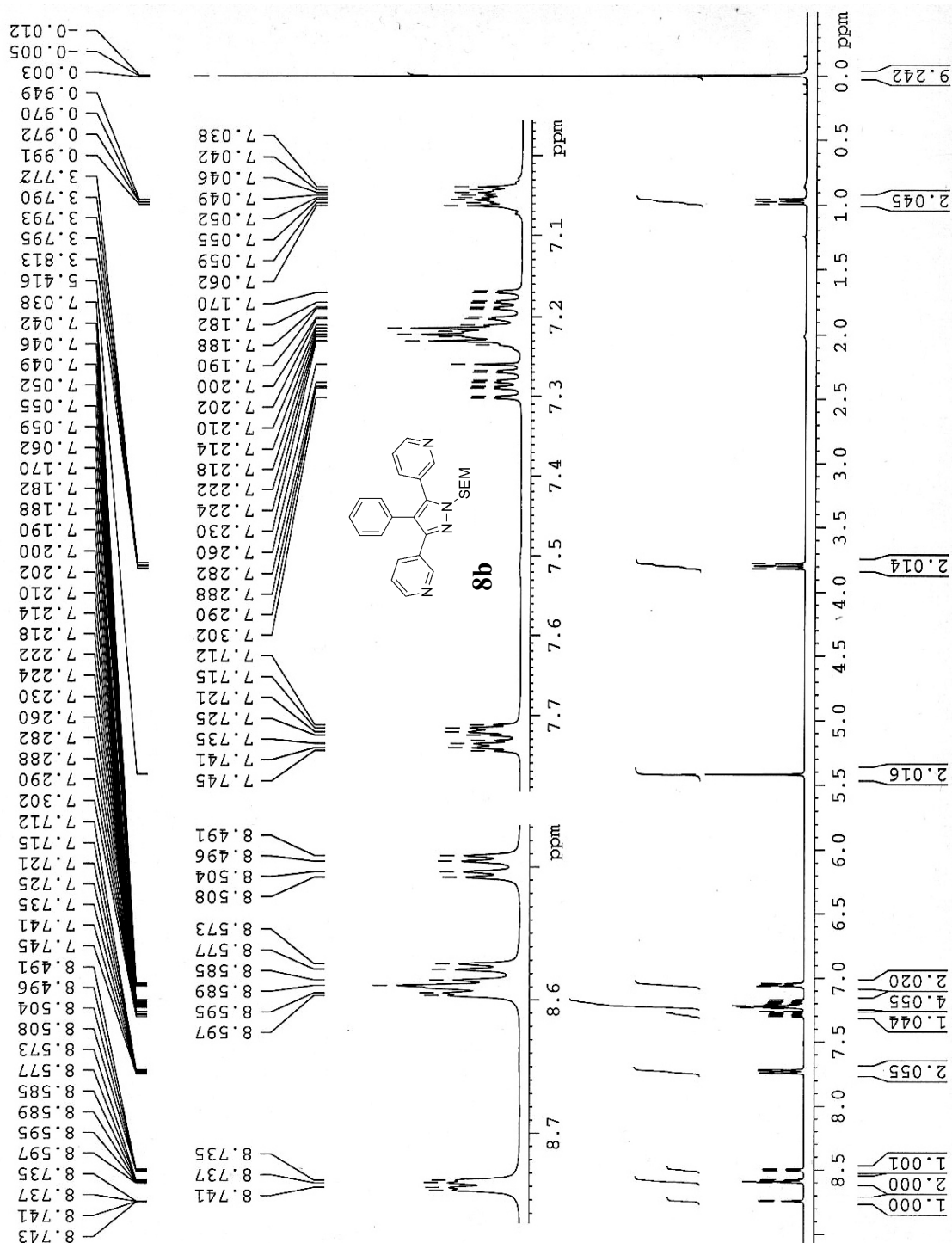


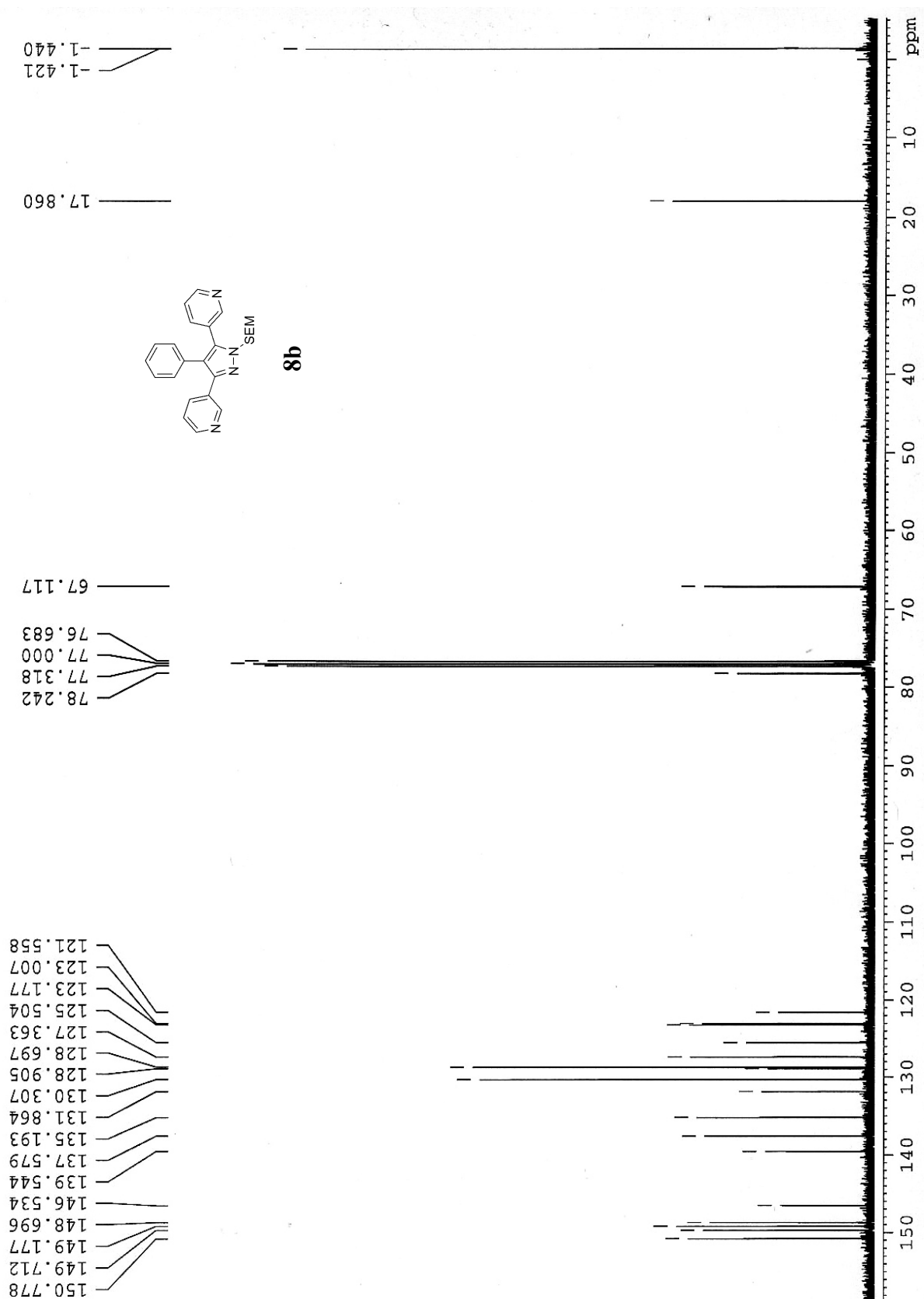


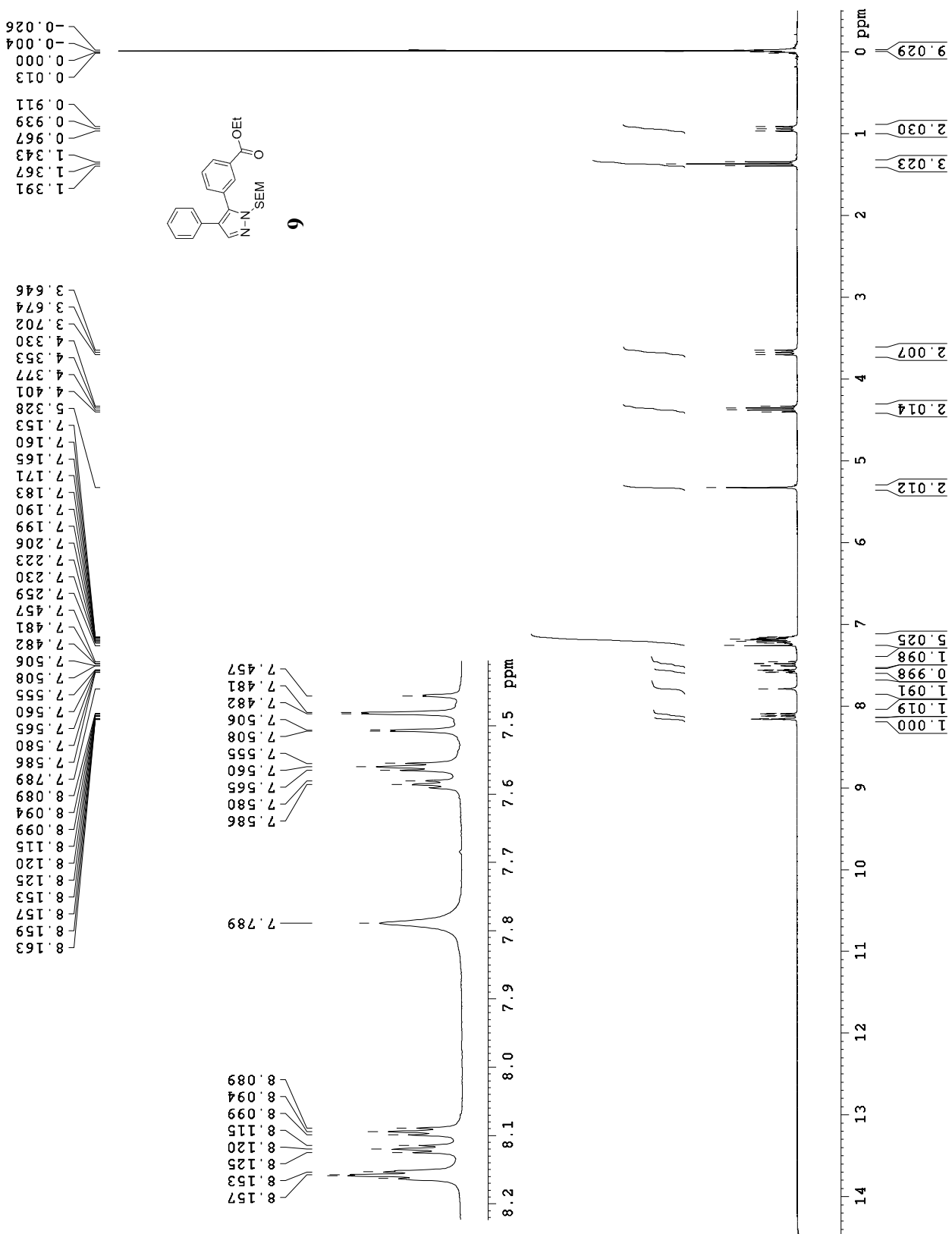


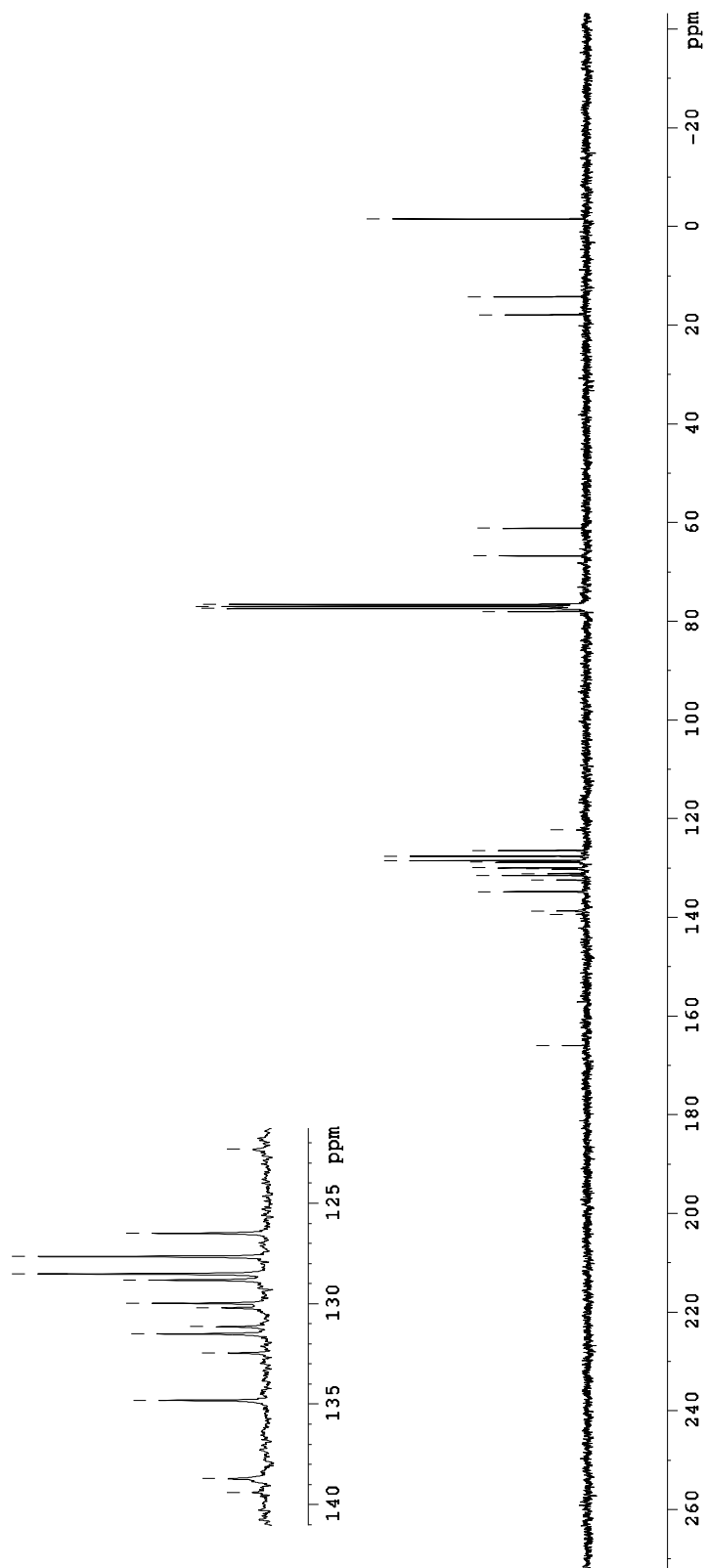




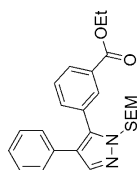








9



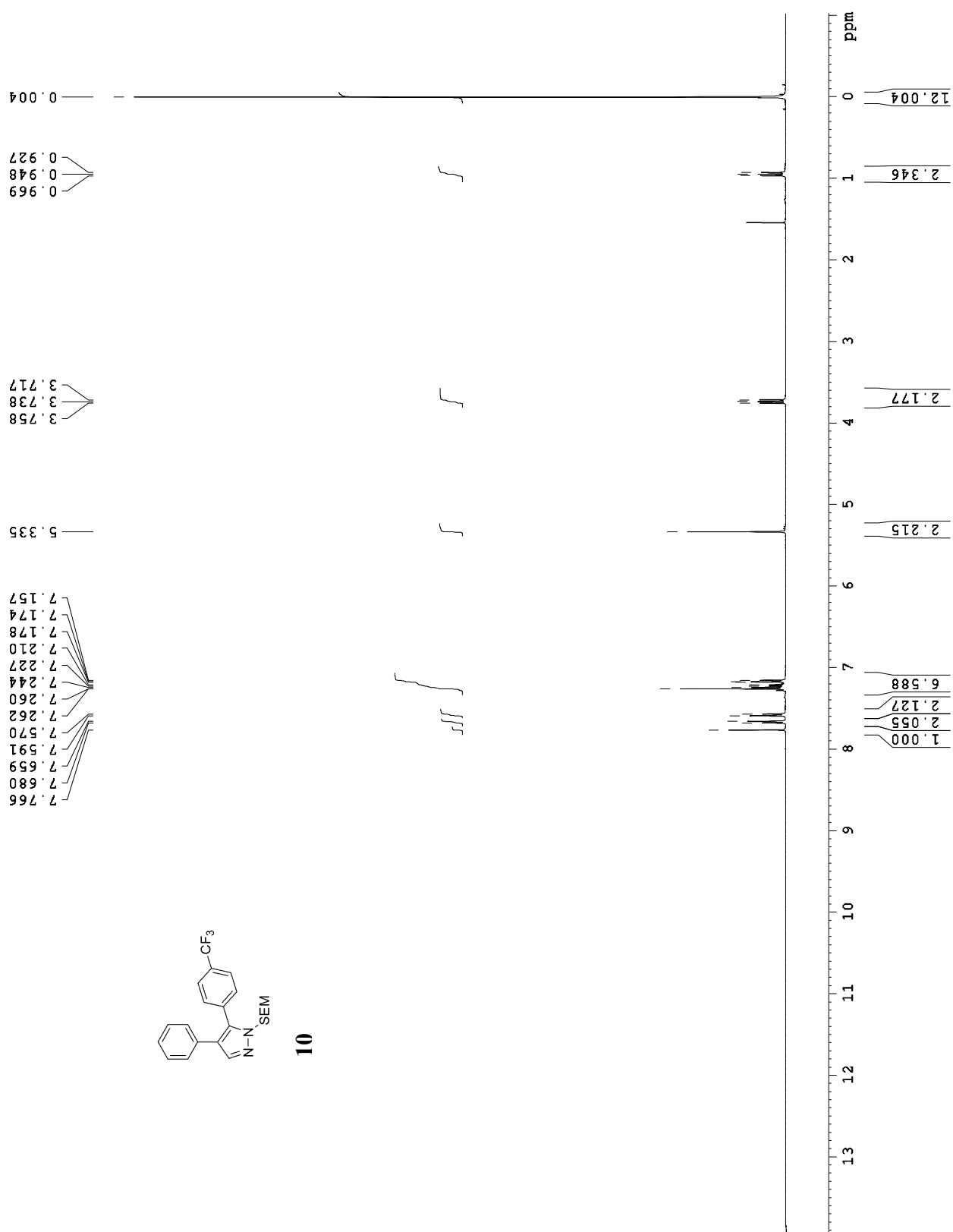
17.925
14.246
-1.471

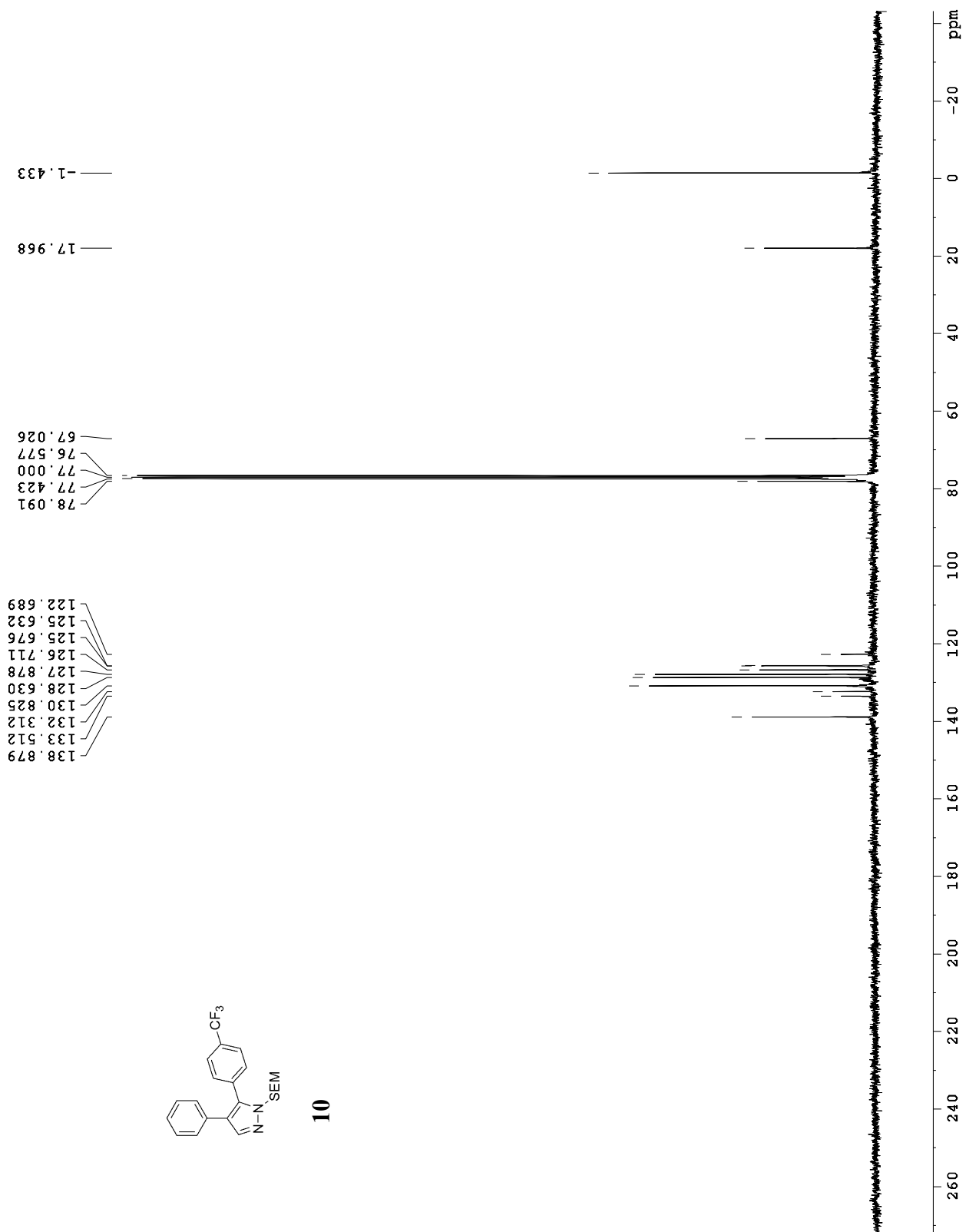
78.007
77.420
76.997
76.573
66.743
61.167

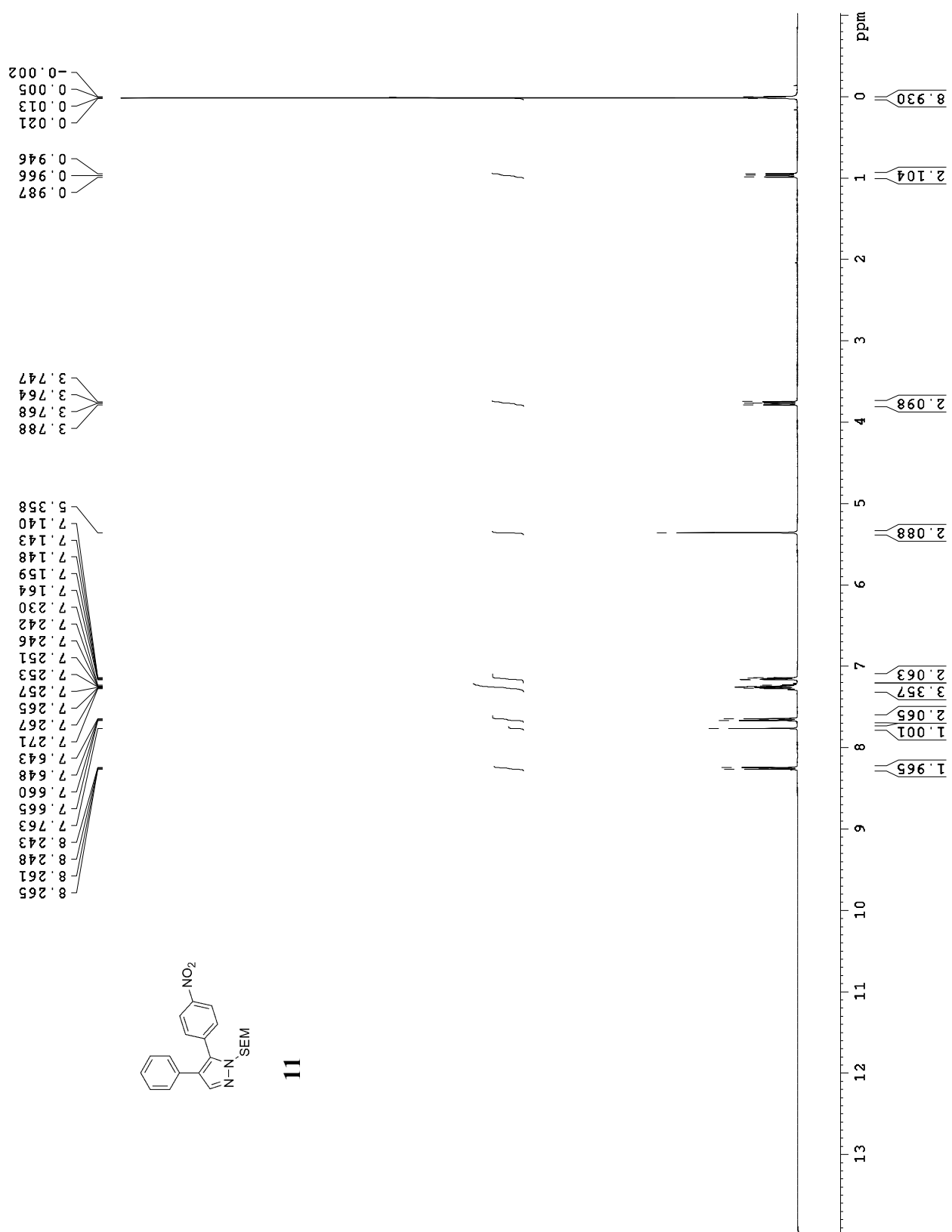
139.388
138.708
134.809
132.456
131.498
131.143
130.198
129.972
128.815
128.506
127.651
126.487
122.311

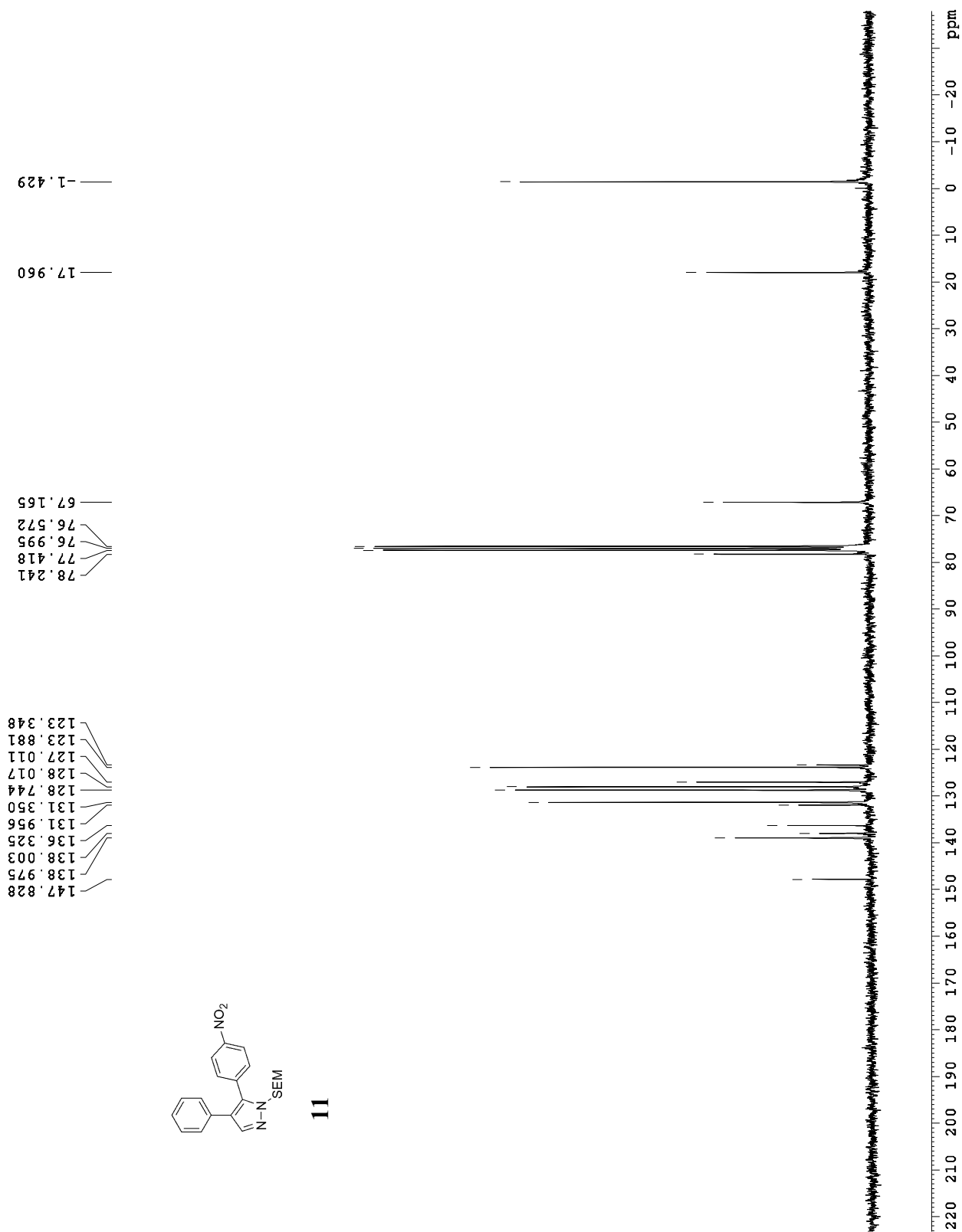
165.970

139.388
138.708
134.809
132.456
131.498
131.143
130.198
129.972
128.815
128.506
127.651
126.487
122.311







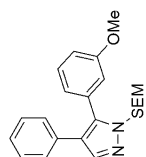


TLJ-1-247 1H 400MHz CDCl₃
after HPLC purification

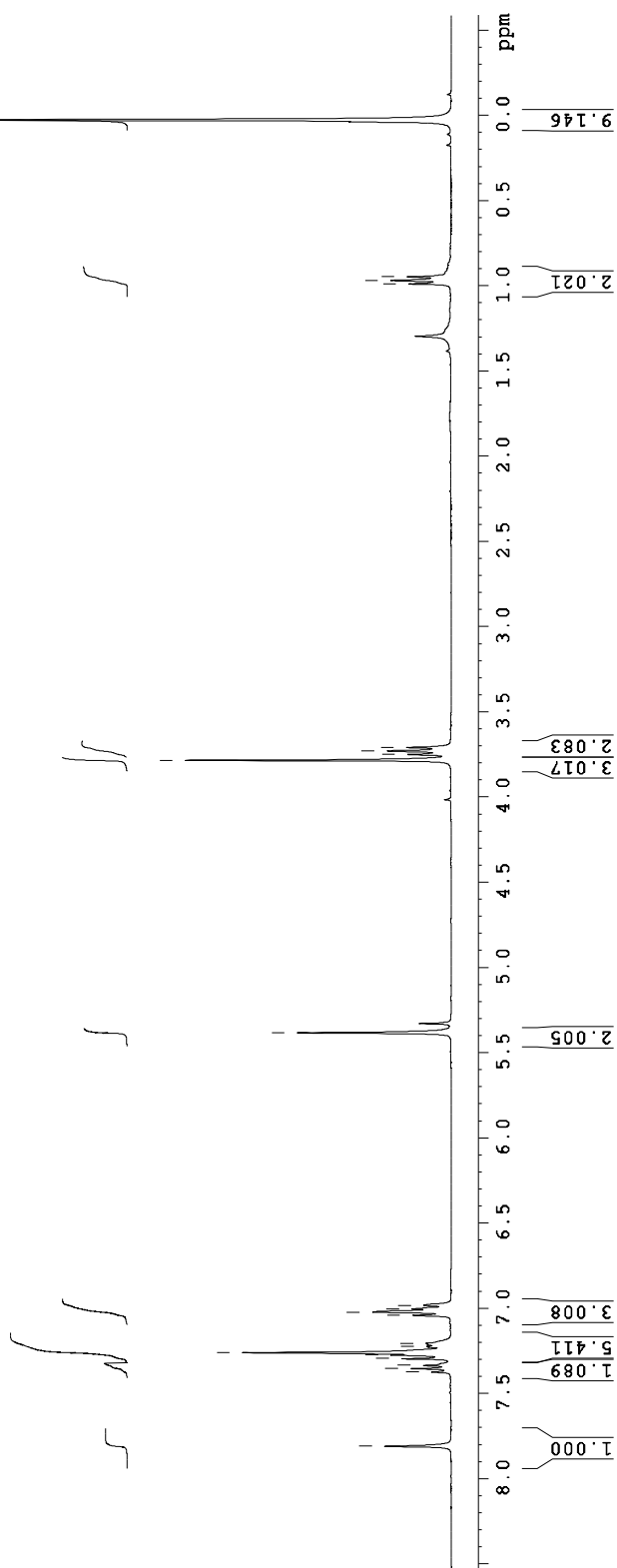
3.784
3.750
3.730
3.709

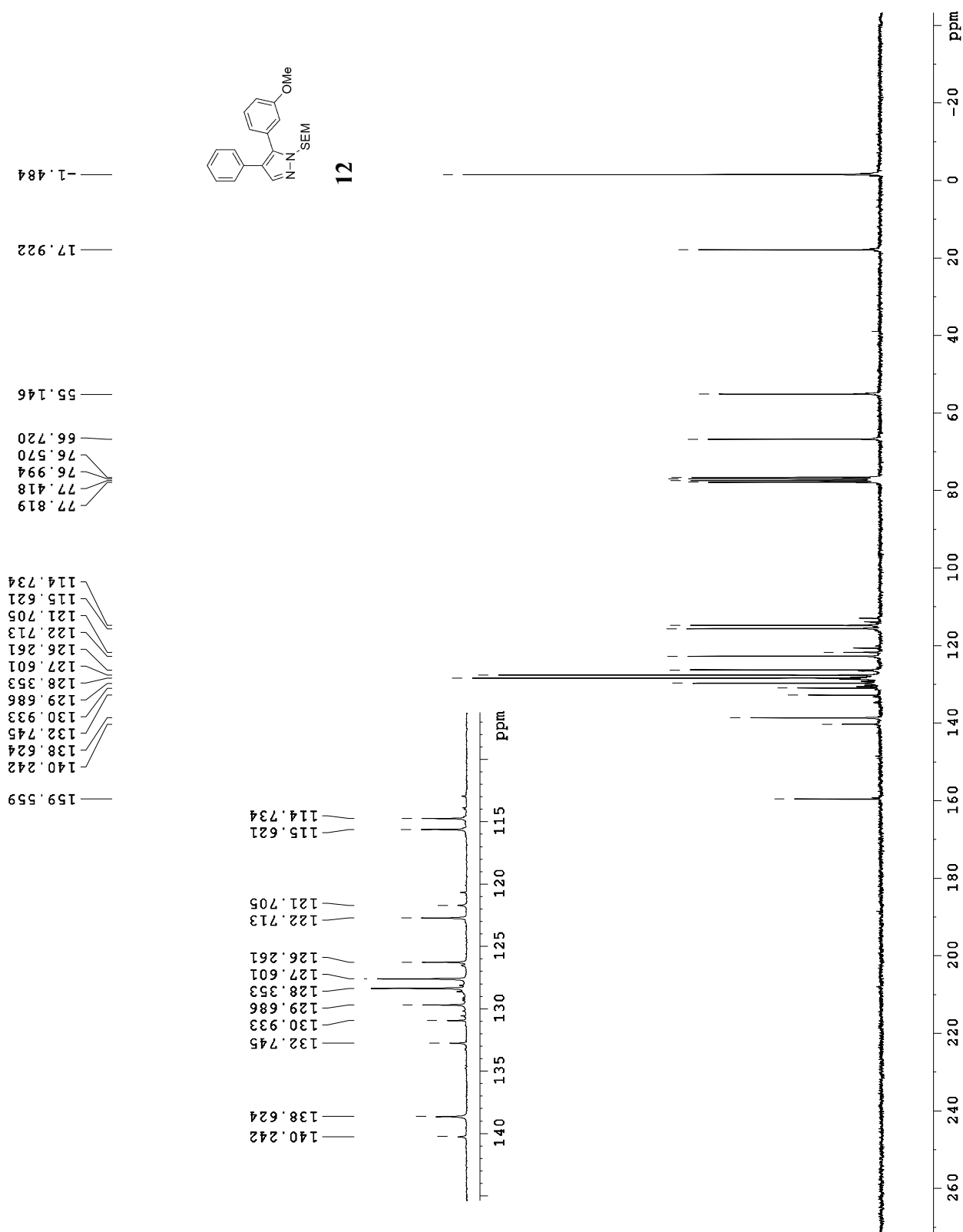
5.383

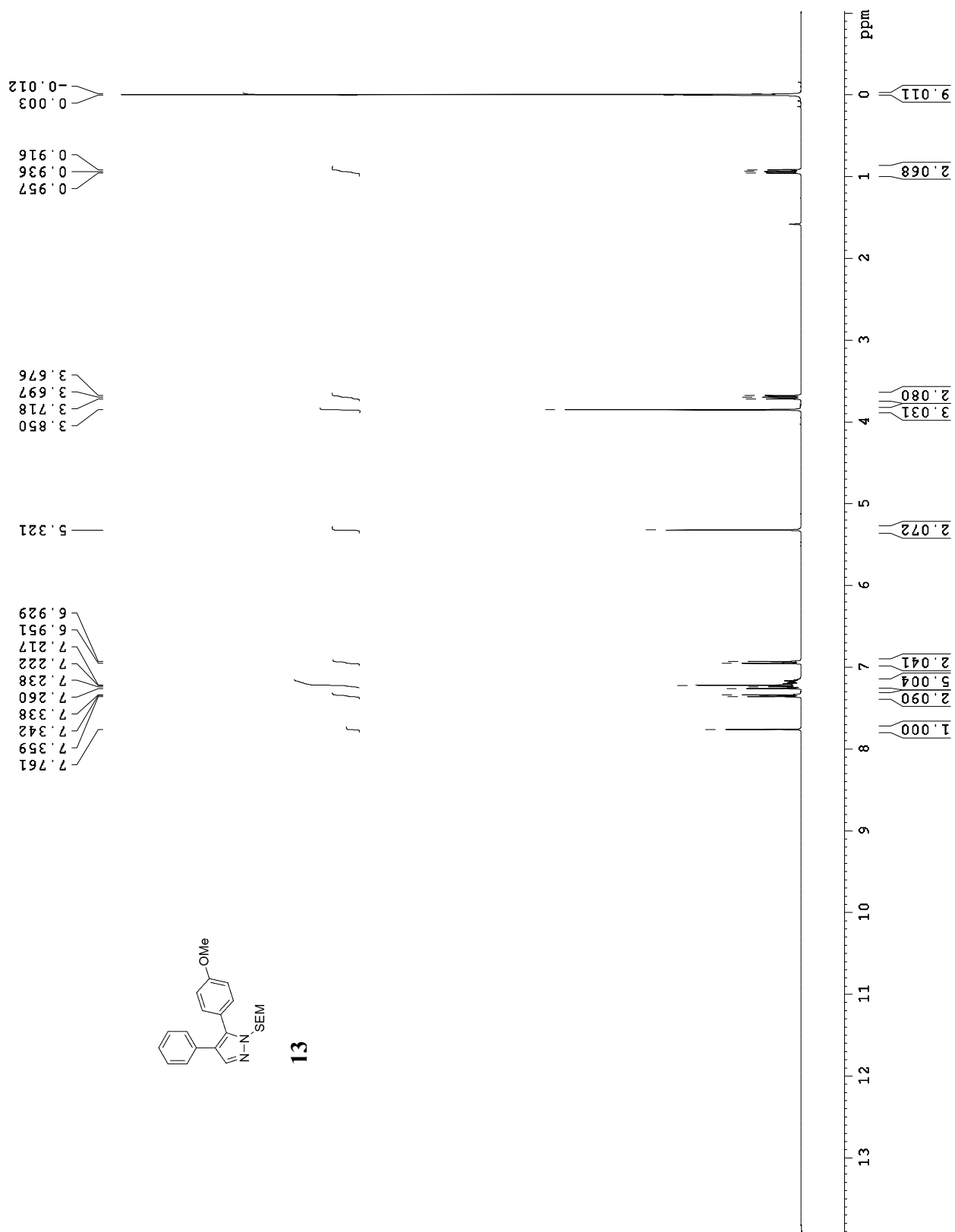
7.809
7.374
7.354
7.334
7.295
7.274
7.259
7.222
7.207
7.042
7.023
7.005
6.984

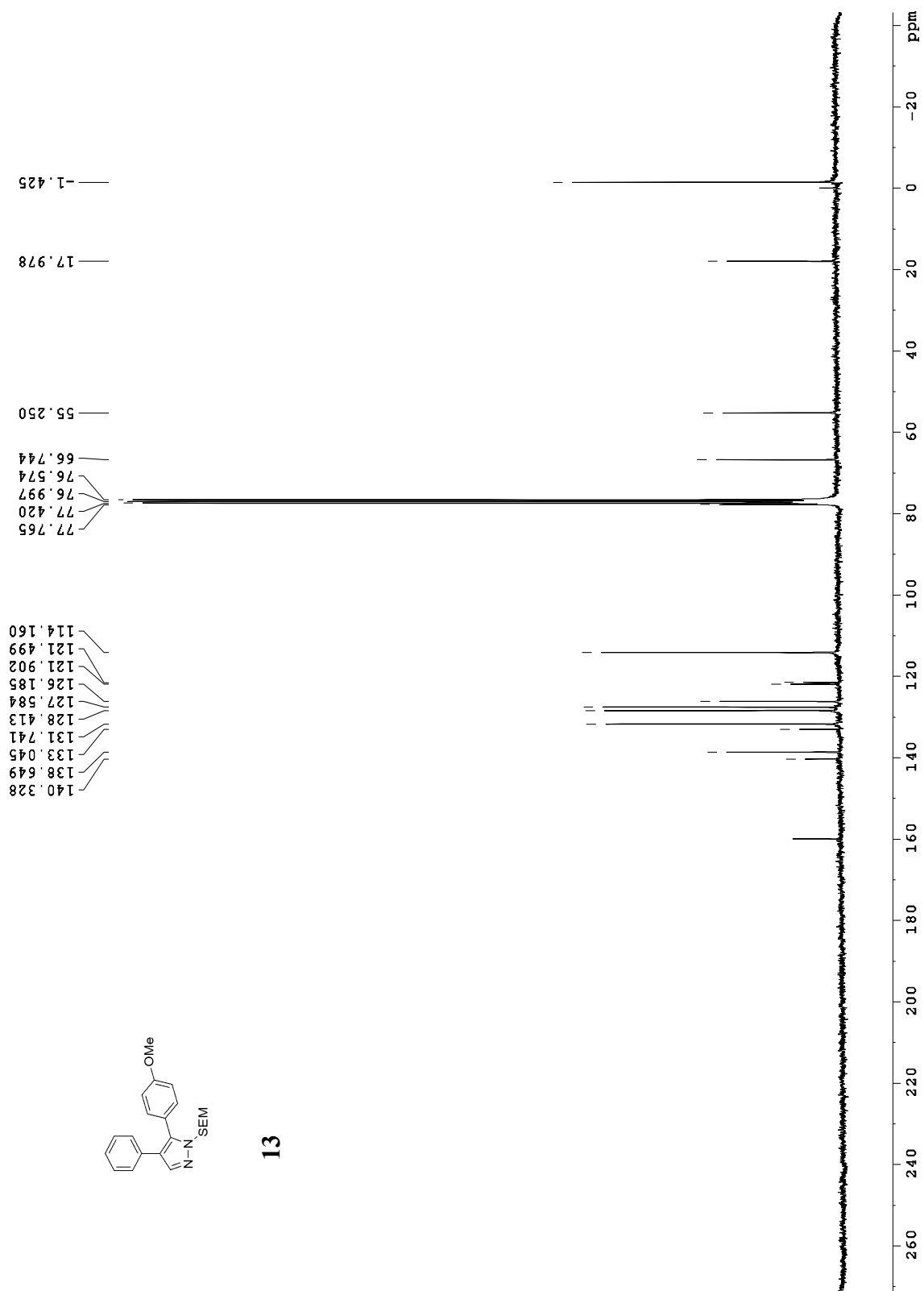


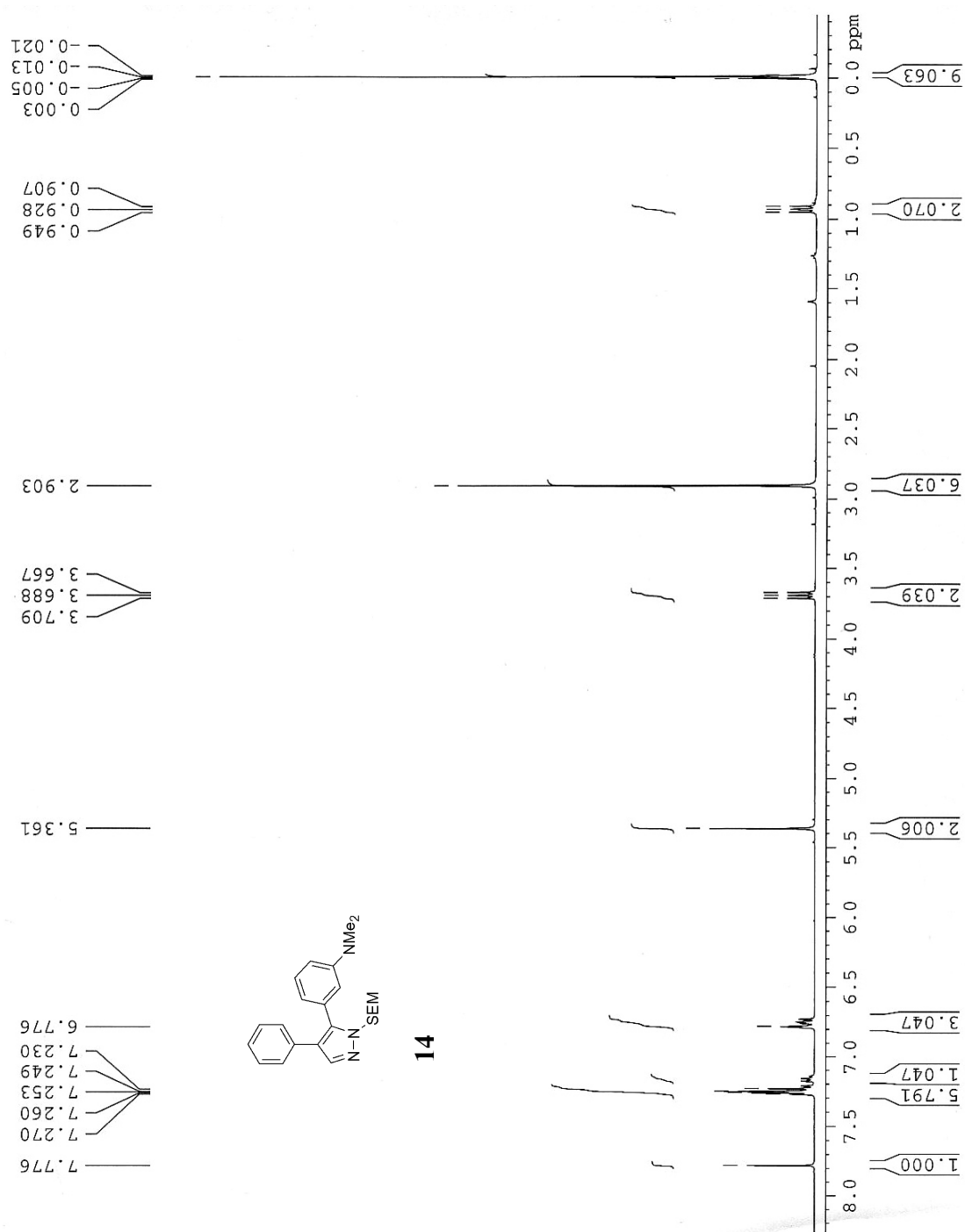
12

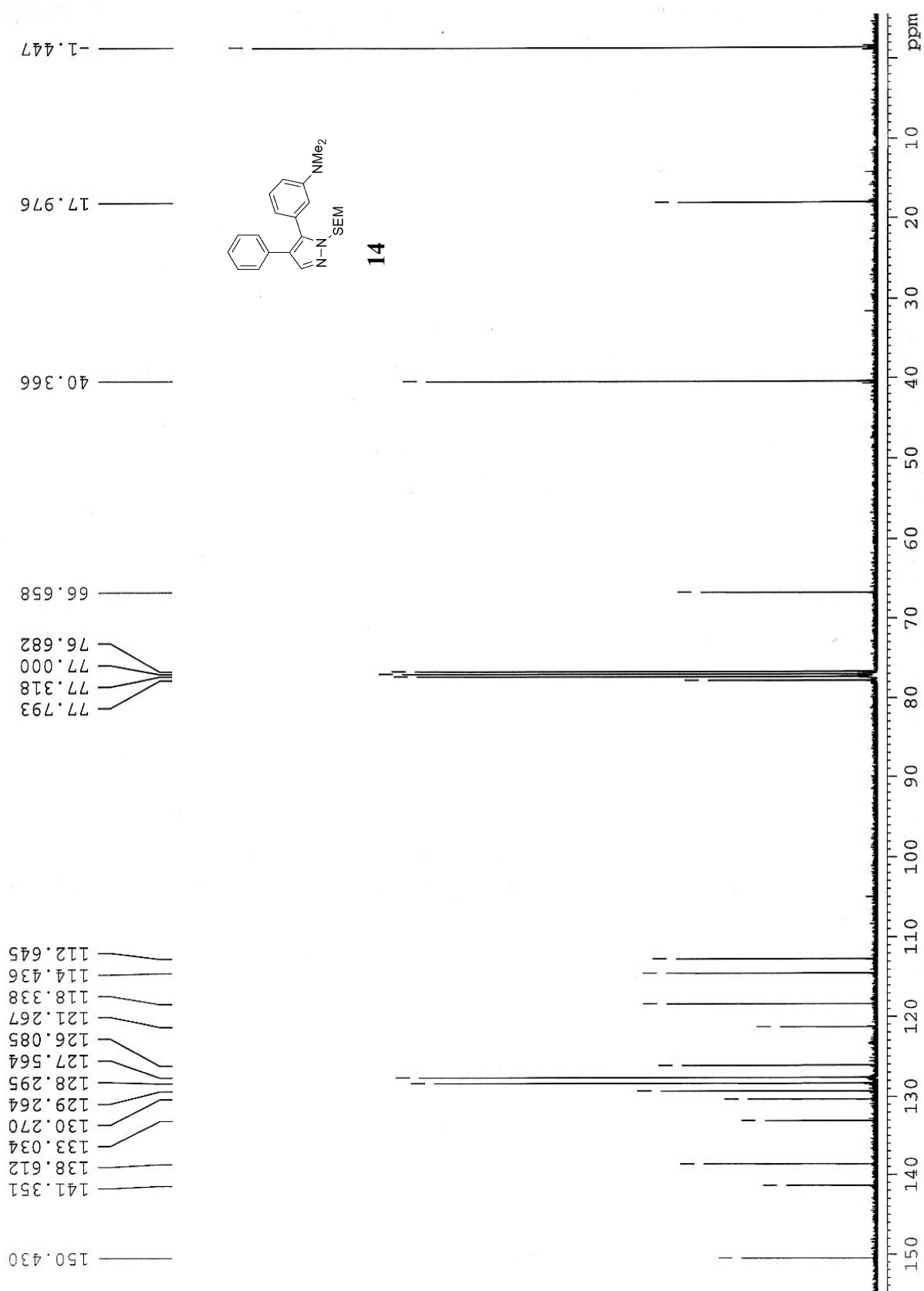


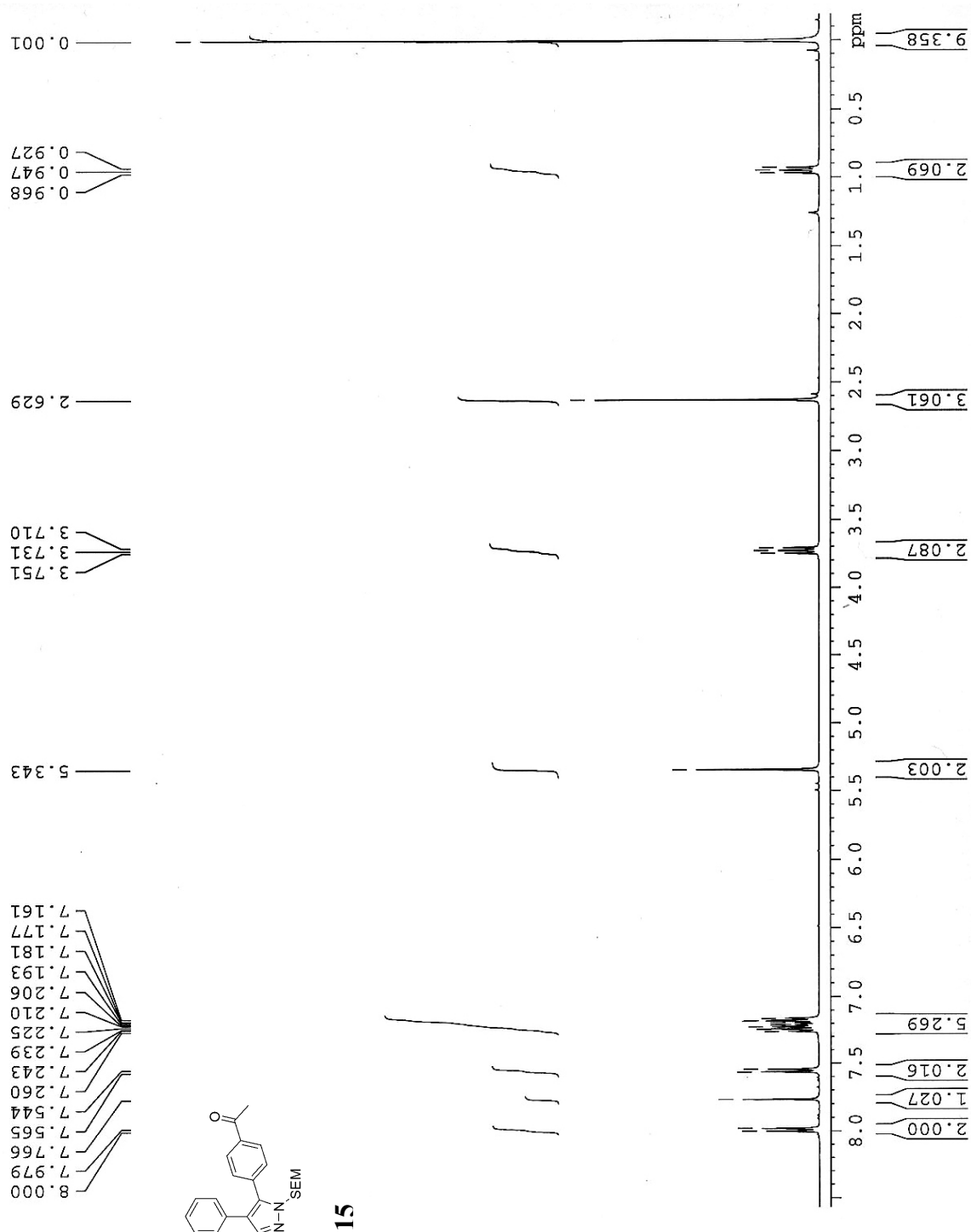


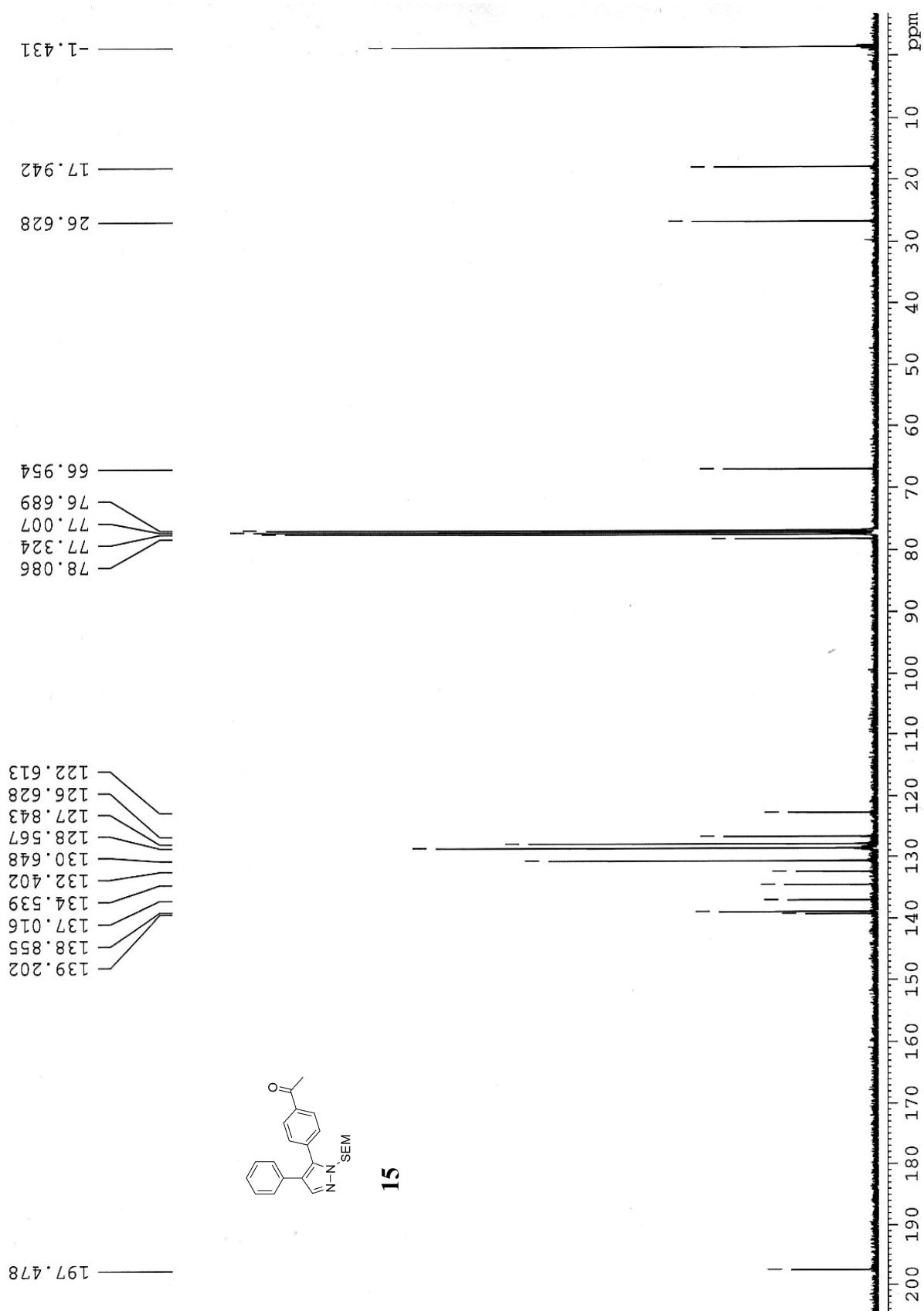


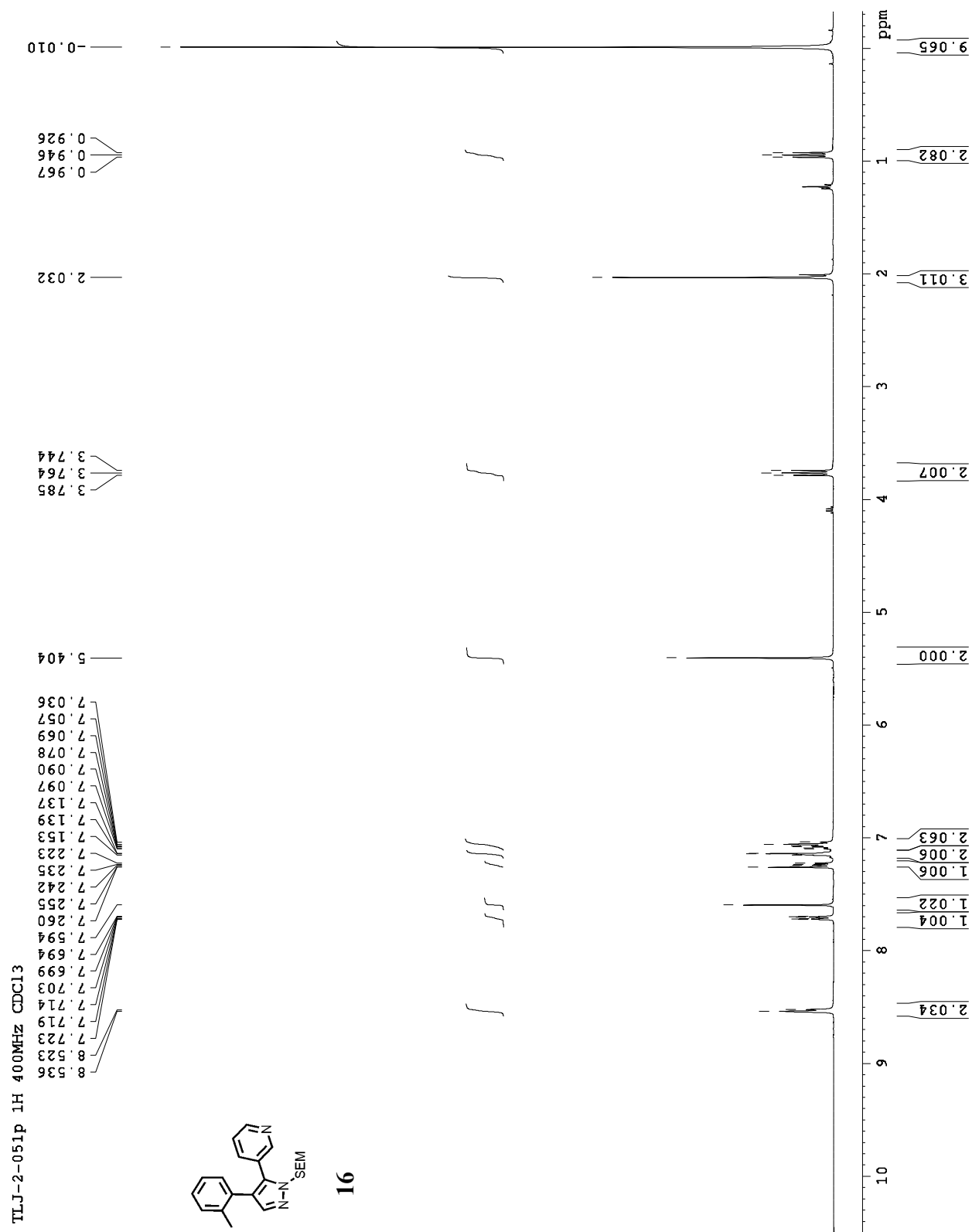


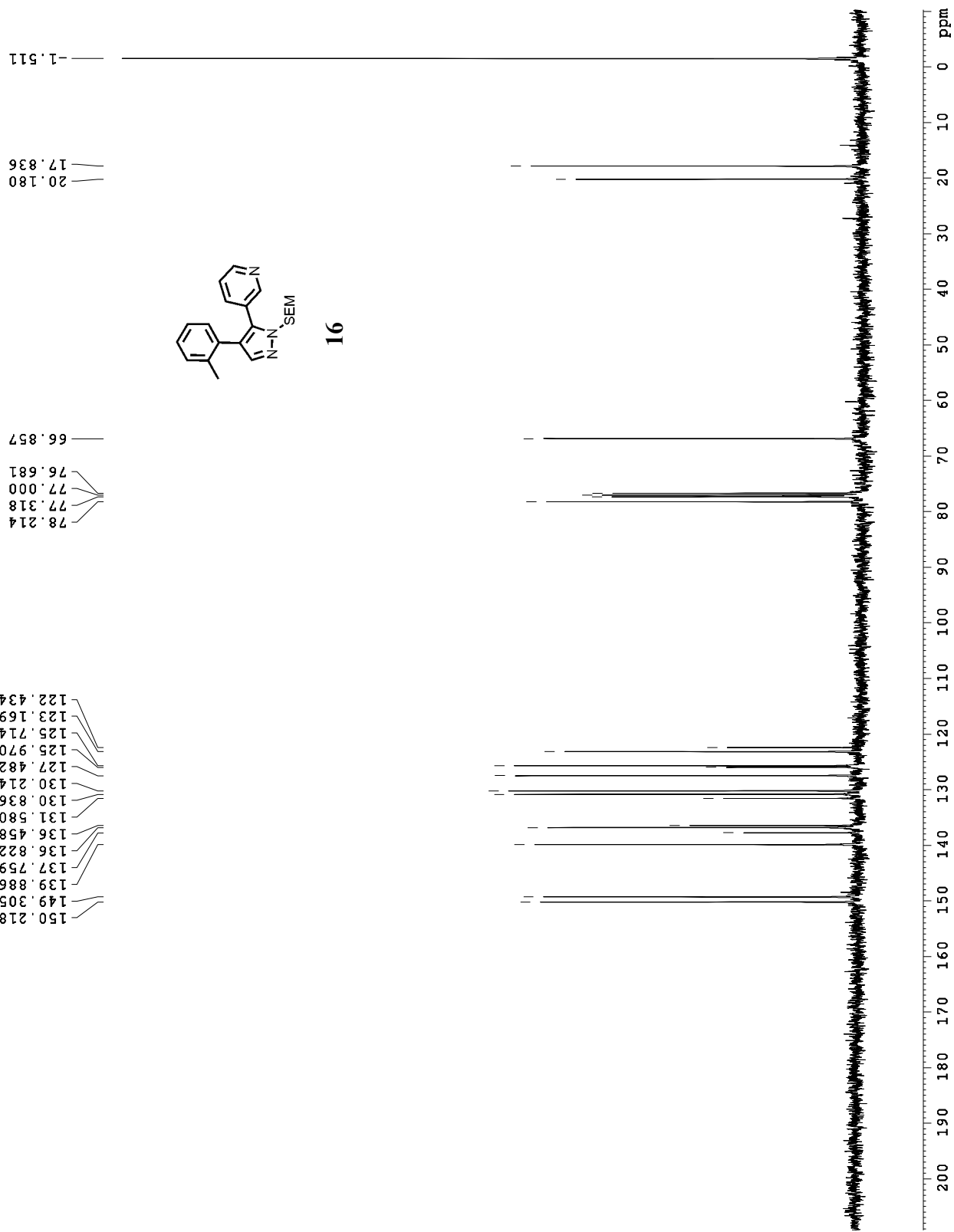


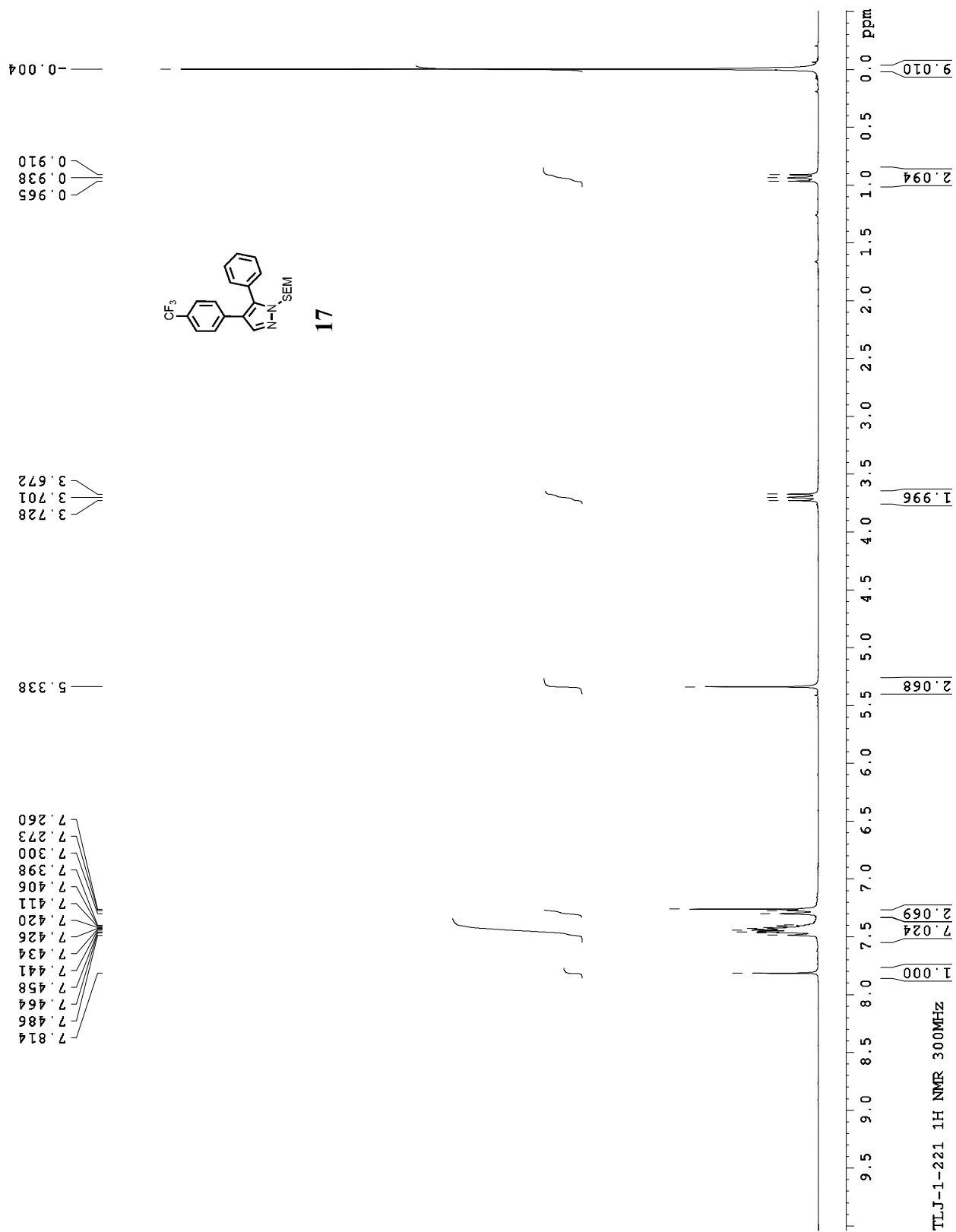


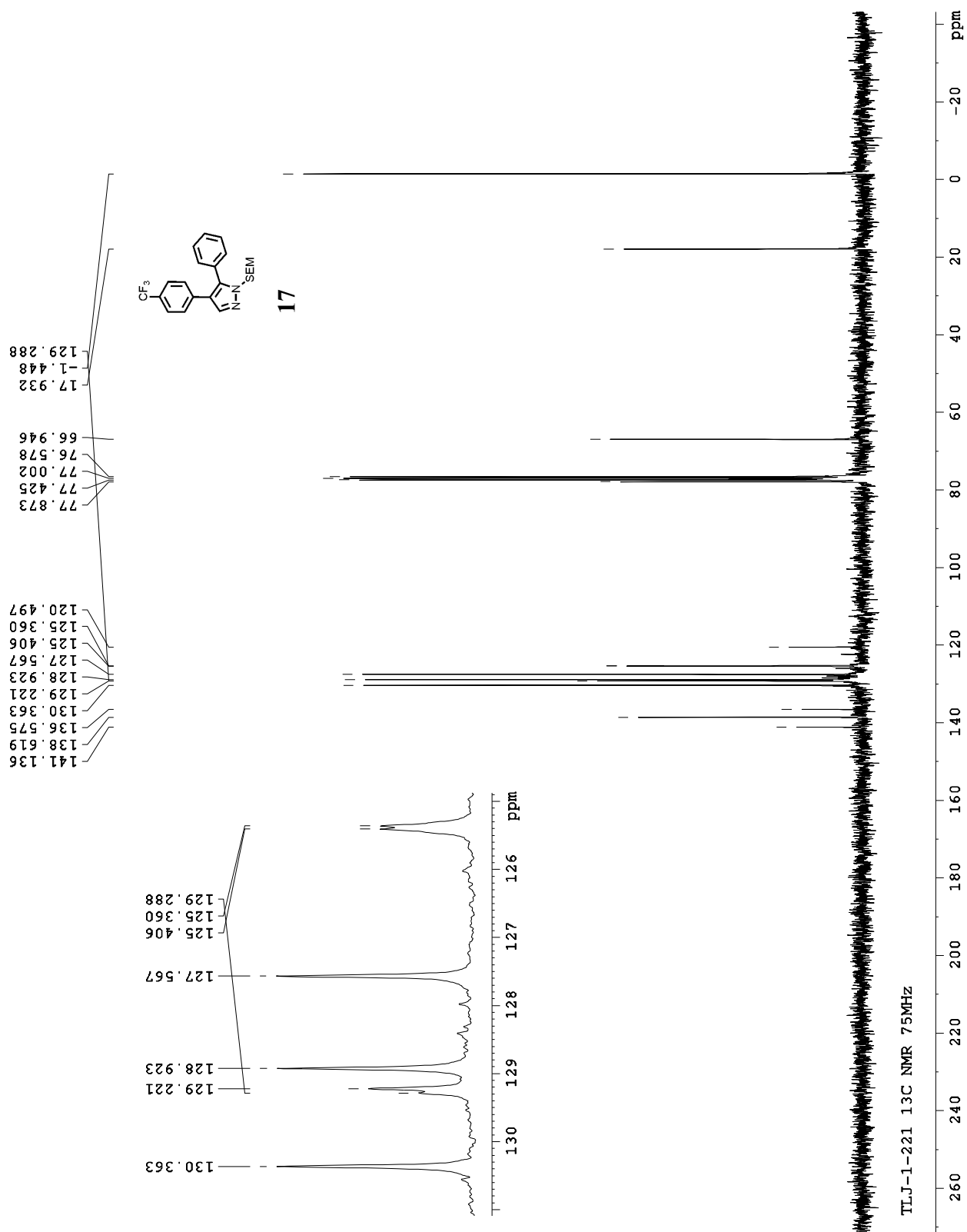


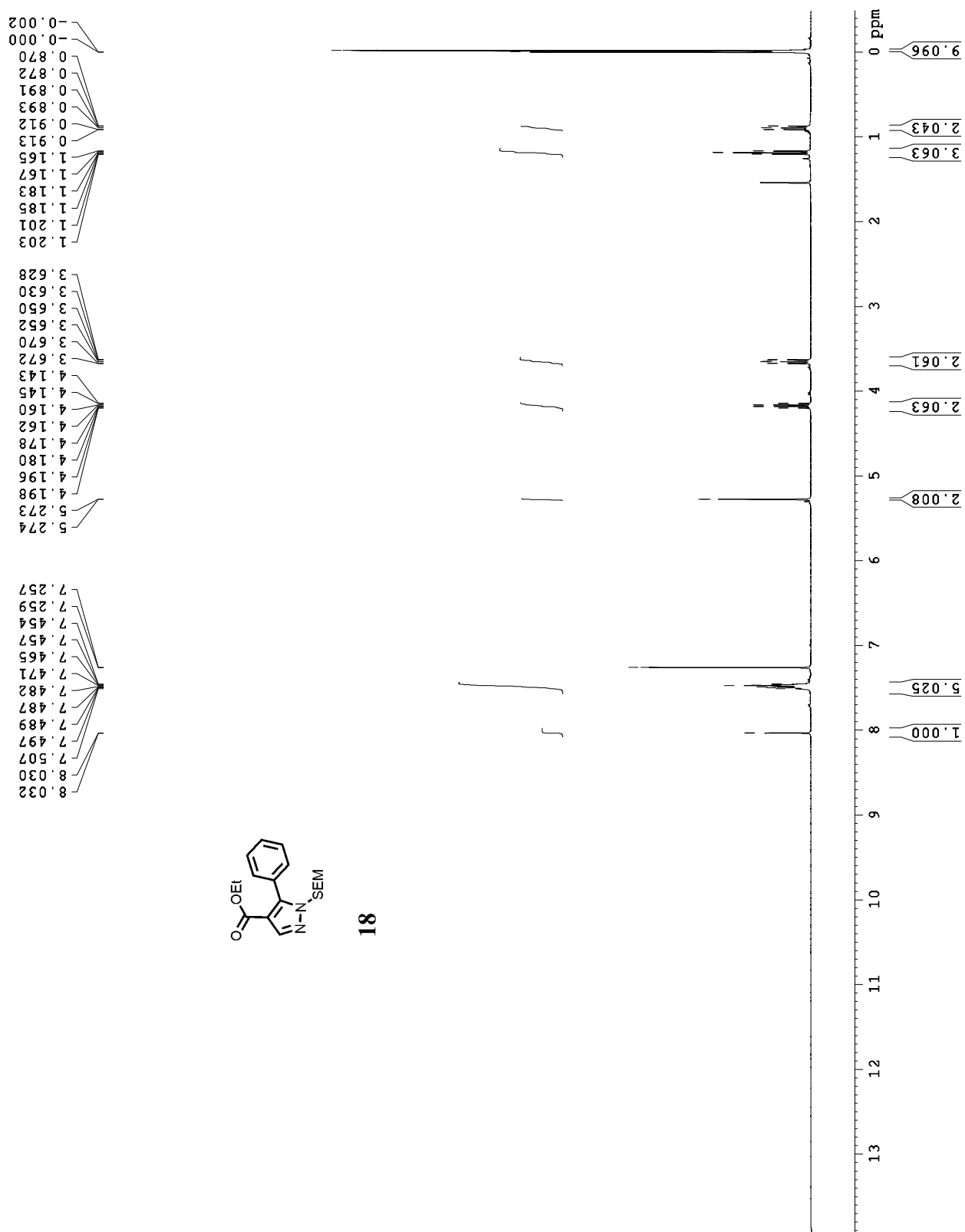


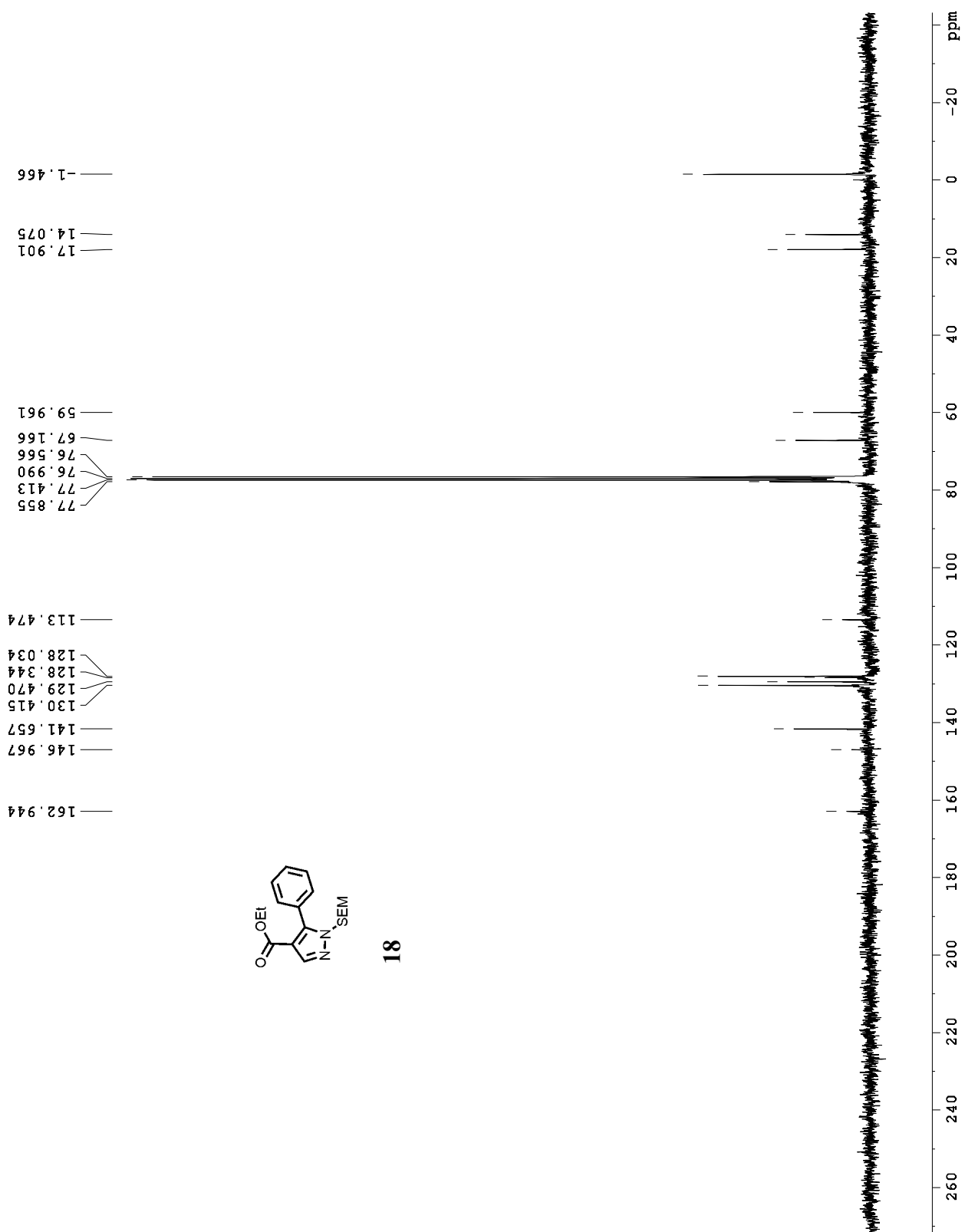


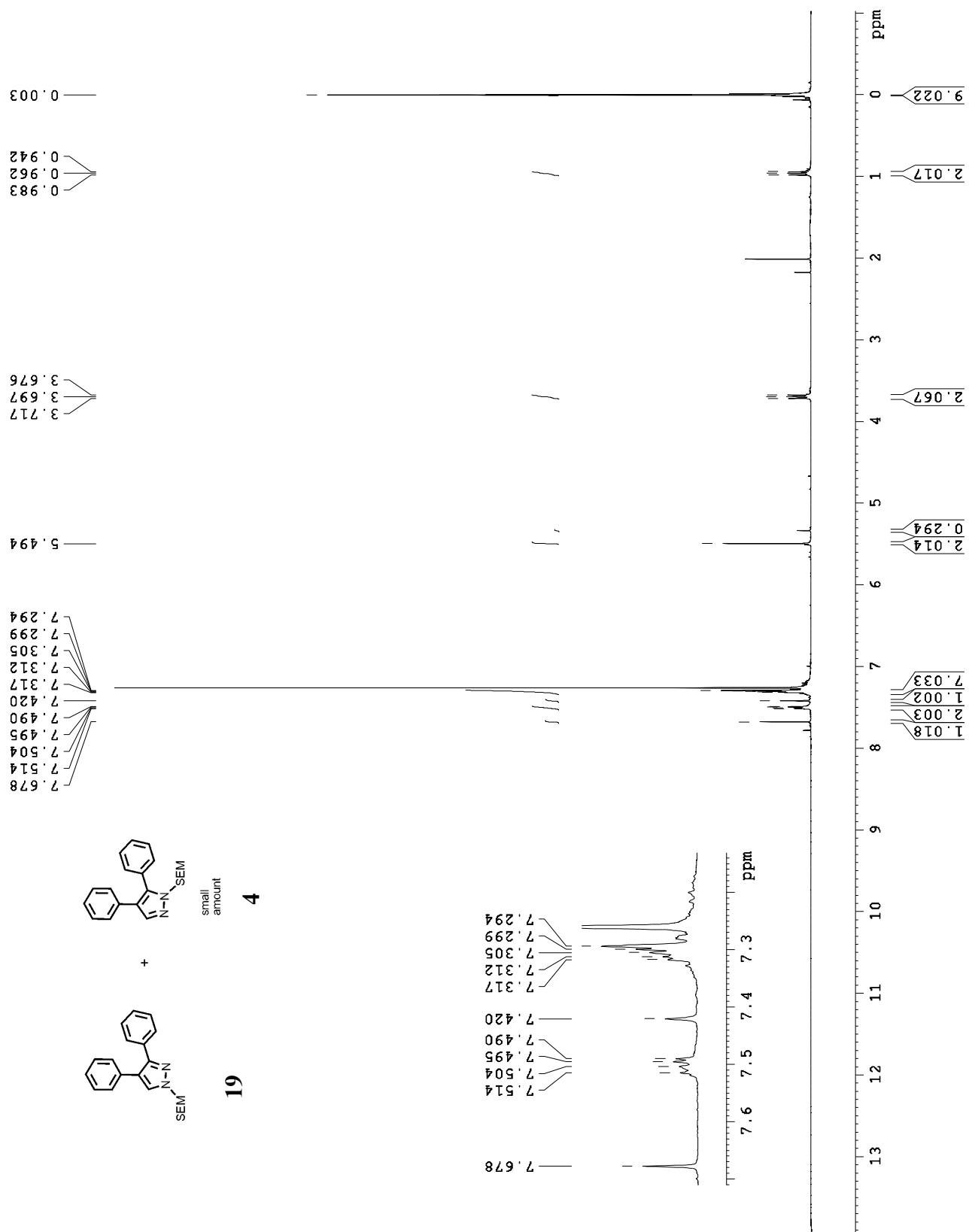


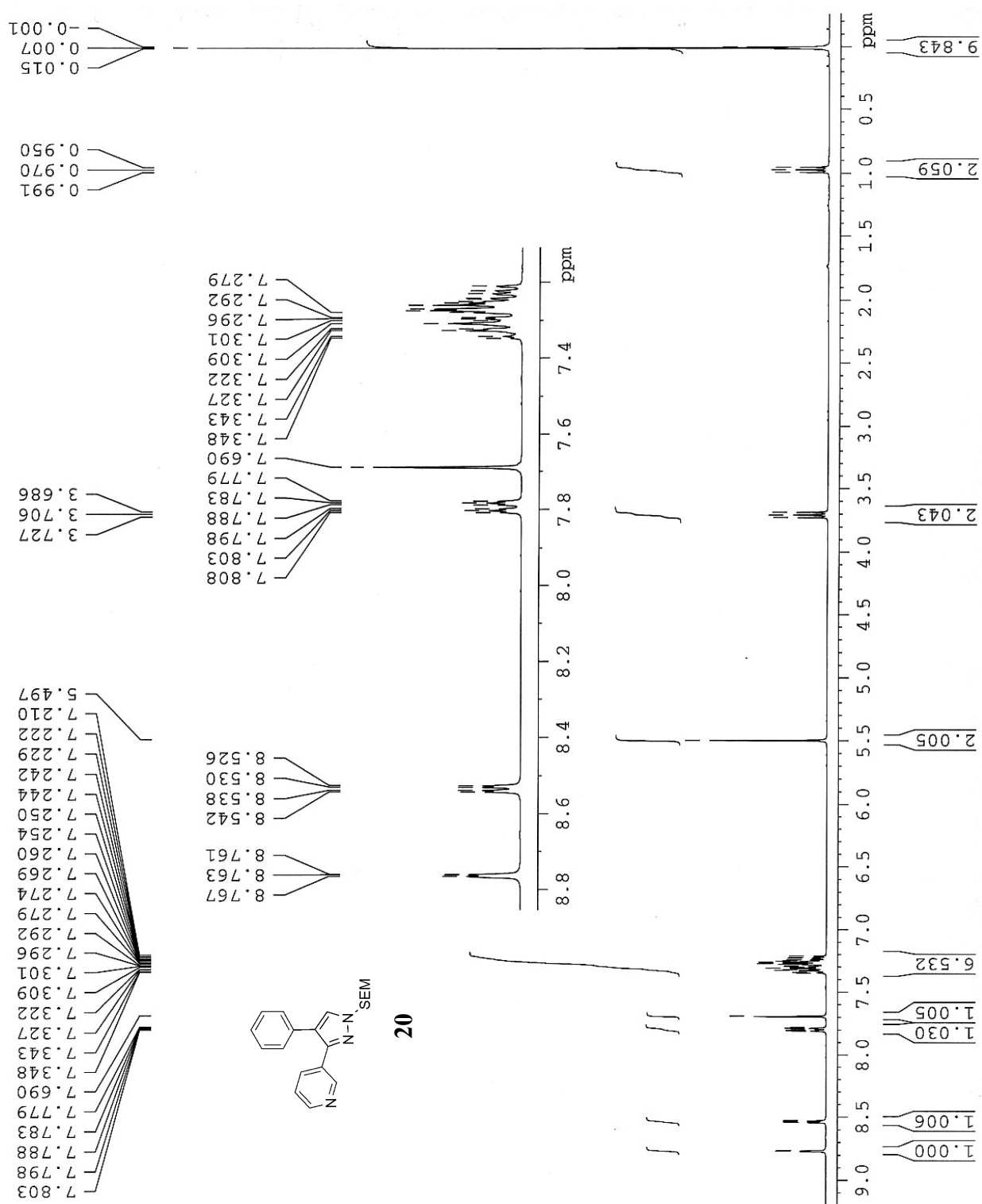


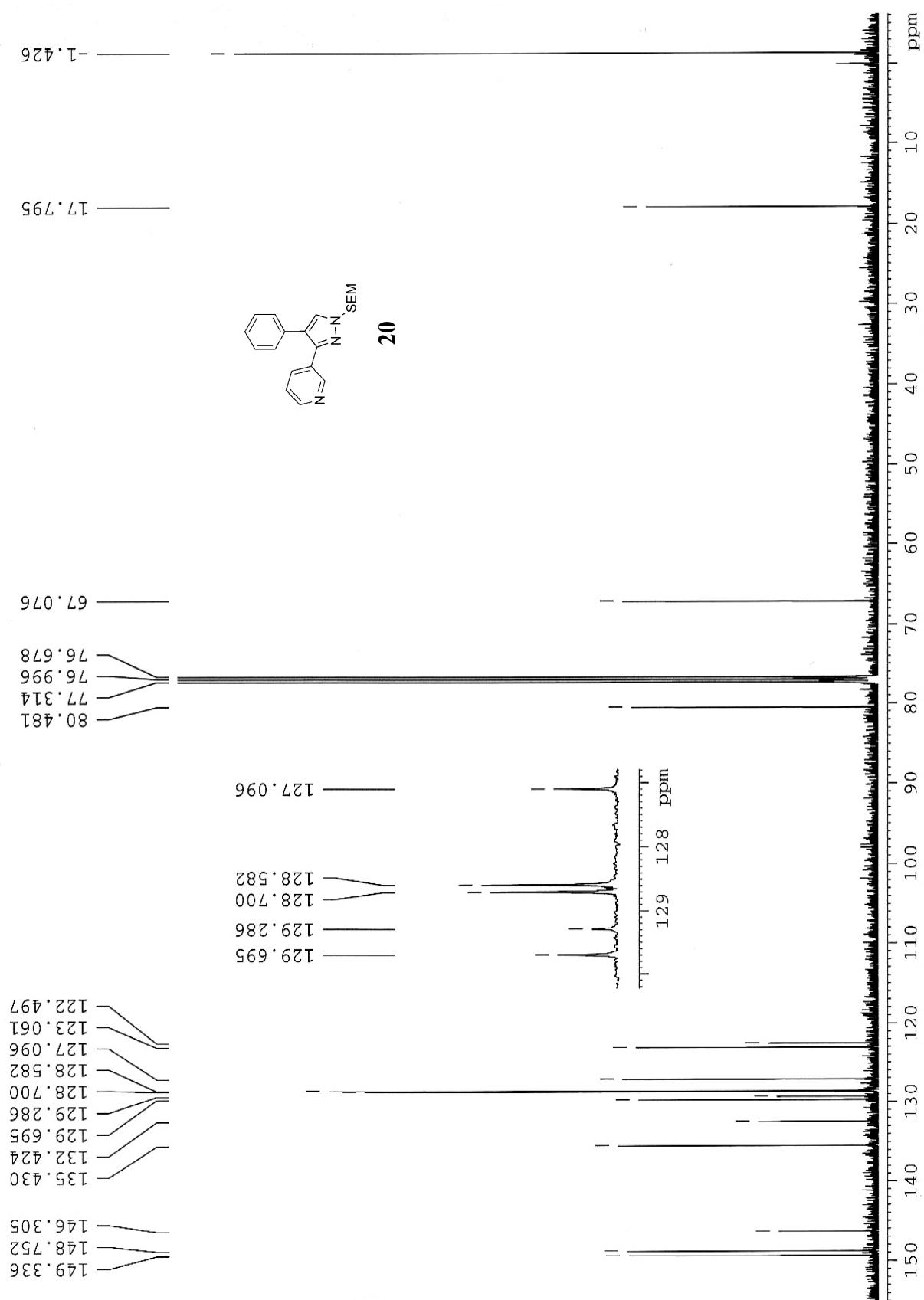


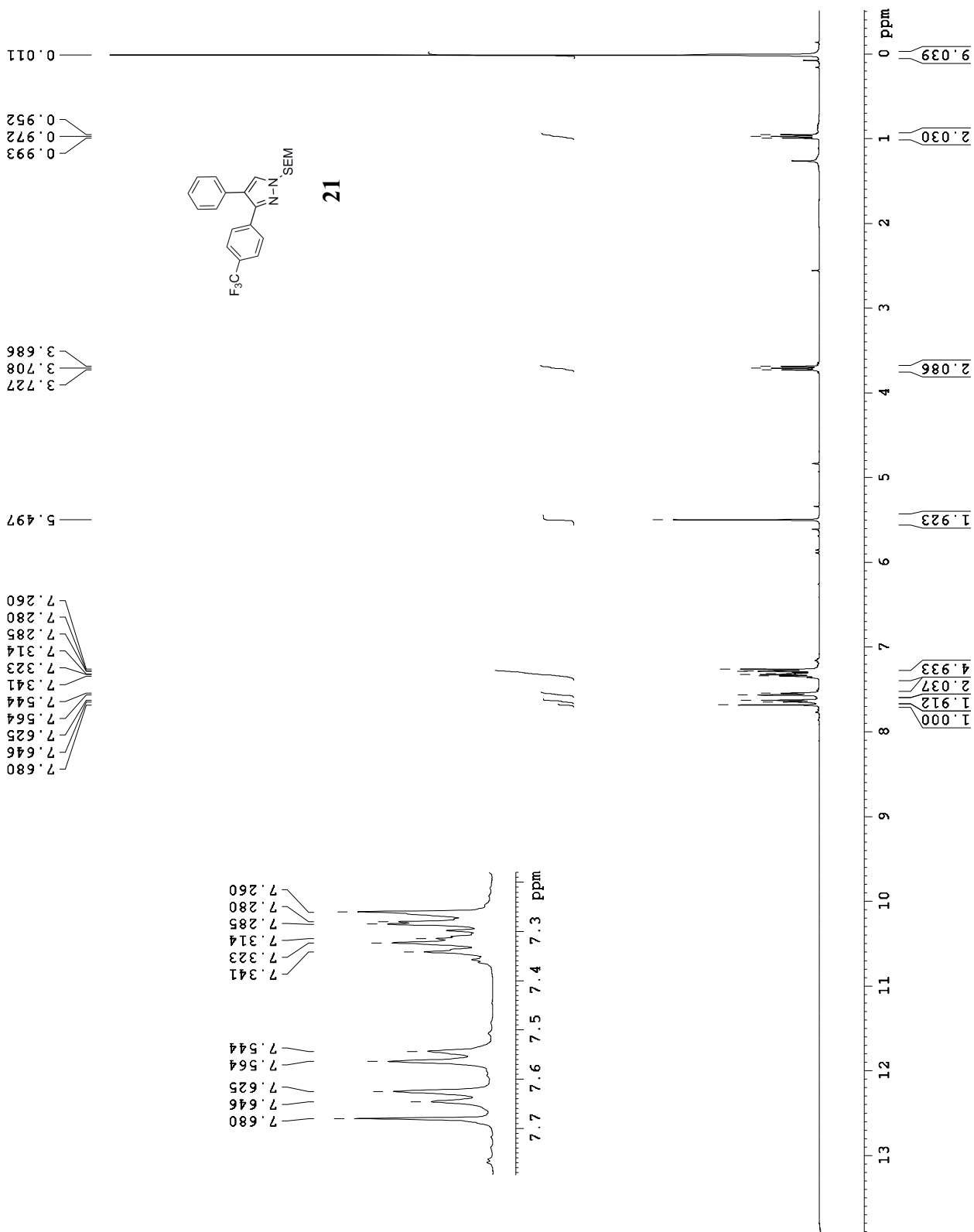


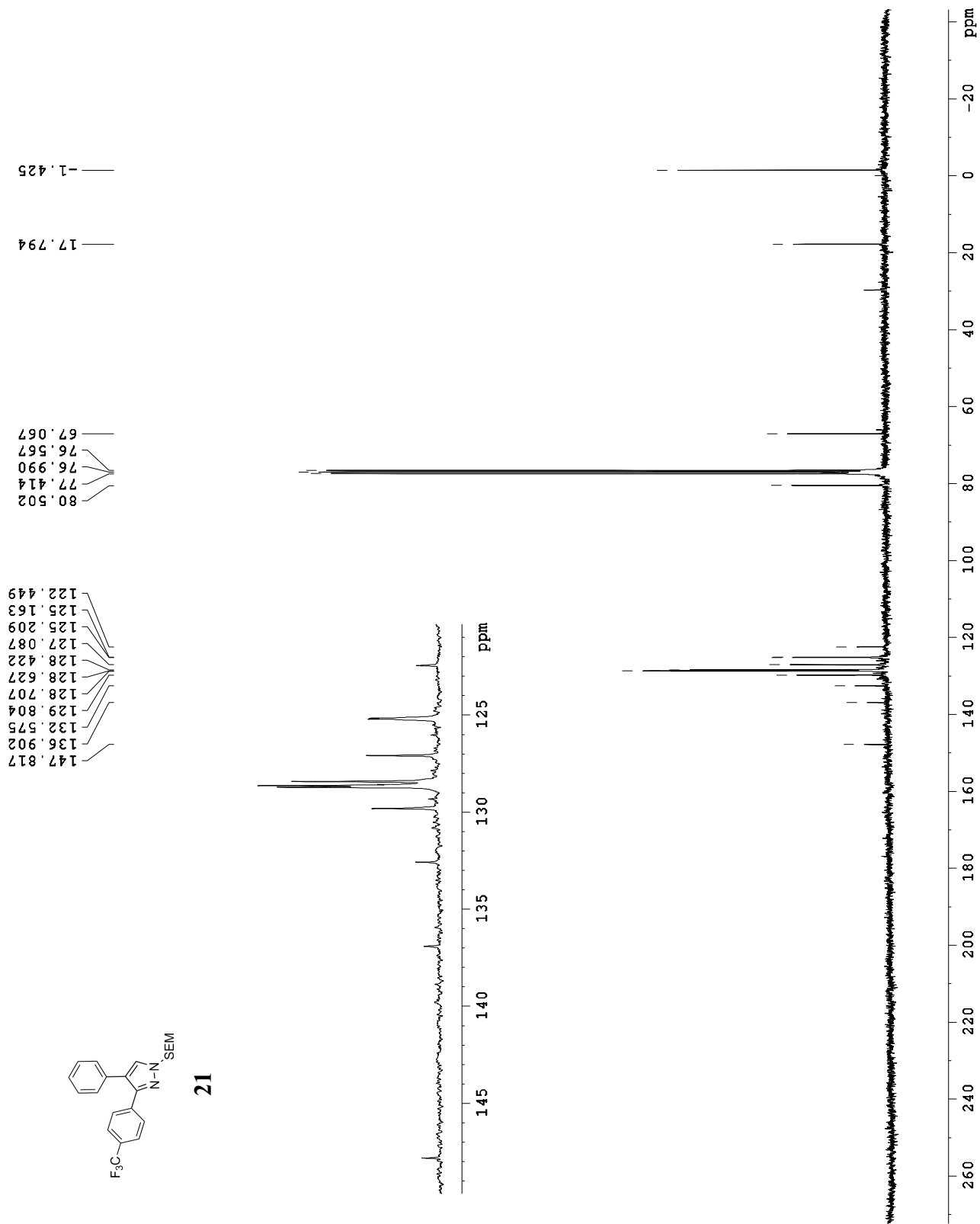


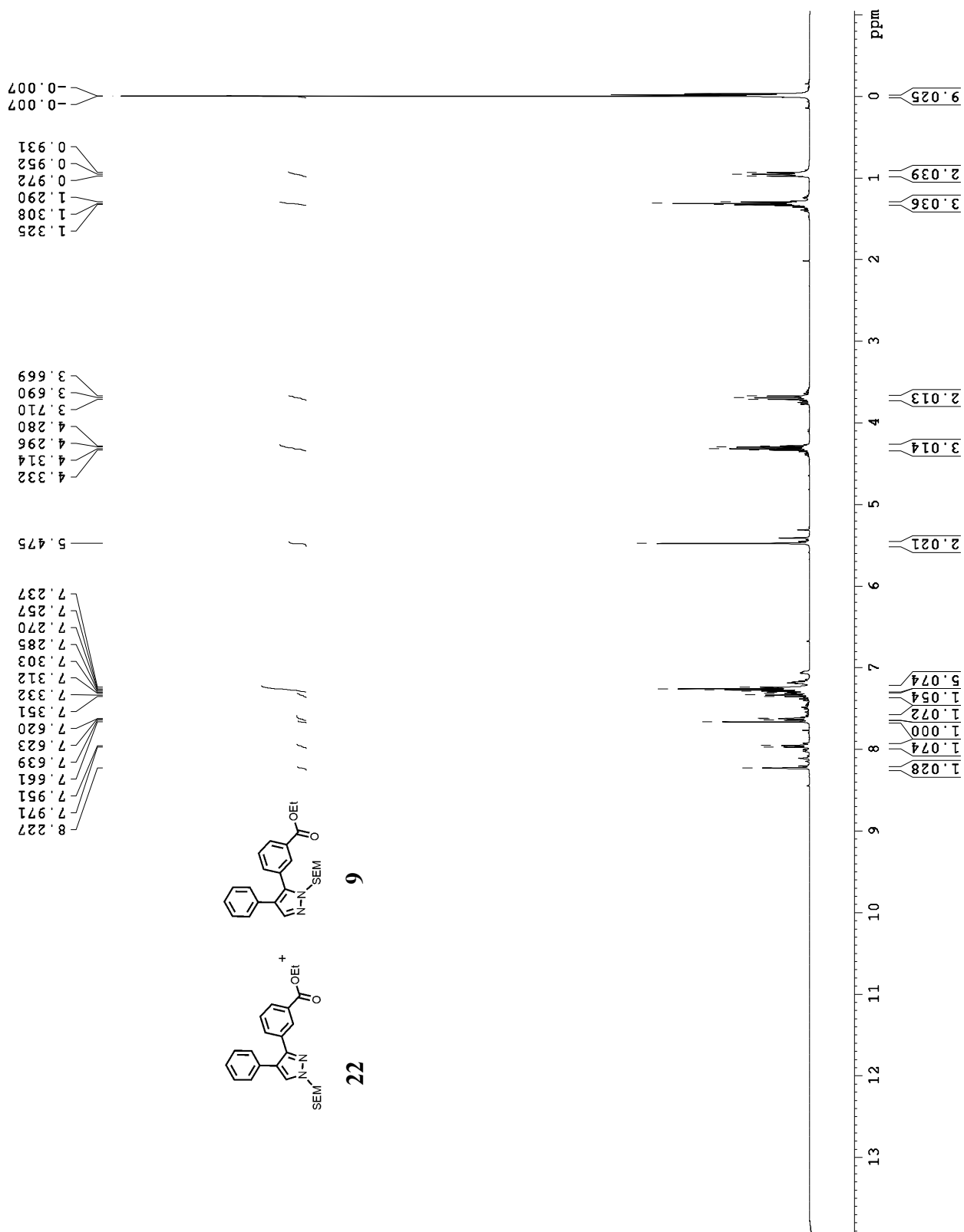


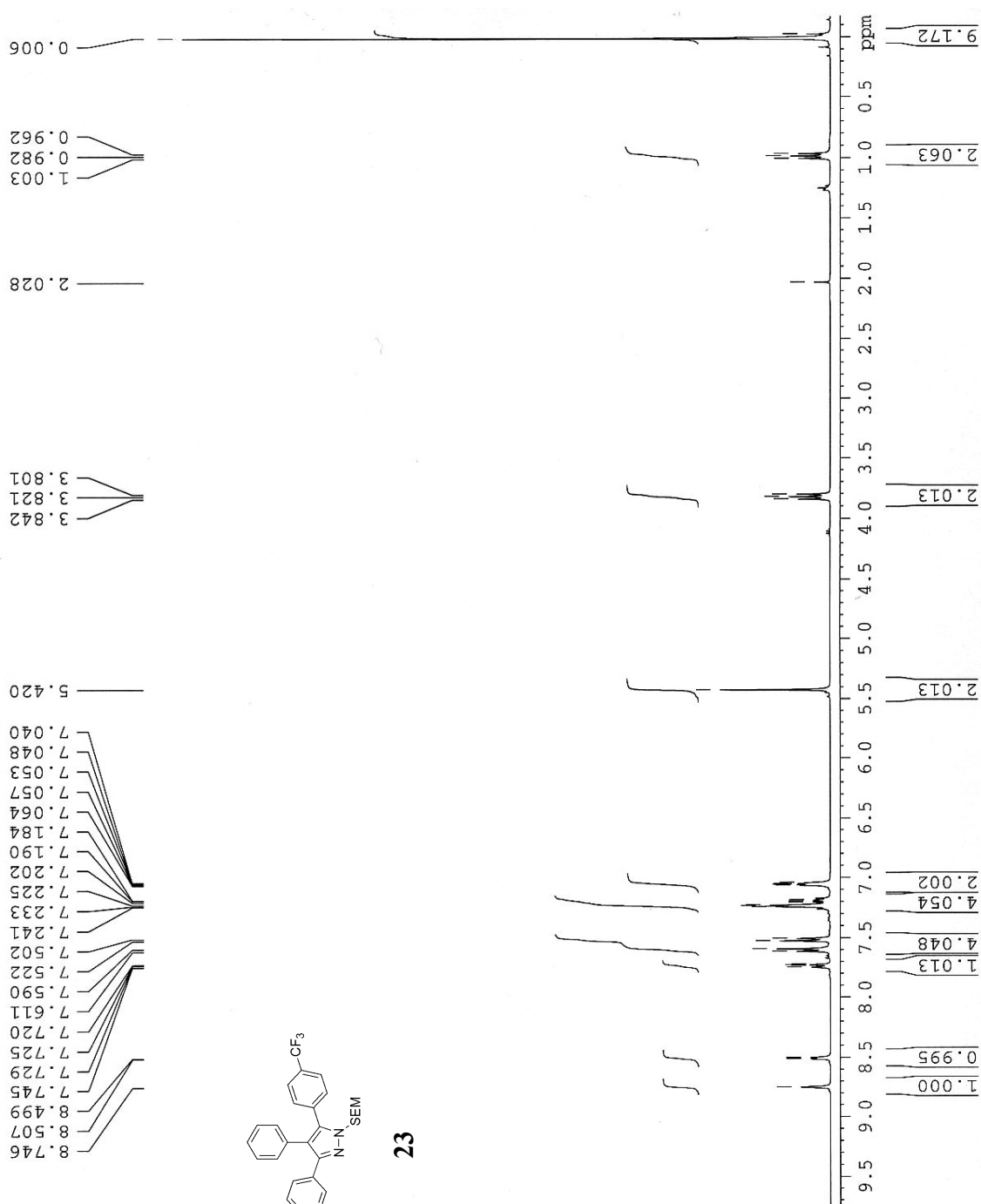


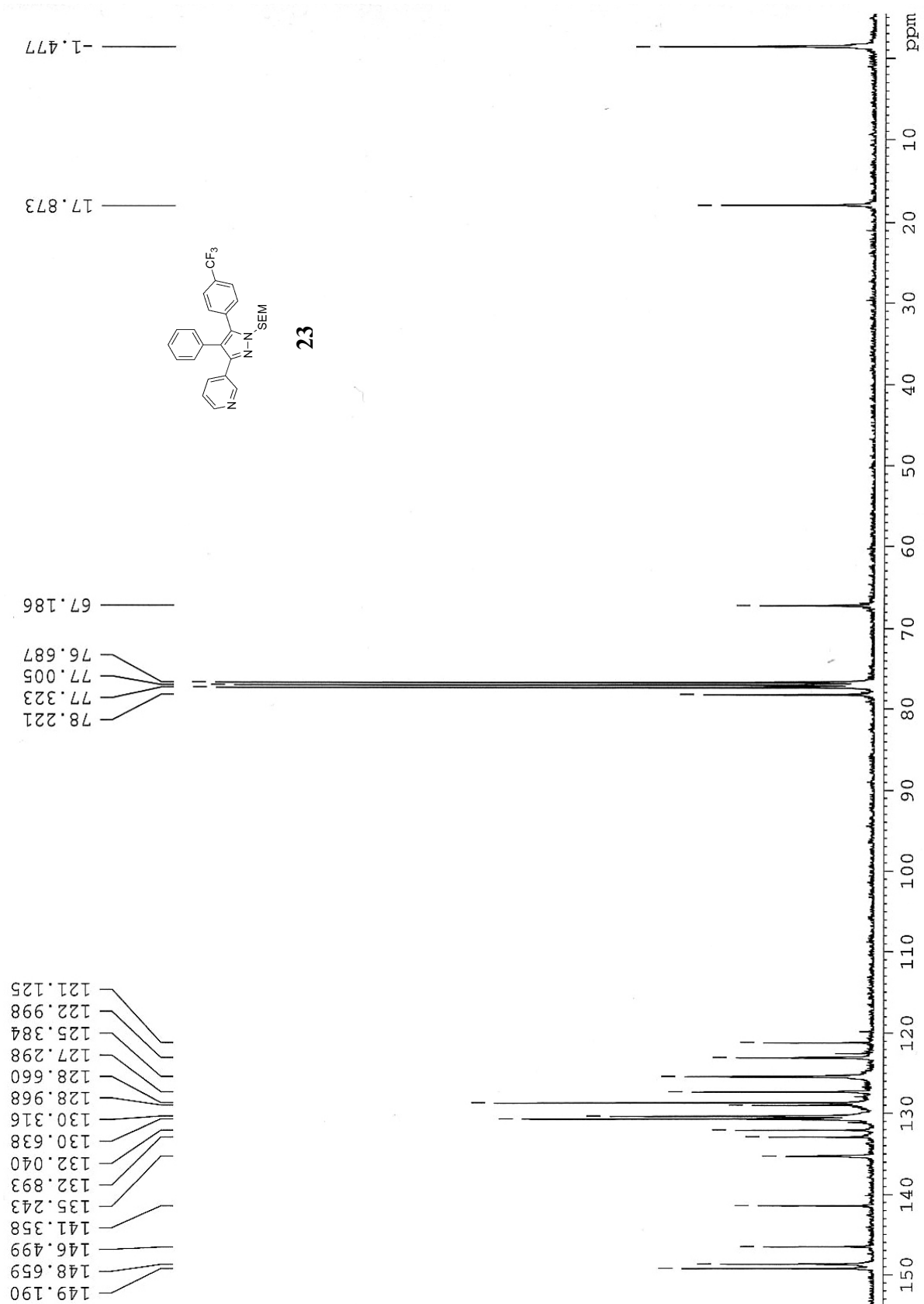


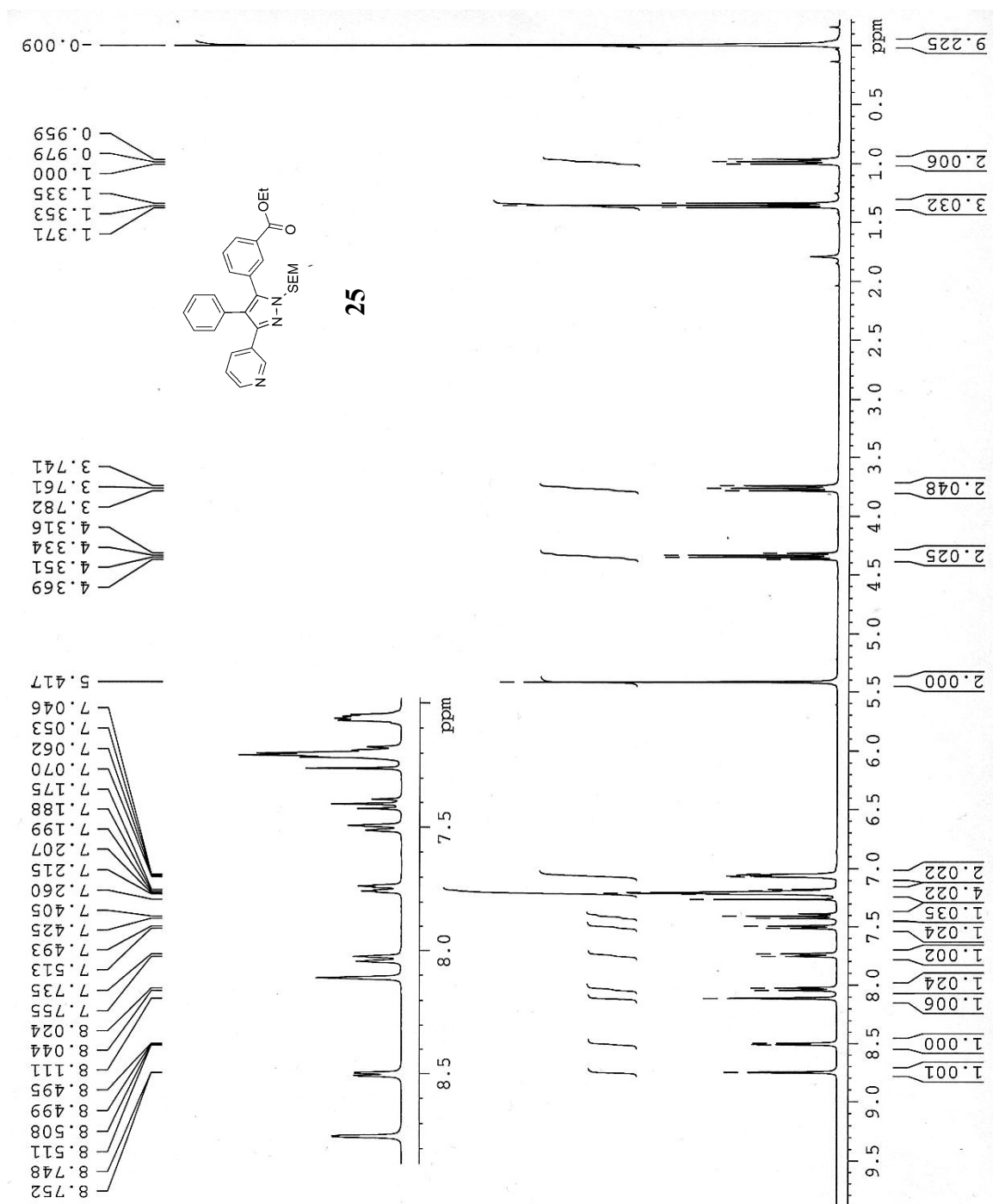


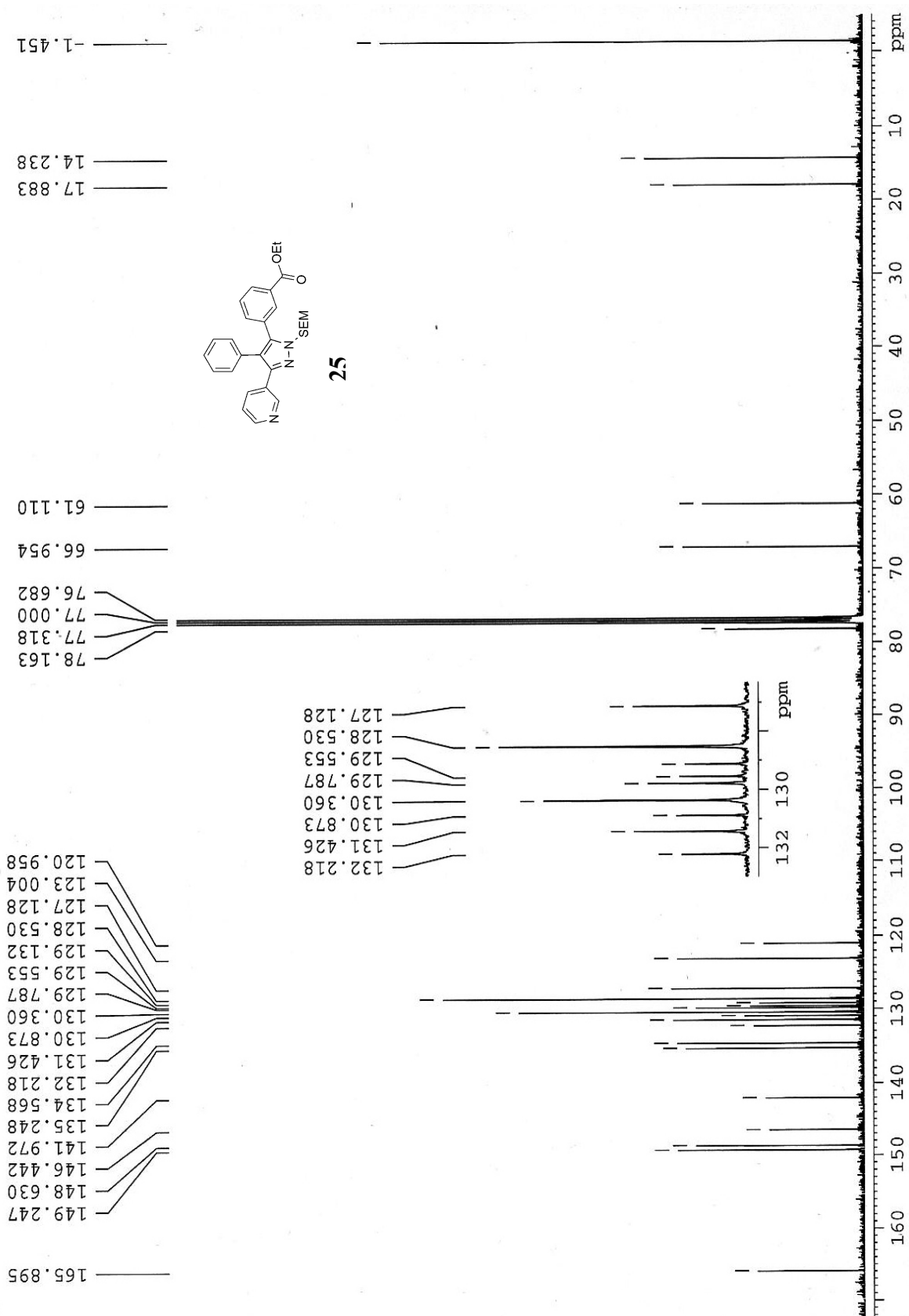


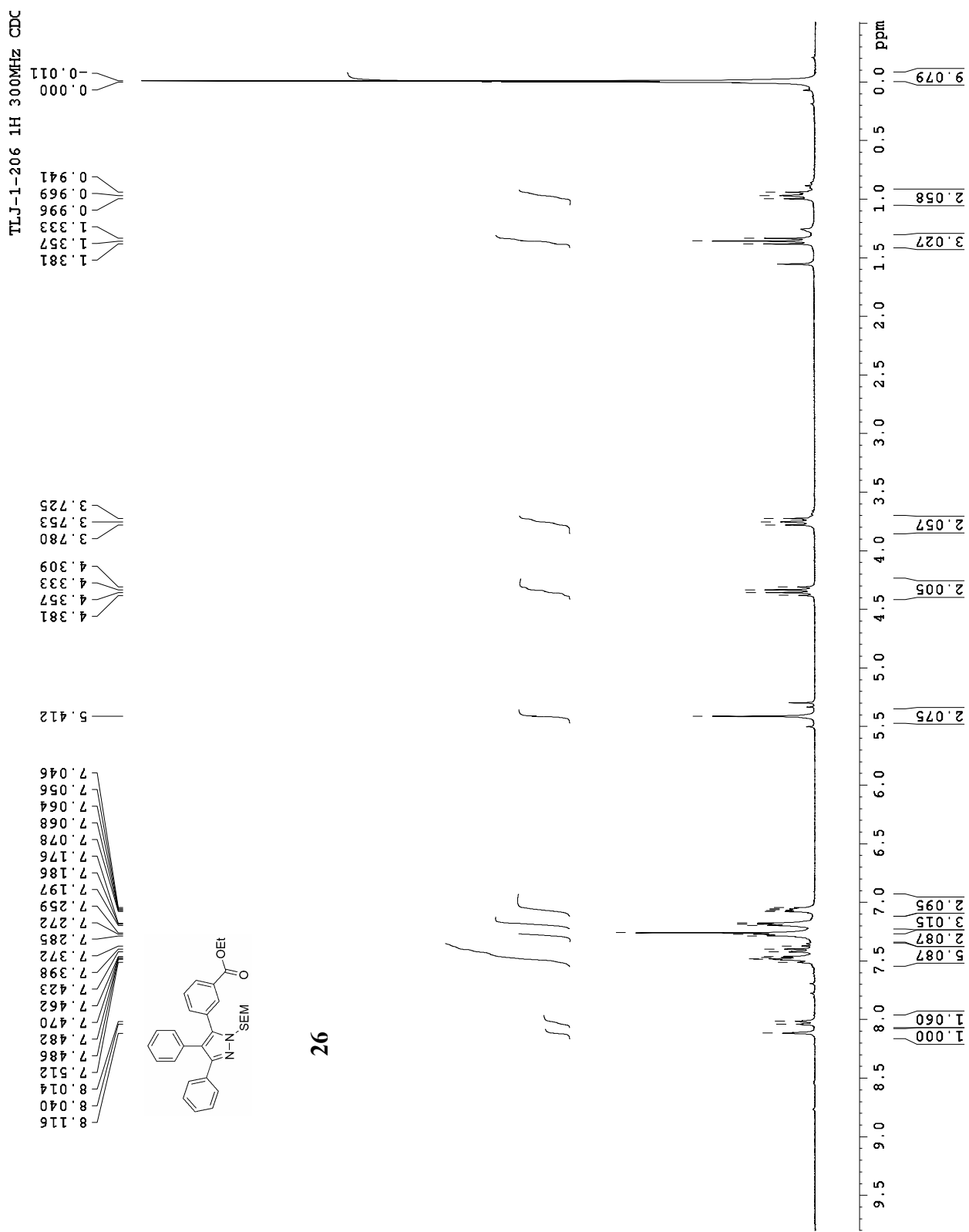




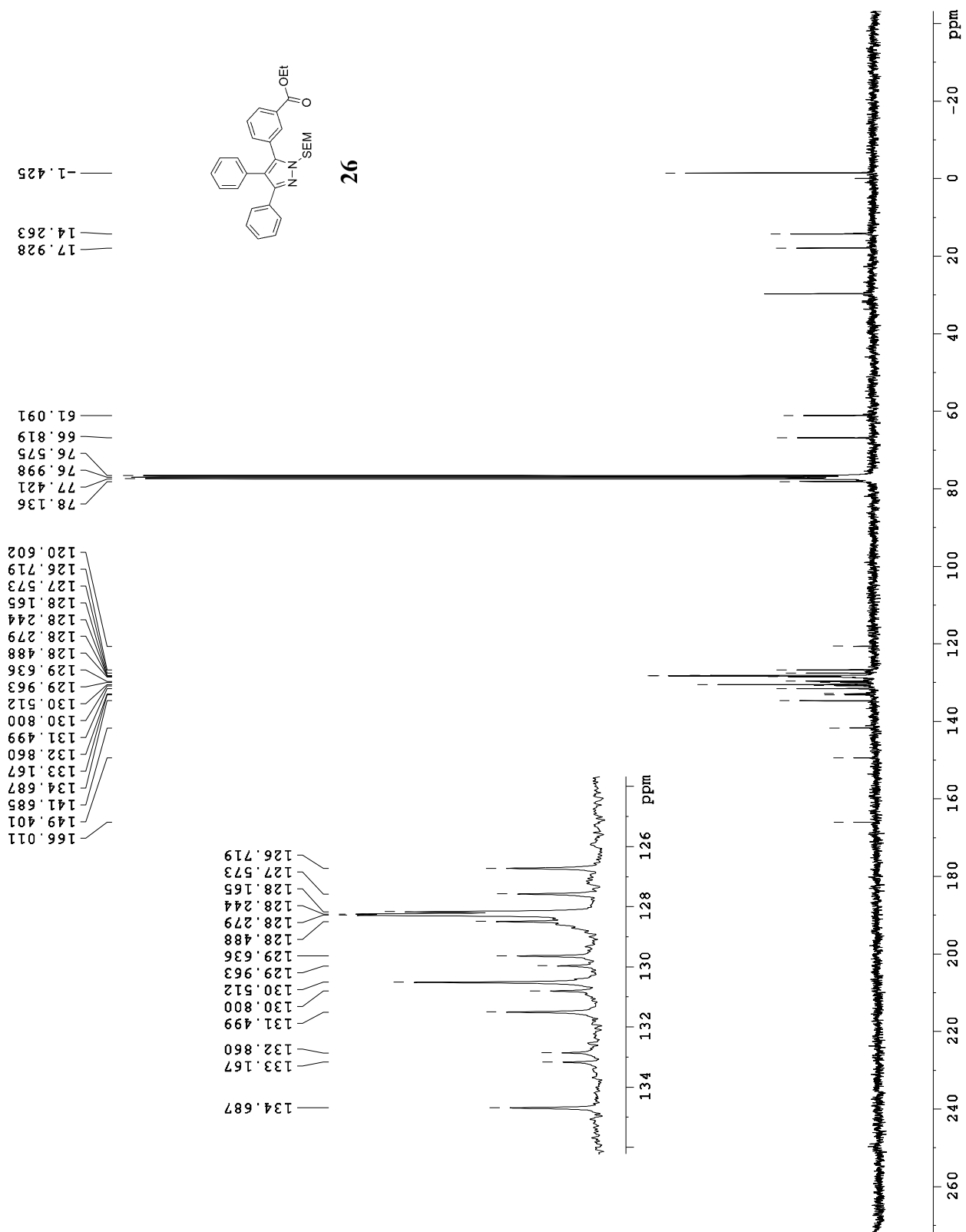


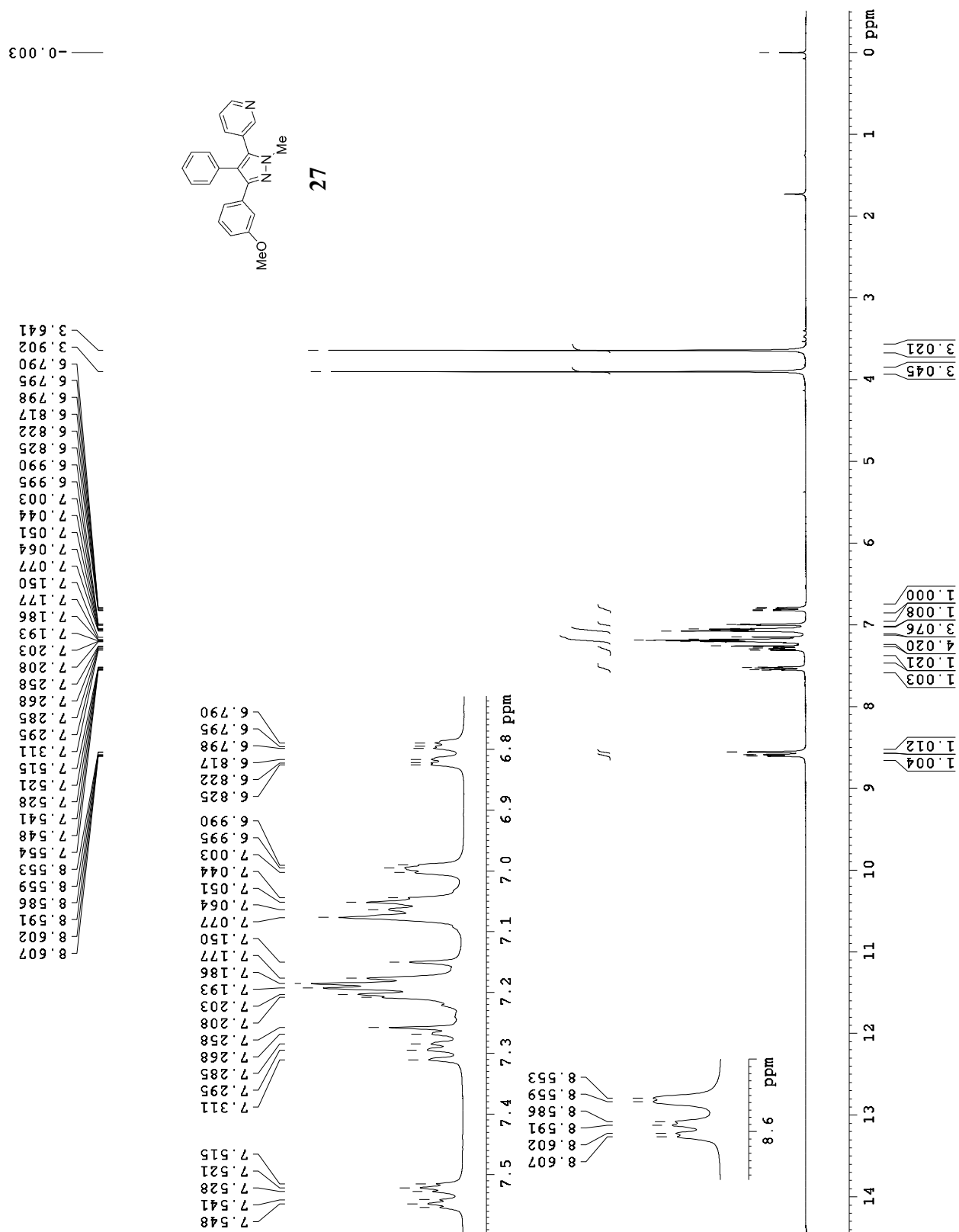


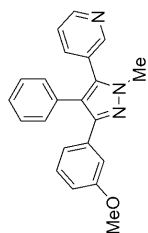




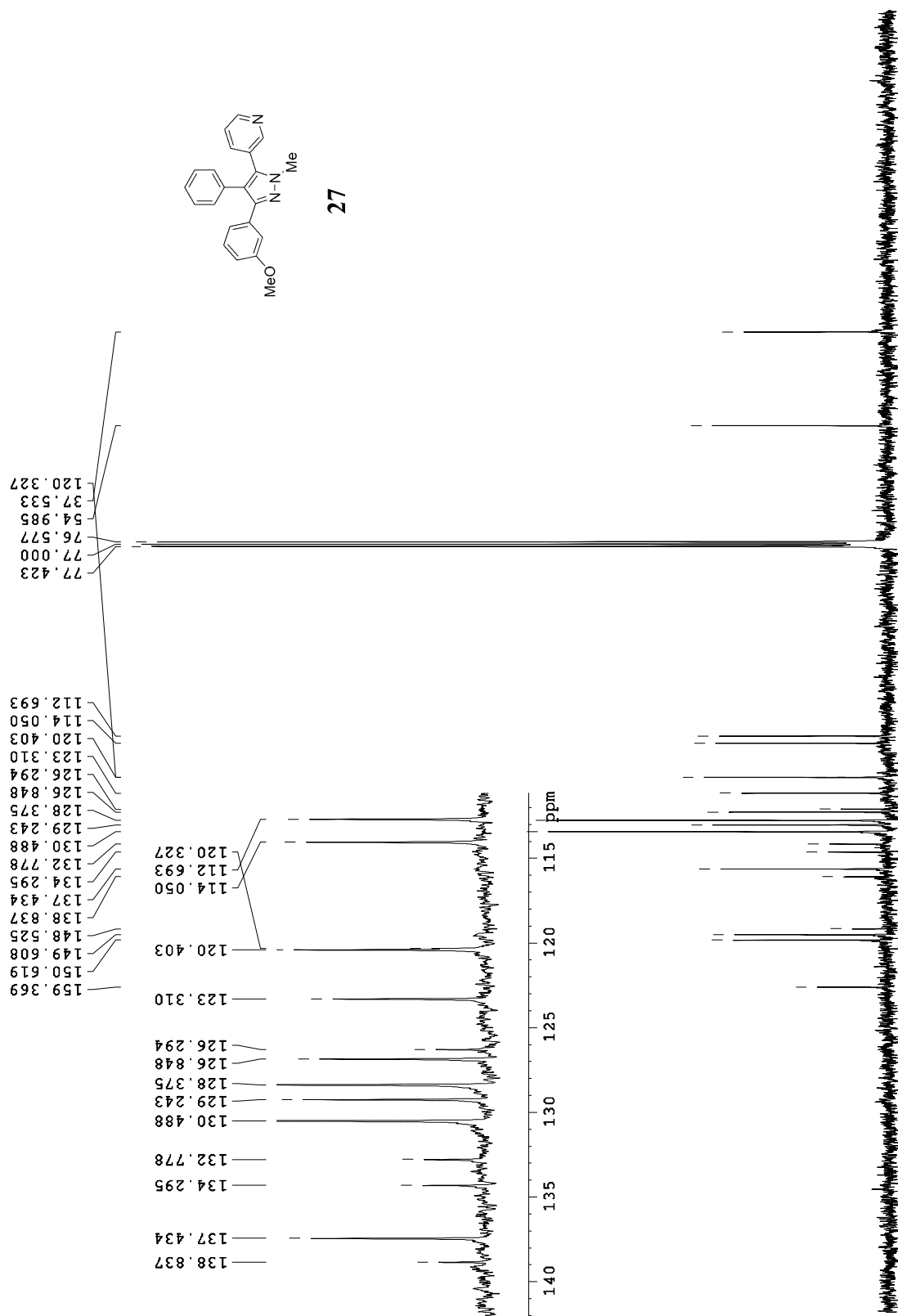
26

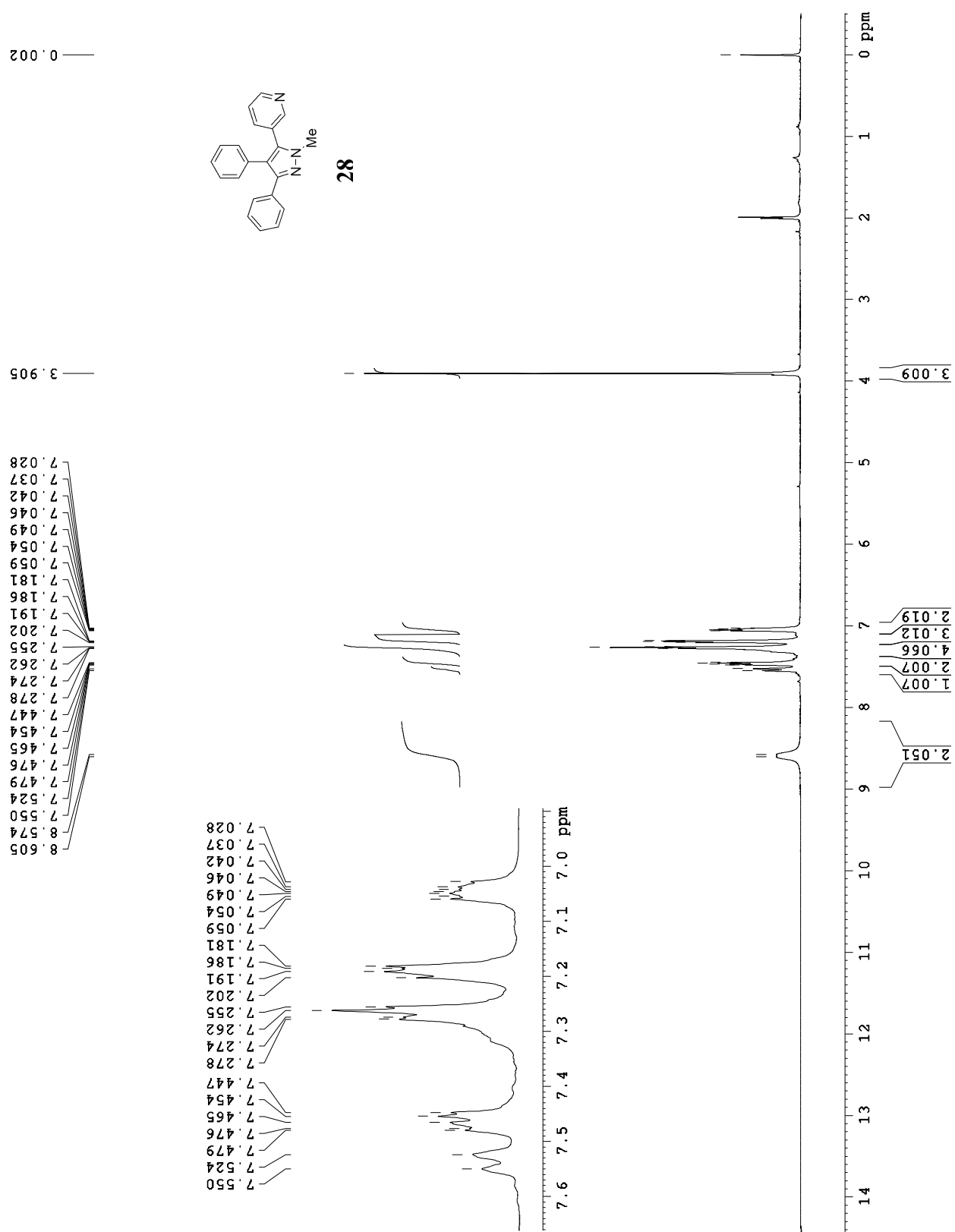


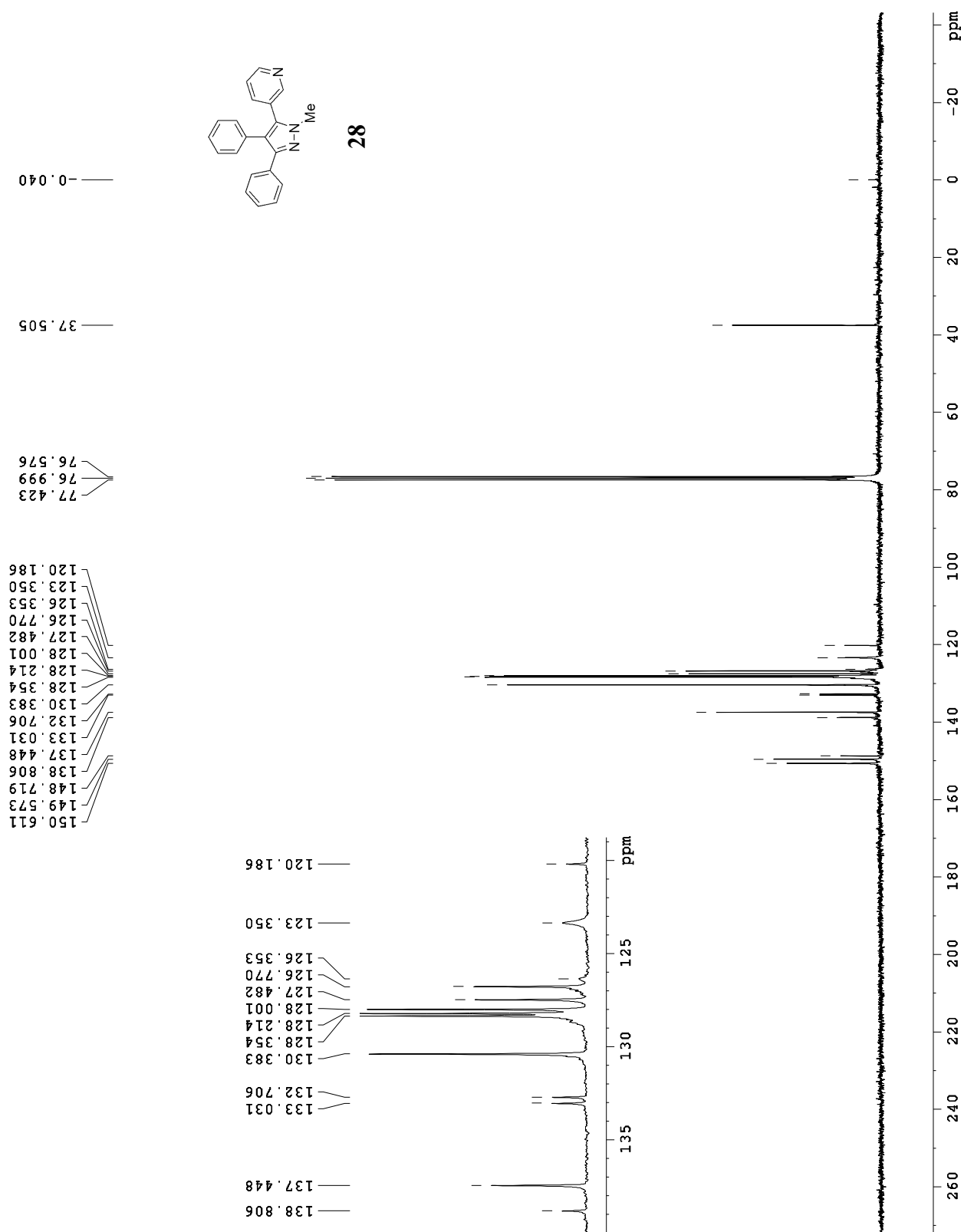


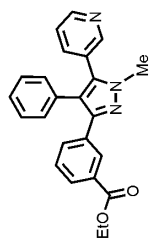


27

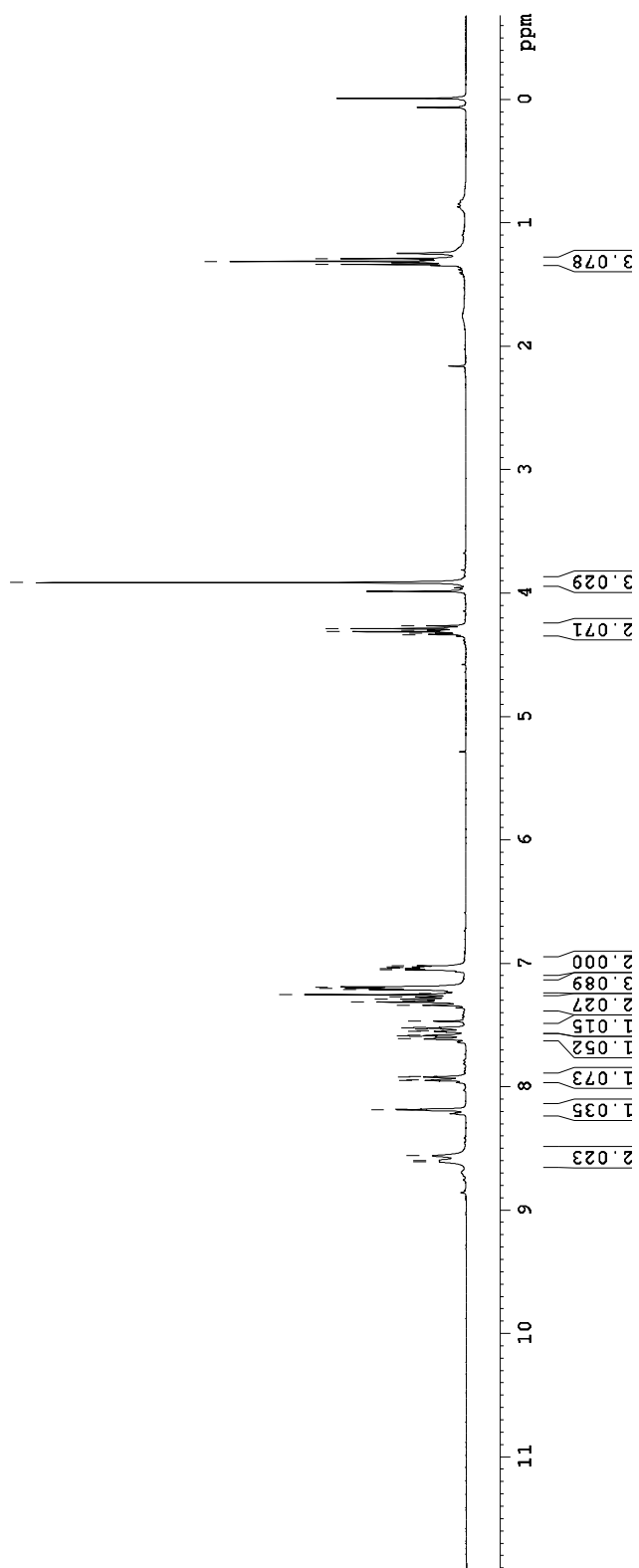


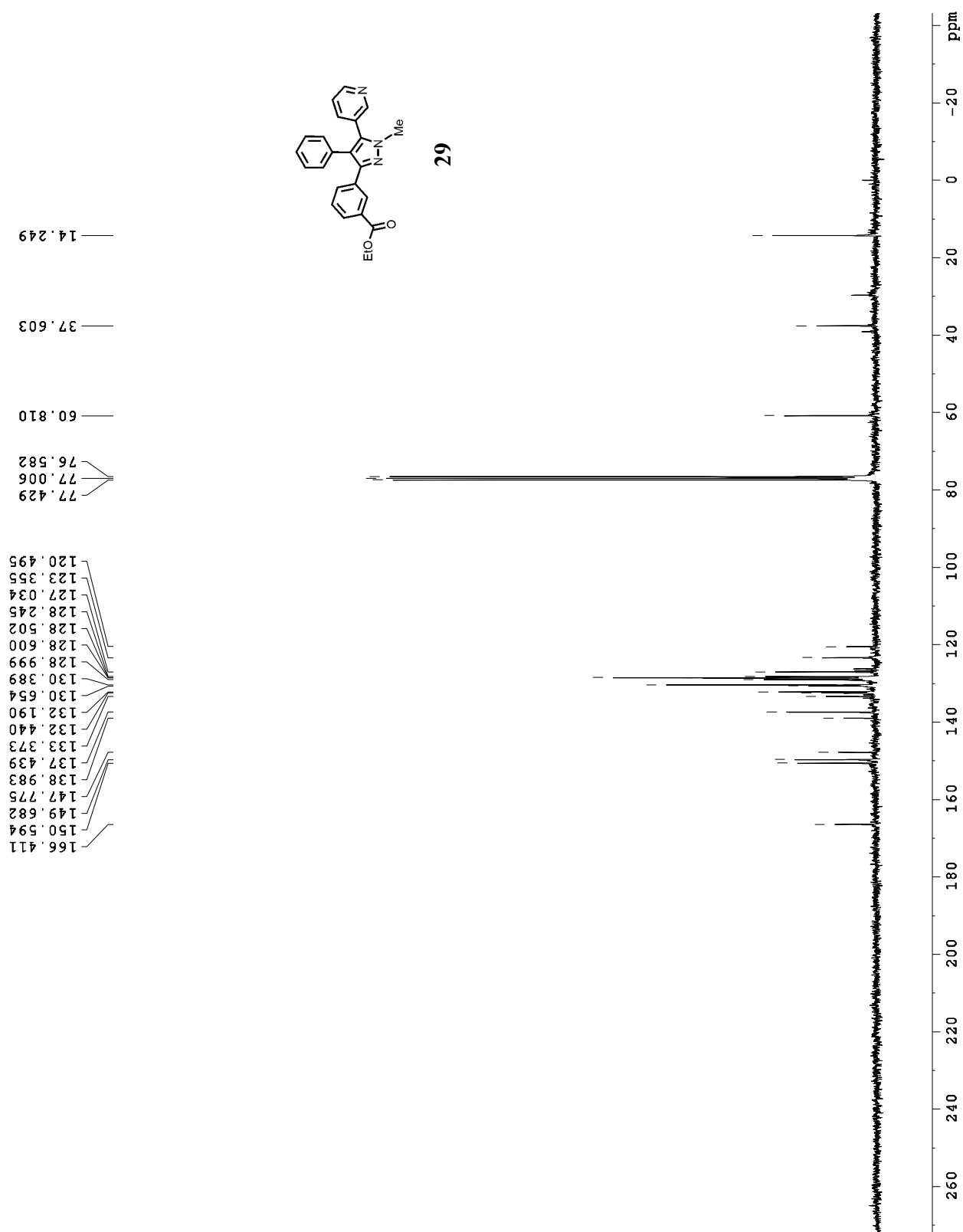


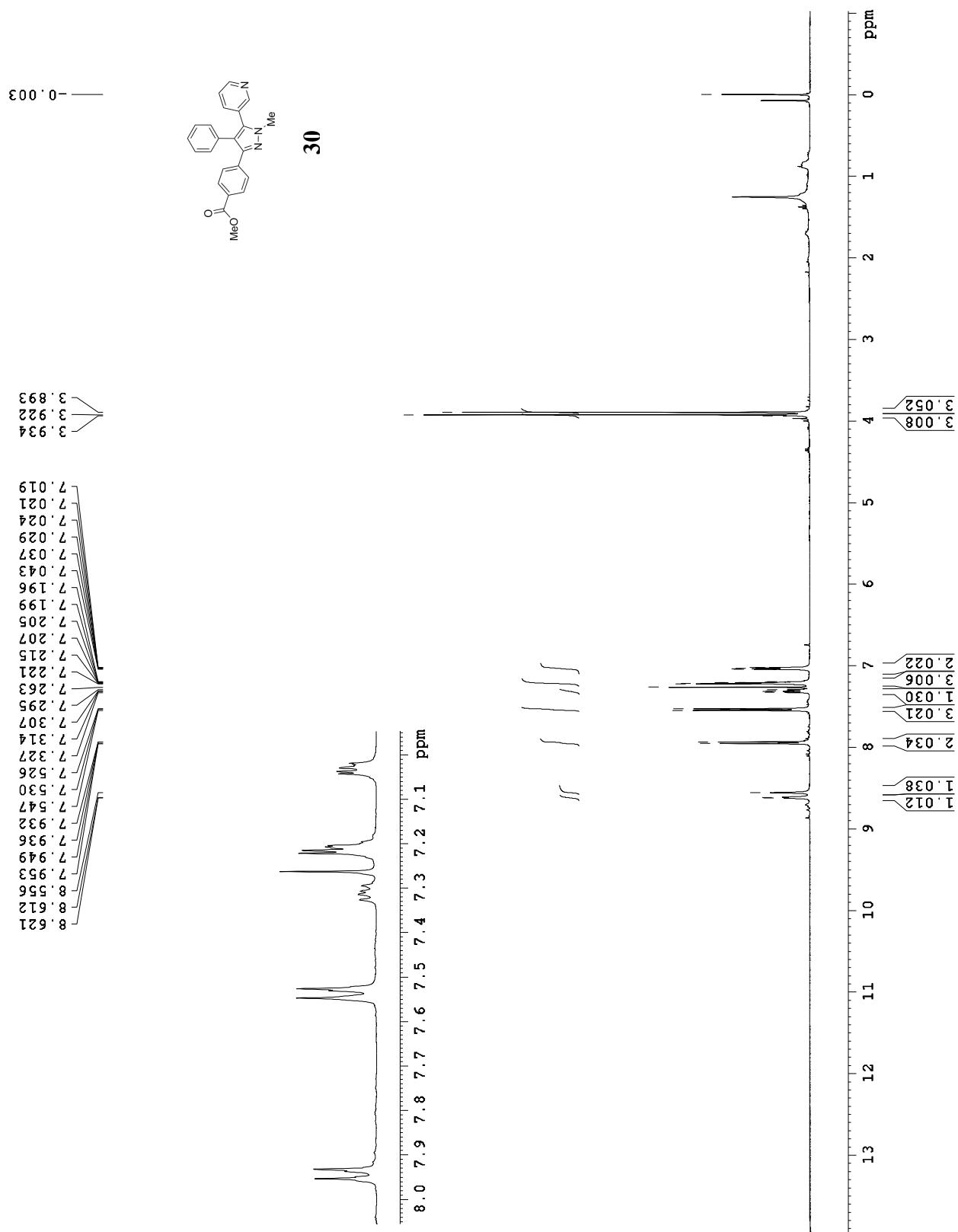


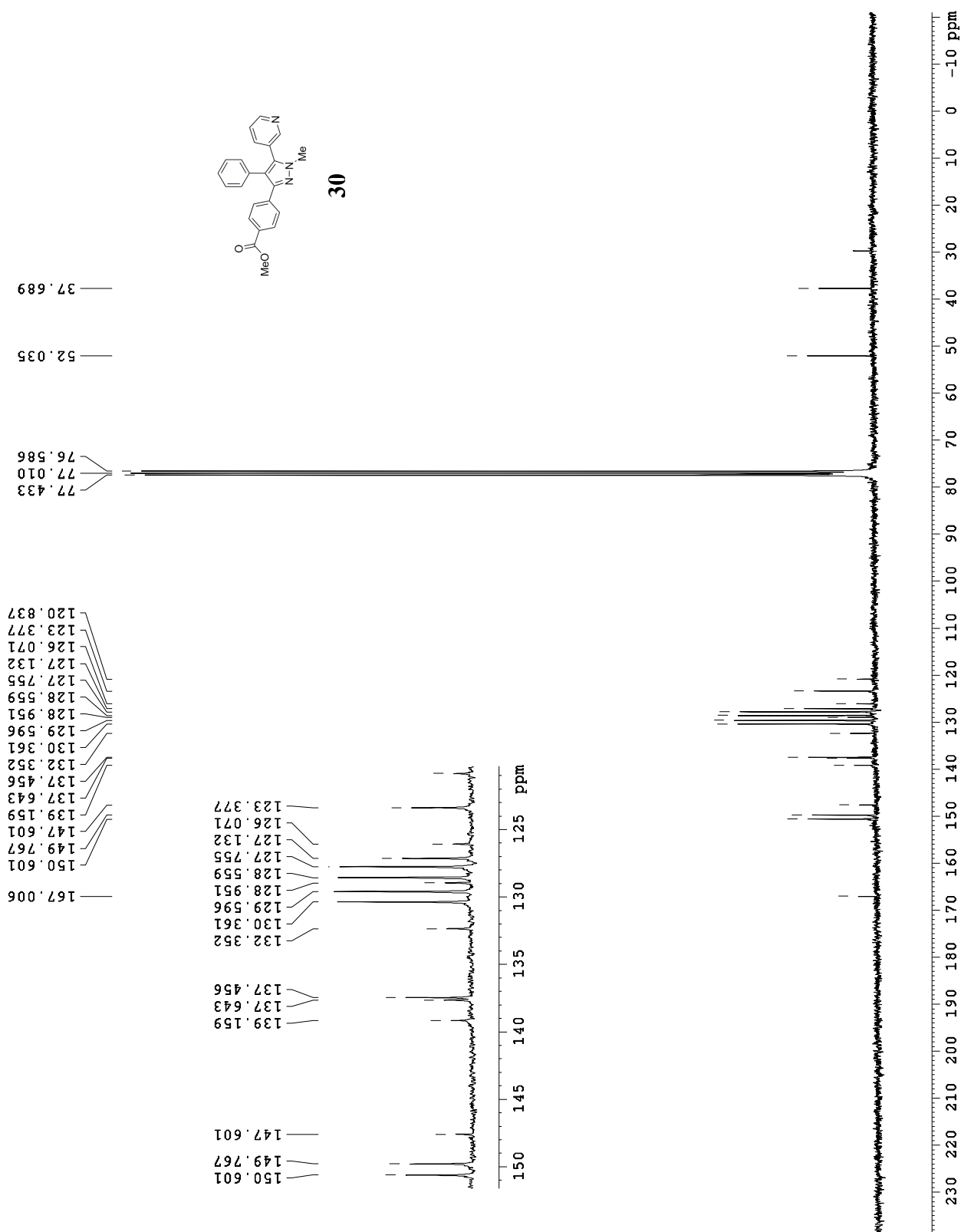
TLJ-1-218 1H 300MHz CDCl₃1.337
1.313
1.2898.607
8.598
8.559
8.188
8.183
7.949
7.945
7.923
7.919
7.613
7.591
7.586
7.582
7.552
7.546
7.532
7.526
7.520
7.471
7.340
7.315
7.303
7.290
7.273
7.255
7.243
7.214
7.203
7.193
7.054
7.044
7.040
7.036
7.032
7.022
4.336
4.326
4.313
4.303
4.289
4.265
3.915

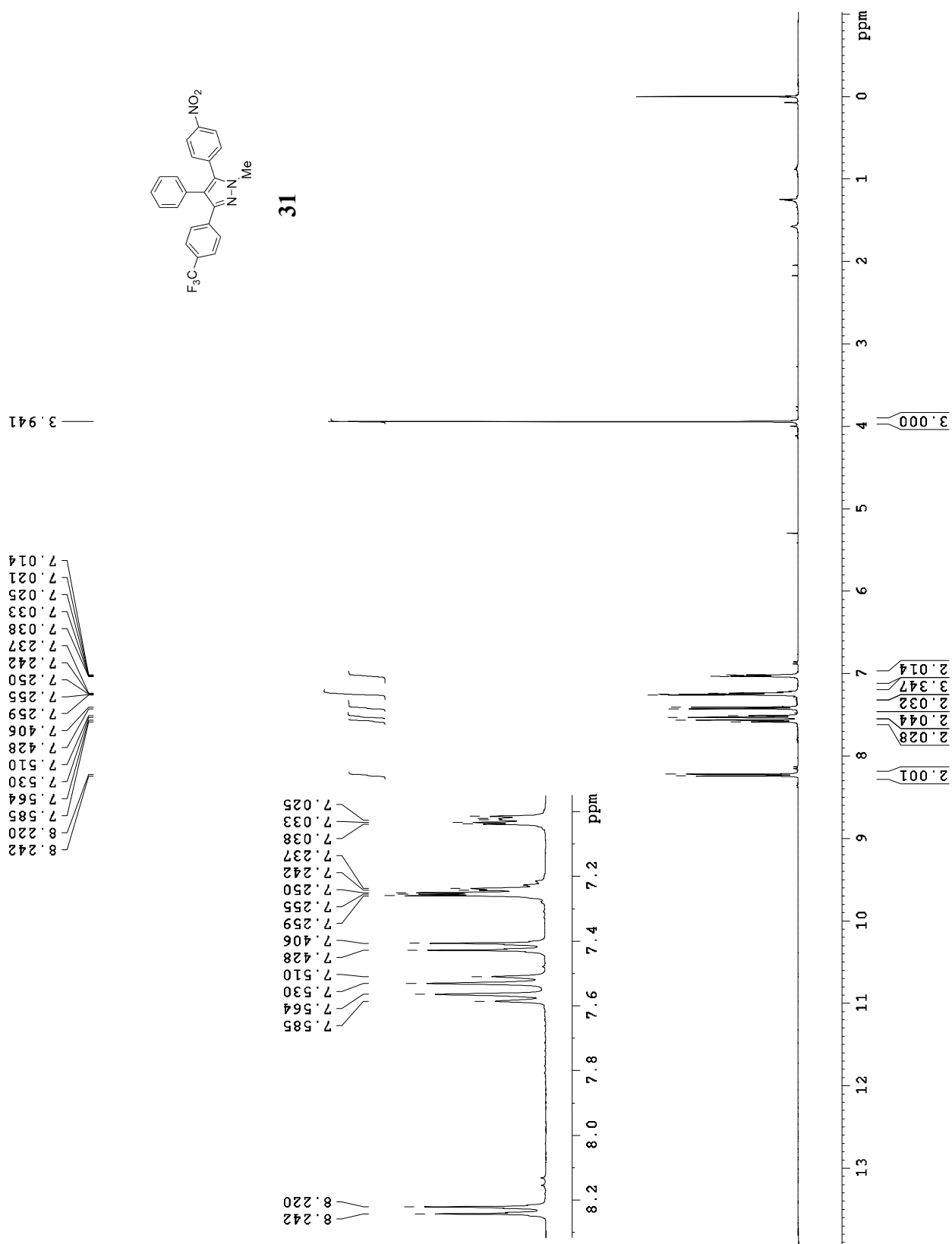
29

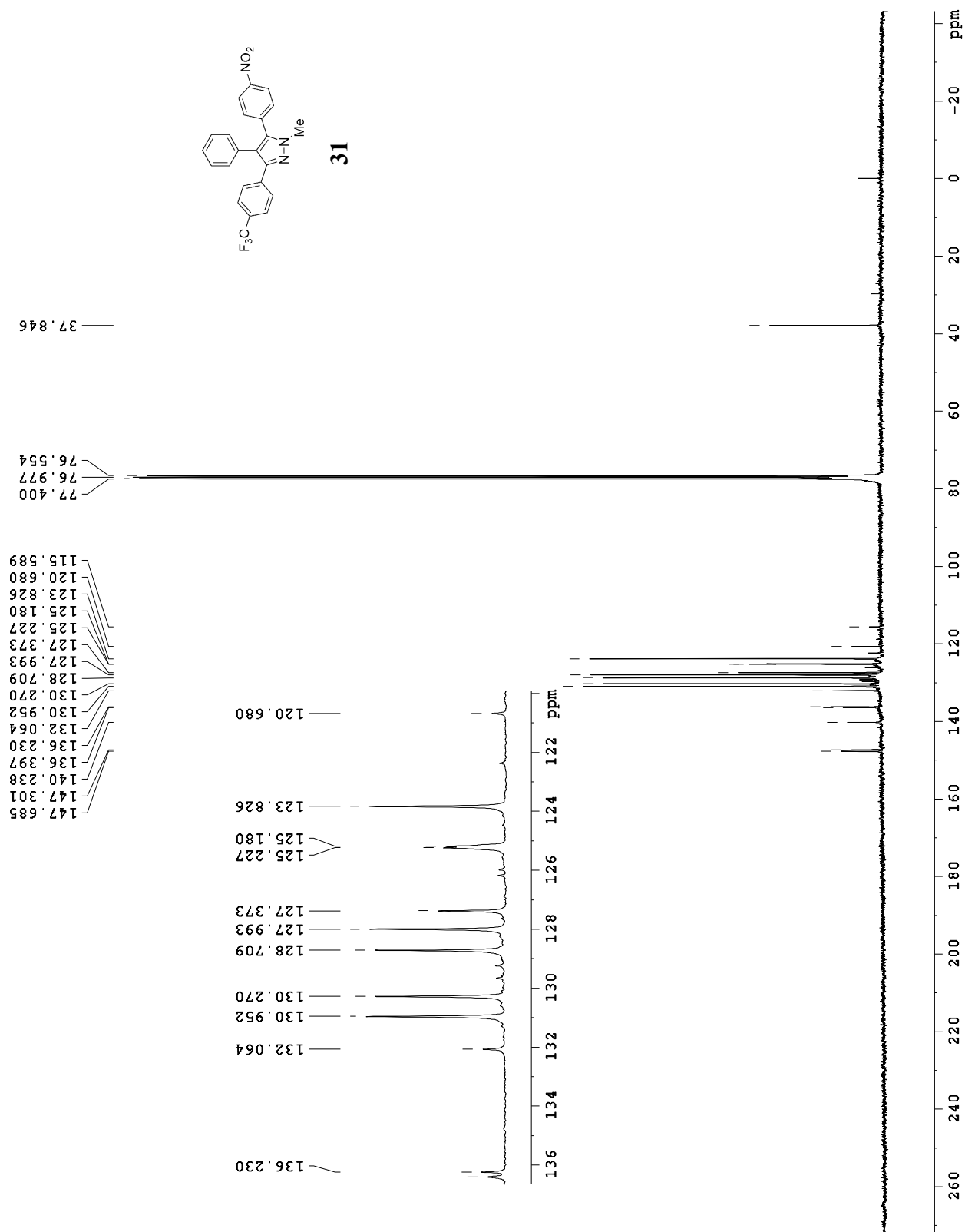


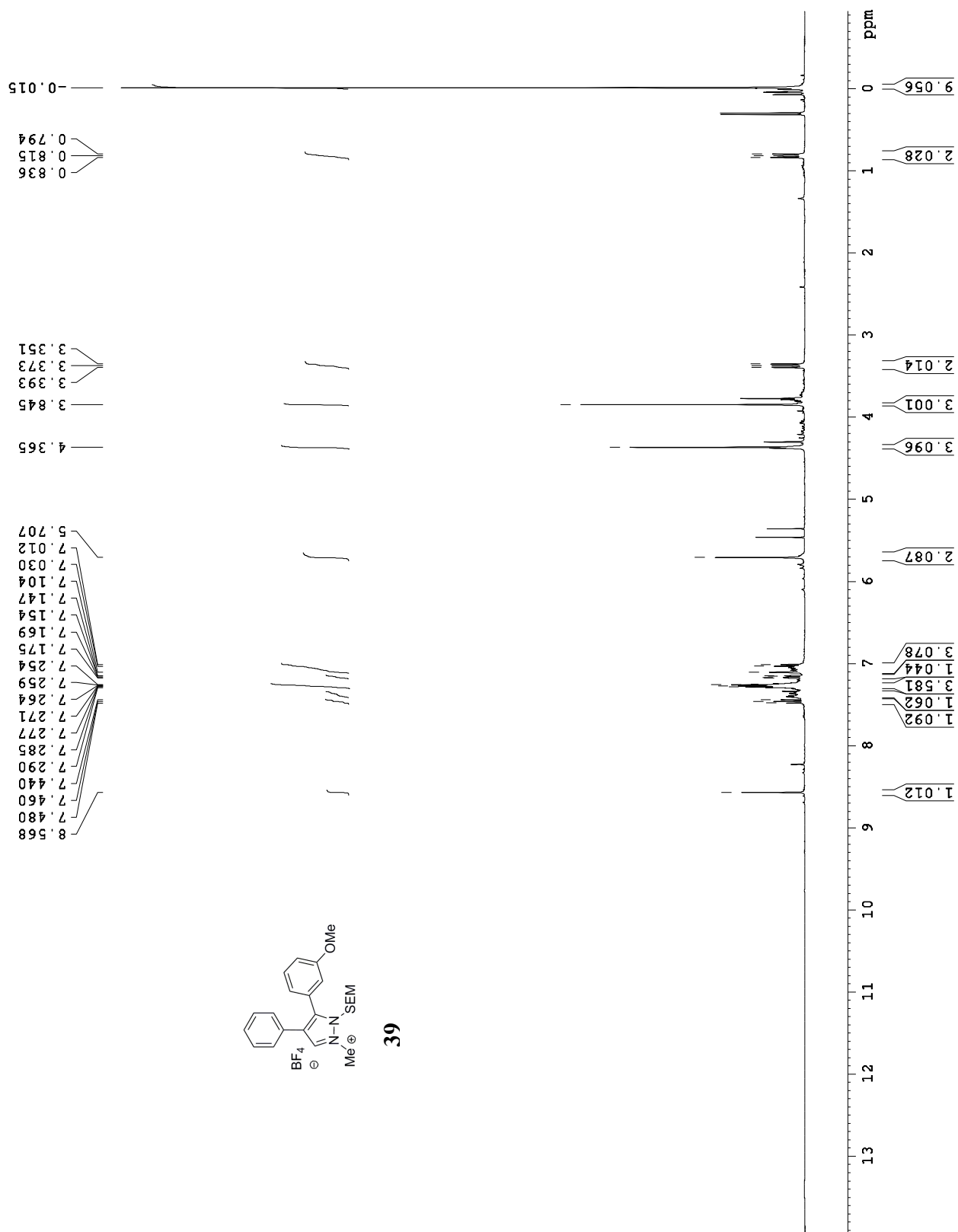


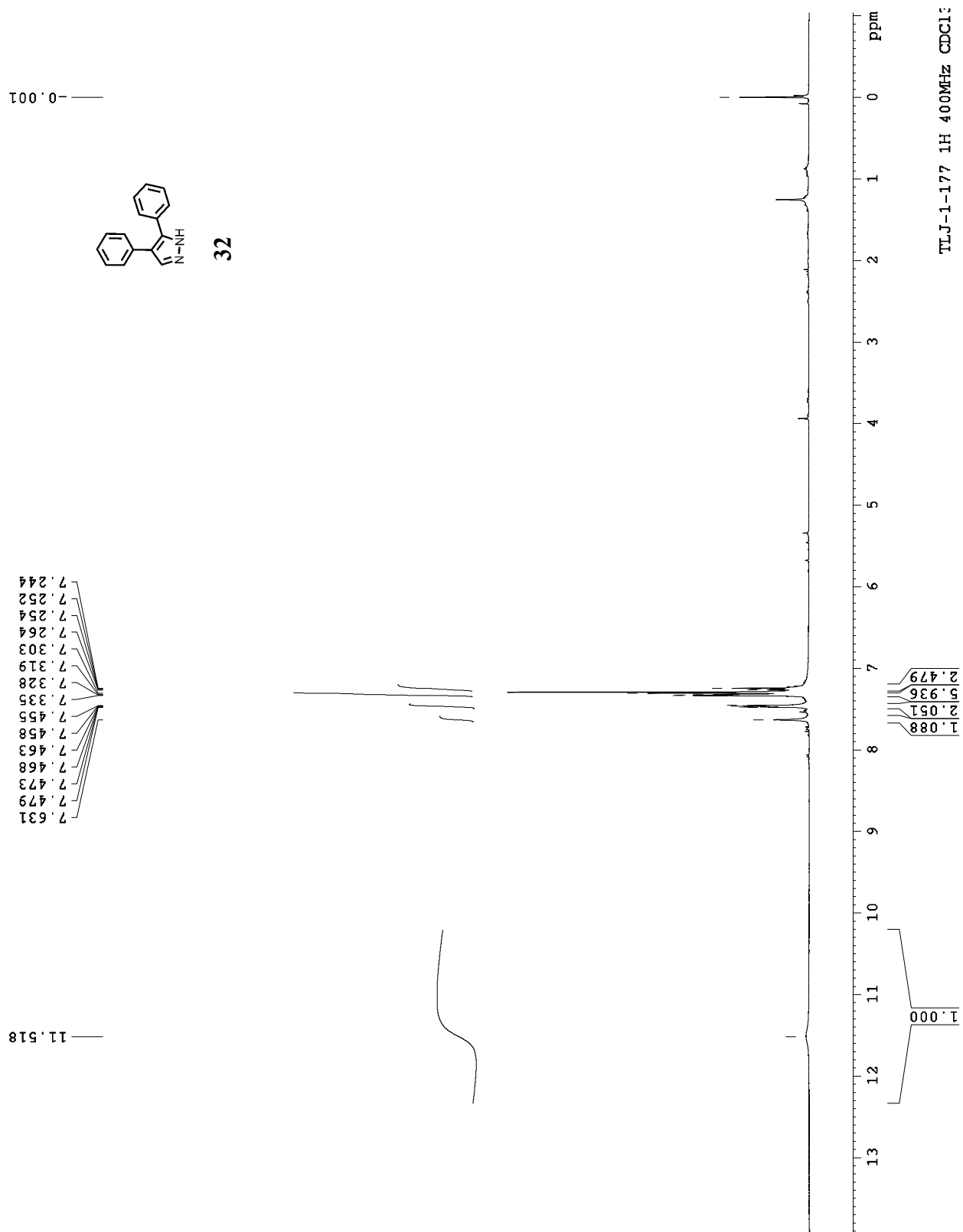




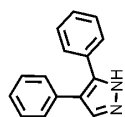






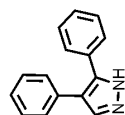


TLJ-1-177 1H 400MHz DMS

**32**
(DMSO-
d₆)2.502
2.4988.314
8.311
7.399
7.327
7.306
7.288
7.268
7.247
7.244
7.22513.193
13.05113.193
13.05113.4 13.2 13.0 ppm
0.399
0.6083.161
6.9520.399
0.608

ppm

TLJ-2-084 13C 75MHz CDCl3



32

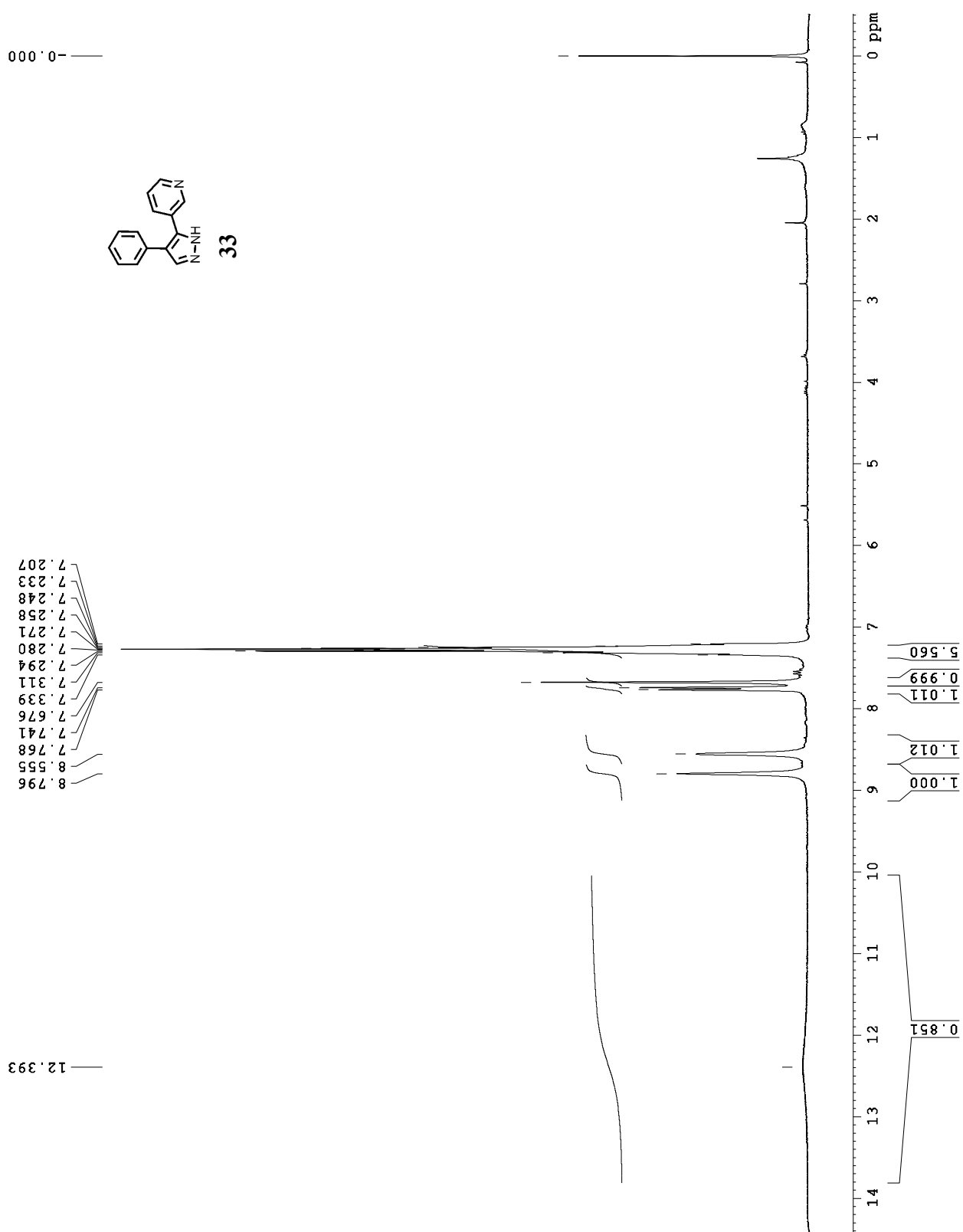
77.416
76.993
76.569

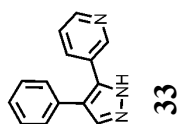
135.052
133.103
131.316
128.600
128.482
128.406
128.178
127.981
127.921
126.559

135.052
133.103
131.316
128.600
128.482
128.406
128.178
127.981
127.921
126.559

135 130 125 ppm

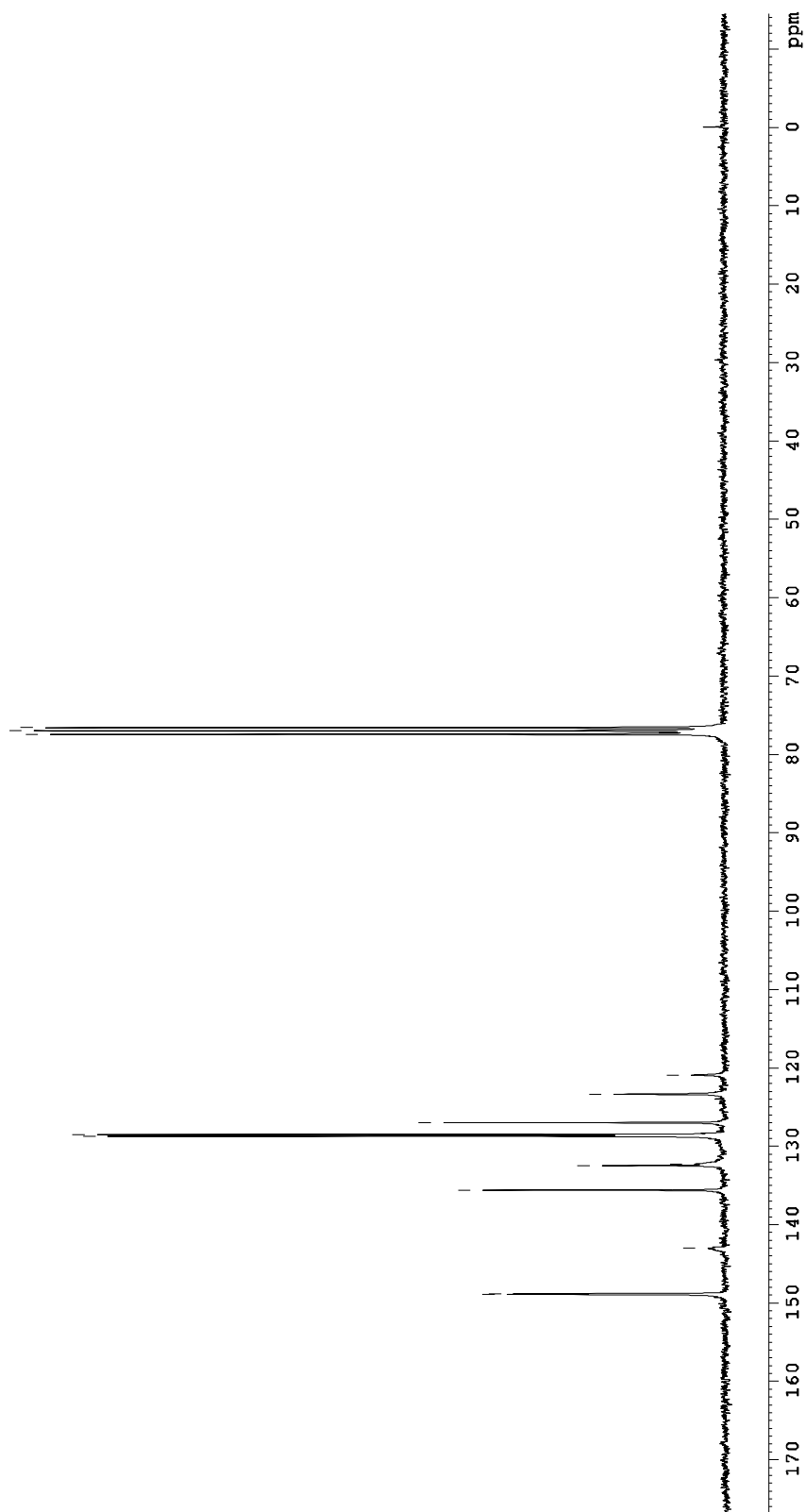
190 180 170 160 150 140 130 120 110 100 90 80 70 60 50 40 30 20 10 ppm

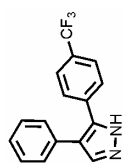




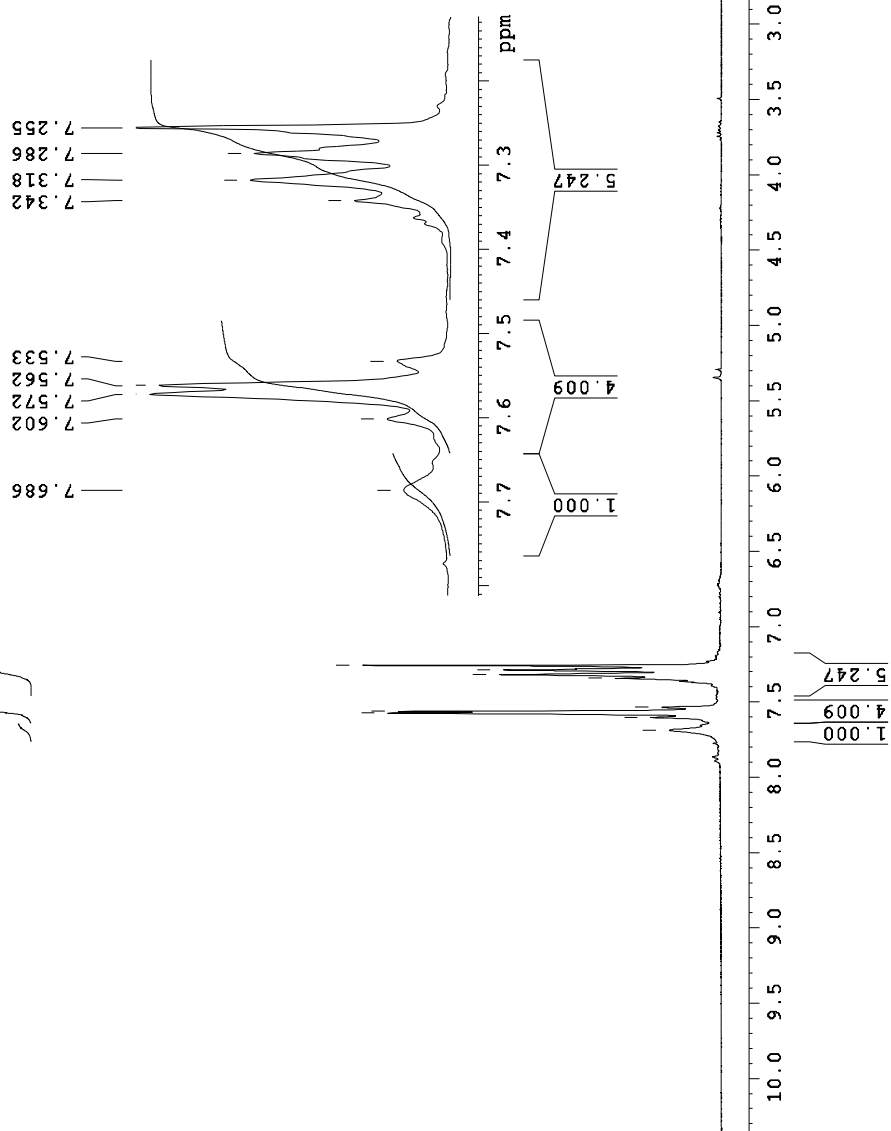
77.426
77.003
76.579

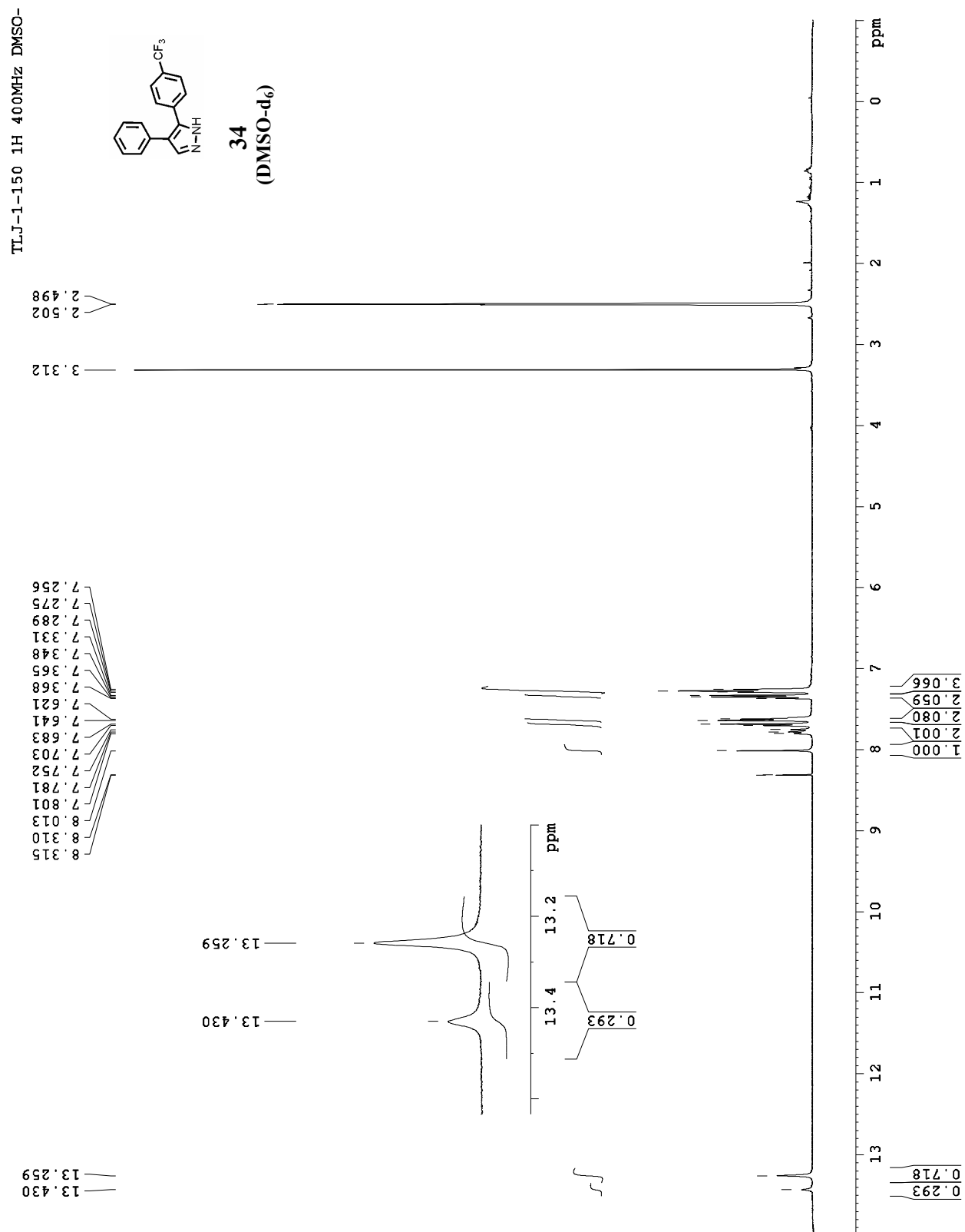
148.913
148.831
143.014
135.594
132.461
128.723
128.517
126.999
123.347
120.909
132.274

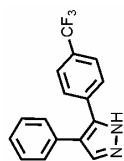


**34**

7.686
7.602
7.572
7.562
7.533
7.342
7.318
7.286
7.255



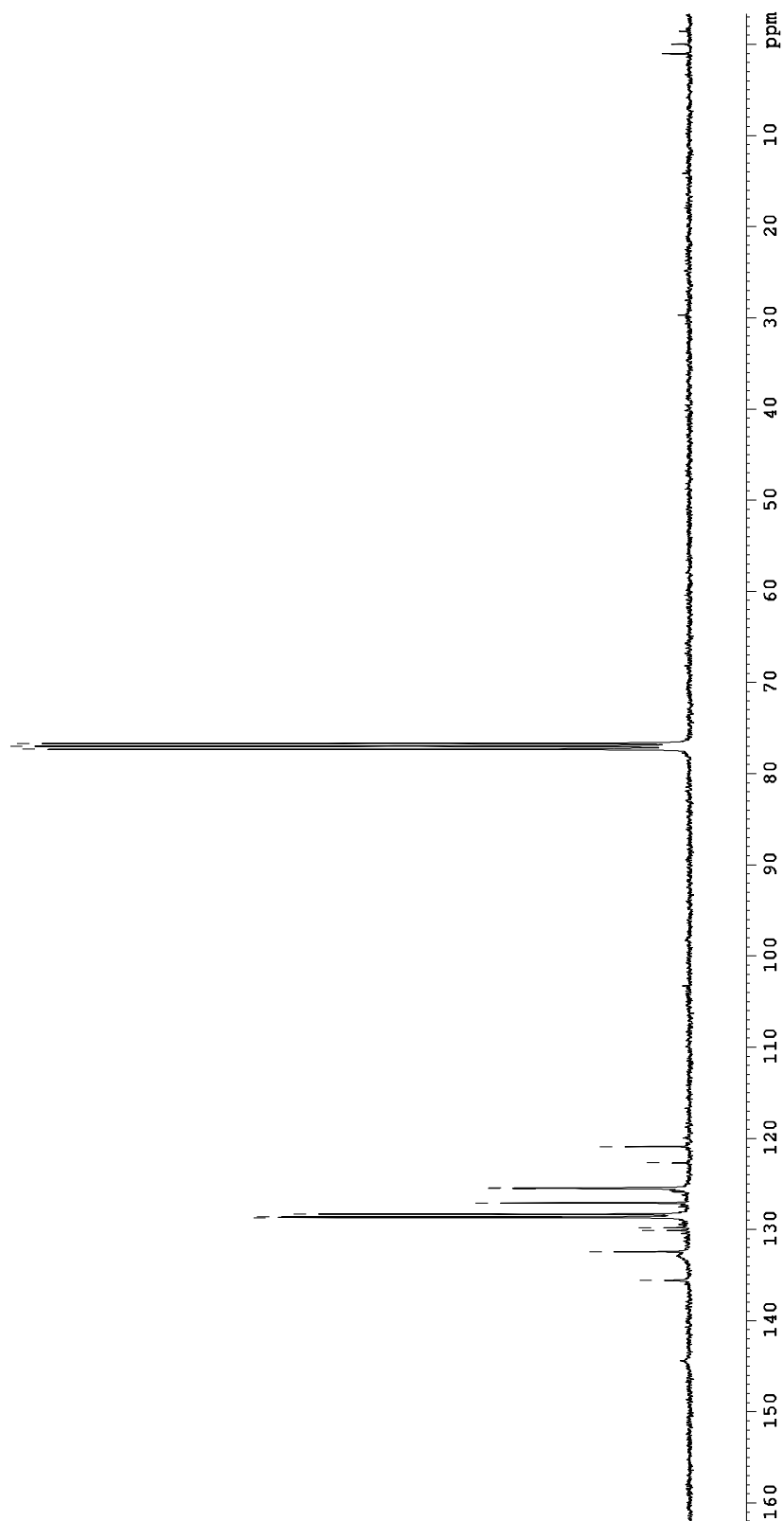


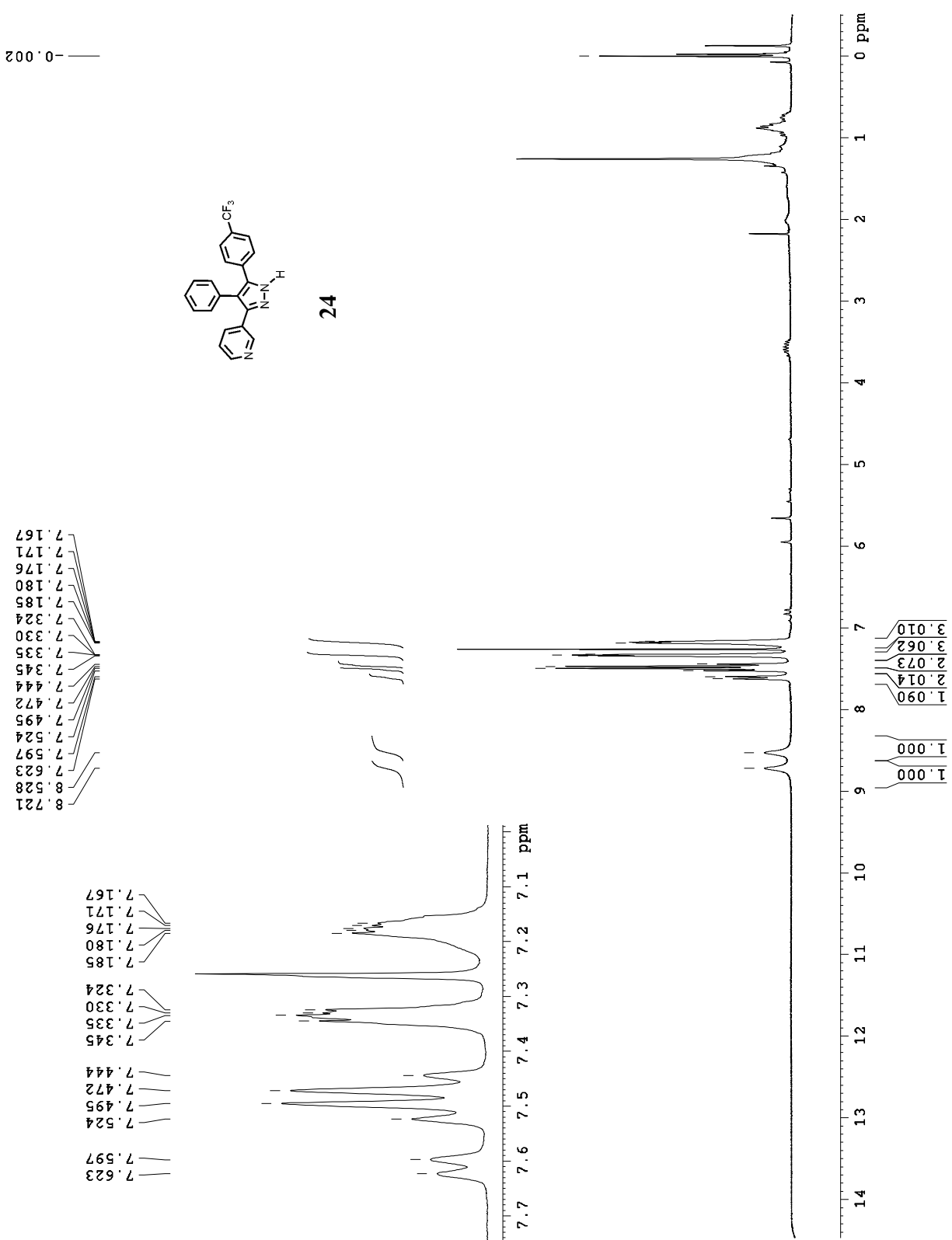


34

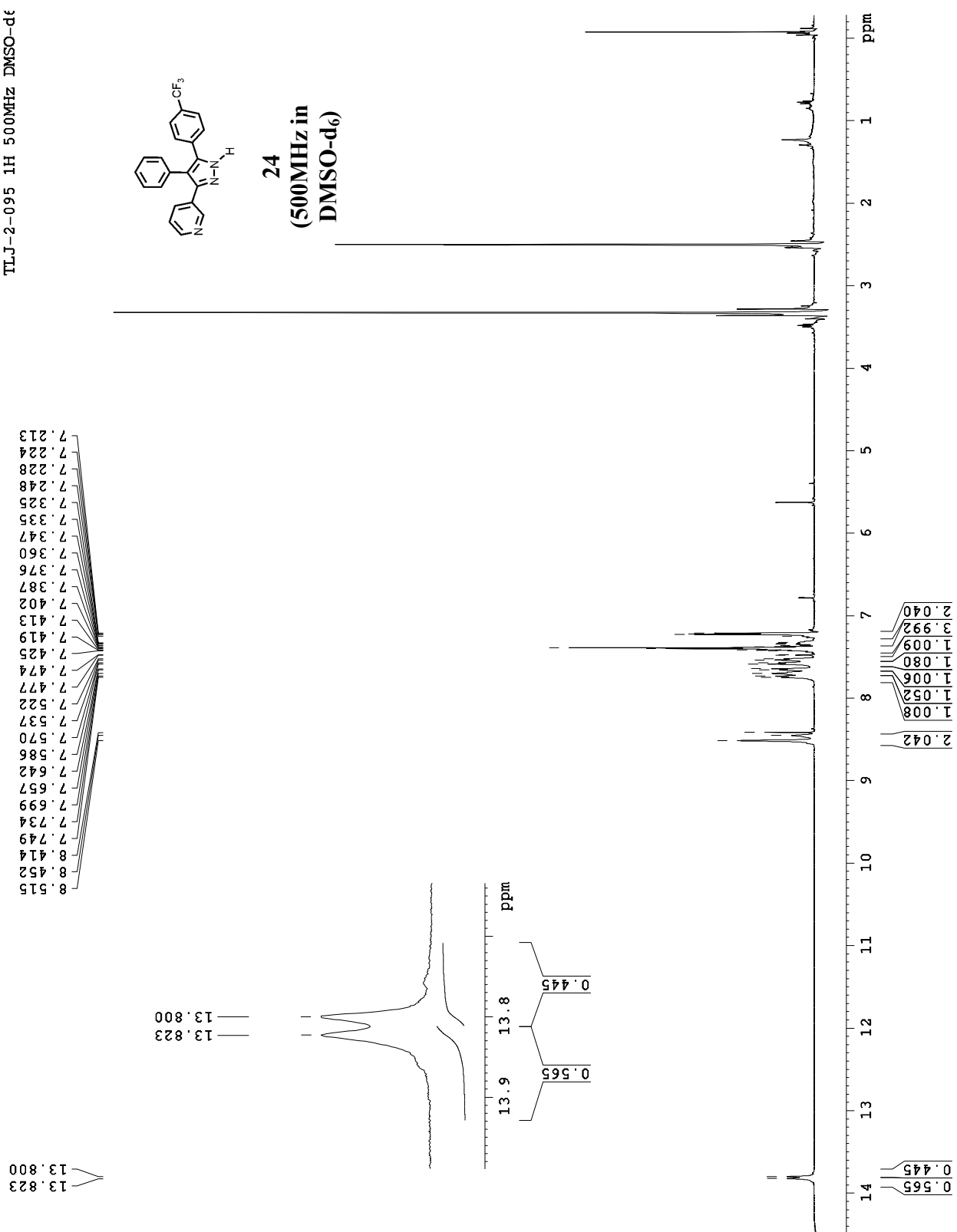
77.316
76.999
76.681

135.568
132.454
130.127
129.803
128.707
128.618
128.318
127.083
125.491
125.457
122.695
120.919

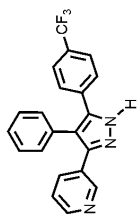


TLJ-2-095 1H NMR 300MHz CDCl₃

TLJ-2-095 1H 500MHz DMSO-d6

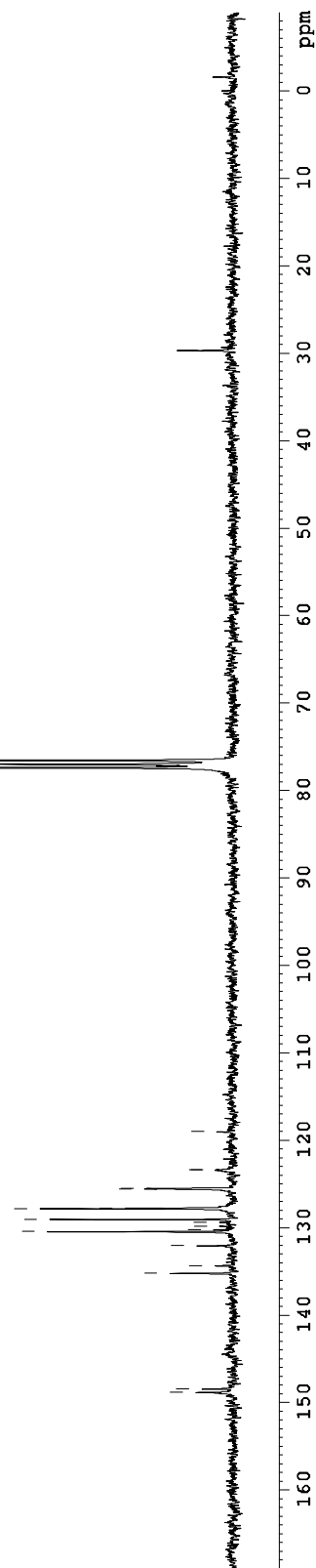
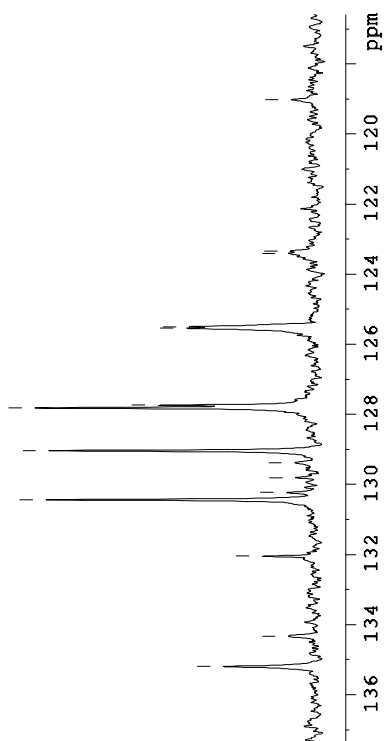


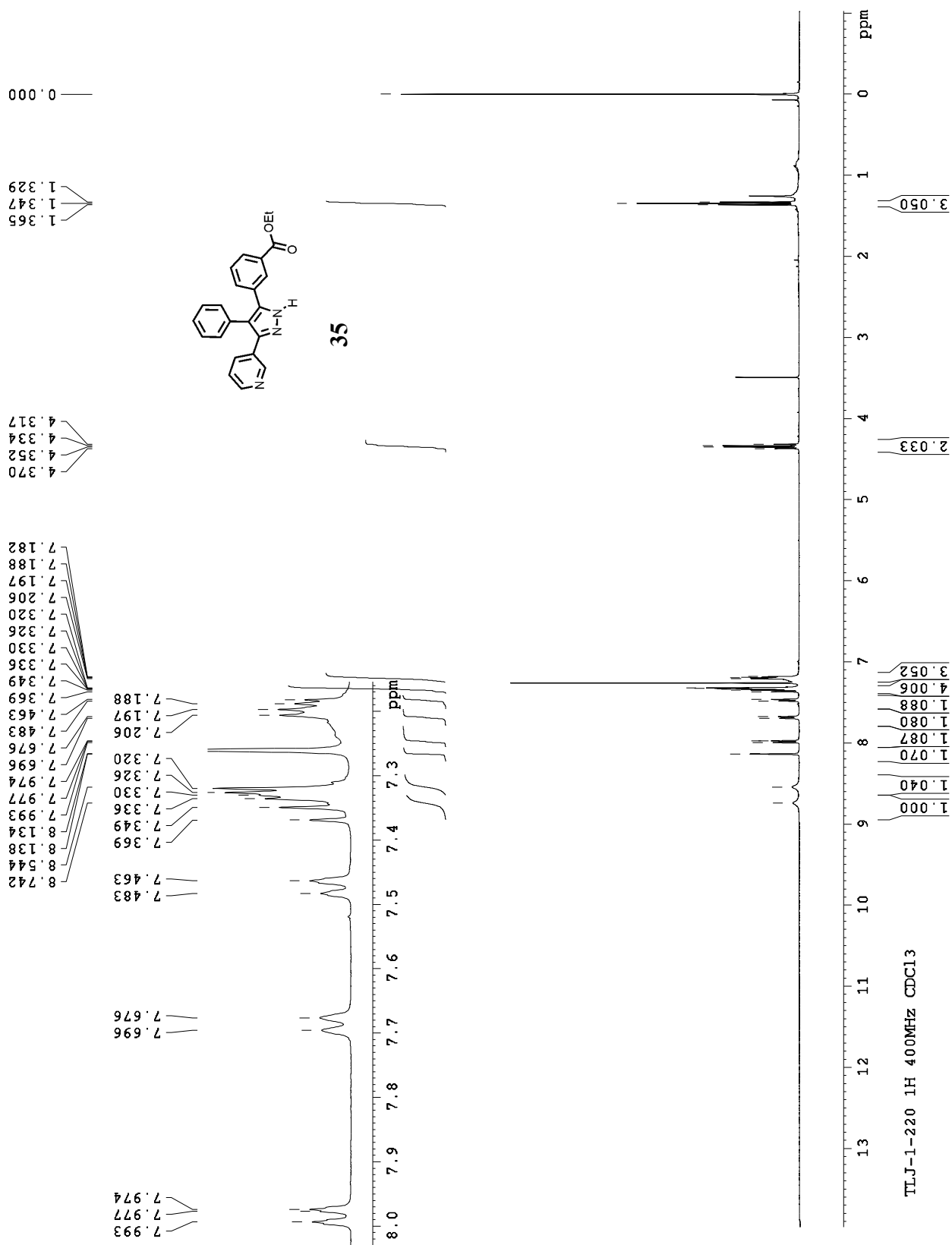
TLJ-2-095 13C 300wb CDCl3 10/13/08

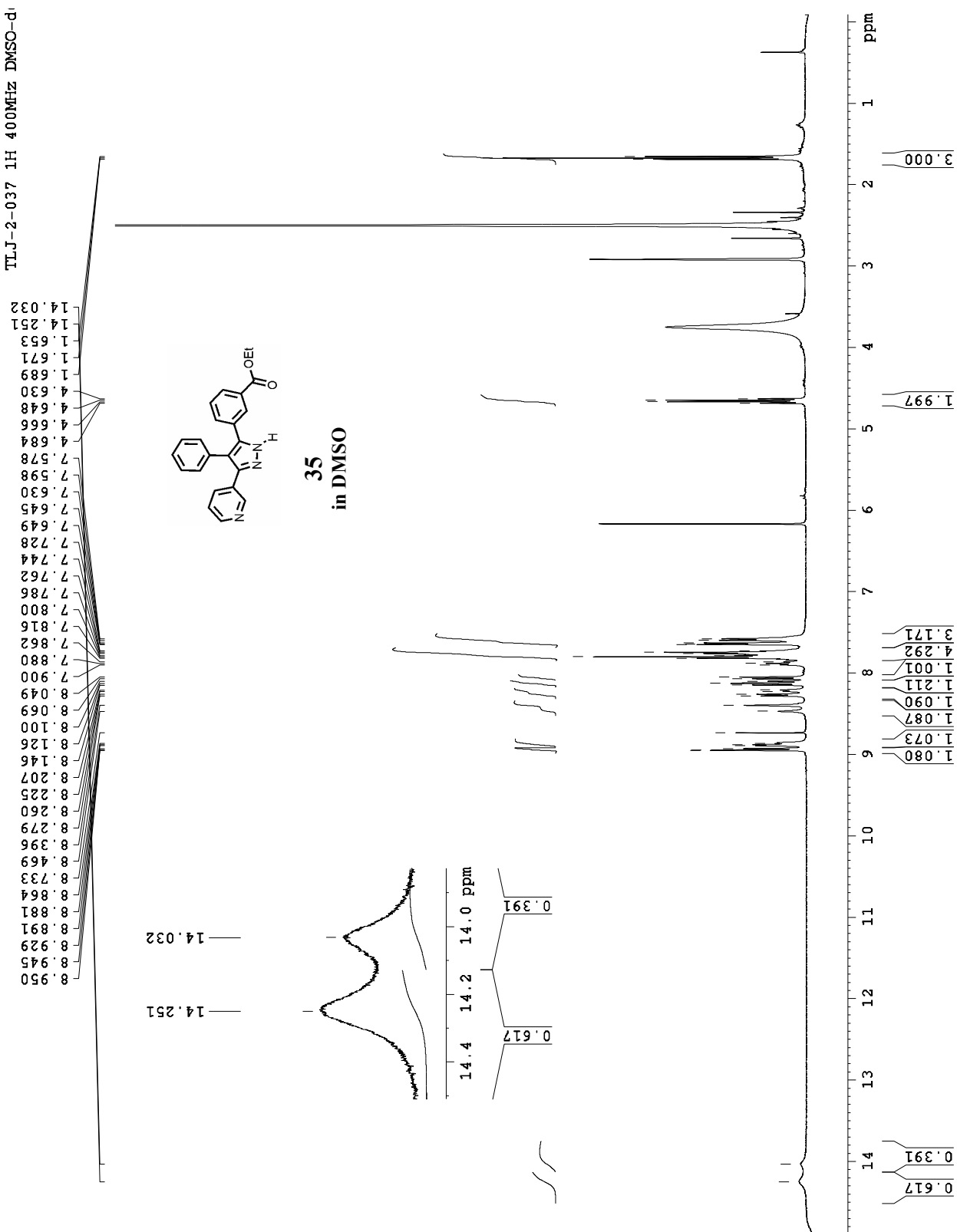
**24**

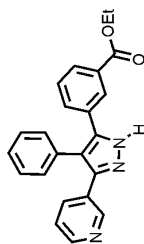
148.830
148.421
148.193
135.327
135.193
134.327
132.044
130.432
130.231
129.031
127.820
127.740
125.541
123.406
119.013
125.498
129.812
129.378
123.346

135.193
134.327
132.044
130.432
130.231
129.031
127.820
127.740
125.541
123.406
119.013
125.498
129.812
129.378
123.346

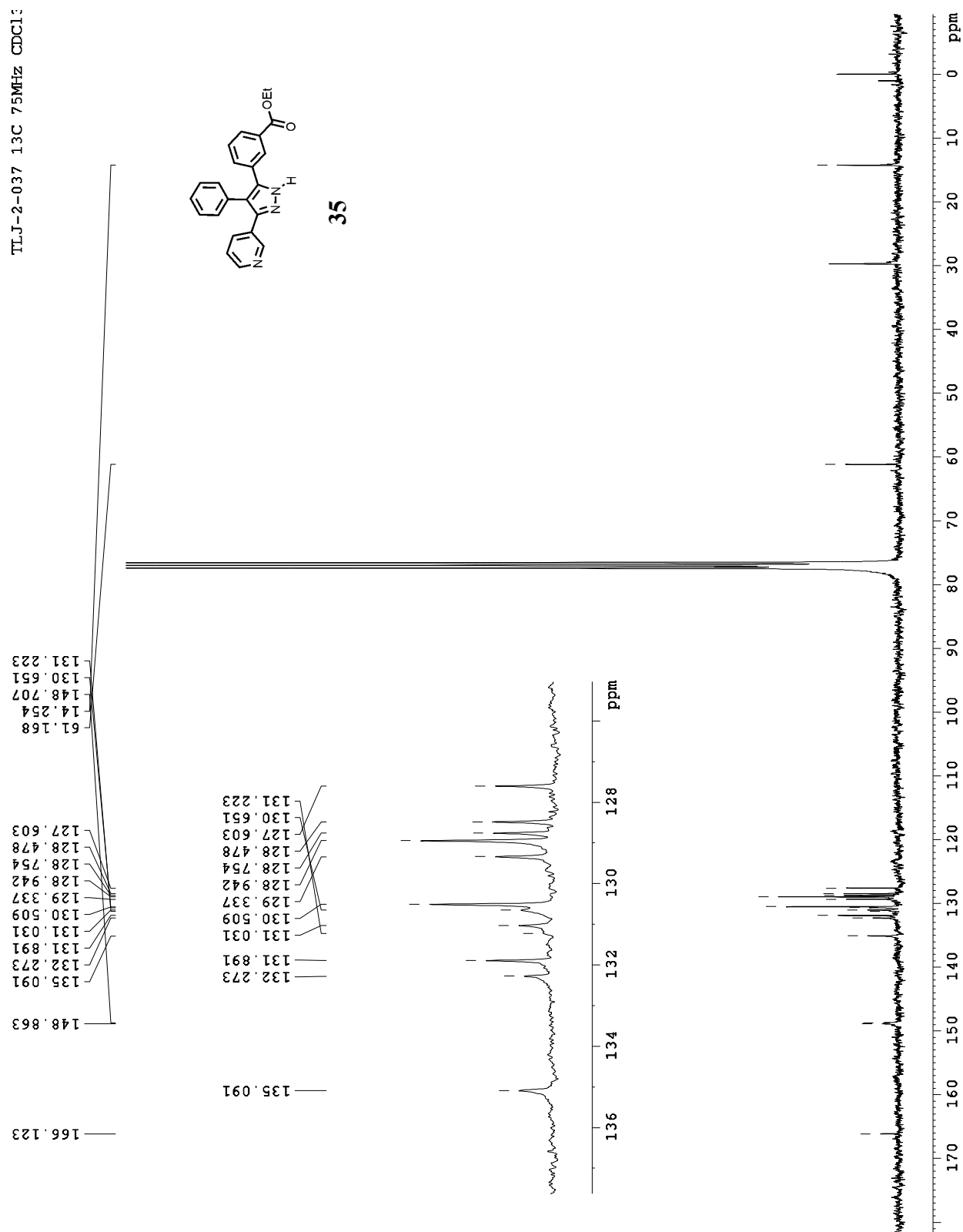


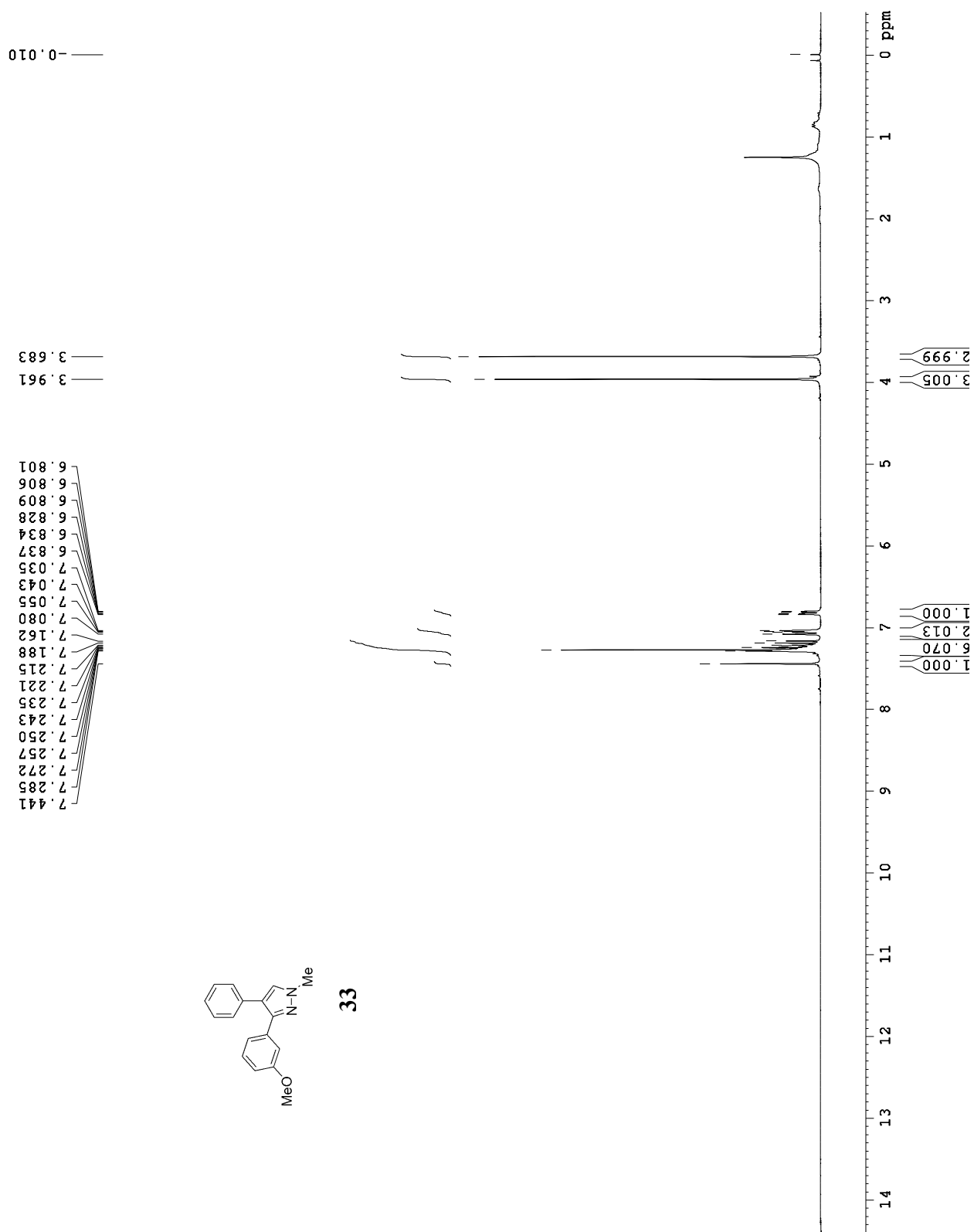


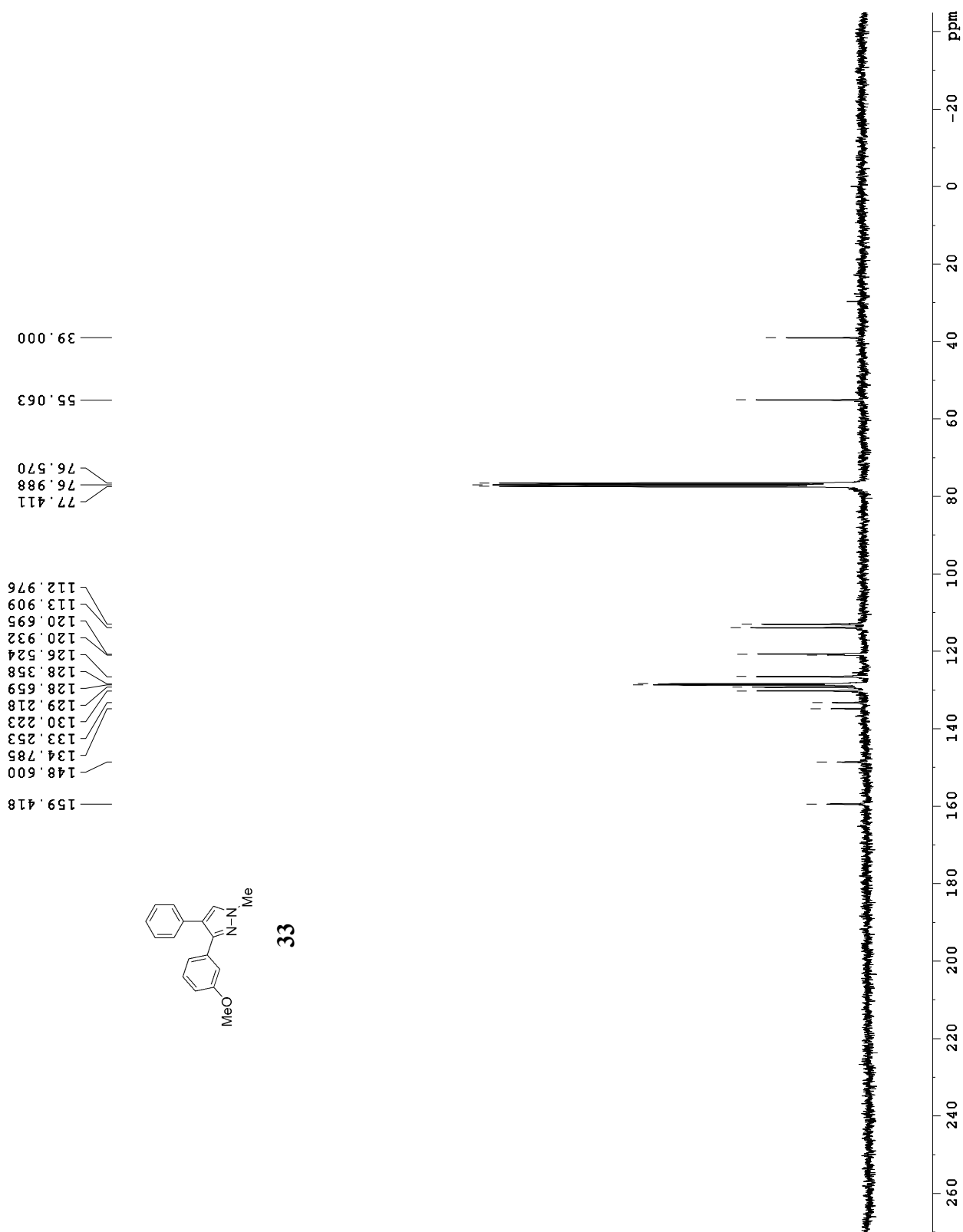
TLJ-2-037 1H 400MHz DMSO-d₆

TLJ-2-037 13C 75MHz CDCl₃

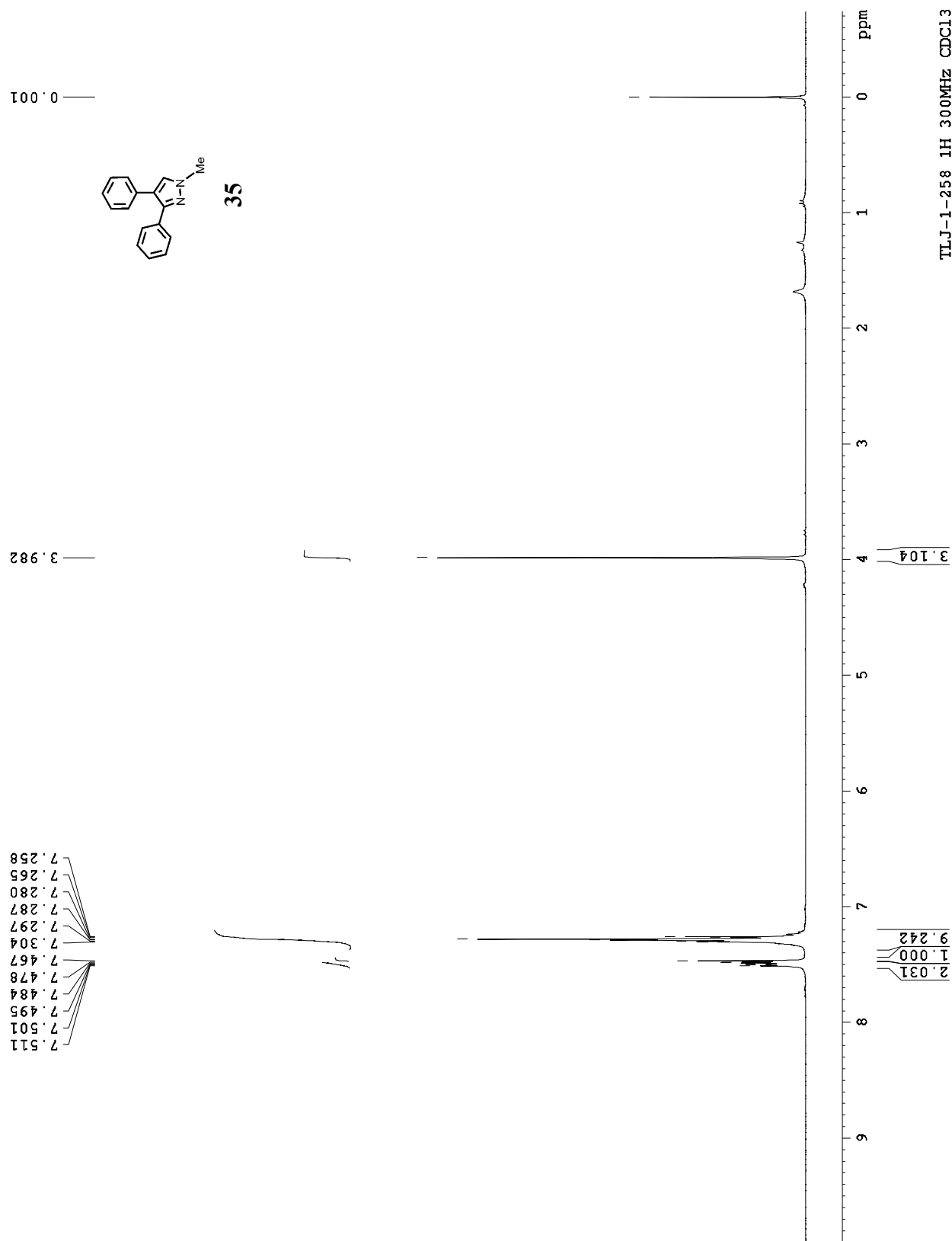
35

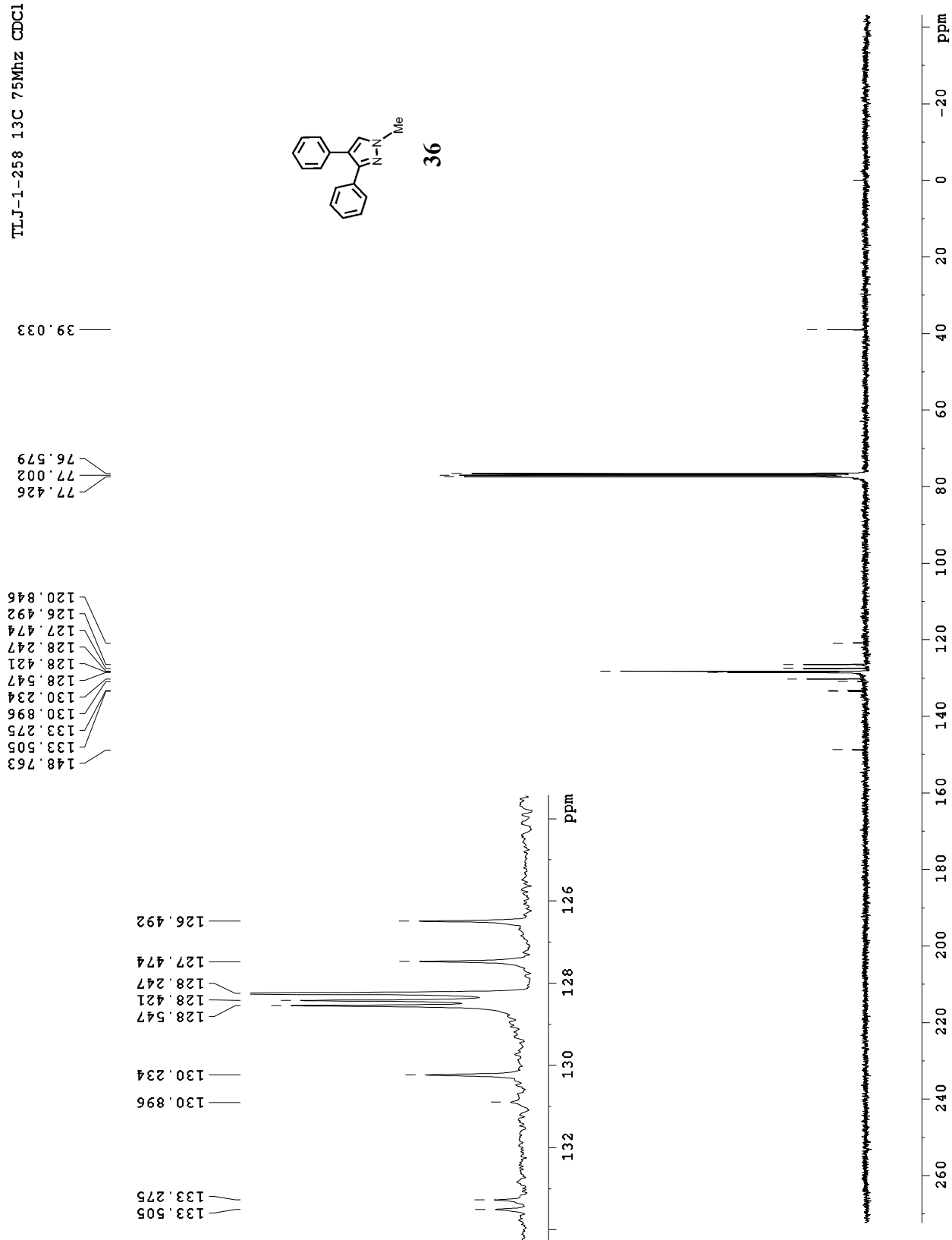


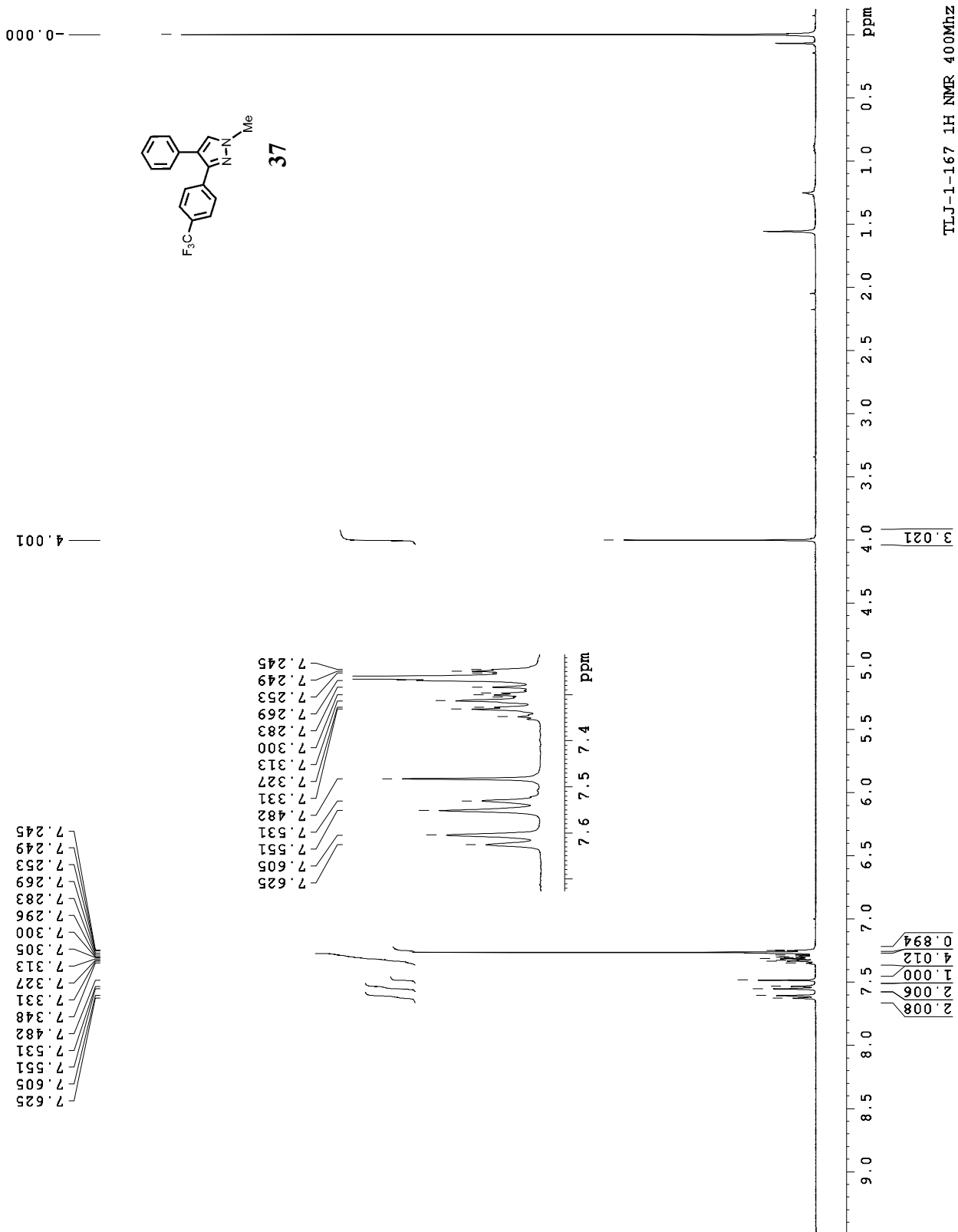




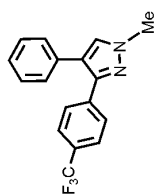
TLJ-1-258 1H 300MHz CDCl3



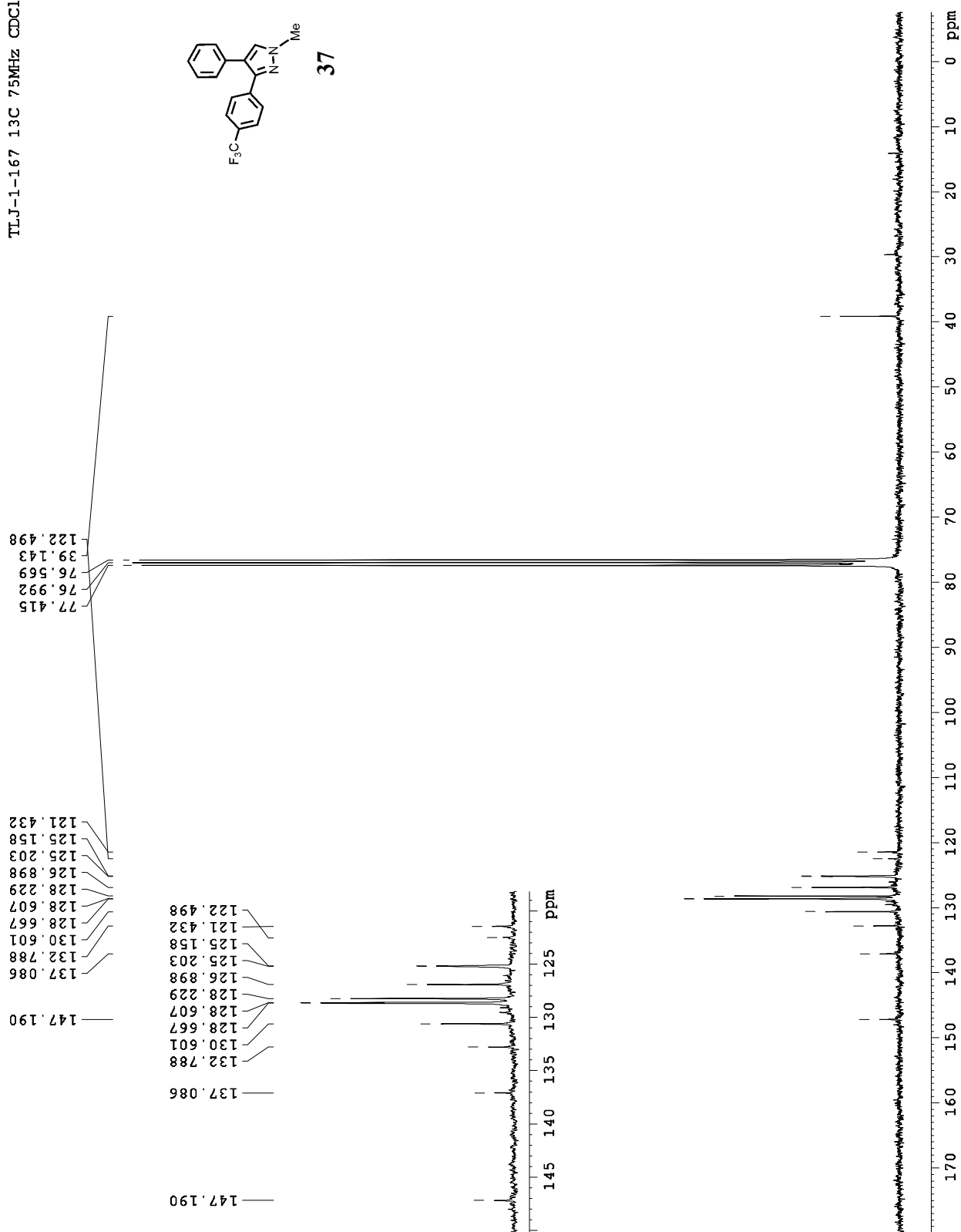
TLJ-1-258 13C 75MHz CDCl₃

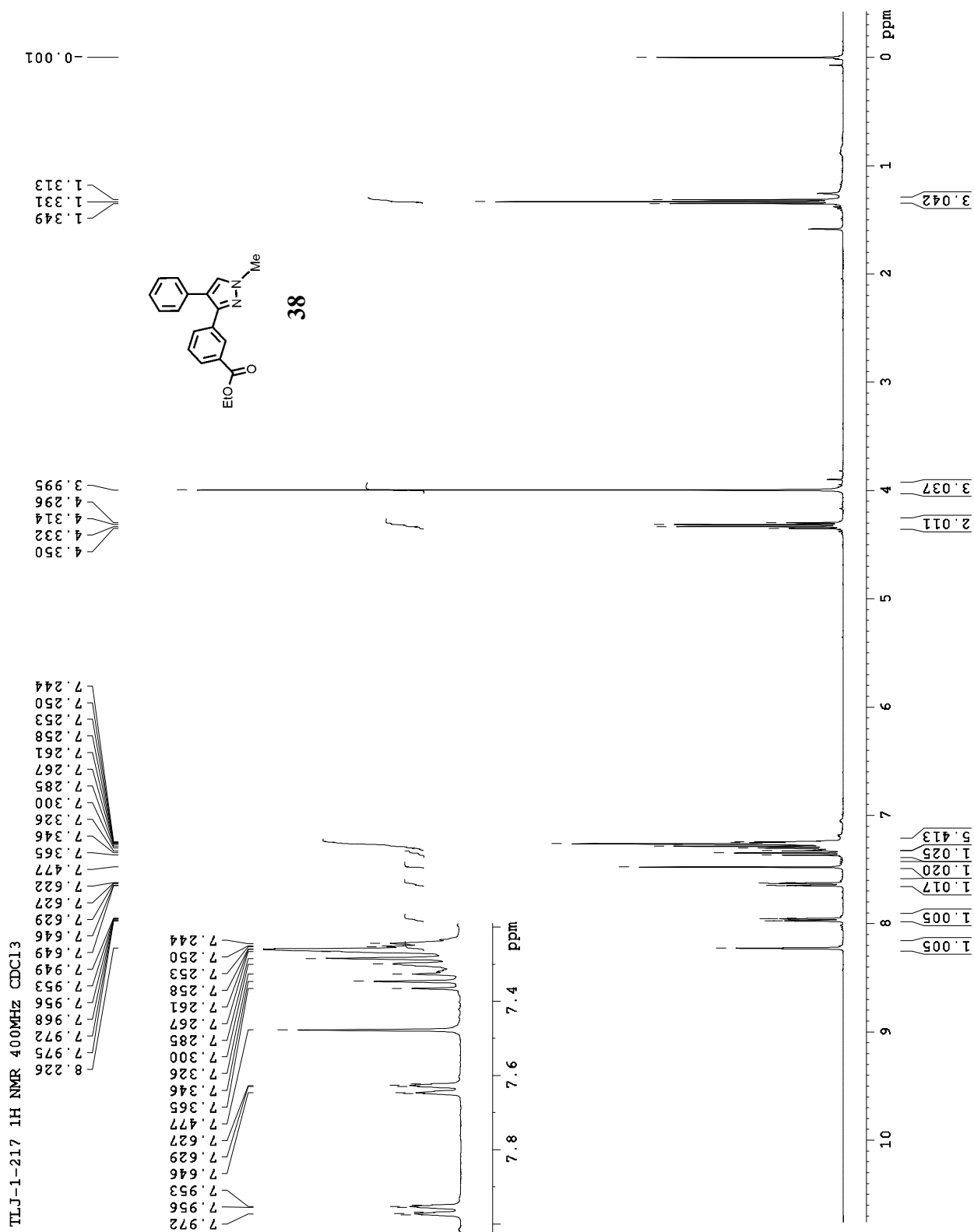


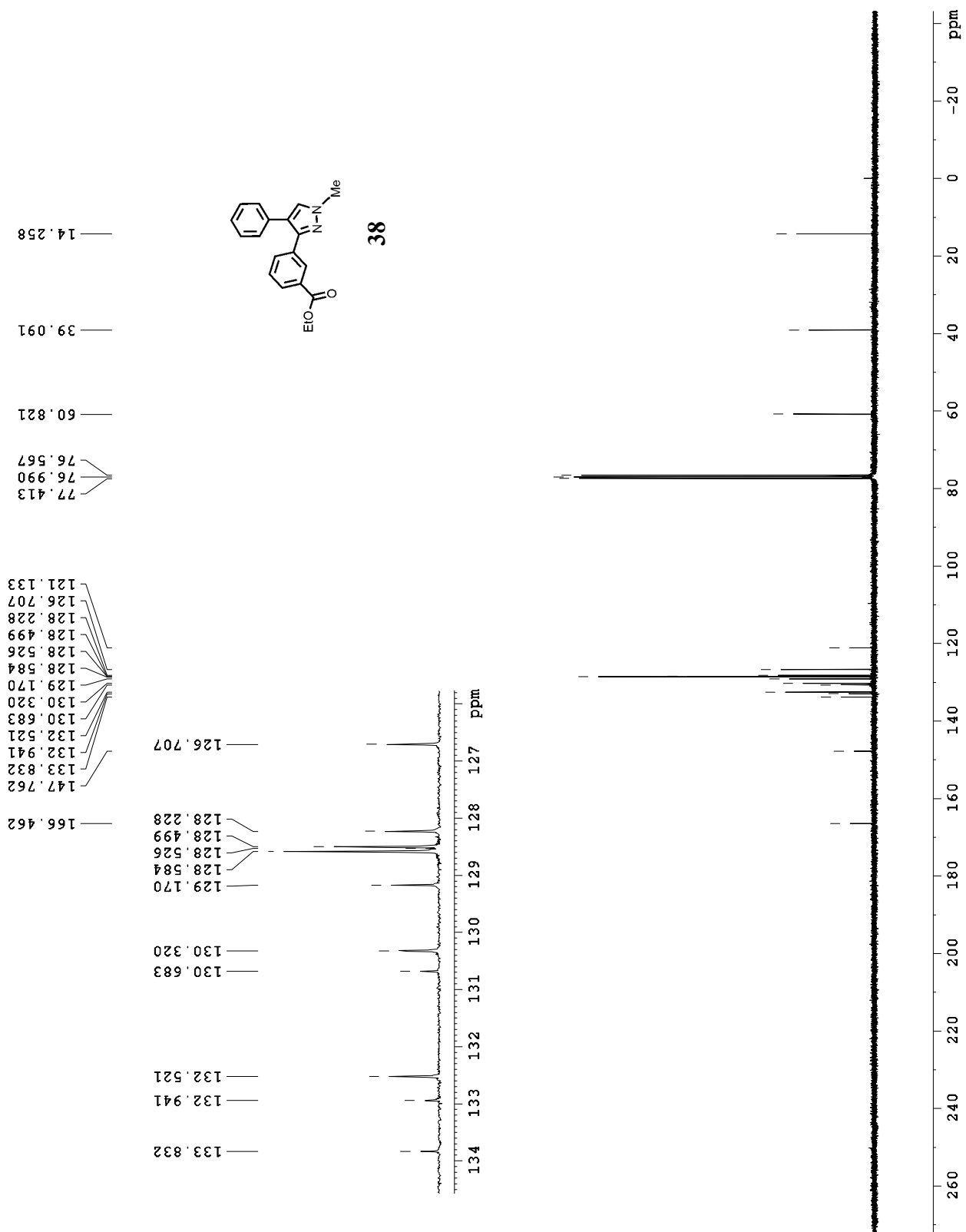
TLJ-1-167 13C 75MHz CDCl



37







V. References

- ¹ Pozharskii, A. F.; Soldatenkov, A. T.; Katritzky, A. R. *Heterocycles in Life and Society*; Wiley: Chichester, U.K., 1997.
- ² (a) Elguero, J. In *Comprehensive Heterocyclic Chemistry*; Katritzky, A. R., Rees, C. W., Scriven, E. F. V., Eds.; Pergamon: Oxford, 1996, Vol 5. (b) Elguero, J.; Goya, P.; Jagerovic, N.; Silva, A. M. S. Pyrazoles as Drugs: Facts and Fantasies. In *Targets in Heterocyclic Systems*; Attanasi, O. A., Spinelli, D., Eds.; Italian Society of Chemistry: Roma, 2002; Vol. 6, pp 52–98.
- ³ Sliskovic, D. R.; Roth, B. D.; Wilson, M. W.; Hoefle, M. L.; Newton, R. S. *J. Med. Chem.* **1990**, *33*, 31–38.
- ⁴ Penning, T. D.; et al. *J. Med. Chem.* **1997**, *40*, 1347–1365.
- ⁵ Stauffer, S. R.; Katzenellenbogen, J. A. *J. Comb. Chem.* **2000**, *2*, 318–329.
- ⁶ Moore, K. W.; Bonner, K.; Jones, E. A.; Emms, F.; Leeson, P. D.; Marwood, R.; Patel, S.; Patel, S.; Rowley, M.; Thomas, S.; Carling, R. W. *Bioorg. Med. Chem. Lett.* **1999**, *9*, 1285–1290.
- ⁷ Danel, A.; He, Z.; Milburna, G. H. W.; Tomasikb, P. **1999**, *9*, 339–342.
- ⁸ Mukherjee, R. *Coordination Chemistry Reviews* **2000**, *203*, 151–218.
- ⁹ Lahm, G. P.; Cordova, D.; Barry, J. D. *Bioorg. Med. Chem.* **2009**, *17*, 4127.
- ¹⁰ *Science of Synthesis*; Stanovnik, B., Svete, J. D. Eds.; Thieme: Stuttgart, 2002; Vol. 12, pp 22–81, pp 84–91.
- ¹¹ (a) Aggarwal, V. K.; De Vicente, J.; Bonnert, R. V. *J. Org. Chem.* **2003**, *68*, 5381–5383. (b) Heller, S. T.; Natarajan, S. R. *Org. Lett.* **2006**, *8*, 2675–78. (c) Deng, X.; Mani, N. S. *Org. Lett.* **2008**, *10*, 1307–1310.
- ¹² Schmidt, A.; Dreger, A. Recent advances in the chemistry of pyrazoles. Properties, biological activities, and syntheses. *Curr. Org. Chem.* **2011**, *15*, 1423–1463.
- ¹³ (a) Godula, K.; Sames, D. *Science* **2006**, *312*, 67–72. (b) Kakiuchi, F.; Chatani, N. *Adv. Synth. Catal.* **2003**, *345*, 1077–1101.
- ¹⁴ There have been a great number of reviews of transition metal-catalyzed C-H functionalization; for recent reviews, see: (a) Alberico, D.; Scott, M. E.; Lautens, M. *Chem. Rev.* **2007**, *107*, 174–238. (b) Ackermann, L.; Vicente, R.; Kapdi, A. R. *Angew. Chem. Int. Ed.* **2009**, *48*, 9792–826. (c) Colby, D. A.; Bergman, R. G.; Ellman, J. A. Rhodium-catalyzed C-C bond formation via heteroatom-directed C-H bond activation. *Chem. Rev.* **2010**, *110*, 624–655. (d) Hirano, K.; Miura, M. Copper-mediated oxidative direct C-C (hetero)aromatic cross-

- coupling. *Chem. Commun.* **2012**, 48, 10704–10714. (e) Kuhl, N.; Hopkinson, M. N.; Wencel-Delord, J.; Glorius, F. Beyond directing groups: Transition-metal-catalyzed C-H activation of simple arenes. *Angew. Chem. Int. Ed.* **2012**, 51, 10236–10254.
- ¹⁵ As recently reported, THP protecting group and its transposition has been used to achieve pyrazole lithiation and regioselective preparation of N-THP-pyrazolylboronate esters: McLaughlin, M.; Marcantonio, K.; Chen, C.-Y.; Davies, I. W. *J. Org. Chem.* **2008**, 73, 4309–4312.
- ¹⁶ (a) Lane, B. S.; Sames, D. *Org. Lett.* **2004**, 6, 2897–2900. (b) Lane, B. S.; Brown, M. A.; Sames, D. *J. Am. Chem. Soc.* **2005**, 127, 8050–8057. (c) Touré, B. B.; Lane, B. S.; Sames, D. *Org. Lett.* **2006**, 8, 1979–1982. (d) Wang, X.; Gribkov, D. V.; Sames, D. *J. Org. Chem.* **2007**, 72, 1476–1479.
- ¹⁷ Wang, X.; Lane, B. S.; Sames, D. *J. Am. Chem. Soc.* **2005**, 127, 4996–4997.
- ¹⁸ For recent reviews of catalytic methods of C-H arylation of arenes & heteroarenes, see: (a) Campeau, L.-C.; Stuart, D. R.; Fagnou, K. *Aldrichimica Acta* **2007**, 40, 35–41. (b) Satoh, T.; Miura, M. *Chem. Lett.* **2007**, 36, 200–205. (c) Seregin, I. V.; Gevorgyan, V. *Chem. Soc. Rev.* **2007**, 36, 1173–1193. (d) Alberico, D.; Scott, M. E.; Lautens, M. *Chem. Rev.* **2007**, 107, 174–238.
- ¹⁹ Recent examples of azole C-arylation reported by others: (a) Yang, S.-D.; Sun, C.-L.; Fang, Z.; Li, B.-J.; Li, Y.-Z.; Shi, Z.-J. *Angew. Chem., Int. Ed.* **2008**, 47, 1473–1476. (b) Blaszykowski, C.; Aktoudianakis, E.; Alberico, D.; Bressy, C.; Hulcoop, D. G.; Jafarpour, F.; Joushaghani, A.; Laleu, B.; Lautens, M. *J. Org. Chem.* **2008**, 73, 1888–1897. (c) Berman, A. M.; Lewis, J. C.; Bergman, R. G.; Ellman, J. A. *J. Am. Chem. Soc.* **2008**, 130, 14926. (d) Phipps, R. J.; Gaunt, M. J. *Science* **2009**, 323, 1593–1597. (e) Čerňová, M.; Pohl, R.; Hocek, M. *Eur. J. Org. Chem.* **2009**, 3698–3701. (f) Duong, H. A.; Gilligan, R. E.; Cooke, M. L.; Phipps, R. J.; Gaunt, M. J. *Angew. Chem. Int. Ed.* **2011**, 50, 463–466. (g) Kirchberg, S.; Tani, S.; Ueda, K.; Yamaguchi, J.; Studer, A.; Itami, K. *Angew. Chem. Int. Ed.* **2011**, 50, 2387–2391. (h) Ye, M.; Gao, G.-L.; Edmunds, A. J. F.; Worthington, P. A.; Morris, J. A.; Yu, J.-Q. *J. Am. Chem. Soc.* **2011**, 133(47), 19090–19093. (i) Funaki, K.; Sato, T.; Oi, S. *Org. Lett.* **2012**, 14(24), 6168–6189. (j) Shibahara, F.; Yamauchi, T.; Yamaguchi, E.; Murai, T. *J. Org. Chem.* **2012**, 77, 8815–8820.
- ²⁰ Intramolecular C-arylation of pyrazoles have been reported via an alkylation/arylation sequence. Blaszykowski, C.; Aktoudianakis, E.; Bressy, C.; Alberico, D.; Lautens, M. *Org. Lett.* **2006**, 8, 2043–2045.
- ²¹ The SEM group is also a directing group for lithiation of azoles including pyrazoles. (a) Edwards, M. P.; Doherty, A. M.; Ley, S. V.; Organ, H. M. *Tetrahedron* **1986**, 42, 3723–3729. (b) Fugina, N.; Holzer, W.; Wasicky, M. *Heterocycles* **1992**, 34, 303–314. (c) Gerard, A.-L.; Bouillon, A.; Mahatsekake, C.; Collot, V.; Rault, S. *Tet. Lett.* **2006**, 47, 4665–4669. (d) Luo, G.; Chen, L.; Dubowchik, G. *J. Org. Chem.* **2006**, 71, 5392–5395.
- ²² Lafrance, M.; Fagnou, K. *J. Am. Chem. Soc.* **2006**, 128, 16496–16497.

- ²³ (a) *Science of Synthesis*; Stanovnik, B., Svete, J. D., Eds.; Thieme: Stuttgart, 2002; Vol. 12, pp 173-203. (b) Gupta, R. R.; Kumar, M.; Gupta, V. *Heterocyclic Chemistry*; Springer: Berlin, 1998; p 452. (c) Behr, L. C.; Fusco, R.; Jarboe, C. H. Pyrazoles, pyrazolines, pyrazolidines, indazoles, and condensed rings. In *The Chemistry of Hetero- cyclic Compounds*; Wiley, R. H., Ed.; Interscience Publishers: New York, 1967; Vol. 22 pp 107-109.
- ²⁴ Park, C.-H.; Ryabova, V.; Seregin, I. V.; Sromek, A. W.; Gevorgyan, V. *Org. Lett.* **2004**, *6*, 1159–1162.
- ²⁵ (a) Joo, J. M.; Touré, B. B.; Sames, D. *J. Org. Chem.* **2010**, *75*, 4911–20. (b) Guo, P.; Joo, J. M.; Rakshit, S.; Sames, D. *J. Am. Chem. Soc.* **2011**, *133*, 16338–41.
- ²⁶ The palladium-carbonate system also showed preference for acidic C-H bonds: Garcia-Cuadrado, D.; Braga, A. A. C.; Maseras, F.; Echavarren, A. M. *J. Am. Chem. Soc.* **2006**, *128*, 1066–1067.
- ²⁷ Tundel, R. Part II: C-H Arylation of Heteroarenes: Mapping the Mechanism of Palladium-Carboxylate Catalyzed Direct Arylation Reactions. Ph.D. Thesis, Columbia University, New York, NY, 2011.
- ²⁸ Zhao, Z.-G.; Wang, Z.-X. *Synth. Commun.* **2007**, *37*, 137–147.
- ²⁹ He, Y.; Chen, Y.; Du, H.; Schmid, L. A.; Lovely, C. J. *Tetrahedron Lett.* **2004**, *45*, 5529–5532.
- ³⁰ Luo, G.; Chen, L.; Dubowchik, G. *J. Org. Chem.* **2006**, *71*, 5392–5395.
- ³¹ (a) Trofimenko, S.; Yap, G. P. A.; Jove, F. A.; Claramunt, R. M.; García, M. A.; Santa Maria, M. D.; Alkorta, I.; Elguero, J. *Tetrahedron* **2007**, *63*, 8104–8111. (b) Vors, J.-P.; Gerbaud, V.; Gabas, N.; Canselier, J. P.; Jagerovic, N.; Jimeno, M. L.; Elguero, J. *Tetrahedron* **2003**, *59*, 555–560. (c) Aguilar-Parrilla, F.; Cativiela, C.; Diaz de Villegas, M. D.; Elguero, J.; Foces-Foces, C.; Laureiro, J. I. G.; Cano, F. H.; Limbach, H.-H.; Smith, J. A. S.; Toiron, C. *J. Chem. Soc. Perkin Trans. 2* **1992**, 1737–1742. (d) Habraken, C. L.; Moore, J. A. *J. Org. Chem.* **1965**, *30*, 1892–1896.
- ³² For considerations regarding the binding of tautomers to protein targets, see: Chimenti, F.; Fioravanti, R.; Bolasco, A.; Manna, F.; Chimenti, P.; Secci, D.; Befani, O.; Turini, P.; Ortuso, F.; Alcaro, S. *J. Med. Chem.* **2007**, *50*, 425–428.
- ³³ (a) Kudo, N.; Perseghini, M.; Fu, G. C. *Angew. Chem., Int. Ed.* **2006**, *45*, 1282–1284. (b) Billingsley, K. L.; Anderson, K. W.; Buchwald, S. L. *Angew. Chem., Int. Ed.* **2006**, *45*, 3484–3488. (c) Billingsley, K.; Buchwald, S. L. *J. Am. Chem. Soc.* **2007**, *129*, 3358–3366.
- ³⁴ Goikhman, R.; Jacques, T. L.; Sames, D. *J. Am. Chem. Soc.* **2009**, *131*, 3042–3048.
- ³⁵ Fustero, S.; Sánchez-Roselló, M.; Barrio, P.; Simón-Fuentes, A. *Chem. Rev.* **2011**, *111*, 6984–7034.

-
- ³⁶ Joo, J. M.; Guo, P.; Sames, D. C-H Bonds As Ubiquitous Functionality: Preparation of Multiple Regioisomers of Arylated 1,2,4-Triazoles via C-H Activation. *J. Org. Chem.* **2013**, *78*, 738–743.
- ³⁷ Fugina, N.; Holzer, W.; Wasicky, M. *Heterocycles* **1992**, *34*, 303 – 313.
- ³⁸ Zhao, Z.-G.; Wang, Z.-X. *Synth. Comm.* **2007**, *37*, 137 – 147.
- ³⁹ Still, W. C.; Kahn, M.; Mitra, A. *J. Org. Chem.* **1978**, *43* (14), 2923 – 2925.
- ⁴⁰ Nakagawa, Y.; Aki, O.; Sirakawa, K. *Chem. Pharm. Bull.* **1972**, *20*, 2209 – 2214.
- ⁴¹ Luo, G.; Chen, L.; Dubowchik, G. *J. Org. Chem.* **2006**, *71*, 5392 – 5395.
- ⁴² (a) Trofimenko, S.; Yap, G. P. A.; Jove, F. A.; Claramunt, R. M.; García, M. A.; Santa Maria, M. D.; Alkorta, I.; Elguero, J. *Tetrahedron* **2007**, *63*, 8104 – 8111. (b) Vors, J.-P.; Gerbaud, V.; Gabas, N.; Canselier, J. P.; Jagerovic, N.; Jimeno, M. L.; Elguero, J. *Tetrahedron* **2003**, *59*, 555 – 560. (c) Aguilar – Parrilla, F.; Cativiela, C.; Diaz de Villegas, M. D.; Elguero, J.; Foces-Foces, C.; Laureiro, J. I. G.; Cano, F. H.; Limbach, H.-H.; Smith, J. A. S.; Toiron, C. *J. Chem. Soc. Perkin Trans. 2*, **1992**, 1737-1742. (d) Habraken, C. L.; Moore, J. A. *J. Org. Chem.* **1965**, *30*, 1892 – 1896.

Chapter 2

Toward Pharmacological Modulation of Neuroplasticity: The Neurotrophin Receptor TrkB as a Potential Target

I.1 Introduction

Neuroplasticity is a broad term that describes the ability of the nervous system to change itself in terms of both connectivity structure and functional parameters as neuronal and neurotransmission signaling. The pathophysiology of many psychiatric and neurodegenerative diseases has been linked to deficiencies or abnormalities in neuronal wiring or neuronal signaling proteins, and neuroplasticity may offer the opportunity to correct these deficiencies. Elucidation and modulation of these abnormalities is an active area of research, as better treatments for psychiatric and neurodegenerative illness that take advantage of the brain's plasticity require a better understanding of the cellular mechanisms underlying their causes and manifestations.

Our group has had a long-standing interest in neuronal transmission¹ and recently became interested in developing pharmacological approaches for neuronal rescue and repair. The idea that a small molecule could be capable of acutely influencing signaling pathways, and potentially resetting relevant dysfunctional circuits in the brain, was extremely intriguing to us. One study in particular that inspired us to enter this field of research was a study of deep-brain stimulation in which Brodmann's Area 25 (BA25, subgenual area 25), a region in the cingulate gyrus of the cerebral cortex of six treatment-resistant depressed patients, was stimulated by electrodes implanted in the subgenual cingulate white matter, resulting in rapid reversal of symptoms in four of the six cases.² While this may prove a powerful therapy for treatment-resistant depression, a pharmacological agent that could deliver a similar outcome, without the several-

week induction period for current pharmacological antidepressant efficacy, would be highly advantageous and would represent a major breakthrough.

The mechanisms of action of many current pharmacological treatments for psychiatric conditions, including schizophrenia, addiction, bi- and unipolar depression, are still poorly understood despite decades of research due to the complexity of brain disorders. With psychiatric and neurodegenerative conditions on the rise, closing the gaps in our knowledge is becoming all the more urgent. Many physiological phenomena, such as changes in neuronal or glial cell density, protein expression and signaling, or neurotransmitter release and neurotransmitter receptor signaling, are tentatively connected to one or more central nervous system (CNS) disorders. Certain specific brain structures also show discernable changes in volume which may be either casually linked to a disease or a consequence of it. An interesting example is the trend that hippocampal volume appears reduced in patients with depression and post-traumatic stress disorder, and antidepressants reverse and prevent this volume reduction,³ either by repairing the damage caused by stress or by inducing hippocampal *neurogenesis*,⁴ which refers to the growth of new neurons from progenitor or neural stem cells. Also, synaptic and glial atrophy have been observed in the prefrontal cortex in depression.⁵ The neurotrophic hypothesis of depression and mood disorders has recently been proposed to account for some of these observations.⁶

The neurotrophic hypothesis suggests that decreased expression of neurotrophins and possibly other growth factors contributes to depression, and that antidepressants reverse this effect.³ When studying which potential target could produce such a reparative or protective effect, the neurotrophic hypothesis led us to examine protein receptors and signaling pathways implicated in neurogenesis. *Growth factors*, which are secreted signaling proteins that induce

the growth, proliferation and differentiation of cells during development and protect mature neurons throughout life, are linked to antidepressant action and increasing growth factor receptor signaling represents an approach to potential treatment for neurodegenerative diseases. A growth factor that protects neurons from death is considered a *neurotrophic factor*, which is by definition tied to the development, function and survival of neurons. The two families of proteins that are considered neurotrophic factors include the neurotrophins and the glial cell-derived neurotrophic factor (GDNF) family of ligands (GFLs). Of these proteins, the neurotrophins in particular are crucial for hippocampal neurogenesis and are heavily implicated in mood disorder neurobiology,⁷ Alzheimer's disease,⁸ and other brain disorders. Proteins, and even peptide mimetics, however, are not often suitable drugs, as they may be metabolized too quickly or not cross the blood-brain barrier,⁹ and so the development of effective delivery systems¹⁰ and neurotrophic small molecule that can mimic neurotrophin action or induce neurotrophin gene expression¹¹ are important areas of research.

I.2 BDNF/TrkB Signaling

The neurotrophin family consists of the secreted proteins *nerve growth factor* (NGF), *brain-derived neurotrophic factor* (BDNF), *neurotrophin-3* (NT-3), and *neurotrophin-4* (NT-4, also NT-4/5 or NT-5). Each protein functions as a relatively selective, high-affinity ligand for one of the neurotrophin receptors: NGF for TrkA (also referred to as the nerve growth factor receptor), BDNF and NT-4 for TrkB (*tropomyosin receptor kinase B*), and NT-3 for TrkC, which are receptor tyrosine kinases (RTKs), phosphorylation of which is capable of inducing a variety of intracellular signaling pathways (Figure 1).¹² The proteins also function as low-affinity ligands for the neurotrophin receptor p75NTR, which is part of the TNF- α family of receptors.

BDNF, like the other neurotrophins, is synthesized in a precursor pro-form, which must be proteolytically cleaved into its mature form.¹³ Pro-BDNF does not share the same function as mature BDNF, and demonstrates a higher affinity for p75NTR; p75NTR at times serves to support and increase the specificity of Trk receptors for their respective ligands, even at times potentiating Trk signaling, but ligand binding to p75NTR in the absence of Trk signaling can also result in activation of apoptotic pathways, earning p75NTR the nickname of ‘death receptor’.¹⁴ Mature BDNF is functional as a noncovalent dimer (thus any reference to BDNF from this point will be referring to the active, dimerized form of the protein), which upon binding induces dimerization and activation of its receptor TrkB.

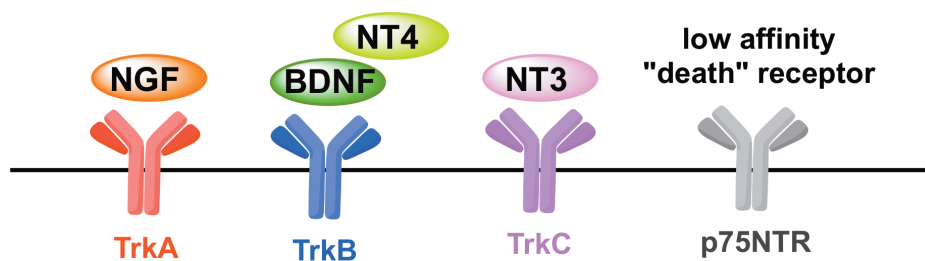


Figure 1. The neurotrophin receptors and their main cognate ligands.

TrkB is a membrane-bound receptor enzyme containing an extracellular domain, a single-pass membrane domain, and an intracellular, catalytic kinase domain. As a tyrosine kinase, it is capable of transferring a phosphate group from adenosine triphosphate (ATP) to tyrosine residues on target proteins, but it itself also requires tyrosine phosphorylation to be activated. Typical of receptor tyrosine kinases (RTKs), it exists primarily as a monomer, and may dimerize spontaneously in conditions of high receptor density or form functional heterodimers with one of the other Trk receptors. It occurs in an immature form, a mature, glycosylated form (145 kDa), and a truncated form T1 (90 kDa) that lacks the intracellular domain (ICD) where

phosphorylation occurs.¹⁵ In response to BDNF-induced dimerization, TrkB may be phosphorylated at multiple sites, each of which may activate different signaling cascades leading to cellular differentiation, survival, and/or synaptic plasticity. Tyr-670, Tyr-674, and Tyr-675 are major sites of autophosphorylation in the kinase domain, and other residues include Tyr-706/707; these are all phosphorylated following neurotrophin binding leading to activation of the kinase, though the signaling cascades are activated following phosphorylation of other specific residues.¹⁶

The primary signaling cascades activated by TrkB are the phosphoinositide-3 kinase/Akt (PI3K/Akt), the mitogen activated protein kinase (MAPK) pathway involving Ras/MAPK/ERK (extracellular related kinase), and phospholipase C- γ 1/protein kinase C (PLC γ /PKC) pathways (Figure 2). Phosphorylation creates docking sites for adaptor proteins that lead to activation of one or more of these pathways. For example, phosphorylation of tyrosine 515 (Y515, commonly referred to as Y490, the corresponding residue in TrkA) creates a binding site for the protein Shc, which results in MAPK signaling and subsequent neurite outgrowth. Phosphorylation of tyrosine 816 (Y816, which is often referred to as Y785, the corresponding residue in TrkA) recruits and activates PLC γ ,¹⁷ resulting in activation of PI3K followed by Akt (also called protein kinase B, PKB), a major signaling protein for neuronal survival. PLC γ activation may also Ca^{2+} release and consequent protein kinase C (PKC) activation, which results in plasticity.¹⁶

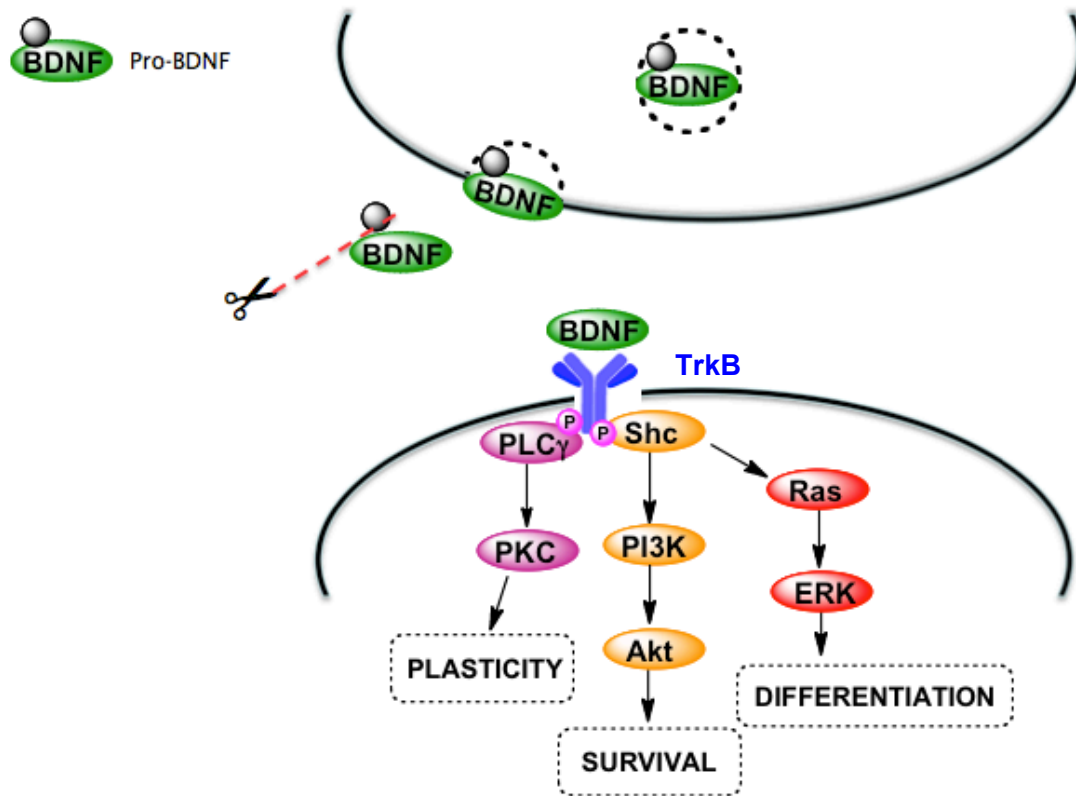


Figure 2. TrkB-activated signaling pathways.

I.3 BDNF/TrkB in Psychiatric and Neurodegenerative Disease

BDNF is a neurotrophin of interest in psychiatric and neurodegenerative disease. A landmark study that demonstrated the antidepressant capacity of BDNF showed that in two animal models of depression, infusion of BDNF into the midbrain of rats was antidepressant and also protective.¹⁸ Abnormal expression of BDNF and potential roles of BDNF-TrkB signaling have been observed in mood and mental disorders, including schizophrenia,¹⁹ major unipolar and bipolar depressive disorders,⁷ Rett syndrome (an autism spectrum disorder)²⁰ and obesity.²¹ Antidepressants have been shown to regulate BDNF expression²² and elicit TrkB activation independently from their serotonergic effects.²³ TrkB activation is required for behavioral effects²⁴ and antidepressant-induced neurogenesis.²⁵ Also, other activities and treatments

known to be antidepressant, such as electroconvulsive therapy, exercise²⁶ and vagal nerve stimulation,²⁷ have also been shown to increase BDNF or lead to TrkB activation. A process likely involved in memory and learning, long term potentiation (LTP), is also dependent on normal BDNF-TrkB function.²⁸ Modulation of pain has also been a putative role of the neurotrophin.²⁹ BDNF and TrkB have also been heavily implicated in neurodegenerative diseases,³⁰ including Parkinson's disease,³¹ Alzheimer's,³² Huntington's,³³ and amyotrophic lateral sclerosis (ALS).³⁴

A *BDNF* gene polymorphism Val66Met has been linked to many conditions as well, providing additional support for a role of BDNF in post-traumatic stress disorder,³⁵ mood disorders and schizophrenia,³⁶ bipolar disorder,³⁷ and others, though not all studies support the connection.³⁸ This, along with the large body of evidence referenced above, motivated us to consider the BDNF/TrkB signaling pathway as a potential target for the development of small molecules capable of neuronal repair or rescue.

With TrkB and its signaling being so important in CNS function, neurodegeneration, and other disease, we examined the literature for TrkB agonists and antagonists/inhibitors and considered the potential therapeutic value of activating or inhibiting TrkB in the brain. The following sections describe the known TrkB-selective agonists and antagonists/inhibitors, which we considered as prospective starting points for our own search for small molecule TrkB signaling modulators.

1.4 TrkB Agonism

There are three major approaches for increasing neurotrophic activity via the BDNF/TrkB signaling system. First, induction of BDNF synthesis and/or release;¹¹ second,

direct agonists including monoclonal antibodies to activate TrkB,³⁹ BDNF peptide mimetics,⁴⁰ RNA aptamers,⁴¹ and direct small molecule agonists;^{11,42} third, transactivation of the receptor via activation of G-protein coupled receptors (GPCRs) or other RTKs. Antibodies and peptides are not as desirable as small molecules for development of research tools and therapeutics due to their metabolic instability and frequent inability to cross the blood-brain barrier.

We originally set out to establish a cell-based ELISA (enzyme linked immunosorbent assay) to measure the release of BDNF into the medium from a model cell line. There are a growing number of small-molecule pharmacological agents known to increase BDNF synthesis or release, including 4-methylcatechol,⁴³ resveratrol,⁴⁴ gangliosides,⁴⁵ and many others.¹¹ Unfortunately, our efforts to establish a release assay using a variety of cell lines did not yield robust release of BDNF into the medium of any of the cell lines tested (differentiated SH-SY5Y, Neuro2a, and SK-N-AS neuroblastomas, primary human hippocampal astrocytes, and C6 rat glioma); only primary human cortical astrocytes and SMS-KCN neuroblastoma cells released enough BDNF to be detected by an *in situ* enzyme-linked immunosorbent assay (ELISA).⁴⁶ While it was possible that our detection of BDNF release was prevented by the lack of a reliable positive control, preventing us from detecting any BDNF release beyond the basal levels that were below the quoted detection limit of the ELISA kit, we opted to focus future studies on developing molecules that interact with TrkB directly, as opposed to increasing signaling by inducing neurotrophin release. Recent advances in the development of small molecule neurotrophin mimetics has yielded only a small handful of reported TrkB agonists (Figure 3) and the elucidation of several transactivation pathways that induce TrkB activation.

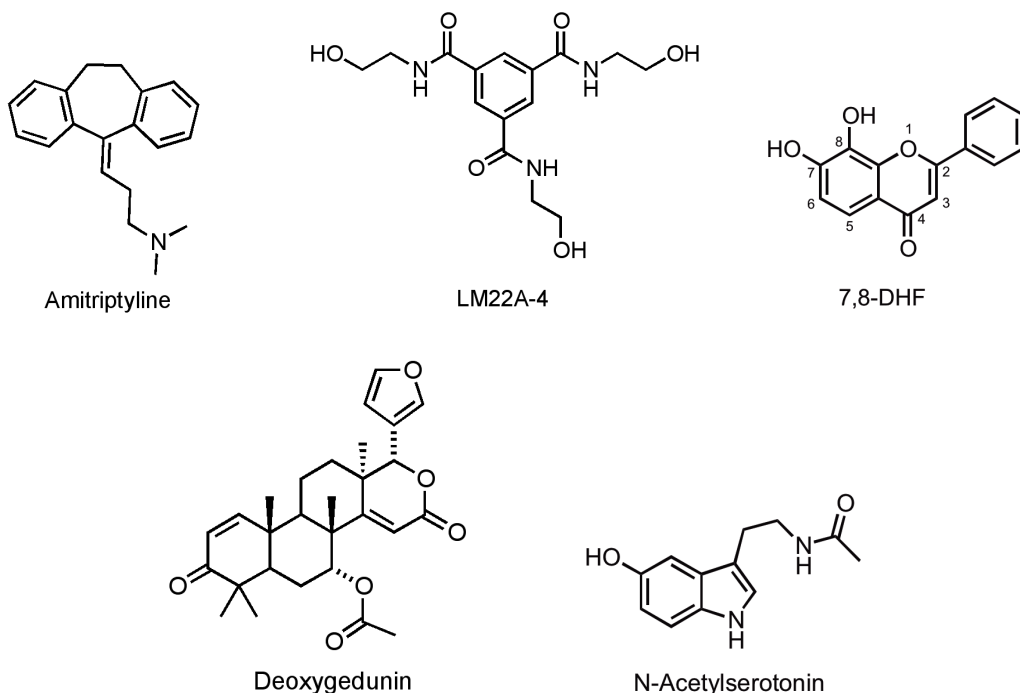


Figure 3. Chemical structures of several putative TrkB agonists.

I.4.1 Amitriptyline

The tricyclic antidepressant amitriptyline (Figure 3) has been in clinical use since the 1960's and has traditionally been thought to elicit its effects via its serotonin-norepinephrine reuptake activity, although it is known to bind to a number of CNS receptors. Interestingly, it was reported in 2009 to be a direct TrkA and TrkB agonist, inducing the homo- and heterodimerization of both receptors.⁴⁷ The authors found that a low, physiologically relevant concentration of amitriptyline (500 nM, whereas 5-7 μ M is the estimated therapeutic concentration in the brain⁴⁸), but not its tricyclic relatives imipramine or clomipramine, induced neurite outgrowth in PC12 cells, which is a common assay for neurotrophic activity. Amitriptyline also protected rat hippocampal neurons from apoptosis by an oxygen-glucose deprivation test, and activated TrkA and TrkB, but not TrkC, heterologously expressed in human embryonic kidney (HEK) cells. The authors used an *in vitro* binding assay, in which

amitriptyline bound to the ECD, but not ICD, of TrkA ($K_d \sim 3\mu\text{M}$) and TrkB ($K_d \sim 14\mu\text{M}$); however, binding was not competitive with NGF or BDNF, respectively. The compound also activated TrkA and B in mouse brain, along with Akt and ERK1/2 over the same time course. These results indicate that amitriptyline is neurotrophic and protective in both *in vitro* and *in vivo* systems, and though it is active against TrkB, greater experimental emphasis is placed on its TrkA activity.

I.4.2 LM22A-4

Massa and colleagues identified LM22A-4 (Figure 3) from a small set of TrkB agonist leads via an extensive *in silico* screen of >1,000,000 compounds based on a model of the likely BDNF binding region.⁴⁹ Fourteen compounds were selected from the hits and seven were screened for neurotrophic activity using E16 mouse hippocampal neurons; four were chosen for further examination and found to activate TrkB selectively using TrkA, B, or C transfected mouse embryonic fibroblast NIH-3T3 cells. LM22A-4, the simplest compound structurally and most amenable to chemical modification, bound selectively to TrkB-ECD, competed for BDNF binding ($\text{IC}_{50} \sim 47 \text{ nM}$), and at $10 \mu\text{M}$ did not bind strongly to other receptors in a commercial binding screen of 57 CNS receptors. The compound also activated TrkB, Akt, and ERK at 60 minutes from $0.01 - 500 \text{ nM}$ in cultured E16 mouse hippocampal neurons and in adult mouse hippocampus and striatum after 7-day treatment (10 mg/kg). The compound was also protective in *in vitro* models of Alzheimer, Huntington, and Parkinson diseases. The authors speculate that though the molecule is small and would not be able to induce dimerization of the receptor by binding two discrete Trk monomers simultaneously, it may bind to a ‘hot spot’ and induce a

conformational change that activates the receptor. In all, the authors deduced that LM22A-4 has selective, partial agonist activity at TrkB.

A recent study found that LM22A-4, when administered three days after induced stroke in mice trained to perform motor tasks, led to decreased recovery time and increased neurogenesis in the region adjacent to the stroke.⁵⁰ The compound also proved to be therapeutic in an animal model of Rett syndrome, returning TrkB phosphorylation to wild-type levels after four weeks of administration and regulating abnormal breathing.⁵¹ Though the efficacy of the small molecule remains to be validated in a completely independent laboratory at this time, the *in vitro* and *in vivo* evidence is accumulating in support of LM22A-4 as a potent, effective TrkB agonist capable of inducing neurogenesis and cell survival signaling.

I.4.3 7,8-Dihydroxyflavone (7,8-DHF)

The same laboratory that reported amitriptyline as a TrkA/TrkB agonist reported another selective TrkB agonist, 7,8-DHF, in 2010.⁵² The compound was identified from a survival screen in T48 cells, which are TrkB-transfected murine basal forebrain SN56 cells, in which apoptosis was induced using staurosporine. Sixty-six compounds that enhanced survival in T48 but not SN56 were identified as potential TrkB agonists; five of these were flavone compounds. 7,8-DHF, cianidanol, pinocembrin, and diosmetin protected primary hippocampal neurons from glutamate toxicity with EC₅₀ values of 35, 100, 100, and 500 nM, respectively. 7,8-DHF also protected the cells from oxygen-glucose deprivation and even protected primary human neurons from H₂O₂-induced apoptosis. It induces homodimerization of the TrkB receptor and activation of TrkB, Akt, and ERK1/2 in primary hippocampal neurons but does not induce signaling in cells with kinase-dead TrkB (TrkB-KD). [3H]-7,8-DHF binding was observed at the TrkB-ECD

($K_d = 320$ nM), but not TrkB-ICD, and not at TrkA or p75NTR. In models of neuronal injury, the compound also proved active; it decreased kainic acid-induced apoptosis in mouse brain and decreased toxicity induced by MPTP (1-methyl-4-phenyl-1,2,3,6-tetrahydropyridine, the neurotoxic precursor to the neurotoxin MPP+), a known model of Parkinson's disease.

Examination of the structure-activity relationship (SAR) of the active and inactive flavones from the original screen indicates that the only required substituent is the 8-position hydroxyl group (Figure 3). A further, more thorough SAR study identified a more potent flavone analog, 4'-dimethylamino-7,8-dihydroxyflavone, which exhibits stronger anti-apoptotic activity compared to 7,8-DHF and more potent antidepressant activity.⁵³ Concerns about the metabolic stability of this compound led to further optimization, where potential metabolism of the dimethylamino group was addressed by replacing it with pyrrolidino, and full metabolic profiling of the best lead led to the compound 2-methyl-8-(4-(pyrrolidin-1-yl)phenyl)chromeno[7,8-d]imidazol-6(1H)-one as an optimized, drug-like TrkB agonist ready for further preclinical development.⁵⁴

The identification of 7,8-DHF as a TrkB agonist has been an important breakthrough in the field, and the compound has been applied to a number of disease models. It has been shown to improve neuromuscular transmission,⁵⁵ activate TrkB in mouse amygdala and improve emotional memory,⁵⁶ restore BDNF-TrkB signaling integrity in an animal model related to post-traumatic stress,⁵⁷ and reduces disease symptoms in Rett syndrome mice.⁵⁸ Excitingly, the compound successfully reverses memory deficits in a mouse model of Alzheimer's, 5XFAD.⁵⁹ In this mouse model, hippocampal BDNF decreases over time, as does the activation and expression of TrkB receptors, while expression of β -secretase enzyme (BACE-1), the enzyme responsible for cleaving amyloid precursor protein (APP) into the amyloid fragments that form

toxic plaques A β ₄₀ and A β ₄₂, increases. Administration of 7,8-DHF for 10 days (5 mg/kg, i.p.) restored BDNF-TrkB signaling, blocked BACE-1 elevations, and lowered levels of APP, A β ₄₀ and A β ₄₂. Another recent pair of studies supports the utility of the compound in hippocampal age-related synaptic dysfunction, as 7,8-DHF led to the rescue of long-term synaptic plasticity and signaling deficits in the hippocampus⁶⁰ as well as other brain regions, including the amygdala.⁶¹ These studies are a testament to the potency and efficacy of 7,8-DHF as a TrkB agonist, especially *in vivo*, across disease models. However, it is likely that the compound exerts neuroprotective action on cells via its antioxidant activity in addition to TrkB activation, as 7,8-DHF protects mouse hippocampal neuronal HT-22 cells against glutamate-induced toxicity.⁶²

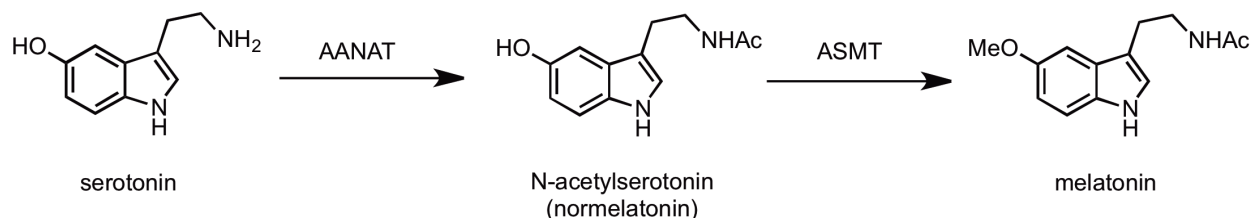
I.4.4 Deoxygedunin

The Ye lab discovered another TrkB agonist in their screening for neuroprotective compounds, deoxygedunin.⁶³ Screening revealed four gedunin family compounds as possible TrkB agonists, with deoxygedunin providing the strongest protective effect against glutamate-induced toxicity. The compound binds weakly to the ECD of TrkB, but not TrkA, with $K_d \sim 1.4 \mu\text{M}$, and induces receptor dimerization but does not displace neurotrophin binding. In TrkA, B, and C-transfected HEK293 cells, it activated TrkB selectively. Immunohistochemistry demonstrates TrkB activation in primary hippocampal neurons. In cultured rat cortical neurons, it dose-dependently phosphorylated TrkB and also induced phosphorylation of Akt and ERK, with maximal activation at 30 minutes and 500 nM. To determine if the neuroprotective effect was TrkB dependent, the authors used TrkB-F616A knock-in mouse cortical neurons to demonstrate that activation by deoxygedunin can be prevented by 1NMPP1, a TrkB-F616A inhibitor, as in their other TrkB agonist studies. TrkB, ERK, and Akt were also activated, though

with different kinetics than in the cultured cell models, in mouse brain. *In vivo* behavioral characterization also supported the activity of the compound: in the forced swim test, a classic paradigm to test antidepressant efficacy, deoxygedunin proved to have an anti-depressant effect, and the compound also enhanced acquisition of conditioned fear, a process which requires BDNF-dependent TrkB activation.

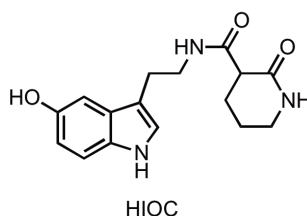
I.4.5 *N*-Acetylserotonin

N-Acetylserotonin (NAS), a serotonin metabolite and direct precursor to melatonin (Scheme 1), was also discovered by the Ye lab to activate TrkB.⁶⁴ The authors examined several serotonin metabolites in primary mouse hippocampal neurons to determine if they activate TrkB, at 100 nM after 30 minutes since serotonin and BDNF are known to cooperate to regulate neuronal survival and plasticity, and they found that only NAS activates TrkB, and in a BDNF- and melatonin (MT₃ subtype) receptor-independent manner. Phosphorylation of TrkB peaked at 30 minutes. TrkB was also phosphorylated in a time-dependent manner correlating to the circadian rhythm in mice with normal arylalkylamine N-acetyltransferase (AANAT), the enzyme responsible for converting serotonin to NAS, but not in mice with the mutated enzyme. NAS was protective against kainite-induced apoptosis in TrkB 616A mice, and this effect was ameliorated by pretreatment with 1NMPP1, which suggests that the protection is TrkB-dependent. The authors also found that NAS, but not melatonin, demonstrated antidepressant activity in the forced swim test.

Scheme 1. Production of melatonin from serotonin via N-acetylserotonin.

(AANAT = arylalkylamine N-acetyltransferase; ASMT = acetylserotonin o-methyltransferase)

Despite the *in vitro* and *in vivo* evidence suggesting that NAS is a TrkB agonist, binding studies did not provide evidence for interaction between the compound and the receptor, which the authors attributed to rapid kinetics of binding and dissociation. Nonetheless, the finding that NAS activates TrkB is interesting in the context of antidepressant research, as the antidepressant fluoxetine is known to induce increased expression of AANAT⁶⁵ and melatonin and disruption in circadian rhythms have been connected to the pathophysiology of depressive disorders.⁶⁶ Fortunately, the authors sought a more stable derivative of NAS that would have a longer biological half-life and found that the derivative N-[2-(5-hydroxy-1H-indol-3-yl)ethyl]-2-oxopiperidine-3-carboxamide (HIOC, Figure 4) activates TrkB and protects retinas from light-induced retinal degeneration.⁶⁷

**Figure 4.** Reported TrkB agonist N-[2-(5-hydroxy-1H-indol-3-yl)ethyl]-2-oxopiperidine-3-carboxamide (HIOC).

I.4.6 L-783,281 (Demethylasterriquinone B1, DAQ B1)

L-783,281 (Figure 5) is a fungal metabolite originally discovered to activate the insulin receptor at micromolar concentrations.⁶⁸ Further exploring the activity of the compound, the authors found that L-783,281, but not its closely related structural isomer L-767,827, activates TrkA, TrkB, and TrkC by 41% of NGF-induced activation, 37% of BDNF, and 14% of NT-3, respectively, by Western blotting, with maximal Trk phosphorylation occurring at 3 minutes.⁶⁹ The compound also induced pTrk in rat and human cortical neuronal cultures and in rat dorsal root ganglion cultures. However, though the compound activated ERK signaling in these lines, it also activated ERK in nontransfected CHO cells, signifying that the molecule acts on an additional target other than the Trk or insulin receptors.

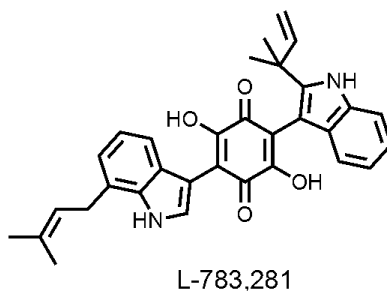


Figure 5. Structure of L-783,281.⁶⁹

Also, no binding studies or pharmacological inhibition of Trk receptors were reported. Intriguingly, the authors used PDGF-Trk receptor chimeras to determine which part of the receptor is required for signaling, and found that the molecule acts at the kinase domain and not the ECD. While the compound does not necessarily activate Trk directly, or if so, does not activate Trk specifically, it is an example of a small molecule that activates relevant and important neurotrophic signaling and the activation of Trk is very likely due to intracellular

transactivation from other receptor or target. It is important to note that this study, as well as the previous studies discussed, does not report a quantitative measure of TrkB activation by a small molecule agonist.

I.4.7 Transactivation

Transactivation is a common phenomenon in which the activation of one receptor signals to activate a second receptor, the classic example of which is G-protein coupled receptor (GPCR) transactivation to receptor tyrosine kinases.⁷⁰ Specifically, several transactivation pathways have been demonstrated for TrkB via very different mechanisms. Activation of the D1 receptor, a GPCR, using the benzapine SKF38393, a D1 agonist, activates TrkB and results in phosphorylation of PLC γ , Akt, and MAPK proteins in striatal neurons, which can be blocked by K252a, a Trk and serine/threonine kinase inhibitor, and by a D1 antagonist.⁷¹ Adenosine and adenosine 2A (A_{2A}) receptor agonists (i.e. CGS 21680) are also capable of activating TrkB via the A_{2A} receptor.⁷² Acetylcholinesterase inhibitors donepezil and galantamine lead to rapid transactivation of both TrkA and TrkB in mouse hippocampus and phosphorylation of Akt and CREB, but not ERK1/2.⁷³ Endocannabinoids acting through the CB₁ cannabinoid receptor (CB₁R) activate TrkB and induce association of CB₁ with TrkB in PC12-TrkB cells transfected with CB₁R; rat cortical interneurons also exhibited TrkB activation following treatment with a CB₁R agonist.⁷⁴ Pituitary adenylate cyclase activating protein (PACAP), a neuromodulating peptide which signals through its GPCR receptor VPAC-1, induces TrkB activity in rat hippocampal neurons.⁷⁵

In addition to the GPCR receptors, at least one intracellular receptor, the glucocorticoid receptor, can activate TrkB, as dexamethasone induces TrkB phosphorylation in rat brain.⁷⁶

Another receptor tyrosine kinase, Ret, has also been shown to activate TrkB in SH-SY5Y and LAN-5 neuroblastoma cell lines, which has been linked to their differentiation by retinoic acid.⁷⁷

Two metal ions have also been shown to activate TrkB: copper in mouse embryonic cortical neurons,⁷⁸ and zinc in rat cortical neurons,⁷⁹ both through metalloproteinase and Src-dependent mechanisms. It is possible that other potential transactivation mechanisms may exist that induce TrkB signaling as well.

1.5 TrkB Antagonism

There is a clear connection between the induction of TrkB signaling and the positive outcomes described above; however, activating a growth factor receptor pathway may have negative consequences. Overexpression of TrkB has been observed in epilepsy,⁸⁰ drug abuse,⁸¹ neuropathic pain,⁸² and cancer,⁸³ implying that increasing TrkB signaling may contribute to the pathogenesis of these conditions, and inhibiting or antagonizing signaling may prove effective for treatment of these conditions. In some parts of the brain, like the ventral midbrain-nucleus accumbens pathway, infusion of BDNF is actually pro-depressive.⁸⁴ Of particular interest is the involvement of BDNF/TrkB signaling in reward circuitry in the brain; for example, self-administration of cocaine is increased by infusion of BDNF into rat nucleus accumbens⁸⁵ and after a single, acute injection of cocaine, TrkB is required for sensitization and conditioned place preference.⁸⁶

Due to the differential effect of BDNF signaling in different brain regions, global administration of an agonist or antagonist/inhibitor poses a concern, which may be addressed with the development of positive or negative modulators of TrkB signaling. A very limited number of TrkB inhibitors are known; K252a, a staurosporine analog, is commonly used as a

supposed selective Trk family inhibitor, though it is known to inhibit PKC and other kinases as well.⁸⁷ Only two low molecular weight, specific negative modulators of TrkB are known and were only recently reported: cyclotraxin B and ANA-12.

I.5.1 Cyclotraxin B

A peptidomimetic approach facilitated the development of cyclotraxin B (CTX-B, CNPMGYTKEGC, cyclized at the terminal cysteine residues) as a potent, allosteric, partial TrkB antagonist.⁸⁸ By proteolytically digesting mature BDNF to create fragments and screening them for TrkB inhibition in a TrkB-inducible cell line, Tet*On*-rhTrkB CHO, the authors were able to use the active fragment sequence and a model of the binding site to design CTX-B. As the compound does not inhibit BDNF binding, the authors postulated that its inhibitory activity is derived from allosteric modulation of the extracellular domain of TrkB, thus preventing both its basal activation and its activation by its endogenous ligand BDNF or even its transactivation by a glucocorticoid, dexamethasone.⁷⁶ The potency of inhibition of BDNF-induced TrkB activation differed in the exogenously TrkB-expressing CHO cells ($-34.8 \pm 8.0\%$, $IC_{50} = 0.28 \pm 0.08$ nM) versus primary mouse cortical neurons ($-53.0 \pm 5.8\%$, $IC_{50} = 65.7 \pm 21.7$ pm), presumably due to the presence of both endogenous TrkB and p75NTR in cortical neurons. This inhibition was also selective up to 1 μ M over TrkA and TrkC, as assessed in nnr5 PC12-TrkA and -TrkC cells, and the compound was not toxic even at 10 μ M after 72 hours. CTX-B inhibits activation at two tyrosine residues that initiates downstream signaling, Y515, which binds Shc and induces MAPK signaling and neurite outgrowth, and Y816, which recruits and activates PLC γ .

The compound was also shown to be biologically active when administered by systemic injection, enabled by fusing CTX-B to the transduction domain of a protein, *tat*, from HIV type I. It was not antidepressant as determined by the forced swim test, but in two models of anxiety/social defeat stress, specifically the open field and elevated-plus maze tests, the compound proved to be anxiolytic. These results are promising, as the inhibitor is only a partial inhibitor of the receptor. This may be an advantageous feature for pharmacological, systemic use, as global and complete inhibition of TrkB in the brain could have deleterious effects from long-term usage. Since the initial publication of the inhibitor, CTX-B has been used to examine the roles of BDNF in an animal model of neuropathic pain⁸⁹ and in amphibian melanocyte growth in response to dark environments.⁹⁰

I.5.2 ANA-12

The second selective TrkB inhibitor to be reported is ANA-12 (Figure 6), a small molecule developed from *in silico* screening hits based on the “specificity patch”, a binding pocket speculated to control the selectivity of BDNF for TrkB.⁹¹ From 22 virtual hits, 12 were assessed in a KIRA-ELISA assay using the same cells as in the CTX-B study to determine TrkB activation, and two of those hits fully inhibited phosphorylation of TrkB by BDNF. However, one of the two compounds did not inhibit TrkB in primary neurons, and the one that did was not very potent, so further screening of the core was performed to arrive on ANA-12, the only of the fourteen second-round hits that was effective in the KIRA-ELISA assay at submicromolar concentrations in the transfected cells. Attaching BODIPY via a linker to ANA-12 allowed the authors to use fluorescence spectroscopy to assess the compound’s binding to recombinant TrkB-ECD, assuming that the BODIPY did not interfere with the binding interaction between ANA-12

and TrkB; a low affinity ($K_d = 12 \mu\text{M}$) and a high affinity ($K_d \sim 10 \text{ nM}$) binding site were identified, and the compound was modeled in the specificity patch of the protein.

The only way, however, that the researchers assessed the compound's ability to inhibit downstream signaling and its specificity for TrkB versus the other Trks was via the PC12 neurite outgrowth assay using nnr5 PC12-Trk cell lines, which are NGF nonresponding mutant PC12 cells stably transfected with TrkA, TrkB or TrkC cDNA. ANA-12 inhibited neurite outgrowth from 10 – 100 μM and was nontoxic by visual inspection.

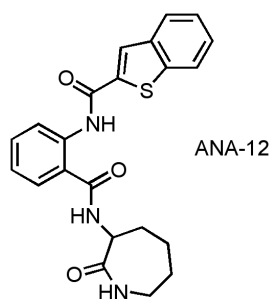


Figure 6. Structure of ANA-12.⁹¹

In the adult mouse brain, the ability of ANA-12 to inhibit TrkB in various brain structures after administration was determined, and it was found that after two hours, TrkB inhibition in the striatum was more robust than in the cortex and hippocampus, but after four hours inhibition was fairly equal across brain regions. When mice were subjected to the elevated plus maze task and the novelty-suppressed feeding paradigm tests for anxiety, and either the forced swim test or the tail suspension test for depression, administration of ANA-12 (0.5 mg/kg) was effective in each behavioral model.

ANA-12 has been used in multiple studies since its initial publication to examine the role of TrkB in several disease models. For example, in a rat model of hypertension and vascular

dementia, 28 days of treatment with telmisartan, an angiotensin II receptor blocker and PPAR- γ (peroxisome proliferator-activated receptor γ) agonist, upregulated BDNF expression in the hippocampus and provided a protective effect against cognitive decline that was dependent on TrkB signaling as evidenced by attenuation using ANA-12.⁹² Another intriguing study found that the male offspring of cocaine-addicted rats demonstrated a delayed acquisition of cocaine-self administration, which was reversed by administration of ANA-12, suggesting that the increase in BDNF mRNA, protein expression, and signaling in the medial prefrontal cortex may dampen the reinforcing effect of cocaine in the offspring (contrary to epidemiological studies in humans).⁹³ Finally, the administration of BDNF or leptin into the medial nucleus tractus solitaries reduced food intake in rats, a phenomenon that was prevented via administration of ANA-12, signifying a probable inverse relationship between TrkB-mediated signaling in the brain region and food intake.⁹⁴ The antagonist will likely be utilized in many more studies of BDNF/TrkB-dependent CNS processes in the near future.

II. Establishing an Assay for Assessment of TrkB Activation

To begin exploring currently published TrkB agonists and antagonists, we chose to use western blotting as the primary tool for semi-quantitatively assessing TrkB phosphorylation. We reasoned that cell line with exogenously expressed TrkB would be a good model system to initiate our studies, and the activity of any promising small molecule candidates would then be confirmed in a cell line that endogenously expresses TrkB. Though we considered designing or purchasing a TrkB assay that could be adapted to a 96-well plate format, for preliminary work we opted to develop western blotting expertise before committing to a more expensive system.

II.1 NIH-3T3-Trk and HEK-TrkB Cells

A former post doctoral colleague, Dr. Shu Li, obtained and began work with NIH-3T3-TrkA, -B, and -C cells. They are Swiss embryonic mouse fibroblast NIH-3T3 cells that have been stably transfected with Trk receptors. Dr. Li found high levels of basal autophosphorylation in NIH-3T3-TrkB, without a reproducible difference between background phospho-TrkB and BDNF-induced phospho-TrkB (pTrkB). Data presented in the literature using this line did not reflect this high level of autophosphorylation,⁴⁹ so we learned about the phenomenon in hopes of finding a way to circumvent it. There are two types of autophosphorylation: *cis* autophosphorylation occurs when a protein kinase activates itself, whereas *trans* autophosphorylation occurs when the partner from the dimer or complex activates the other member of the complex. Both types of phosphorylation rely on the ICD of the receptor being accessible to ATP in order to accept a phosphate group. After lysis and denaturation, the conformation of the ICD is no longer as prohibitive toward phosphorylation and free ATP can more easily access the tyrosine residues. Chelation of Mg^{2+} or Mn^{2+} , which stabilizes ATP, via ethylenediamine tetraacetic acid (EDTA) is one way that this process is prevented. It has been reported that TrkB autophosphorylation is dependent on time, concentration of ATP, and density of the TrkB receptor, where autophosphorylation increases as receptor density increases.⁹⁵ This has obvious implications for cell lines overexpressing TrkB, as in the case of NIH-3T3-TrkB.

In my hands, basal TrkB activation was also extremely high, despite efforts to reduce receptor autophosphorylation by working with cell lysates exclusively at 4°C to slow enzymatic activity and by using a tenfold excess of EDTA. Initially, we presumed that the observed basal activation was intrinsic to the activity of Trk receptors, since they are known to be easily phosphorylated, as described in the quotation below:⁹⁶

“... high local membrane density of Trk proteins may promote spontaneous activation in the absence of neurotrophins. Although such spontaneous activation has been observed for many receptor tyrosine kinases under scenarios of overexpression, the Trk proteins are especially prone to this behavior. Indeed, this tendency to undergo spontaneous activation represented a difficult impediment to pioneering studies aiming to prove that TrkA was an NGF receptor by demonstrating NGF-dependent activation of TrkA in transfected cell lines (Dr. Moses Chao, personal communication). Although the apparent hair-trigger behavior of Trk activation has been a continual annoyance for investigators studying Trk signaling mechanisms, it may be argued that leaving Trk proteins delicately poised at the brink of activation represents an essential feature of Trk function, as it allows diverse forms of modulation of the cellular environment to impinge on Trk activation.”⁹⁶

However, after attempts to reduce the apparent basal pTrkB with cautious handling of lysates, loading various concentrations of protein in the western, serum deprivation prior to the experiment, different degrees of confluency, and experimenting with several phospho-specific antibodies (selective for Y490, Y816, and Y706) at various dilutions without success, we decided to consult with members of Prof. Moses Chao's laboratory at the NYU medical center. From these discussions, we determined that the over-activity of the receptor was likely due to high constitutive activity of the specific NIH-3T3-TrkB line, and that our BDNF (Aldrich) was potentially not as active as the BDNF their group routinely uses (Peprotech); the group generously donated a new exogenously transfected secondary cell line, HEK-TrkB cells, to our group.

Human embryonic kidney (HEK) cells are a commonly used system for the heterologous expression of recombinant receptors and proteins.⁹⁷ We found these cells to have low basal TrkB activity, and Peprotech BDNF to be more potent than that from Aldrich, thus establishing an effective system for us to test human TrkB activity with a reliable positive control (Figure 7).

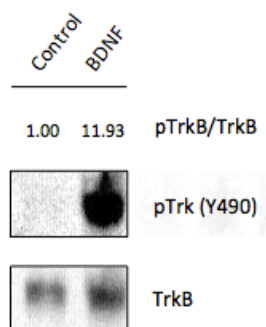


Figure 7. Activation of TrkB in HEK-TrkB by BDNF. HEK-TrkB cells were incubated for 10 minutes in the presence or absence of 50 ng/mL human BDNF. Lysates were analyzed by western blotting using a phospho-specific Trk antibody, followed by stripping and reprobing the membrane for total TrkB. pTrkB/TrkB indicates quantification of the relative ratio of phosphorylated TrkB induced by BDNF to the control, from densitometry analysis by ImageJ. Representative image of at least five separate experiments.

Comparing pTrkB or activated downstream signaling enzymes like ERK1/2, with nontransfected HEK cells would allow us to determine if activation is due to the presence of TrkB. To determine specificity of the molecules we work with, activation of Trks A and C can be determined with the respective NIH-3T3 transfected lines and compared to nontransfected 3T3. In my hands, NIH-3T3-TrkA cells were functional and selectively activated by NGF but not BDNF, independently of confluence (Figure 8).

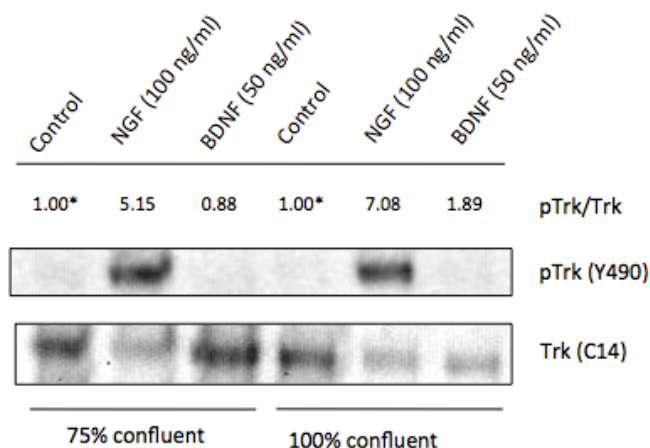


Figure 8. Activation of TrkA in NIH-3T3-TrkA cells by NGF. NIH-3T3-TrkA cells were incubated for 10 minutes in the presence or absence of 50 ng/mL human NGF. Lysates were analyzed by western blotting using a phospho-specific Trk antibody, followed by stripping and reprobing the membrane for total Trk. pTrk/Trk indicates quantification of the relative ratio of phosphorylated Trk induced by NGF to the control, from densitometry analysis by ImageJ. Representative image of three separate experiments.

II.2 Efforts to Establish Small Molecule Controls: HEK-TrkB

With functional cell lines with easily distinguishable receptor activation and reliable neurotrophin positive controls, we sought to confirm the activity of the previously discussed published agonists (I.4) and antagonists (I.5) in hopes of determining a lead compound for further development. In contrast to our expectations, we found that amitriptyline, LM224-A (the triamide), and 7,8-DHF did not activate TrkB in HEK-TrkB cells at the published incubation times and concentrations (Figure 9). We reasoned that perhaps in this particular cell line, Y490 was not activated, but despite probing for multiple tyrosine-phosphorylated Trk receptors, we did not observe reproducible activation of the receptor using western blotting. To address the possibility that tyrosine residue(s) other than Y490 or Y816 were phosphorylated, despite most reports reporting activation at those specific residues including by the putative agonists, we developed immunoprecipitation protocols for isolation of TrkB from HEK-TrkB and of TrkA

from NIH-3T3-TrkA, but we still did not observe pTrk despite probing the blots for any phospho-tyrosines.

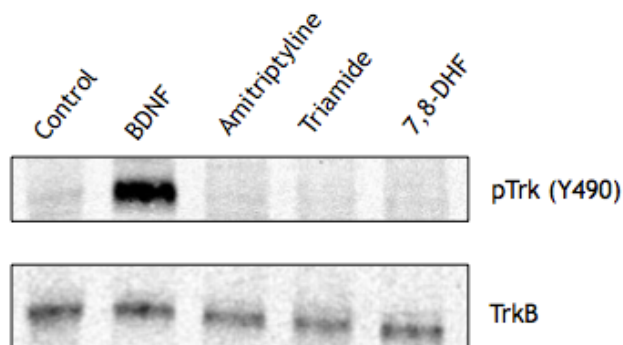


Figure 9. Published TrkB agonists do not activate TrkB in HEK-TrkB cells. HEK-TrkB cells were incubated in the presence of BDNF (50 ng/mL) for 10 minutes, amitriptyline (500 nM) for 30 minutes, Triamide LM22A-4 (500 nM) for 60 minutes, and 7,8-DHF (500 nM) for 30 minutes. Lysates were analyzed by western blotting using a phospho-specific Trk antibody, followed by stripping and reprobing the membrane for total TrkB. The data indicate that the small molecules do not activate TrkB, despite robust activation by the positive control, BDNF. Representative image of at least two separate experiments.

While it was clear that TrkB was not activated by these small molecules in our system, to be thorough we considered probing other downstream signaling proteins that are known to be phosphorylated following TrkB activation. We chose to detect ERK1/2 in the event that either the phospho-specific Trk antibodies were not picking up on a low level of activation, as signaling to ERK1/2 may be amplified, or that another target was possibly activated instead of TrkB that would lead to subsequent ERK1/2 activation. We found that only BDNF activated ERK1/2 as expected, but not the triamide, amitriptyline, 7,8-DHF, or NAS at the published concentrations or incubation times (Figure 10). Also, ANA-12 was not very effective at inhibiting BDNF-induced ERK1/2 activation after 30 minutes of pre-incubation compared to K252a, a compound that is selective for Trk receptors at low concentrations,⁹⁸ in HEK-TrkB cells.

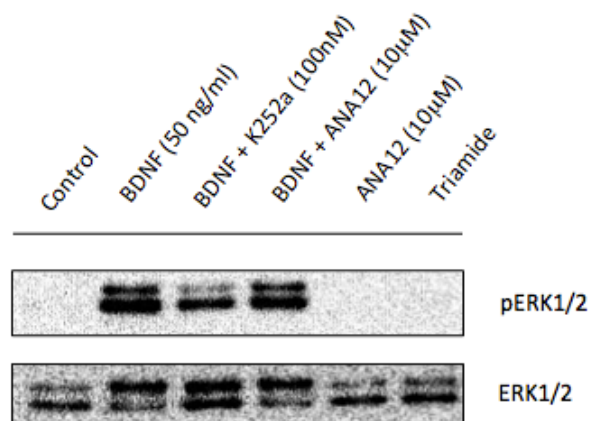


Figure 10. Inhibition of BDNF-induced ERK1/2 activation by Trk inhibitors in HEK-TrkB. HEK-TrkB cells were pre-treated with the Trk inhibitors ANA12 (10 μ M) or K252a (100 nM) for 1 hour followed by incubation with BDNF (50 ng/mL) for 10 minutes. The cells were also treated with triamide LM22A-4 (500 nM) for 1 hour. Lysates were analyzed by western blotting using a phospho-specific ERK1/2 antibody, followed by stripping and reprobing the membrane for total ERK1/2. The data indicate that ANA12 does not inhibit ERK1/2 activation as well as K252a, and the triamide compound does not activate ERK1/2. Representative image of two separate experiments.

II.3 Efforts to Establish Small Molecule Controls: SH-SY5Y

We surmise that the cause of these negative results may be inherent to the recombinant system or due to species differences. Each molecule had proven effective in more than one system, often in a transfected cell line and in primary culture or even *in vivo*, but in our hands none of molecules achieved TrkB activation or inhibition in HEK-TrkB cells. It is known that endogenous Trk receptor signaling is mediated by the presence of p75NTR,⁹⁹ so we opted to try a cell line that contains both endogenous TrkB and p75NTR, human neuroblastoma SH-SY5Y,^{77,100} to determine if the experimental molecules were not functioning as expected due to a lack of inadequate signaling partners in the recombinant-expressed systems. In this line, TrkB expression is induced by differentiation by retinoic acid. In retinoic acid-differentiated SH-SY5Y cells, 10 μ M of 7,8-DHF, NAS, or LM224-A did not activate ERK1/2 at any time points

tested between 1 minute and 3 hours. We chose to use a large excess of compound in the event that the low concentration did not induce a detectable change in ERK1/2 phosphorylation.

Though the agonists tested do not produce increased ERK1/2 activation, ANA-12 inhibits BDNF-induced ERK1/2 activation reproducibly by approximately 50%, which is consistent with the magnitude of inhibition reported for cyclotraxin B.⁸⁸ It should be noted, however, that dose-response studies were not successful due to insolubility of the compound in the aqueous experimental medium at concentrations higher than 10-20 μ M.

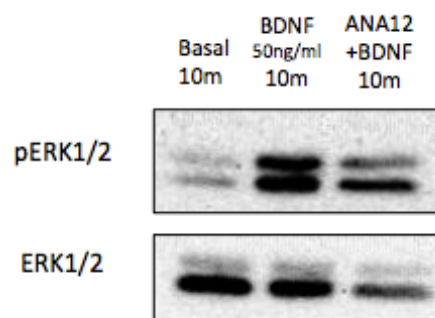


Figure 11. Inhibition of BDNF-induced ERK1/2 activation by ANA-12. SH-SY5Y neuroblastoma cells were differentiated for 72 hours in the presence of 10 μ M retinoic acid followed by overnight incubation in low serum (1% FBS) medium, then pretreated with ANA12 (10 μ M) for 1 hour before incubation with BDNF (50 ng/mL) for 10 minutes. Lysates were analyzed by western blotting using a phospho-specific ERK1/2 antibody, followed by stripping and reprobing the membrane for total ERK1/2. Representative image of at least four separate experiments.

Despite our lack of success with published TrkB agonists, both in recombinant cell lines and in SH-SY5Y, we may conclude that ANA-12 may be an adequate lead for partial antagonism of the TrkB receptor based on these western results.

II.4 Development of High-Throughput Screening Assays for TrkB Agonists

Since we were unable to establish a small molecule positive control for TrkB agonism, we decided to pursue higher-throughput assays in hopes of developing a system to test and discover small molecule TrkB modulators. Dr. Yves Meyer, a postdoctoral researcher in our group, has established a cell-based ERK1/2 activation assay using HEK-TrkB cells and the Phospho-ERK1 (T202/Y204)/ERK2 (T185/Y187) Cell-Based ELISA kit from R&D Systems. This immunohistochemical assay uses a fluorescent readout to detect both phosphorylated and total ERK in fixed cells. He found that though BDNF induced a rapid phosphorylation of ERK1/2 with a maximum at five min, none of the small molecules tested did after 60 minutes (Figure 12). Interestingly, gedunin, the precursor to deoxygedunin, did induce a small increase in ERK1/2 phosphorylation after 30 minutes. However, ANA-12 did not inhibit ERK1/2 activation by BDNF in this assay (data not shown).

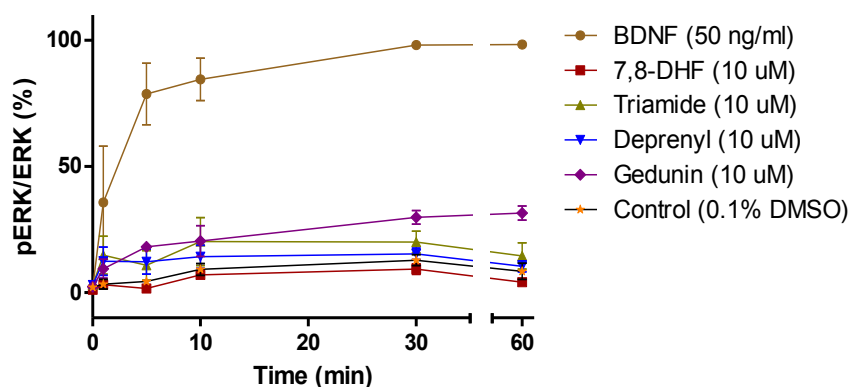


Figure 12. ERK phosphorylation time-course by treatment with BDNF and small molecules in HEK-TrkB cells. HEK-TrkB cells were cultured in collagen (rat tail)-coated 96-well plates and incubated with the indicated treatments for various times (x-axis), followed by fixation and immunohistochemical detection of phospho- and total ERK1/2 using the Phospho-ERK1 (T202/Y204)/ERK2 (T185/Y187) Cell-Based ELISA kit from R&D Systems, according to the manufacturer's instructions. Data is representative of three independent experiments; courtesy of Dr. Yves Meyer.

Dr. Meyer is also attempting to assess TrkB activation using a cell line with a β -lactamase reporter, CellSensor® TrkB-NFAT-*bla* CHO-K1 Cell Line from Invitrogen. In this line, after TrkB activation, signaling via the PLC γ /PKC/Ca²⁺ pathway activates the transcription factor NFAT (Nuclear Factor of Activated T-Cells), which then translocates into the nucleus where it binds to DNA response elements driving β -lactamase expression. Cleavage of a small molecule organic reporter substrate allows quantification of β -lactamase induction, measured five hours after the beginning of incubation of the cells with the experimental treatment. The assay is amenable to high-throughput screening in 384-well plates.¹⁰¹

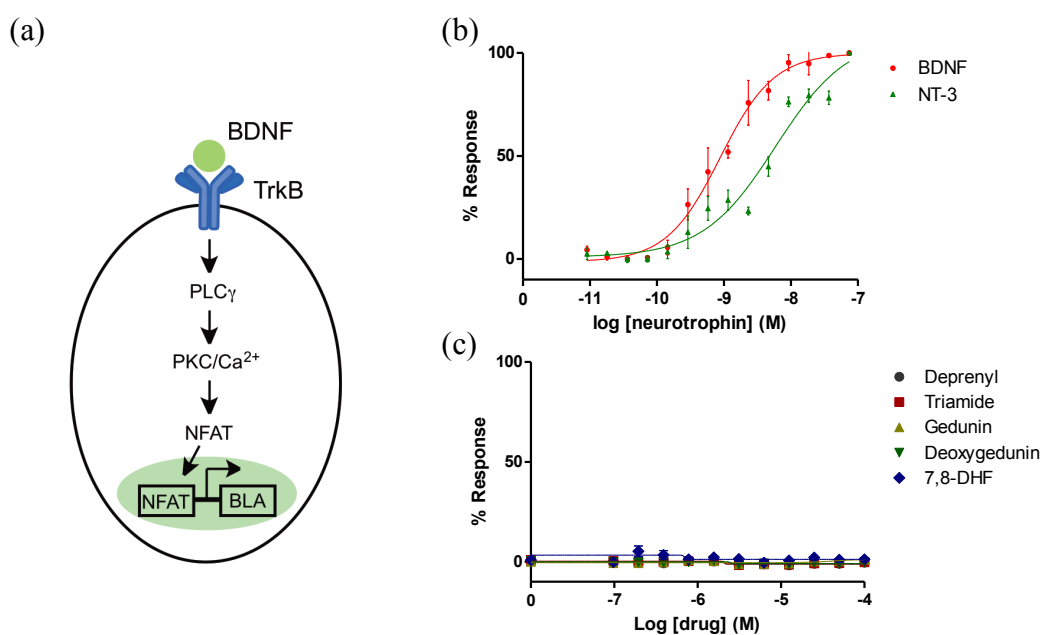


Figure 13. (a) NFAT activation induced by TrkB activation. (Graphical model adapted from reference 101.) (b) BDNF, NT-3 dose-responses, with concentrations from 0.05 ng/ml to 400 ng/mL. Data is representative of three independent experiments. (c) Reported small-molecule agonists dose-responses; this experiment has been performed once in duplicate. hTrkB-NFAT CHO K1 cells were cultured in 384-well plates and incubated with NT proteins or compounds at different concentrations for 5 h at 37°C, followed by addition of a β -lactamase activatable fluorescent substrate (CCF4-AM, Invitrogen) for 2 h at room temperature, according to the manufacturer's instructions. Compound concentrations are from 0.1 to 100 μ M. [BLA = β -lactamase] Courtesy of Dr. Yves Meyer.

This assay is a viable option for high-throughput TrkB agonist screening, though care must be taken with hits due to the variety of sources of PKC activation and/or Ca^{2+} release.

III. Conclusions and Future Directions

TrkB signaling is crucial for CNS development and maintenance and identification of small molecule ligands is an important area of research. In our hands, there was no suitable cell line that released significant amounts of BDNF into the culture medium, so we sought to activate TrkB directly. Unfortunately, none of the small molecule agonists described in the literature activated TrkB in our hands as determined by western blotting in two separate cell lines, one with heterologously expressed and the other with endogenously expressed TrkB, nor was a change in ERK1/2 activation detectable in a cell-based ERK1/2 assay. We speculate that this may be due to species differences, as the TrkB that has been transfected into the NIH-3T3 and HEK293 cells is a human protein, whereas the primary cultures and *in vivo* studies have been rodent-based. Also, it is highly possible that the activation of TrkB requires a co-receptor or other signaling partner that is not present in the model cell lines but is present in primary culture. Furthermore, the primary target of the reported compounds may be a different receptor that transactivates TrkB, but experimentally appears to be a direct agonist.

However, the antagonist ANA-12 did inhibit ERK1/2 activation induced by BDNF, reproducibly in SH-SY5Y as determined by western blotting. ANA-12 may then serve as an adequate lead for a partial TrkB antagonist, and we are pursuing structural modifications which may increase its potency and solubility. Also, we intend to continue development of a high-throughput screening assay to discover more leads for TrkB agonism or antagonism, in hopes of developing a small, drug-like molecule capable of modulating endogenous TrkB activity to

protect and repair neurons in disease states, the impact of which would be considerable. We are not convinced of the validity of TrkB as the true target of the published agonists, and high-throughput screening may offer us a chance to find a true, selective TrkB agonist or antagonist.

IV. Experimental

Materials

SH-SY5Y cells were purchased from American Type Culture Collection (#CRL-2266; Rockville, MD) and routinely grown in a 5% CO₂ atmosphere at 37°C in DMEM (high glucose with GlutaMax, #10569; Life Technologies Corp., Grand Island, NY) supplemented with 10% FBS (Premium Select, Atlanta Biologicals; Atlanta, GA) and 100 U/mL penicillin and 100 µg/mL streptomycin (#15140, Life Technologies). NIH-3T3-TrkB cells were generously provided by Dr. David Kaplan (Hospital for Sick Kids, Toronto, ON, Canada) and NIH-3T3-TrkA cells were a kind gift from Dr. William Mobley (Department of Neurosciences, University of California, San Diego) and grown in DMEM supplemented with 10% FBS, 100 U/mL penicillin, 100 µg/mL streptomycin, and 200 mg/mL G418 (Life Technologies). HEK-TrkB cells were a generous gift from Dr. Moses Chao (NYU School of Medicine, New York, NY), and were grown in the same medium as NIH-3T3-TrkB cells. 100 mm polystyrene tissue culture plates were purchased from Corning (#430169; Corning, NY), and 6-well plates (#657165) were from Greiner Bio-One (Monroe, NC). Protein assays were performed using Costar 96-well plates (3370, Corning).

BDNF (#450-02) and β -NGF (#450-01) were purchased from Peprtech (Rocky Hill, NJ). *N*-acetyl-5-hydroxytryptamine (*N*-acetylserotonin, NAS) was purchased from Sigma-Aldrich (Saint Louis, MO). 7,8-Dihydroxyflavone was obtained from TCI (Portland, OR). *N,N',N''*-Tris(2-hydroxyethyl)-1,3,5-benzenetricarboxamide (LM22A-4, #CHS0233913) was purchased from ChemBridge Corp (San Diego, CA) but was also synthesized in our laboratory. *N*2-(2-{[(2-oxoazepan-3-yl)amino]carbonyl}phenyl)benzo[*b*]thiophene-2-carboxamide (ANA-

12; #BTB06525) was obtained from Maybridge (Cambridge, UK) but also synthesized in our laboratory. Protease inhibitor cocktail (#P8340), phosphatase inhibitor cocktails 2 (#P5726) and 3 (#P0044), and bovine serum albumin (BSA) were also purchased from Sigma-Aldrich. ERK1/2 rabbit polyclonal antibody (#9102), phospho-ERK1/2 (Thr202/Tyr204) XP™ rabbit monoclonal antibody (#4370), phospho-Trk (Tyr490) polyclonal rabbit (#9141), phospho-TrkA/TrkB (Tyr706/707) rabbit monoclonal (#4621), phospho-TrkA/TrkB (Tyr816) rabbit monoclonal (#4168), TrkB (80E3) rabbit monoclonal (#4603), TrkA rabbit polyclonal (#2505), and anti-rabbit HRP-linked (#7074) antibodies were acquired from Cell Signaling Technology (Beverly, MA). Anti Trk (C14) (sc-11) was obtained from Santa Cruz Biotechnology (Santa Cruz, CA). Pierce RIPA buffer, Pierce ECL 2 Western Blotting Substrate, and Pierce BCA Protein Assay kit were purchased from Thermo Scientific (Rockford, IL).

Trk and ERK1/2 activation

Cells were grown until confluence and subcultured into 6-well plates at 1 million cells/well and grown for 24 hours in 2 to 3 mL of complete medium. For experiments with SH-SY5Y cells, the wells were washed and the medium was replaced with experimental medium containing 1% FBS and incubated overnight. On the day of the experiment, a small volume was removed from the well and replaced with an equal volume (100 - 1000 mL) of a concentrated solution of the experimental compound or control condition in the culture medium at the appropriate time. Compounds were diluted from 1000x concentrated stock solutions in DMSO or sterile water. For time course experiments, a control well was run for every time point, since basal ERK1/2 phosphorylation rises approximately 10 – 15 minutes after a treatment is added. To stop the experiment, the medium was removed and the plates were rinsed twice with cold

PBS while on ice. 150 to 200 mL of lysis buffer (Pierce RIPA buffer + 1:100 protease inhibitor cocktail, phosphatase inhibitor 2 and 3 cocktails, and 0.5M EDTA solution) was immediately added to the wells and incubated over ice for 15 minutes to an hour, after which cells were scraped and the lysates were transferred into microcentrifuge tubes. After homogenizing the samples with a sonicator, the tubes were centrifuged at 14,000 rpm for 10 minutes, the supernatant was transferred to fresh tubes, and the protein content was measured using the Pierce BCA assay. Equal quantities of protein were added to each well of a 10% bis-tris acrylamide gel and were blotted onto Immobilon P PVDF transfer membranes. Blots were blocked in 3% BSA in TBS for at least 1 hour, followed by overnight incubation with the primary antibody with rocking at 4°C. The next day, the blots were washed 3 x 5 minutes with TBST (0.05% Tween 20), incubated for 1 hour with secondary antibody (typically 1:1000) in the buffer indicated on the antibody's corresponding data sheet, then washed again for 3 x 5 minutes prior to development with the ECL kit. Chemiluminescence was visualized with a Kodak Image Station 440CF imager. Membranes were stripped and reprobed following the same detection procedure. Data were routinely quantified using densitometry by the gel analysis tools in ImageJ (NIH, Bethesda, MD).

V. References

- ¹ (a) Gubernator, N. G.; Zhang, H.; Staal, R. G. W.; Mosharov, E. V.; Pereira, D. B.; Yue, M.; Balsanek, V.; Vadola, P. A.; Mukherjee, B.; Edwards, R. H.; Sulzer, D.; Sames, D. Fluorescent false neurotransmitters visualize dopamine release from individual presynaptic terminals. *Science* **2009**, *324*, 1441–1444. (b) Rodriguez, P. C.; Pereira, D. B.; Borgkvist, A.; Wong, M. Y.; Barnard, C.; Sonders, M. S.; Zhang, H.; Sames, D.; Sulzer, D. Fluorescent dopamine tracer resolves individual dopaminergic synapses and their activity in the brain. *Proc. Nat. Acad. Sci. U.S.A.* **2013**, *110*(3), 870–875.
- ² Mayberg, H. S.; Lozano, A. M.; Voon, V.; McNeely, H. E.; Seminowicz, D.; Hamani, C.; Schwab, J. M.; Kennedy, S. H. Deep brain stimulation for treatment-resistant depression. *Neuron* **2005**, *45*, 651–660.
- ³ Duman, R. S.; Monteggia, L. M. A neurotrophic model for stress-related mood disorders. *Biol. Psychiatry* **2006**, *59*, 1116–1127.
- ⁴ Malberg, J. E.; Blendy, J. Antidepressant action: to the nucleus and beyond. *Trends Pharmacol. Sci.* **2005**, *26*, 631–638.
- ⁵ Kang, H. J.; Voleti, B.; Hajszan, T.; Rajkowska, G.; Stockmeier, C. A.; Licznarski, P.; Lepack, A.; Majik, M. S.; Jeong, L. S.; Banasr, M.; Son, H.; Duman, R. S. Decreased expression of synapse-related genes and loss of synapses in major depressive disorder. *Nature Med.* **2012**, *18*, 1413–1417.
- ⁶ Duman, R. S.; Malberg, J.; Nakagawa, S.; D'Sa, C. Neuronal plasticity and survival in mood disorders. *Biol. Psychiatry* **2000**, *48*, 732–739.
- ⁷ Neto, F. L.; Borges, G.; Torres-Sanchez, S.; Mico, J. A.; Berrocoso, E. Neurotrophins role in depression neurobiology: A review of basic and clinical evidence. *Curr. Neuropharmacol.* **2011**, *9*, 530–552.
- ⁸ Allen, S. J.; Dawbarn, D. Clinical relevance of the neurotrophins and their receptors. *Clin. Sci.* **2006**, *110*, 175–191.
- ⁹ Poduslo, J. F.; Curran, G. L. Permeability at the blood-brain and blood-nerve barriers of the neurotrophic factors: NGF, CNTF, NT-3, BDNF. *Brain Res. Mol. Brain Res.* **1996**, *36*(2), 280–286.
- ¹⁰ Wu, D. Neuroprotection in experimental stroke with targeted neurotrophins. *NeuroRx* **2005**, *2*(1), 120–128.
- ¹¹ (a) Skaper, S. D.; Walsh, F. S. Neurotrophic molecules: strategies for designing effective therapeutic molecules in neurodegeneration. *Mol. Cell. Neurosci.* **1998**, *12*, 179–193. (b) Saragovi, H. U.; Gehring, K. Development of pharmacological agents for targeting

-
- neurotrophins and their receptors. *Trends Pharmacol. Sci.* **2000**, *21*(3), 93–98. (c) Xie, Y.; Longo, F. M. Neurotrophin small-molecule mimetics. *Prog. Brain Res.* **2000**, *128*, 333–347. (d) Price, R. D.; Milne, S. A.; Sharkey, J.; Matsuoka, N. Advances in small molecules promoting neurotrophic function. *Pharmacol. Ther.* **2007**, *115*, 292–306.
- ¹² (a) Huang, E. J.; Reichardt, L. F. Trk receptors: Roles in neuronal signal transduction. *Annu. Rev. Biochem.* **2003**, *72*, 609–642. (b) Patapoutian, A.; Reichardt, L. F. Trk receptors: mediators of neurotrophin action. *Curr. Opin. Neurobiol.* **2001**, *11*, 272–280.
- ¹³ Mowla, S. J.; Farhadi, H. F.; Pareek, S.; Atwal, J. K.; Morris, S. J.; Seidah, N. G.; Murphy, R. A. Biosynthesis and post-translational processing of the precursor to brain-derived neurotrophic factor. *J. Biol. Chem.* **2001**, *276*(16), 12660–12666.
- ¹⁴ Teng, K. K.; Felice, S.; Kim, T.; Hempstead, B. L. Understanding proneurotrophin actions: Recent advances and challenges. *Develop. Neurobiol.* **2010**, *70*, 350–359.
- ¹⁵ Ohira, K.; Hayashi, M. A new aspect of the TrkB signaling pathway in neural plasticity. *Curr. Neuropharmacol.* **2009**, *7*, 276–285.
- ¹⁶ Kaplan, D. R.; Miller, F. D. Neurotrophin signal transduction in the nervous system. *Curr. Opin. Neurobiol.* **2000**, *10*, 381–391.
- ¹⁷ Middlemas, D. S.; Meisenhelder, J.; Hunter, T. Identification of TrkB autophosphorylation sites and evidence that phospholipase C- γ 1 is a substrate of the TrkB receptor. *J. Biol. Chem.* **1994**, *269*(7), 5458–5466.
- ¹⁸ Siuciak, J. A.; Lewis, D. R.; Weigand, S. J.; Lindsay, R. M. Antidepressant-like effect of brain-derived neurotrophic factor (BDNF). *Pharmacol. Biochem. Behav.* **1997**, *56*, 131–137.
- ¹⁹ (a) Weickert, C. S.; Ligons, D. L.; Romanczyk, T.; Ungaro, G.; Hyde, T. M.; Herman, M. M.; Weinberger, D. R.; Kleinman, J. E. Reductions in neurotrophin receptor mRNAs in the prefrontal cortex of patients with schizophrenia. *Mol. Psych.* **2005**, *10*, 637–650. (b) Chen, D. C.; Wang, J.; Wang, B.; Yang, S. C.; Zhang, C. X.; Zheng, Y. L.; Li, Y. L.; Wang, N.; Yang, K. B.; Xiu, M. H.; Kosten, T. R.; Zhang, X. Y. Decreased levels of serum brain-derived neurotrophic factor in drug-naïve first-episode schizophrenia: relationship to clinical phenotypes. *Psychopharmacology* **2009**, *207*, 375–380. (c) Balu, D. T.; Coyle, J. T. Neuroplasticity signaling pathways linked to the pathophysiology of schizophrenia. *Neurosci. Biobehav. Rev.* **2011**, *35*(3), 848–870. (d) Hashimoto, T.; Bergen, S. E.; Nguyen, Q. L.; Xu, B.; Monteggia, L. M.; Pierri, J. N.; Sun, Z.; Sampson, A. R.; Lewis, D. A. Relationship of brain-derived neurotrophic factor and its receptor TrkB to altered inhibitory prefrontal circuitry in schizophrenia. *J. Neurosci.* **2005**, *25*(2), 372–383.
- ²⁰ (a) Ogier, M.; Wang, H.; Hong, E.; Wang, Q.; Greenberg, M. E.; Katz, D. M. Brain-derived neurotrophic factor expression and respiratory function improve after ampakine treatment in a mouse model of Rett syndrome. *J. Neurosci.* **2007**, *27*(40), 10912–10917. (b) Ricceri, L.; De

-
- Filippis, B.; Laviola, G. Rett syndrome treatment in mouse models: Searching for effective targets and strategies. *Neuropharmacology* **2012**, <http://dx.doi.org/10.1016/j.neuropharm.2012.08.010> (*in press*)
- ²¹ (a) Rios, M.; Fan, G.; Fekete, C.; Kelly, J.; Bates, B.; Kuehn, R.; Lechan, R. M.; Jaenisch, R. Conditional deletion of brain-derived neurotrophic factor in the postnatal brain leads to obesity and hyperactivity. *Mol. Endocrinol.* **2001**, *15*(10), 1748–1757. (b) Tsao D.; Thomsen, H. K.; Chou, J.; Stratton, J.; Hagen, M.; Loo, C.; Garcia, C.; Sloane, D. L.; Rosenthal, A.; Lin, J. C. TrkB agonists ameliorate obesity and associated metabolic conditions in mice. *Endocrinology* **2008**, *149*(3), 1038–1048. (c) Rosas-Vargas, H.; Martínez-Enzquerro, J. D.; Bienvenu, T. Brain-derived neurotrophic factor, food intake regulation, and obesity. *Arch. Med. Res.* **2011**, *42*(6), 482–494.
- ²² Dias, B. G.; Banjeree, S. B.; Duman, R. S.; Vaidya, V. A. Differential regulation of brain-derived neurotrophic factor transcripts by antidepressant treatments in the adult rat brain. *Neuropharmacology* **2003**, *45*(4), 553–563.
- ²³ Rantamäki, T.; Vesa, L.; Antila, H.; Di Lieto, A.; Tammela, P.; Schmitt, A.; Lesch, K.-P.; Rios, M.; Castrén, E. Antidepressant drugs transactivate TrkB neurotrophin receptors in the adult rodent brain independently of BDNF and monoamine transporter blockade. *PloS One* **2011**, *6*(6), e20567.
- ²⁴ (a) Saarelainen, T.; Hendolin, P.; Lucas, G.; Koponen, E.; Sairanen, M.; MacDonald, E.; Agerman, K.; Haapasalo, A.; Nawa, H.; Aloyz, R.; Ernfors, P.; Castrén, E. Activation of the TrkB neurotrophin receptor is induced by antidepressant drugs and is required for antidepressant-induced behavioral effects. *J. Neurosci.* **2003**, *23*, 349–357. (b) Rantamäki, T.; Hendolin, P.; Kankaanpää, A.; Mijatovic, J.; Piepponen, P.; Domenici, E.; Chao, M. V.; Männistö, P. T.; Castrén, E. Pharmacologically diverse antidepressants rapidly activate brain-derived neurotrophic factor receptor TrkB and induce phospholipase-C γ signaling pathways in mouse brain. *Neuropsychopharmacology* **2007**, *32*, 2151–2162. (c) Kozisek, M. E.; Middlemas, D.; Bylund, D. B. Brain-derived neurotrophic factor and its receptor tropomyosin-related kinase B in the mechanism of action of antidepressant therapies. *Pharmacol. Ther.* **2008**, *117*(1), 30–51.
- ²⁵ Li, Y.; Luikart, B. W.; Birnbaum, S.; Chen, J.; Kwon, C.-H.; Kernie, S. G.; Bassel-Duby, R.; Parada, L. F. TrkB regulates hippocampal neurogenesis and governs sensitivity to antidepressive treatment. *Neuron* **2008**, *59*(3), 399–412.
- ²⁶ Griesbach, G. S.; Hovda, D. A.; Gomez-Pinilla, F. Exercise-induced improvement in cognitive performance after traumatic brain injury in rats is dependent on BDNF activation. *Brain Res.* **2009**, *1288*, 105–115.
- ²⁷ Furmaga, H.; Carreno, F. R.; Frazer, A. Vagal nerve stimulation rapidly activates brain-derived neurotrophic factor receptor TrkB in rat brain. *PloS One* **2012**, *7*(5), e34844.

-
- ²⁸ Minichiello, L. TrkB signaling pathways in LTP and learning. *Nature Rev. Neurosci.* **2009**, *10*(12), 850–860.
- ²⁹ (a) Pezet, S.; McMahon, S. B. Neurotrophins: Mediators and modulators of pain. *Annu. Rev. Neurosci.* **2006**, *29*, 507–538. (b) Merighi, A.; Salio, C.; Ghirri, A.; Lossi, L.; Ferrini, F.; Betelli, C.; Bardoni, R. BDNF as a pain modulator. *Prog. Neurobiol.* **2008**, *85*(3), 297–317.
- ³⁰ Zuccato C.; Cattaneo E. Brain-derived neurotrophic factor in neurodegenerative diseases. *Nature Rev. Neurol.* **2009**, *5*, 311–322.
- ³¹ (a) Siegel, G. J.; Chauhan, N. B. Neurotrophic factors in Alzheimer's and Parkinson's disease brain. *Brain Res. Rev.* **2000**, *33*, 199–227. (b) Fumagalli, F.; Racagni, G.; Riva, M. A. Shedding light into the role of BDNF in the pharmacotherapy of Parkinson's disease. *Pharmacogenomics J.* **2006**, *6*(2), 95–104.
- ³² (a) Peng, S.; Wu, J.; Mufson, E. J.; Fahnstock, M. Precursor form of brain-derived neurotrophic factor and mature brain-derived neurotrophic factor are decreased in the pre-clinical stages of Alzheimer's disease. *J. Neurochem.* **2005**, *93*, 1412–1421. (b) Schindowski, K.; Belarbi, K.; Buée, L. Neurotrophic factors in Alzheimer's disease: role of axonal transport. *Genes Brain Behav.* **2008**, *7*(suppl 1), 43–56.
- ³³ Zuccato, C.; Cattaneo, E. Role of brain-derived neurotrophic factor in Huntington's disease. *Prog. Neurobiol.* **2007**, *81*(5–6), 294–330.
- ³⁴ (a) Ekestern, E. Neurotrophic factors and amyotrophic lateral sclerosis. *Neurodegen. Dis.* **2004**, *1*, 88–100. (b) Ochs, G.; Penn, R. D.; York, M.; Giess, R.; Beck, M.; Tonn, J.; Haigh, J.; Malta, E.; Traub, M.; Sendtner, M.; Toyka, K. V. A phase I/II trial of recombinant methionyl human brain derived neurotrophic factor administered by intrathecal infusion to patients with amyotrophic lateral sclerosis. *Amyotroph Lateral Scler Other Motor Neuron Disord* **2000**, *1*, 201–206.
- ³⁵ Frielingsdorf, H.; Bath, K. G.; Soliman, F.; DiFede, J.; Casey, B. J.; Lee, F. S. Variant brain-derived neurotrophic factor Val66Met endophenotypes: implications for posttraumatic stress disorder. *Ann. N.Y. Acad. Sci.* **2010**, *1208*, 150–157.
- ³⁶ Rybakowski, J. K. BDNF gene: functional Val66Met polymorphism in mood disorders and schizophrenia. *Pharmacogenomics* **2008**, *9*(11), 1589–1593.
- ³⁷ Fan, J.; Sklar, P. Genetics of bipolar disorder: focus on BDNF Val66Met polymorphism. *Novartis Found Symp.* **2008**, *289*, 60–72.
- ³⁸ Hong, C.-J.; Liou, Y.-J.; Tsai, S.-J. Effects of BDNF polymorphisms on brain function and behavior in health and disease. *Brain Res. Bull.* **2011**, *86*, 287–297.

-
- ³⁹ Qian, M. D.; Zhang, J.; Tan, X.-Y.; Wood, A.; Gill, D.; Cho, S. Novel agonist monoclonal antibodies activate TrkB receptors and demonstrate potent neurotrophic activities. *J. Neurosci.* **2006**, *26*(37), 9394–9403.
- ⁴⁰ a.) O’Leary, P. D.; Hughes, R. A. Structure–activity relationships of conformationally constrained peptide analogues of loop 2 of brain-derived neurotrophic factor. *J. Neurochem.* **1998**, *70*, 1712–1721. b.) O’Leary, P. D.; Hughes, R. A. Design of potent peptide mimetics of brain-derived neurotrophic factor. *J. Biol. Chem.* **2003**, *278*, 25738–25744. c.) Fletcher, J. M.; Hughes, R. A. Novel monocyclic and bicyclic loop mimetics of brain-derived neurotrophic factor. *J. Pept. Sci.* **2006**, *12*, 515–524.
- ⁴¹ Huang, Y. Z.; Hernandez, F. J.; Gu, B.; Stockdale, K. R.; Nanapaneni, K.; Scheetz, T. E.; Behlke, M. A.; Peek, A. S.; Bair, T.; Giangrande, P. H.; McNamara, J. O. RNA Aptamer-based functional ligands of the neurotrophin receptor, TrkB. *Mol. Pharmacol.* **2012**, *82*, 623–635.
- ⁴² Obianyo, O.; Ye, K. Novel small molecule activators of the Trk family of receptor tyrosine kinases. *Biochim. Biophys. Acta* **2012**, *2*, 6–11.
- ⁴³ Sometani, A.; Nomoto, H.; Nitta, A. Furukawa, Y. Furukawa, S. 4-Methylcatechol stimulates phosphorylation of Trk family neurotrophin receptors and MAP kinases in cultured rat cortical neurons. *J. Neurosci. Res.* **2002**, *70*, 335–339.
- ⁴⁴ Rahvar, M.; Nikseresht, M.; Shafiee, S. M.; Naghibalhossaini, F.; Rasti, M.; Panjehshahin, M. R.; Owji, A. A. Effect of oral resveratrol on the BDNF gene expression in the hippocampus of the rat brain. *Neurochem. Res.* **2011**, *36*, 761–765.
- ⁴⁵ Rabin, S. J.; Bachis, A.; Mocchetti, I. Gangliosides activate Trk receptors by inducing the release of neurotrophins. *J. Biol. Chem.* **2002**, *277*(51), 49466–49472.
- ⁴⁶ Balkowiec, A.; Katz, D. M. Activity-dependent release of endogenous brain-derived neurotrophic factor from primary sensory neurons detected by ELISA *in situ*. *J. Neurosci.* **2000**, *20*, 7417–7423.
- ⁴⁷ Jang, S.-W.; Liu, X.; Chan, C.-B.; Weinshenker, D.; Hall, R. A.; Xiao, G.; Ye, K. Amitriptyline is a TrkA and TrkB receptor agonist that promotes TrkA/TrkB heterodimerization and has potent neurotrophic activity. *Chem. Biol.* **2009**, *16*, 644–656.
- ⁴⁸ Glotzbach, R. K.; Preskorn, S. H. Brain concentrations of tricyclic antidepressants: single-dose kinetics and relationship to plasma concentrations in chronically dosed rats. *Psychopharmacology* **1982**, *78*, 25–27.
- ⁴⁹ Massa, S. M.; Yang, T.; Xie, Y.; Shi, J.; Bilgen, M.; Joyce, J. N.; Nehama, D.; Rajadas, J.; Longo, F. M. Small molecule BDNF mimetics activate TrkB signaling and prevent neuronal degeneration in rodents. *J. Clin. Invest.* **2010**, *120*(5), 1774–1785.

-
- ⁵⁰ Han, J.; Pollak, J.; Yang, T.; Siddiqui, M. R.; Doyle, K. P.; Taravosh-Lahn, K.; Cekanaviciute, E.; Han, A.; Goodman, J. Z.; Jones, B.; Jing, D.; Massa, S. M.; Longo, F. M.; Buckwalter, M. S. Delayed administration of a small molecule tropomyosin-related kinase B ligand promotes recovery after hypoxic-ischemic stroke. *Stroke* **2012**, *43*, 1918–1924.
- ⁵¹ Schmid, D. A.; Yang, T.; Ogier, M.; Adams, I.; Mirakhur, Y.; Wang, Q.; Massa, S. M.; Longo, F. M.; Katz, D. M. A TrkB small molecule partial agonist rescues TrkB phosphorylation deficits and improves respiratory function in a mouse model of Rett syndrome. *J. Neurosci.* **2012**, *32*(5), 1803–1810.
- ⁵² Jang, S.-W.; Liu, X.; Yepes, M.; Shepherd, K. R.; Miller, G. W.; Liu, Y.; Wilson, W. D.; Xiao, G.; Bianchi, B.; Sun, Y. E.; Ye, K. A selective TrkB agonist with potent neurotrophic activities by 7,8-dihydroxyflavone. *Proc. Nat. Acad. Sci. U.S.A.* **2010**, *107*(6), 2687–2692.
- ⁵³ Liu, X.; Chan, C.-B.; Jang, S.-W.; Pradoldej, S.; Huang, J.; He, K.; Phun, L. H.; France, S.; Xiao, G.; Jia, Y.; Luo, H. R.; Ye, K. A synthetic 7,8-dihydroxyflavone derivative promotes neurogenesis and exhibits potent antidepressant effect. *J. Med. Chem.* **2010**, *53*, 8274–8286.
- ⁵⁴ Liu, X.; Chan, C.-B.; Qi, Q.; Xiao, G.; Luo, H. R.; He, X.; Ye, K. Optimization of a small tropomyosin-related kinase B (TrkB) agonist 7,8-dihydroxyflavone active in mouse models of depression. *J. Med. Chem.* **2012**, *55*, 8524–8537.
- ⁵⁵ Mantilla, C.; Ermilov, L. G. The novel TrkB receptor agonist 7,8-dihydroxyflavone enhances neuromuscular transmission. *Muscle Nerve* **2012**, *45*, 274–276.
- ⁵⁶ Andero, R.; Heldt, S. A.; Ye, K.; Liu, X.; Armario, A.; Ressler, K. J. Effect of 7,8-dihydroxyflavone, a small-molecule TrkB agonist, on emotional learning. *Am. J. Psychiatry* **2011**, *168*, 163–172.
- ⁵⁷ Andero, R.; Daviu, N.; Escorihuela, R. M.; Nadal, R.; Armario, A. 7,8-Dihydroxyflavone, a TrkB receptor agonist, blocks long-term spatial memory impairment caused by immobilization stress in rats. *Hippocampus* **2012**, *22*, 399–408.
- ⁵⁸ Johnson, R. A.; Lam, M.; Punzo, A. M.; Li, H.; Lin, B. R.; Ye, K.; Mitchell, G. S.; Chang, Q. 7,8-Dihydroxyflavone exhibits therapeutic efficacy in a mouse model of Rett syndrome. *J. Appl. Physiol.* **2012**, *112*, 704–710.
- ⁵⁹ Devi, L.; Ohno, M. 7,8-Dihydroxyflavone, a small-molecule TrkB agonist, reverses memory deficits and BACE1 elevation in a mouse model of Alzheimer's disease. *Neuropsychopharmacology* **2012**, *37*, 434–444.
- ⁶⁰ Zeng, Y.; Tan, M.; Kohyama, J.; Sneddon, M.; Watson, J. B.; Sun, Y. E.; Xie, C.-W. Epigenetic enhancement of BDNF signaling rescues synaptic plasticity in aging. *J. Neurosci.* **2011**, *31*(49), 17800–17810.

-
- ⁶¹ Zeng, Y.; Liu, Y.; Wu, M.; Liu, J.; Hu, Q. Activation of TrkB by 7,8-dihydroxyflavone prevents fear memory defects and facilitates amygdalar synaptic plasticity in aging. *J. Alzheimer's Dis.* **2012**, *31*, 765–778.
- ⁶² Chen, J.; Chua, K. W.; Chua, C. C.; Yu, H.; Pei, A.; Chua, B. H.; Hamdy, R. C.; Xu, X.; Liu, C.-F. Antioxidant activity of 7,8-dihydroxyflavone provides neuroprotection against glutamate-induced toxicity. *Neurosci. Lett.* **2011**, *499*, 181–185.
- ⁶³ Jang, S.-W.; Liu, X.; Chan, C. B.; France, S. A.; Sayeed, I.; Tang, W.; Lin, X.; Xiao, G.; Andero, R.; Chang, Q.; Ressler, K. J.; Ye, K. Deoxygedunin, a natural product with potent neurotrophic activity in mice. *PloS One* **2010**, *5*, e11528.
- ⁶⁴ Jang, S.-W.; Liu, X.; Pradoldej, S.; Tosini, G.; Chang, Q.; Iuvone, P. M.; Ye, K. N-acetylserotonin activates TrkB receptor in a circadian rhythm. *Proc. Nat. Acad. Sci. U.S.A.* **2010**, *107*(8), 3876–3881.
- ⁶⁵ Uz, T.; Manev, H. Chronic fluoxetine administration increases the serotonin N-acetyltransferase messenger RNA content in rat hippocampus. *Biol. Psychiatry* **1999**, *45*, 175–179.
- ⁶⁶ Quera Salva, M. A.; Hartley, S.; Barbot, F.; Alvarez, J. C.; Lofaso, F.; Guilleminault, C. Circadian rhythms, melatonin and depression. *Curr. Pharm. Des.* **2011**, *17*(15), 1459–1470.
- ⁶⁷ Shen, J.; Ghai, K.; Sompol, P.; Liu, X.; Cao, X.; Iuvone, P. M.; Ye, K. N-acetyl serotonin derivatives as potent neuroprotectants for retinas. *Proc. Nat. Acad. Sci. U.S.A.* **2012**, *109*(9), 3540–3545.
- ⁶⁸ Zhang, B.; Salituro, G.; Szalkowski, D.; Li, Z.; Zhang, Y.; Royo, I.; Vilella, D.; Díez, M. T.; Pelaez, F.; Ruby, C.; Kendall, R. L.; Mao, X.; Griffin, P.; Calaycay, J.; Zierath, J. R.; Heck, J. V.; Smith, R. G.; Moller, D. E. Discovery of a small molecule insulin mimetic with antidiabetic activity in mice. *Science* **1999**, *284*, 974–977.
- ⁶⁹ Wilkie, N.; Wingrove, P. B.; Bilsland, J. G.; Young, L.; Harper, S. J.; Hefti, F.; Ellis, S.; Pollack, S. J. The non-peptidyl fungal metabolite L-783,281 activates TRK neurotrophin receptors. *J. Neurochem.* **2001**, *78*, 1135–1145.
- ⁷⁰ (a) Malarkey, K.; Belham, C. M.; Paul, A.; Graham, A.; McLees, A.; Scott, P. H.; Plevin, R. The regulation of tyrosine kinase signalling pathways by growth factor and G-protein-coupled receptors. *Biochem. J.* **1995**, *309*(2), 361–375. (b) Lopez-Ilasaca, M. Signaling from G-protein-coupled receptors to mitogen-activated protein (MAP)-kinase cascades. *Biochem. Pharmacol.* **1998**, *56*, 269–277. (c) Werry, T. D.; Sexton, P. M.; Christopoulos, A. 'Ins and outs' of seven-transmembrane receptor signalling to ERK. *Trends Endocrin. Metab.* **2005**, *16*(1), 26–33. (d) Delcourt, N.; Bockaert, J.; Marin, P. GPCR-jacking: from a new route in

-
- RTK signalling to a new concept in GPCR activation. *Trends Pharmacol. Sci.* **2007**, *28*, 602–607.
- ⁷¹ Iwakura, Y.; Nawa, H.; Sora, I.; Chao, M. V. Dopamine D1 receptor-induced signaling through TrkB receptors in striatal neurons. *J. Biol. Chem.* **2008**, *283*(23), 15799–15806.
- ⁷² (a) Lee, F. S.; Chao, M. V. Activation of Trk neurotrophin receptors in the absence of neurotrophins. *Proc. Nat. Acad. Sci. U.S.A.* **2001**, *98*, 3555–3560. (b) Wiese, S.; Jablonka, S.; Holtmann, B.; Orel, N.; Rajagopal, R.; Chao, M. V.; Sendtner, M. Adenosine receptor A_{2A}-R contributes to motoneuron survival by transactivating the tyrosine kinase receptor TrkB. *Proc. Nat. Acad. Sci. U.S.A.* **2007**, *104*, 17210–17205. (c) Assaife-Lopes, N.; Sousa, V. C.; Pereira, D. B.; Ribeiro, J. A.; Chao, M. V.; Sebastião, A. M. Activation of adenosine A_{2A} receptors induces TrkB translocation and increases BDNF-mediated phospho-TrkB localization in lipid rafts: Implications for neuromodulation. *J. Neurosci.* **2010**, *30*, 8468–8480.
- ⁷³ Autio, H.; Mätlik, K.; Rantamäki, T.; Lindemann, L.; Hoener, M. C.; Chao, M.; Arumäe, U.; Castrén, E. Acetylcholinesterase inhibitors rapidly activate Trk neurotrophin receptors in the mouse hippocampus. *Neuropharmacology* **2011**, *61*, 1291–1296.
- ⁷⁴ Berghuis, P.; Dobszay, M. B.; Wang, X.; Spano, S.; Ledda, F.; Sousa, K. M.; Schulte, G.; Ernfors, P.; Mackie, K.; Paratcha, G.; Hurd, Y. L.; Harkany, T. Endocannabinoids regulate interneuron migration and morphogenesis by transactivating the TrkB receptor. *Proc. Nat. Acad. Sci. U.S.A.* **2005**, *102*, 19115–19120.
- ⁷⁵ Lee, F. S.; Rajagopal, R.; Kim, A. H.; Chang, P. C.; Chao, M. V. Activation of Trk neurotrophin receptor signaling by pituitary adenylate cyclase-activating polypeptides. *J. Biol. Chem.* **2002**, *277*(11), 9096–9102.
- ⁷⁶ Jeanneteau, F.; Garabedian, M. J.; Chao, M. V. Activation of Trk neurotrophin receptors by glucocorticoids provides a neuroprotective effect. *Proc. Natl. Acad. Sci. U.S.A.* **2008**, *105*, 4862–4867.
- ⁷⁷ Esposito, C. L.; D'Alessio, A.; de Franciscis, V.; Cerchia, L. A cross-talk between TrkB and Ret tyrosine kinases receptors mediates neuroblastoma cells differentiation. *PLoS One* **2008**, *3*(2), e1643.
- ⁷⁸ Huang, J. J.; Park, M.-H.; Koh, J.-Y. Copper activates TrkB in cortical neurons in a metalloproteinase-dependent manner. *J. Neurosci. Res.* **2007**, *85*, 2160–2166.
- ⁷⁹ Huang, Y. Z.; Pan, E.; Xiong, Z.-Q.; McNamara, J. O. Zinc-mediated transactivation of TrkB potentiates the hippocampal mossy fiber-CA3 pyramid synapse. *Neuron* **2008**, *57*, 546–558.
- ⁸⁰ Binder, D. K.; Croll, S. D.; Gall, C. M.; Scharfman, H. E. BDNF and epilepsy: too much of a good thing? *Trends Neurosci.* **2001**, *24*(1), 47–53.

-
- ⁸¹ (a) Ghitza, U. E.; Zhai, H.; Wu, P.; Airavaara, M.; Shaham, Y.; Lu, L. Role of BDNF and GDNF in drug reward and relapse: A review. *Neurosci. Biobehav. Rev.* **2010**, *35*, 157–171. (b) McGinty, J. F.; Whitfield, Jr., T. W.; Berglind, W. J. Brain-derived neurotrophic factor and cocaine addiction. *Brain Res.* **2010**, *1314*, 183–193.
- ⁸² Wang, X.; Ratnam, J.; Zou, B.; England, P. M.; Basbaum, A. I. TrkB signaling is required for both the induction and maintenance of tissue and nerve injury-induced persistent pain. *J. Neurosci.* **2009**, *29*(17), 5508–5515.
- ⁸³ Thiele, C. J.; Li, Z.; McKee, A. E. On Trk--The TrkB signal transduction pathway is an increasingly important target in cancer biology. *Clin. Cancer Res.* **2009**, *15*, 5962–5967.
- ⁸⁴ Eisch, A. J.; Bolaños, C. A.; de Wit, J.; Simonak, R. D.; Pudiak, C. M.; Barrot, M.; Verhaagen, J.; Nestler, E. J. Brain-derived neurotrophic factor in the ventral midbrain–nucleus accumbens pathway: a role in depression. *Biol. Psych.* **2003**, *54*, 994–1005.
- ⁸⁵ (a) Horger, B. A.; Iyasere, C. A.; Berhow, M. T.; Messer, C. J.; Nestler, E. J.; Taylor, J. R. Enhancement of locomotor activity and conditioned reward to cocaine by brain-derived neurotrophic factor. *J. Neurosci.* **1999**, *19*, 4110–4122. (b) Vargas-Perez, H.; Kee, R. T.-A.; Walton, C. H.; Hansen, M.; Razavi, R.; Clarke, L.; Bufalino, M. R.; Allison, D. W.; Steffensen, S. C.; van der Kooy, D. Ventral tegmental area BDNF induces an opiate-dependent-like reward state in naïve rats. *Science* **2009**, *324*, 1732–1734.
- ⁸⁶ Crooks, K. R.; Kleven, D. T.; Rodriguiz, R. M.; Wetsel, W. C.; McNamara, J. O. TrkB signaling is required for behavioral sensitization and conditioned place preference induced by a single injection of cocaine. *Neuropharmacology* **2010**, *58*, 1067–1077.
- ⁸⁷ (a) Knüsel, B.; Hefti, F. K-252 compounds : Modulators of neurotrophin signal transduction. *J. Neurochem.* **1992**, *59*(6), 1987–1996. (b) Kase, H.; Iwahashi, K.; Nakanishi, S.; Matsuda, Y.; Yamada, K.; Takahashi, M.; Murakata, C.; Sato, A.; Kaneko, M. K-252 compounds, novel and potent inhibitors of protein kinase C and cyclic nucleotide-dependent protein kinases. *Biochem. Biophys. Res. Comm.* **1987**, *142*(2), 436–440.
- ⁸⁸ Cazorla, M.; Jouvenceau, A.; Rose, C.; Guilloux, J.-P.; Pilon, C.; Dranovsky, A.; Prémont, J. Cyclotraxin-B, the first highly potent and selective TrkB inhibitor, has anxiolytic properties in mice. *PLoS One* **2010**, *5*, e9777.
- ⁸⁹ Constandil, L.; Goich, M.; Hernández, A.; Bourgeais, L.; Cazorla, M.; Hamon, M.; Villanueva, L.; Pelissier, T. Cyclotraxin-B, a new TrkB antagonist, and glial blockade by propentofylline, equally prevent and reverse cold allodynia induced by BDNF or partial infraorbital nerve constriction in mice. *J. Pain* **2012**, *13*(6), 579–89.
- ⁹⁰ Kuribara, M.; Hess, M. W.; Cazorla, M.; Roubos, E. W.; Scheenen, W. J. J. M.; Jenks, B. G. Brain-derived neurotrophic factor stimulates growth of pituitary melanotrope cells in an autocrine way. *Gen. Comp. Endocrinol.* **2011**, *170*, 156–161.

-
- ⁹¹ Cazorla, M.; Prémont, J.; Mann, A.; Girard, N.; Kellendonk, C.; Rognan, D. Identification of a low-molecular weight TrkB antagonist with anxiolytic and antidepressant activity in mice. *J. Clin. Invest.* **2011**, doi: 10.1172/JCI43992.
- ⁹² Kishi, T.; Hirooka, Y.; Sunagawa, K. Telmisartan protects against cognitive decline via up-regulation of brain-derived neurotrophic factor/tropomyosin-related kinase B in hippocampus of hypertensive rats. *J. Cardiol.* **2012**, *60*, 489–494.
- ⁹³ Vassoler, F. M.; White, S. L.; Schmidt, H. D.; Sadri-Vakili, G.; Pierce, R. C. Epigenetic inheritance of a cocaine-resistance phenotype. *Nat. Neurosci.* **2013**, *16*(1), 42–49.
- ⁹⁴ Spaeth, A. M.; Kanoski, S. E.; Hayes, M. R.; Grill, H. J. TrkB receptor signaling in the nucleus tractus solitarius mediates the food intake-suppressive effects of hindbrain BDNF and leptin. *Am. J. Physiol. Endocrinol. Metab.* **2012**, *302*, E1252–E1260.
- ⁹⁵ Iwasaki, Y.; Nishiyama, H.; Suzuki, K.; Koizumi, S. Sequential *cis/trans* autophosphorylation in TrkB tyrosine kinase. *Biochemistry* **1997**, *36*, 2964–2700.
- ⁹⁶ Schecterson, L. C.; Bothwell, M. Neurotrophin receptors: Old friends with new partners. *Develop. Neurobiol.* **2010**, *70*, 332–338.
- ⁹⁷ Thomas, P.; Smart, T. G. HEK293 cell line: A vehicle for the expression of recombinant proteins. *J. Pharm. & Tox. Methods* **2005**, *51*, 187–200.
- ⁹⁸ Tapley, P.; Lamballe, F.; Barbacid, M. K252a is a selective inhibitor of the tyrosine protein kinase activity of the trk family of oncogenes and neurotrophin receptors. *Oncogene* **1992**, *7*(2), 371–381.
- ⁹⁹ Chao, M.; Hempstead, B. p75 and Trk: a two-receptor system. *Trends Neurosci.* **1995**, *18*, 321–326.
- ¹⁰⁰ Kaplan, D. R.; Matsumoto, K.; Lucarelli, E.; Thielet, C. J. Induction of TrkB by retinoic acid mediates biologic responsiveness to BDNF and differentiation of human neuroblastoma cells. *Neuron* **1993**, *11*, 321–331.
- ¹⁰¹ Wang, J.; Hancock, M. K.; Dudek, J. M.; Bi, K. Cellular assays for high-throughput screening for modulators of Trk receptor tyrosine kinases. *Curr. Chem. Gen.* **2008**, *1*, 27–33.

Chapter 3

Isoquinuclidine-Induced GDNF Release in C6 Glioma Cells: Studies Toward the Mechanism of Action

I.1 GDNF in the CNS

Glial-derived neurotrophic factor (GDNF) is a neurotrophic protein with important roles in the development and maintenance of the central nervous system (CNS). As discussed in Chapter 2, neurotrophic factors are crucial for protection and plasticity of the adult CNS. GDNF was first isolated from the rat glial cell line B49 and identified as a trophic molecule for dopaminergic neurons.¹ It is critical for normal neural development,² and in the adult brain it is located mainly in the midbrain, where it is transported to dopaminergic neurons from the striatum.

Roles for GDNF and/or its receptor, *rearranged during transfection* receptor (Ret), have been demonstrated or suggested in psychostimulant, opioid, and alcohol addiction,³ neuropathic pain,⁴ cancer,⁵ epilepsy,⁶ and Hirschsprung's disease.⁷ Briefly, alcohol addiction is a chronic neuropsychiatric disorder with limited pharmacological means of treatment, and GDNF has been shown reduce alcohol self-administration and withdrawal in mice.^{3b,c} In addition to alcohol, GDNF also counteracts behavioral and biochemical adaptations in mice chronically treated with cocaine and morphine, showing that GDNF plays a beneficial role in reversing the biochemical and behavioral adaptations associated with chronic drug use.⁸ GDNF is protective after stroke,⁹ and since GDNF protects dopaminergic neurons, GDNF is implicated in the pathophysiology of Parkinson's disease as well.¹⁰

I.2 GDNF/Ret Signaling

GDNF exists as a disulfide-linked, glycosylated homodimer of 33-45 kDa and is a member of the GDNF-family of ligands (GFL), which also includes neurturin,¹¹ and persephin,¹² artemin.¹³ These proteins are synthesized in a preproGFL form, and once secreted from a cell, are cleaved to the proGFL form, which is finally proteolytically cleaved to the active, mature GDNF. They signal through the single-pass transmembrane receptor tyrosine kinase Ret, and each is selective for a particular glycosylphosphatidylinositol (GPI)-anchored GFR α co-receptor; primarily, GDNF for GFR α 1, neurturin for GFR α 2, artemin for GFR α 3 and persephin for GFR α 4 (Figure 1). Neurturin and artemin may also weakly cross-activate GFR α 1, and GDNF GFR α 2 and GFR α 3.⁴

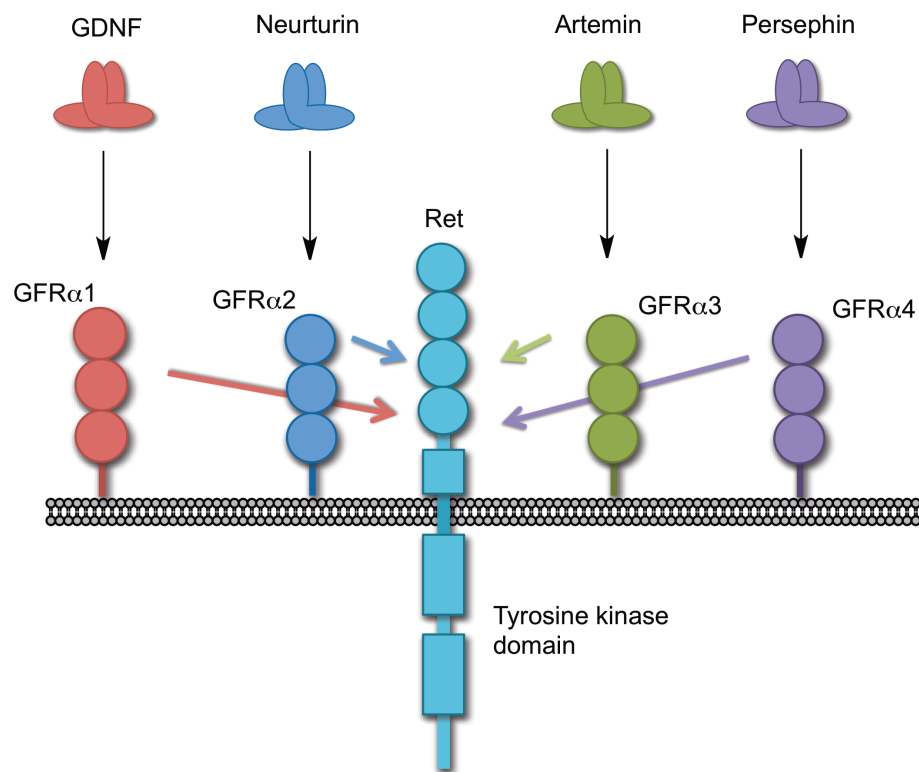


Figure 1. Ret co-receptors and their cognate GDNF-family ligands. Graphic adapted from Reference 4.

The exact sequence of events in the assembly of the receptor complex is not known, but homodimeric GDNF induces the dimerization of Ret with two GFR α 1 units; *cis* signaling occurs when Ret couples to membrane-bound GFR α 1, since both co-receptor units approach each other from the same membrane, and *trans* signaling occurs via association of Ret with soluble GFR α 1.¹⁴ The formation of this complex results in the auto-phosphorylation of the intracellular tyrosine kinase domain of Ret, which constitutes the activated GFR α 1/Ret complex, triggering the intracellular signaling.¹⁵ Alternatively, signaling may occur independently of Ret,¹⁶ including via the neural cell adhesion molecule (NCAM).¹⁷

There are several known sites of phosphorylation that lead to docking of specific adaptor proteins: Y905 docks Grb7/10, Y1015 for PLC γ , Y981 for s-Src, Y1096 for Grb2, and most importantly, Y1062, which docks Shc, IRS1/2, FRS2, DOK1/4/5, and Enigma. Ret induces the same major signaling pathways as TrkB, namely MEK/ERK1/2 and PI3K/Akt from Y1062 phosphorylation, and PLC γ /PKC from Y1015.¹⁸

I.3 Ibogaine and GDNF

Derived from the root bark of the West African shrub *Tabernaemontana iboga*, the natural product ibogaine (12-methoxyibogamine, Figure 2) has attracted the attention of medicinal chemists and pharmacologists owing to anecdotal reports of experiments in humans. Rigorous animal studies also showed that ibogaine suppresses self-administration for a broad range of drugs of abuse.¹⁹ However, high doses are required for the desired effects described above, which cause ataxia, bradycardia, and hallucinations, likely due to its molecular promiscuity in the brain. Pharmacological profiling of the compound shows that it is active at multiple CNS receptors, including α_1 adrenergic, nicotinic acetylcholine (nAChR), kappa opioid (κ OR), 5HT₂,

5HT₃, and *N*-methyl-D-aspartate glutamate (NMDAR) receptors, as well as dopamine transporter (DAT), vesicular monoamine transporter (VMAT), and serotonin transporter (SERT) proteins; however, it binds to these molecules with weak (μ M) affinities.²⁰ Of particular interest is its interaction with the sigma receptors σ 1R and σ 2R, as will be demonstrated in this chapter; ibogaine demonstrates a higher affinity for σ 2R (σ 2R $K_i \sim 200$ nM; σ 1R $K_i \sim 8500$ nM).²¹ It is metabolized by cytochrome P4502D6 to 12-hydroxyibogamine (noribogaine), which also shows anti-addictive properties.²² Despite its highly desired affect on addiction, ibogaine is currently a Schedule I controlled substance in the United States, which includes substance with high abuse potential, no accepted medical use, and poor safety standards. Thus, the design and synthesis of ibogaine analog or derivatives is a logical route to harness the desirable properties of the molecule and increase its specificity for particular target(s) and increasing potency at these targets, while removing the undesirable side effects, namely hallucinations. 18-Methoxycoronaridine (18-MC) is one example of a structurally related compound that retains the ability to reduce self-administration of a number of drugs of abuse²³ but does not retain the negative side effects, presumably because it functions via a different mechanism, as a nAChR antagonist.²⁴

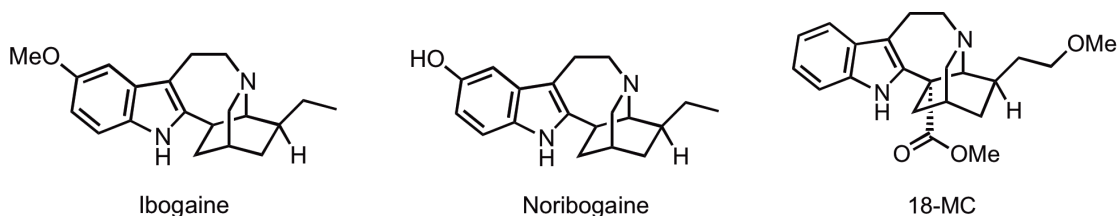


Figure 2. Chemical structures of ibogaine, noribogaine, and 18-MC.

An intriguing effect of ibogaine is the induction of GDNF synthesis *in vitro* and *in vivo*, which has been linked to its anti-addictive effects by the Ron laboratory.^{25,26} Ron's group proposed that the induction of GDNF expression in the ventral tegmental area (VTA) leads to activation of an autocrine loop, in which GDNF signaling through its receptors Ret/GFR α 1 results in increased synthesis and release of GDNF.²⁶ Such an autocrine loop would explain the long-term effects of acute doses of ibogaine on drug self-administration, craving and relapse. GDNF in turn was shown to reset the firing pattern of VTA dopaminergic neurons and thus presumably repair the function of the mesolimbic dopamine system involved in motivational processes. Based on these studies and unpublished preliminary results, the authors believe that ibogaine may act as a direct agonist of GFR α 1/Ret, which initially triggers the loop (Figure 3). The use of a small molecule to mimic the action of a neurotrophic factor is, as described in Chapter 2, highly attractive to us as medicinal chemists interested in neurotrophic small molecules for neuroprotection and repair.

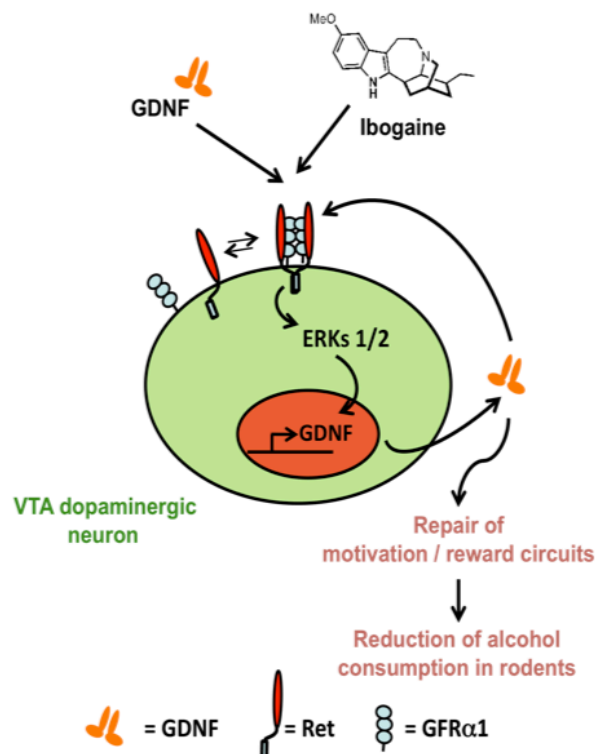


Figure 3. Mechanism of ibogaine-induced GDNF expression proposed by the Ron group (UCSF). Preliminary results indicated that ibogaine directly activates the GFR α 1/Ret complex, leading to activation of the MAP kinase pathway and expression of GDNF. GDNF positively regulates its own production and modulates the reward circuits, which underlies the decrease of alcohol self-administration and relapse in rodents. GDNF, Glial cell line-Derived Neurotrophic Factor; GFR α 1, GDNF Family Receptor α 1; Ret, receptor tyrosine kinase Ret; VTA, Ventral Tegmental Area (of midbrain).

Considering the trophic and repair effects of GDNF on dopamine and motor neurons, the development of methods to increase the release or synthesis of GDNF in the brain may provide treatments for neurological disorders, most notably Parkinson's disease and addiction. As GDNF is a protein, it has a poor pharmacokinetic profile and is not suitable as a direct treatment,²⁷ so similar approaches to those discussed in Chapter 2 to increase BDNF/TrkB signaling also apply to increase GDNF expression and GDNF/Ret signaling. Small molecules can increase expression or release of GDNF,²⁸ small molecules or peptide mimetics may be direct agonists of the Ret/GFR α 1 receptor complex,²⁹ or transactivation may occur from another

target.³⁰ The molecular design, profiling, and systematic examination of the mechanism of a small library of novel potential pharmacological agents to induce GDNF synthesis and release from neurons or astrocytes will be described.

II. Development & Pharmacological Profiling of Isoquinuclidine Ibogaine Analogs

II.1 Development of GDNF Release Assay & Identification of Lead Compounds

Measurement of GDNF release from model cell lines into the culture medium is a facile, widely used way to examine the effect of experimental treatments on GDNF induction and is biologically relevant. We selected an enzyme-linked immunosorbent assay (ELISA) to measure the GDNF content of the medium, since this 96-well microplate assay enables moderate throughput evaluation of compounds in comparison to western blotting or northern blotting for protein or mRNA expression, respectively. To establish this assay, post doctoral researcher Dr. Shu Li screened cell lines known to express GDNF against small molecule positive controls from the respective reports: Neuro2A,²⁹ SH-SY5Y,³¹ SK-N-AS,^{40b} or primary human cortical astrocytes did not secrete more than 15 pg/mL of GDNF as measured by ELISA assay (Promega), but rat C6 glioma cells released a basal level of approximately 100-200 pg/mL as measured by *conventional ELISA*. In the conventional ELISA, GDNF in the growth medium is detected in a separate plate (using an ELISA kit from Promega; see Experimental section), whereas in the *in situ* adaptation of the assay, the cells are grown on the ELISA plate coated with GDNF primary monoclonal antibody so that any GDNF released is instantly captured on the surface. We primarily use the conventional ELISA, as GDNF release concentrations after 48 hours are higher when measured this way, as opposed to the *in situ* version; we reasoned that the

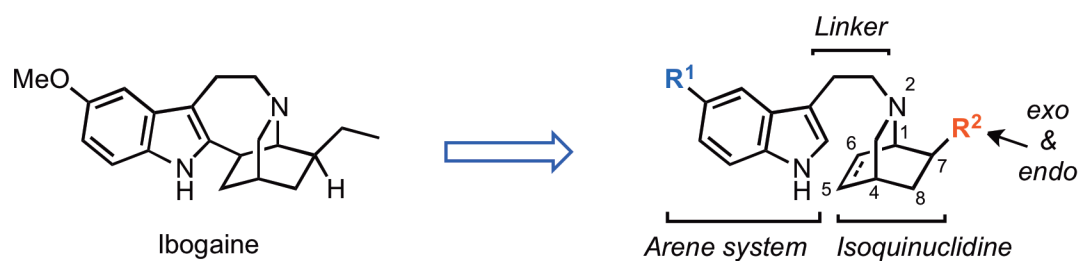
in situ assay does not allow for possible activation of the autoregulatory loop, and thus we prefer to measure free GDNF in the medium.

C6 cells express both Ret and GFR α 1, with higher expression than human glioma cell lines; the C6 line is reported to contain $2,837 \pm 813$ pg GDNF/g of cells³² and basal GDNF release varies between reports (6 to 81 pg/mL)³³ and between experiments in our laboratory. Receptor and growth factor expression is relatively well-characterized in this cell line, which is commonly used as a model for glioblastoma growth and invasion as well as a model of glia cells.³⁴ C6 cells have been used extensively to measure GDNF mRNA and protein expression as well as protein release. For example, NMDA antagonists amantadine and memantine induce the expression of the glial cell line-derived neurotrophic factor in C6 glioma cells.³⁵ Riluzole, a neuroprotective small molecule, has been reported to increase GDNF synthesis and release from the same cell line.³⁶ The antipsychotic haloperidol (5–25 μ M) and atypical antipsychotics quetiapine and clozapine induce secretion of GDNF from C6 cells,³⁷ and different classes of antidepressants, including the tricyclics amitriptyline and clozapine (10–25 μ M), tetracyclic mianserin, and selective serotonin reuptake inhibitors (SSRIs) fluoxetine and paroxetine, but not antipsychotics haloperidol (10–1000 nM), diazepam or diphenhydramine (1–25 μ M) induced GDNF synthesis and release from the same cell line as well.³⁸ Another study of antidepressants found that the synthesis and release may be linked to a β -arrestin, CREB-interactive pathway.³⁹ Lastly, one particular report by Verity characterized GDNF release from C6 cells after 24-hour treatment with a variety of growth factors and cytokines.^{40a} This cell line is therefore a well-characterized, established line to use for GDNF release. Dr. Li in the Sames group measured increases in GDNF release from C6 cells using clozapine as a positive control, and then

proceeded to screen the ibogaine analog library developed by our group in the GDNF release assay. These results served as the fundamental basis for the work described in this chapter.

II.2 Structural Design

We used ibogaine as a starting point for the design of analogs. Pursuing the original goal of developing selective GFR α 1/Ret agonists using ibogaine as the structural lead, the first order requirement was to eliminate or diminish binding to as many CNS off-target receptors as possible, most notably nAChRs. Considering the structural features common to both ibogaine and nicotine - the heteroarene attached to the saturated cyclic amine - we decided to remove this bond and explore *N*-indolyethyl-isoquinuclidines (Scheme 1).



Scheme 1. Structural design of *N*-indolyethyl-isoquinuclidines.

Following this structural design hypothesis, postdoctoral researcher Dr. Xiaoguang Li synthesized several compounds in a racemic form; compounds 1-5 are shown (Table 1). These compounds induce the release of GDNF from C6 cells (see Section II.1). We submitted these compounds to PDSP (Psychoactive Drug Screening Program of NIMH) for screening against 50 common CNS targets. Compound **1**, XL-167, shows no binding to nAChR receptors (7 forms tested), NMDA (PCP binding site), and SERT receptors (performed by PDSP). Thus, the structural changes (disconnection of the indole and isoquinuclidine ring and removal of the

indole methoxy substituent) led to compounds with favorable pharmacological profile (low off-target receptor binding).

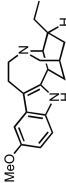
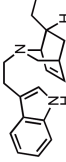
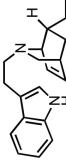
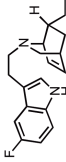
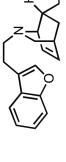
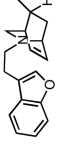
	 Ibogaine	 XL-167	 XL-166	 XL-008	 XL-026	 ACK-1-090
	1	2	3	4	5	
GDNF release (EC ₅₀)	~15 μ M	10.2 \pm 0.3 μ M	18.2 \pm 0.2 μ M	3.3 \pm 0.1 μ M	22.4 \pm 6.6 μ M	ND
DAT (K _i)	4 μ M	0.15 μ M	no	> 10 μ M	no	no
nAChRs (K _i)	0.02 μ M, antag.	no	no	no	no	no
NMDA receptor (K _i)	1-3 μ M, antag.	no	no	no	no	no
SERT (K _i)	0.5 μ M, inhib.	no	no	0.23 μ M	no	3.90 μ M
σ 1 receptor (K _i)	8.5 μ M	no	no	0.13 μ M	2.3 nM	0.39 μ M
σ 2 receptor (K _i)	0.1-0.2 μ M	no	no	0.015 μ M	1.1 nM	0.015 μ M

Table 1. Pharmacological characterization of isoquinclidines 1-5 as compared to ibogaine. EC₅₀ values were experimentally obtained in our laboratory, K_i values for 1-4 were obtained from PDSP, and K_i values for ibogaine were obtained from the literature.

Compounds **3** (XL-008) and **4** (XL-026) were prepared to examine the indole substitution and its effect on GDNF release and PDSP profile. Both compounds are relatively strong inducers of GDNF release, whereas ibogaine was not (Table 1). Compound XL-008, containing the 5-fluoroindole ring, shows no binding to nAChR or NMDA but does bind σ -1 and σ -2 receptors; it binds very weakly to DAT ($>10\ \mu\text{M}$), but shows relatively strong binding to SERT ($0.23\ \mu\text{M}$). XL-026, containing benzofuran in place of indole, shows no binding to DAT or SERT, but it binds to κ - and μ -opioid receptors (0.69 and $0.63\ \mu\text{M}$). These preliminary results demonstrate that the aromatic ring substitution is very important for both potency and binding selectivity at CNS receptors. The stereoisomer of **4**, **5** (compound ACK-I-090), induces less GDNF as measured at $10\ \mu\text{M}$ (Figure 4), but this is not mirrored in σ receptor affinity as compared to XL-026 or XL-008. We also prepared the saturated analog of XL-167 (where the alkene is saturated), which has similar activity to XL-167 in the GDNF release assay, while the compound with a deleted ethyl group is inactive (not shown), demonstrating the importance of a substituent in the 7-position of the isoquinuclidine (see Scheme 1).

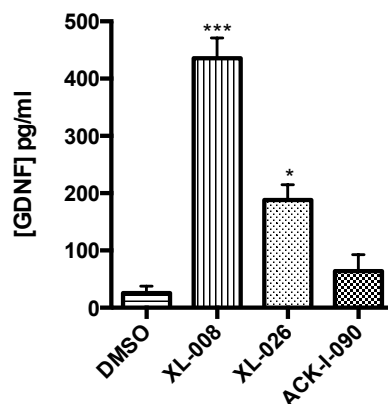


Figure 4. GDNF release from C6 cells (passage number 41) treated with compounds (10 μ M) for 48 hours. GDNF protein concentrations (pg/mL) in the conditioned medium were measured using ELISA. Data represent \pm SEM of biological duplicates within one experiment, representative of > 4 independent experiments. * $p < 0.05$, *** $p < 0.001$ indicate statistical significance compared to control as calculated by one-way ANOVA followed by Tukey's post-hoc test.

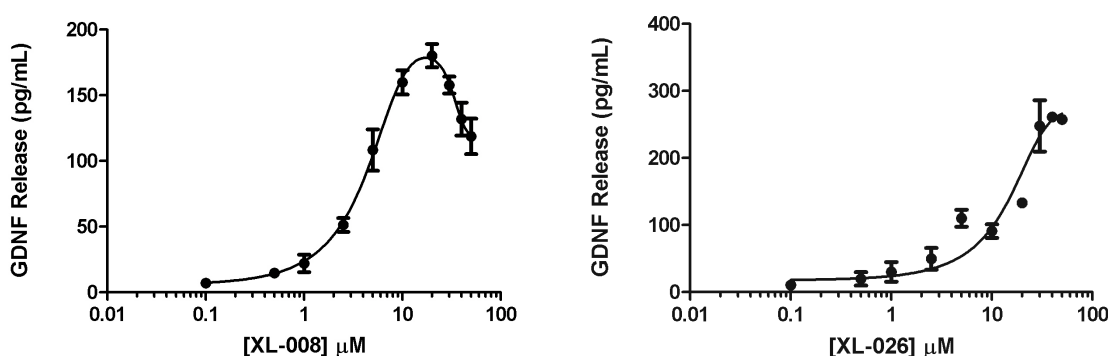


Figure 5. Representative dose-response curves of XL-008 and XL-026-induced GDNF release. GDNF release (pg/mL, measured by ELISA) from C6 (cell passage numbers 45 and 47) treated with compounds at various concentrations for 48 hours. Data represent \pm SEM of biological duplicates within one experiment, representative of 3 independent experiments. Data and graphics provided by Rich Karpowicz.

One challenge associated with the use of C6 cells relates to the known phenotypic instability of this cell line. Specifically, we found that GDNF release from C6 cells in response to small molecules and growth factors decreases over time with increasing passage numbers, which is consistent with the literature,^{40a} but poses a problem when performing statistical

analyses on averages across several sets of data. We also observe variability in release across distinct cell batches acquired from the American Type Culture Collection (ATCC) as well as within our own laboratory thawed from identical batches of cryopreserved cells. For example, the C6 cells that Dr. Li performed her initial screening with happened to release GDNF constitutively, with average basal levels ~ 200 pg/mL for several passages. Since the basal was high and decreased with passage number, we were able to utilize the cells for GDNF release experiments until a relatively high passage number, 46 – 47. A new batch of C6 cells we have acquired since then, however, do not release such high amounts of GDNF under basal conditions, and this basal release is highly variable, between 0 pg/mL and 100 pg/mL. Due to the lower basal release, the cells only produce a statistically significant amount of GDNF in response to stimulus for two to three passages only, so we are restricted to using passage 41 and 42 in experiments with these lines (see Experimental section for details). Quantification of results, therefore, may only be performed on an intra-assay basis; any standard deviation or error calculated from the biological replicates within each experiment is all that we may use to calculate statistical significance, and any graphical representation found in this work is a single representative experiment. We consider an experiment demonstrating a change in GDNF release as representative if it has been repeated at least three times. Negative results are considered reproducible after two experiments yield similar results. Importantly, we consider an increase or decrease of GDNF release statistically significant overall only if we observe statistical significance within each experiment. We find that biological duplicates within each experiment, and each sample being measured three times in the ELISA plate, provides sufficiently small standard error of the mean (SEM) when error is measured from biological replicates.

An interesting aspect of release by the isoquinuclidines is that release of GDNF cannot be

measured after 24 hours. However, if the cells are incubated with the compound for 24 hours, and then washed out and the medium replaced, GDNF release is still induced. This implies that whatever process is responsible for inducing GDNF is triggered within the initial 24-hour period.

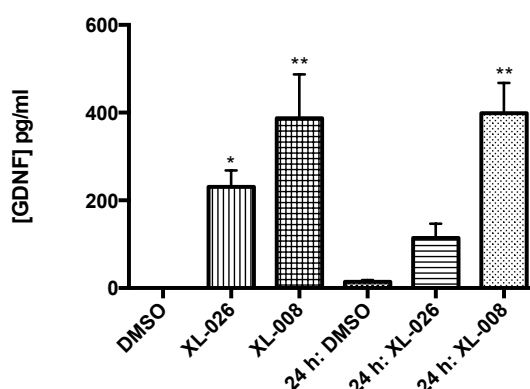


Figure 6. GDNF release from C6 cells (passage number 41) treated with compounds (10 μ M) for 48 or 24 hours followed by washing indicates that a 24-hour pulse of the compounds (10 μ M) leads to similar release as normal 48-hour incubation. GDNF protein concentrations (pg/mL) in the conditioned medium were measured using ELISA. Data represent \pm SEM of biological duplicates within one experiment, representative of 3 independent experiments. * $p < 0.05$, ** $p < 0.01$ indicate statistical significance compared to control as calculated by one-way ANOVA followed by Tukey's post-hoc test.

We questioned why release would take over 24 hours to appear, and tested if GDNF release is synthesis-dependent (or merely activity-dependent, not requiring synthesis of new GDNF). Use of cycloheximide, an inhibitor of translational elongation and thus a protein synthesis inhibitor, enabled us to conclude that the mechanism of GDNF release requires protein synthesis, as it reduced GDNF release by XL-026 down to the level of the control (Figure 7). This is in agreement with the necessary incubation period for release to occur.

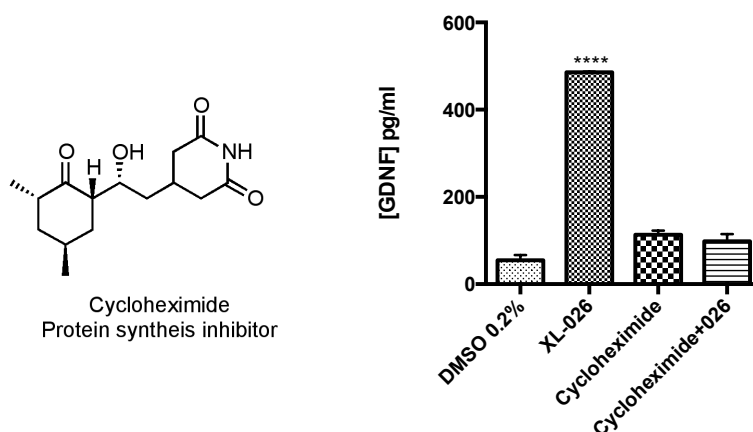


Figure 7. Structure of cycloheximide and its abolishment of GDNF release by XL-026. GDNF release from C6 cells (passage number 44) treated with XL-026 (10 μ M) for 24 hours after 1-hour preincubation with cycloheximide (1 μ g/mL, 3.6 μ M). GDNF protein concentrations (pg/mL) in the conditioned medium were measured using ELISA. Data represent \pm SEM of biological duplicates within one experiment, representative of 2 independent experiments. **** $p < 0.0001$ indicates statistical significance compared to the control as calculated by one-way ANOVA followed by Tukey's post-hoc test.

As we characterized GDNF release from C6 cells, Rich Karpowicz also performed extensive cytotoxicity and morphology experiments to understand the link between cytotoxicity and GDNF release, which we routinely measure using a colorimetric assay for lactate dehydrogenase (LDH) release. LDH is a stable cytoplasmic enzyme that is released upon membrane lysis (see Experimental), and we performed the LDH assay for every experiment alongside GDNF detection. GDNF release tends to parallel small increases in LDH release that typically are in the range of 4 – 10%, and do not rise above 20% of an intracellular control in response to any given treatment.

The morphology of C6 is fibroblastic (Figure 8A), but may change in response to treatments. Interestingly, 48-hour treatment of C6 with one of our early small molecule ‘hits,’ XL-008, at various concentrations induces morphological changes at concentrations as low as 10 μ M (Figure 8B). The cells become rounder and begin to display spindly processes, which are

dramatically evident at 40 μ M (Figure 8C). We reason that the mechanism of GDNF release may be intricately tied to the mechanism of this phenotypic change.

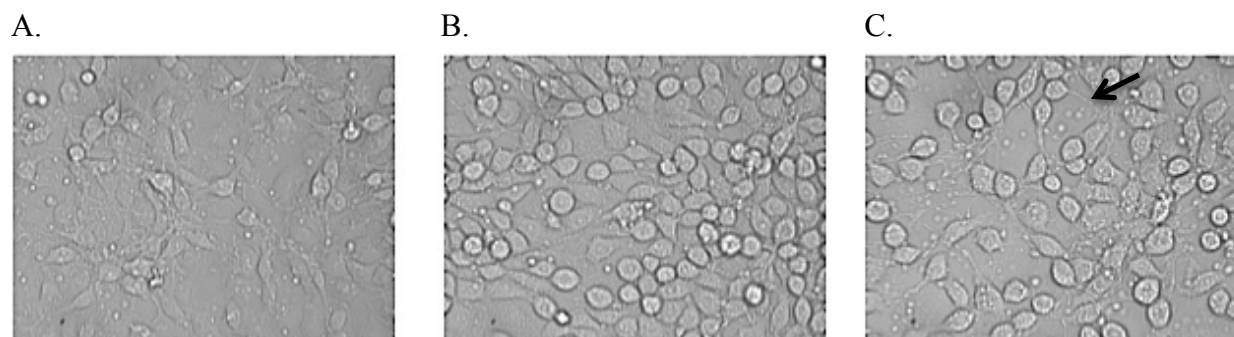


Figure 8. Brightfield images (400X) of C6 morphology in response to 48-hour treatment with XL-008 at (A) 0.1% DMSO control, showing normal, flat, fibroblastic morphology, (B) 10 μ M, and (C) 40 μ M. An example process induced by XL-008 is indicated with an arrow. Images courtesy of Rich Karpowicz.

Thus, we have characterized the time- and protein synthesis-dependent GDNF release induced by our compounds. We know that more than 24 hours is required for GDNF synthesis and release to occur, but the signaling cascade is activated within a 24-hour period. Treatment with the compounds induces dose-dependent GDNF release (Figure 5). C6 cell morphology changes dose-dependently after 48-hour treatment with the compounds. This information will aid us as we seek to elucidate the mechanism of action of these neurotrophin-releasing compounds.

III. Hypotheses for the Mechanism of Action of Isoquinuclidines

Preliminary results in the C6 cell release assay, combined with a thorough examination of the literature on receptor expression and GDNF production in these cells led us to utilize pharmacological tools for examining the signaling pathways involved in isoquinuclidine-induced

GDNF release from C6 cells and further characterizing GDNF release from this cell line.⁴⁰ We also utilized western blotting to examine phosphorylation of Ret and extracellular signal-regulated kinase (ERK) in the presence of the compounds to determine if Ret might be involved in induction of a GDNF autoregulatory loop as hypothesized by the Ron group about ibogaine. As we accumulated information about the signaling involved in GDNF synthesis and release by our compounds, we addressed the following potential hypotheses to structure our approach to the elucidation of the mechanism: *1. Transactivation from a G-protein coupled receptor (GPCR) to a receptor tyrosine kinase (RTK); 2. Sigma receptor involvement; 3. Lysosomal or endoplasmic reticulum (ER) stress; 4. GDNF release as a secondary effect of receptor up-regulation or protein release.*

III.1 Transactivation or Direct Signaling Through Receptor Tyrosine Kinase(s)

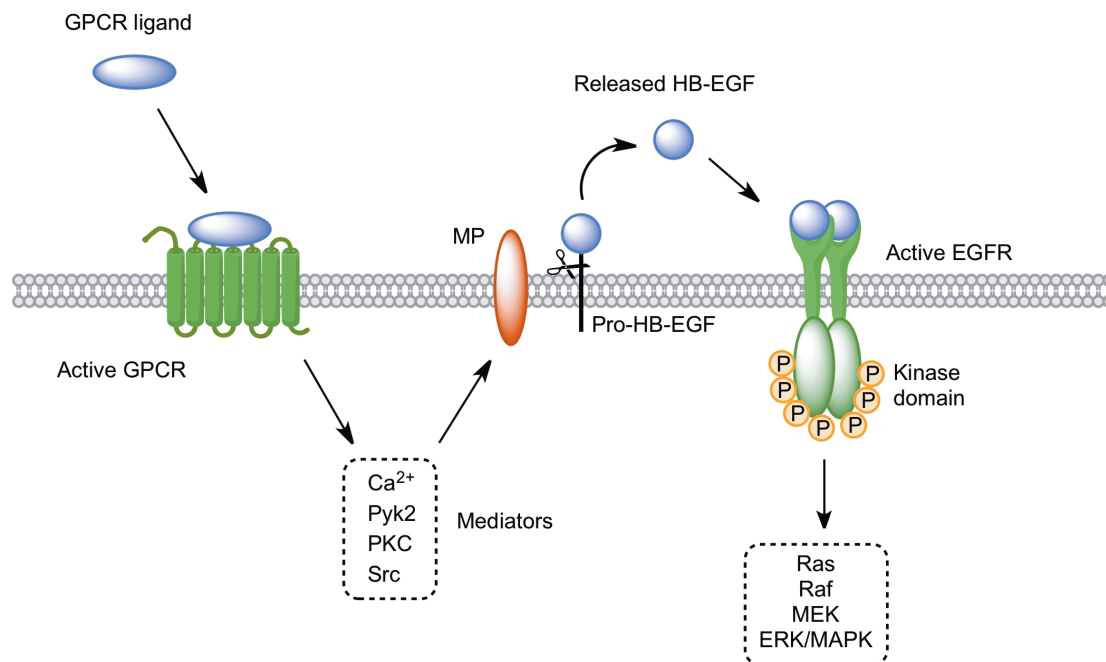


Figure 9. Transactivation from a G-protein coupled receptor (GPCR) to the epidermal growth factor receptor (EGFR).^{43a} Ligand activation of a GPCR induces signaling via mediators, which activate a metalloproteinase (MP) to release heparin-bound epidermal growth factor (HB-EGF) to activate EGFR. [P = phosphate.]

Transactivation, as briefly mentioned in Chapter 2, occurs when ligand binding to its cognate receptor induces not only activation of this receptor, but also the indirect activation of additional receptors as well. The classic system that exemplifies transactivation is from GPCRs to the epidermal growth factor receptor (EGFR)⁴¹ or another RTK (Figure 9).⁴² In this model, GPCR activation leads to second messenger signaling, which varies depending on the cell type, that activates a metalloproteinase to release heparin-bound EGF (HB-EGF), the endogenous cognate ligand for EGFR. Upon this proteolytic cleavage from the pro-form to the free ligand, EGFR is activated, resulting in ERK1/2 phosphorylation.⁴³

RTKs may be transactivated by intracellular mechanisms, also, independently of RTK ligand binding. Second messenger mediators may directly activate the RTK at the kinase

domain via the intracellular tyrosine kinases Src (or Src family kinases), protein tyrosine kinase 2 (Pyk2), reactive oxygen species (ROS), or other modes of signaling.⁴³ For example, it was reported that treatment of C6 cells with serotonin leads to an increase in GDNF release,^{44a} and the release occurs through an increase of GDNF mRNA caused by transactivation through the fibroblast growth factor receptor 2 (FGFR2) which may be mediated by Src family kinases and is not dependent on release of FGF.^{44b} Due to its ubiquitous appearance in nature, transactivation is a reasonable mechanistic possibility for the action of our isoquinuclidines, as we have observed clear evidence of RTK involvement based on extensive use of pharmacological inhibitors (Section IV.4).

We have not ruled out the possibility that these small molecules are direct agonists of any given RTK; for example, it is possible that the isoquinuclidines are agonists of the Ret/GFR α 1 complex, as ibogaine was hypothesized to be.²⁵ There is literature precedent for the direct agonism of RTKs by small molecules⁴⁵; in addition to the TrkB agonists discussed in Chapter 2,⁴⁶ small molecules have been developed as mimetics for insulin,⁴⁷ human granulocyte colony-stimulating factor,⁴⁸ p75NTR,⁴⁹ and TrkA.⁵⁰ Thus, this possibility must be considered alongside other potential direct receptor agonism⁵¹ that may result in transactivation.

III.2 Sigma Receptor Involvement

Pharmacological profiling of our compounds (XL-008 and XL-026) revealed high selectivity and high affinity for the σ -receptors (Section II.2). Both types, σ 1R and σ 2R, are expressed by C6 cells,⁵² though at least one report suggests that only σ 2R is present due to lack of binding by 1 μ M pentazocine, a σ 1R-selective ligand (Figure 10).⁵³ Using known pharmacological agonists and antagonists for σ 1R and σ 2R also supports sigma receptor involvement in isoquinuclidine-induced GDNF release from C6 cells.

The σ 1R is a transmembrane protein chaperone anchored on the endoplasmic reticulum (ER) that translocates to nuclear or plasma membrane upon activation, though whether or not it induces intracellular signaling is highly dependent on cell type.⁵⁴ It is also thought to associate with another molecular chaperone, BiP (binding immunoglobulin protein, a heat shock protein) and stabilize the inositol triphosphate (IP₃) receptor (IP₃R) at the ER.⁵⁵ In fact, the ability to dissociate BiP from σ 1R forms the basis of the first definition of an agonist of the receptor, whereas an antagonist inhibits the dissociation in the presence of an agonist.⁵⁶ Calcium, IP₃, and PKC signaling have been associated with σ 1R, and as a molecular chaperone, it may also translocate other proteins to the plasma membrane, such as protein kinase C (PKC).⁵⁷ In primary mixed cortical and hippocampal neurons, σ 1R agonists PRE-084 and 4-PPBP activated ERK1/2, but not p38 MAPK or JNK,⁵⁸ which is relevant because of ERK1/2-dependence of GDNF release by our isoquinuclidines (Section IV.2). Also pertinent is a report demonstrating that *in vivo*, the σ 1R-selective agonist PRE-084 (Figure 10) increases GDNF and BiP expression after rat root avulsion injury, and the protective effect is antagonized by a σ 1R antagonist.⁵⁹ The agonist cutamesine (SA4503, Figure 10) dissociates the σ 1R receptor from BiP, and this effect lasts for two days; it also potentiates the post-translational processing and release of BDNF from rat B104 neuroblastoma cells⁶⁰ and increases BDNF protein expression in rat hippocampus.⁶¹ Perhaps it is possible, then, that σ 1R could also have the same effect on GDNF expression and release. σ 1R is closely tied to disorders that include schizophrenia, depression, anxiety, memory deficits and pain, and many antipsychotics, antidepressants, and neurosteroids are known to bind with high affinity to this receptor.⁵⁶

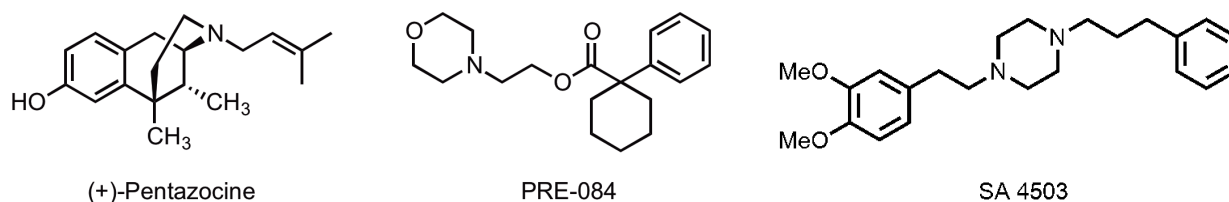


Figure 10. Structures of selected σ 1R ligands.

σ 2R, however, is not well characterized. Ligands of this receptor subtype are often associated with cell proliferation and viability, with selective ligands inducing cell death.⁶² It has recently been suggested that σ 2R is identical to the progesterone receptor membrane component 1 (Pgrmc1).⁶³ Pgrmc1 has been shown to be upregulated in many types of tumor and is known to associate with EGFR and increase EGFR plasma membrane levels.⁶⁴ Pgrmc1 signaling by progesterone also leads to the PKC-dependent activation of *VEGF* gene expression and protein synthesis in porcine retinal glial cells.⁶⁵ This receptor is expressed in C6 cells, as progesterone-treated C6 cells, which express membrane-associated progesterone receptors (PR), including Prgmc1, but not classical nuclear PR, release BDNF in an ERK5- and Prgmc1-dependent manner.⁶⁶ Thus, σ 2R, as Pgrmc1, has been known to increase RTK expression and neurotrophin release from C6 cells, making it a target of interest.

Another aspect of sigma receptor signaling that is critical to our hypothesis (i.e. that sigma receptors are involved in the mechanism of GDNF release by our compounds) is its ability to potentiate signaling at other receptors. For example, the σ 1R ligands (+)-pentazocine, imipramine, and fluvoxamine, the latter two being antidepressants, potentiate nerve growth factor (NGF)-induced neurite outgrowth in PC12 rat pheochromacytoma cells and increase the expression of σ 1R.⁶⁷ Our experimental observations and implications of the phenomenon based on the literature will be discussed in depth in Section V.

III.3 GDNF Release as a Response to Stress

Cellular response to stress is mediated by a number of signaling pathways. Small molecules may induce stress in specific ways; two examples potentially relevant to us involve ER stress and collapse of lysosomal pH gradient or permeabilization of the lysosomal membrane. There are two known pathways a cell may activate to respond to ER stress, caused by the accumulation of unfolded proteins: the unfolding protein response (UPR), which triggers several specific signaling and transcription events, and the ER-overloaded response (EOR), which activates the transcription factor NF- κ B, may require Ca^{2+} , and produces reactive oxygen species (ROS).⁶⁸ UPR is linked to the pathophysiology of depression, stroke, Alzheimer's, and amyotrophic lateral sclerosis, and $\sigma 1$ regulates protein folding and degradation, which further strengthens the connection between $\sigma 1$ and these conditions.⁶⁰ The connection prompted the development of this hypothesis as a potential mechanism for GDNF release by our compounds. Also of interest is that C6 cells have been shown to synthesize VEGF mRNA in response to glucose and oxygen deprivation, both of which can result in ER stress,⁶⁹ and breast cancer cells can secrete vascular endothelial growth factor (VEGF) in response to ER stress,⁷⁰ raising the question of which other growth factors may be secreted as well.

$\sigma 2$ R ligands, on the other hand, have been shown to induce oxidative stress⁷¹ and some $\sigma 2$ R ligands act as lysosomotropic detergents in several cancer cell lines.⁷² Lysosomes are organelles in cells that serve to digest and turnover intracellular macromolecules and organelles in an acidic environment, which is maintained by vacuolar H^+ -ATPase (V-type ATPase), a membrane enzyme that maintains the pH gradient between the organelle's lumen and the cytoplasm. Disruption of this gradient leads to loss of lysosome function, which causes oxidative stress and release of destructive enzymes into the cell. Siramesine, a $\sigma 2$ R selective

ligand, as well as the σ 2R selective rimcazole and σ 1/ σ 2R nonselective ligand haloperidol also induced alkalinization of lysosomes, whereas (+)-pentazocine did not. However, this rise only persisted for 16 hours in the case of siramesine, and rimcazole and haloperidol only induced a rise in pH for four hours.⁷²

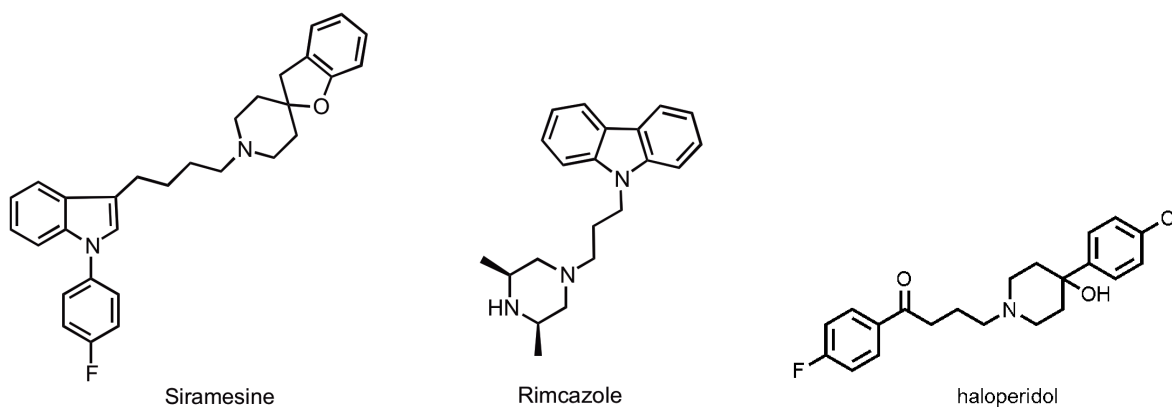


Figure 11. Chemical structures of σ 2R ligands siramesine and rimcazole, and nonselective σ ligand haloperidol.

Regardless, it has been confirmed that σ 2R ligands lead to stress and lysosomal membrane permeabilization in cancer cells.⁷³ This process is known to induce GDNF release from C6, human glioblastomas U87MG and T98G, and primary human astrocyte cultures, as inhibitors of vacuolar H^+ -ATP-ase, concanamycin A and bafilomycinA1, induce GDNF release in these lines.³³ The release of GDNF in response to lysosomal permeabilization caused by collapse of the pH gradient in response to σ 2 ligands and V-type ATPase inhibitors may result in triggering a protective mechanism.

III.4 GDNF Release as a Secondary Effect

The hypothesis that GDNF release may be the result of a prerequisite change in receptor expression or stability, or even a prerequisite protein release that induces GDNF synthesis, is

based on the fact that there is a 24-hour induction period before GDNF is detectable in the conditioned medium in response to XL-008 or XL-026. Does GDNF signaling lead to up-regulation of any growth factor receptors, or release of a growth factor, that could account for activation of some kind of autoregulatory loop as in the case of GDNF/Ret/GFR α 1? It is possible that GDNF release is caused by a factor in the growth medium, and isoquinuclidines prime the cell for potentiated, endogenous signaling by up-regulating, stabilizing, or shuttling receptor proteins to the surface (possibly via σ 1R). Also, it is equally possible that the small molecules lead to release of a different protein first, which then leads to GDNF synthesis and release. Pharmacological inhibition studies will provide us with clues as to which receptor systems may be implicated in the mechanism of release, and using that information we will be able to determine if receptor-mediated GDNF release is dependent on previous growth factor expression and secretion.

IV. Results & Discussion

Our search for the molecular target of the isoquinuclidines that triggers signaling pathways responsible for GDNF induction in C6 cells began with Ret/GFR α 1. One major method used in our studies has been western blotting, to examine activation of relevant signaling proteins. We assessed Ret and downstream ERK1/2 activation in C6 cells and in human neuroblastoma SH-SY5Y cells, which also contains a functional Ret/GFR α 1 system.³⁰ Since our isoquinuclidines are similar in structure to ibogaine, which was suggested to be a direct Ret/GFR α 1 agonist, and since Ret is known to transactivate TrkB in SH-SY5Y cells,³⁰ we also questioned if TrkB is activated by treatment with several isoquinuclidines in HEK-TrkB cells. ERK1/2 phosphorylation became our primary route to examine the activity of the compounds

once we were convinced of MEK/ERK involvement in the mechanism of GDNF release on the basis of pharmacological inhibition studies in C6 cells.

Our second major approach to examining the signaling pathway(s) responsible for GDNF induction in C6 cells rested on pharmacological modulation of relevant receptors and intracellular signaling proteins. While inhibition and/or antagonism alone do not provide conclusive evidence for the involvement of any given species, we used chemical biological and pharmacological tools with the intention of identifying probable pathways that could then be probed further with other techniques. Early experiments focused on ERK1/2, as it is activated by many receptor proteins, to determine if its activation is required for GDNF release; we also considered the known mechanisms leading to GDNF release in C6 cells, which include serotonin receptors (5HTRs),⁴⁴ and the fibroblast growth factor receptors (FGFRs).⁴⁴ To probe receptor involvement, we used a two-pronged approach by utilizing an agonist of the receptor to determine if it was capable of inducing GDNF release, and an antagonist or inhibitor for the receptor or intracellular signaling module to modulate XL-026-induced release. We applied this approach to most of the potential targets we considered, each of which we selected based on their connection to GDNF synthesis or release in C6 cells or primary astrocytes, expression in C6, and/or ability to trigger ERK1/2 activation, as reported in the literature. Below, each potential target is briefly described with a rationale and the results. First, those we deemed the most probable receptor targets will be addressed, followed by the remaining receptors in alphabetical order grouped by receptor type (GPCRs, nuclear hormone receptors, and RTKs). Lastly, intracellular signaling components are also considered, which we hoped would help elucidate or rule out potential pathways in the context of the receptor results. These studies address the receptor activation/transactivation, sigma involvement, and preliminarily address the idea that

isoquinuclidine-induced GDNF release may be reliant on secretion of either growth factors or cytokines. Proposed future work to address each hypothesis will be summarized in Section VII.

IV.1 Ret Activation

Our initial hypothesis was strongly driven by both published and unpublished preliminary results generated in Ron group (UCSF), postulates that ibogaine is a direct Ret/GFR α 1 modulator. Therefore, we sought to confirm Ret activation by ibogaine in SH-SY5Y, the cell line used by the Ron group.²⁵ After optimization of antibodies for use in western blotting experiments, we spent a great deal of time trying to observe activation of Ret in response to ibogaine, to no avail, despite seeing robust activation of Ret by GDNF as a positive control (Figure 12).

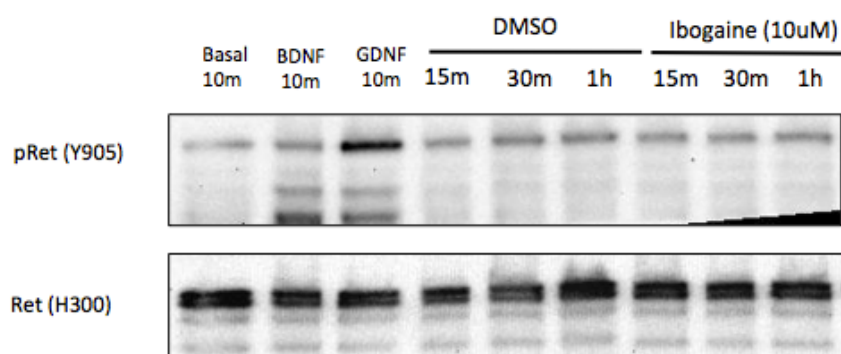


Figure 12. Ibogaine (10 μ M) does not activate Ret in differentiated SH-SY5Y cells. Positive controls GDNF and BDNF give strong activation. SH-SY5Y cells were differentiated for 72 hours in the presence of 10 μ M retinoic acid followed by overnight incubation with low serum medium. The cells were incubated with ibogaine (10 μ M) or DMSO (0.1%) control for the indicated times, and separate wells were incubated with BDNF (50 ng/mL), GDNF (50 ng/mL), or medium only (basal) as a control for 10 minutes. Lysates were analyzed by western blotting using a phospho-specific Ret antibody, followed by stripping and reprobing the membrane for total Ret. Representative image of three separate experiments.

Though one-hour activation of Ret was reported in the literature,²⁵ we also examined Ret phosphorylation at 3 hours to determine if one hour was not long enough to induce activation of

the receptor. However, we did not observe Ret or downstream ERK1/2 activation even at 3 hours in the presence of ibogaine (Figure 13).

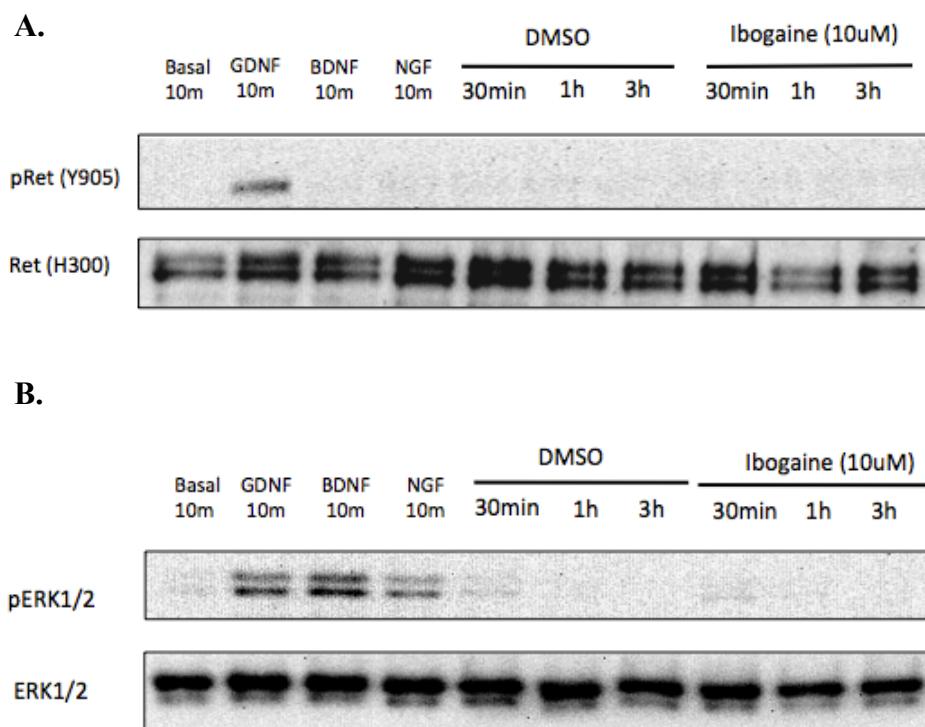


Figure 13. Ibogaine does not activate Ret (A) or ERK1/2 (B) in SH-SY5Y cells from 30 minutes to 3 hours as determined by western blotting. SH-SY5Y cells were differentiated for 72 hours in the presence of 10 μ M retinoic acid followed by overnight incubation in low serum medium. The cells were incubated with ibogaine (10 μ M) or DMSO (0.1%) control for the indicated times, and separate wells were incubated with BDNF (50 ng/mL), GDNF (50 ng/mL), NGF (50 ng/mL), or medium only (basal) as a control for 10 minutes. Lysates were analyzed by western blotting using a phospho-specific ERK1/2 antibody, followed by stripping and reprobing the membrane for total ERK1/2. Representative image of two separate experiments with ibogaine, and of at least six with the neurotrophins.

Ret is difficult to detect in C6 cells

C6 cells express both Ret and GFR α 1 proteins,⁷⁴ so we considered that ibogaine might phosphorylate Ret in this cell line. However, we noticed that regardless of the antibody used or amount of protein loaded on the gel, we could not clearly detect bands corresponding to the Ret

receptor despite extensive optimization by more than one group member. Deeper searching of the literature revealed that there had only been one example of Ret detection by western in this line,^{74a} so we abandoned our efforts to determine if ibogaine or our isoquinuclidines activated Ret in C6. Our results suggest that Ret protein expression is very low. It is also plausible that the receptor may be inactive due to the presence of NCAM,⁷⁵ which may occupy GFR α 1 monomers and thwart binding to Ret. In summary, our results do not support Ron's hypothesis that ibogaine activates Ret and ERK1/2 at the reported concentration (10 μ M).

IV.2 ERK1/2 involvement

ERK1/2 are downstream signaling proteins that are activated in response to countless receptor proteins and signaling events, from RTKs to GPCRs and as a hub between various signaling pathways.^{43a} ERK kinases are activated by phosphorylation, which is catalyzed by the upstream kinases MEK1/2. Since ERK1/2 is downstream from Ret, we wanted to know early on in our investigations if GDNF release by our compounds was ERK1/2-dependent. Pharmacological inhibition with the two most commonly used MEK1/2 inhibitors, PD98059 and U0126, confirmed that MEK/ERK signaling is very likely to be involved, as both inhibitors dose-dependently inhibited GDNF release (Figure 14, Figure 15). However, some reports argue that at the concentrations necessary for MEK1/2 inhibition by these compounds result in cross-inhibition of MEK1/2 versus MEK5, a closely related kinase.⁷⁶ To resolve this ambiguity, we used the MEK inhibitor PD184352, which is less potent at MEK5,⁷⁷ at a low concentration (2 μ M) that is reported to be selective.⁷⁸ BIX02189, a MEK5 inhibitor at 10 μ M, also completely inhibits GDNF release by XL-026. These results indicate that ERK1/2 plays a crucial role in induction of GDNF release by XL-026 in C6 cells; they also indicate that ERK5 may be involved as well (Figure 16).

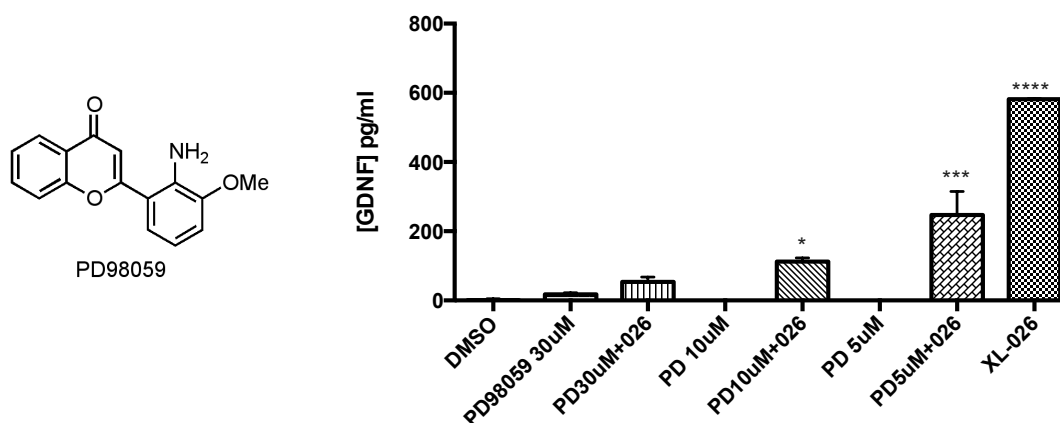


Figure 14. PD98059, the MEK1/2 inhibitor, dose-dependently inhibits GDNF release from C6 cells (passage number 42) induced by XL-026 (10 μ M). GDNF protein concentrations (pg/mL) in the conditioned medium were measured using ELISA after 48 hours. Data represent \pm SEM of biological replicates within one experiment, representative of 2 independent experiments. * $p < 0.05$, *** $p < 0.001$, and **** $p < 0.0001$ indicate statistical significance compared to the control as calculated by one-way ANOVA followed by Tukey's post-hoc test.

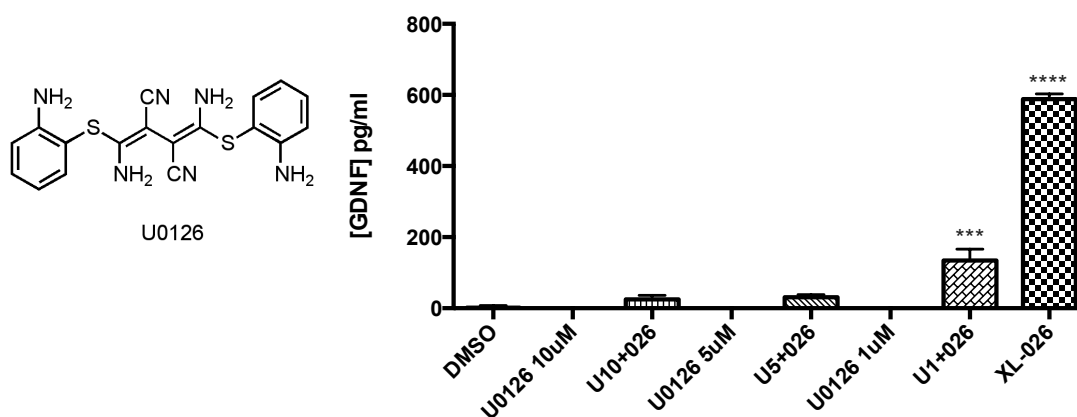


Figure 15. U0126, the MEK1/2 inhibitor, dose-dependently inhibits GDNF release from C6 cells (passage number 42) induced by XL-026 (10 μ M). GDNF protein concentrations (pg/mL) in the conditioned medium were measured using ELISA after 48 hours. Data represent \pm SEM of biological replicates within one experiment, representative of 2 independent experiments. *** $p < 0.001$ and **** $p < 0.0001$ indicates statistical significance compared to the control as calculated by one-way ANOVA followed by Tukey's post-hoc test.

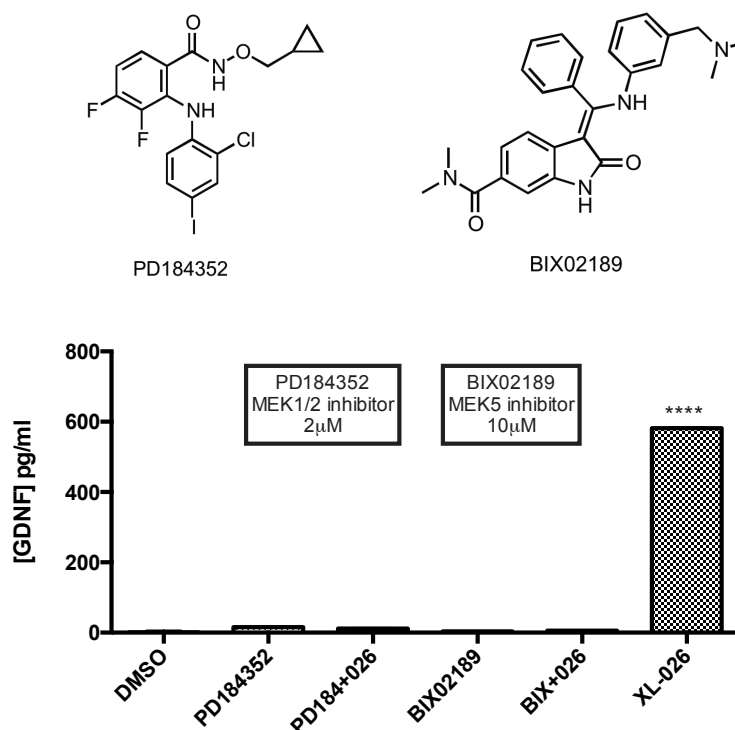


Figure 16. MEK inhibitors implicate MEK1/2 signaling in GDNF release from C6 cells (passage number 42) induced by XL-026 (10 μ M). GDNF protein concentrations (pg/mL) in the conditioned medium were measured using ELISA after 48 hours. Data represent \pm SEM of biological replicates within one experiment, representative of 2 independent experiments. **** $p < 0.0001$ indicates statistical significance compared to the control as calculated by one-way ANOVA followed by Tukey's post-hoc test.

IV.3 GPCR Involvement

IV.3.1 Serotonin (5HT) Receptors

C6 cells express 5HT_{2A} receptors and it has been reported that this receptor transactivates FGFR-2, which activates ERK1/2, resulting in induction of GDNF release.⁴⁴ Since our isoquinuclidines showed affinities for 5-HT receptors, we first wanted to confirm the ability of this receptor to induce GDNF release. Treatment with 5-HT (10 μ M) did not elicit GDNF release (5.4 pg/mL vs 6.7 pg/mL in the control of a representative experiment), likely due to rapid metabolism or transport into the cell via organic ion transporters, but the racemic 5HT₂

receptor agonist 2,5-dimethoxy-4-iodoamphetamine, (\pm)-DOI (Figure 17), which is known to bind to C6 cells (displaces ^3H -5-HT binding with $\text{IC}_{50} = 750 \text{ nM}$),⁷⁹ induced a statistically significant increase in GDNF release. However, the use of 5HT₂ receptor antagonist, cyproheptadine, which was used by Tsuchioka^{44b} to demonstrate that 5HT-induced ERK1/2 activation and subsequent GDNF release was initiated by 5HT₂ receptors in C6 cells, had no effect on XL-026-induced GDNF release (Figure 18). These data suggest that 5HT_{2A} is not involved in the mechanism of XL-026-induced release.

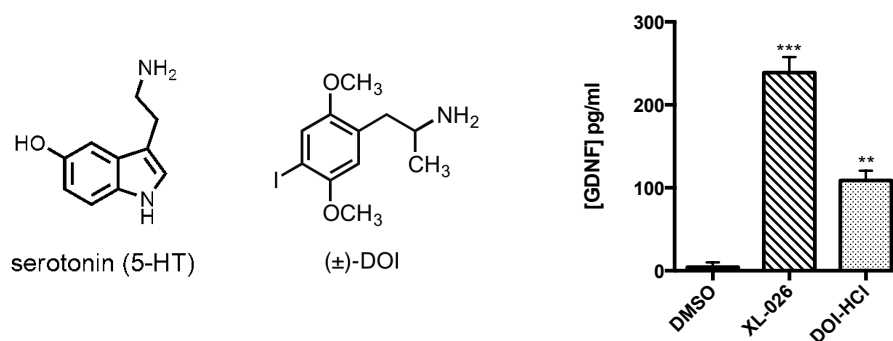


Figure 17. (A) Chemical structure of serotonin and 5HT₂ agonist (\pm)-DOI. (B) (\pm)-DOI (10 μM) induces GDNF release from C6 cells (passage number 42). GDNF protein concentrations (pg/mL) in the conditioned medium were measured using ELISA after 48 hours. Data represent \pm SEM of biological replicates within one experiment, representative of 4 independent experiments. ** $p < 0.01$, *** $p < 0.001$ indicates statistical significance compared to the control as calculated by one-way ANOVA followed by Tukey's post-hoc test.

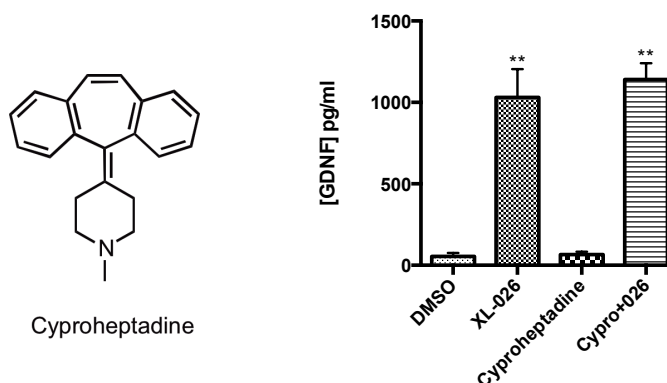


Figure 18. 5HT₂ antagonist cyproheptadine. Cyproheptadine (1 μ M, 30 minutes pretreatment) does not attenuate XL-026-induced GDNF release from C6 (passage 41). GDNF protein concentrations (pg/mL) in the conditioned medium were measured using ELISA after 48 hours. Data represent \pm SEM of biological replicates within one experiment, representative of 2 independent experiments. ** $p < 0.01$ indicates statistical significance compared to the control as calculated by one-way ANOVA followed by Tukey's post-hoc test.

IV.3.2 Opioid Receptors

The κ OR and μ OR receptors are expressed in C6 cells⁸⁰ and both activate ERK1/2, though μ OR activates ERK1/2 through transactivation of FGFR1.⁸¹ This makes these receptors of particular interest, especially in light of the fact that sigma antagonists potentiate opioid-induced analgesia in rats.⁸² To probe the potential involvement of this receptor in GDNF release, we utilized the selective κ OR pharmacological agonist U50,488, endogenous μ OR agonist endomorphin-1, the nonselective antagonist naltrexone, and κ OR-specific antagonist norbinaltorphimine (norBNI). Both agonists tended to increase GDNF release, but this increase was not statistically significant in every experiment (endomorphin-1 induced 17.5 ± 4.8 pg/mL and U50,488 induced 92.4 ± 7.1 pg/mL vs. 6.7 ± 1.7 pg/mL from the control in a representative experiment). Also, neither antagonist had an effect on GDNF release by XL-026 (Figure 19), leading us to conclude that opioid receptors are likely not involved.

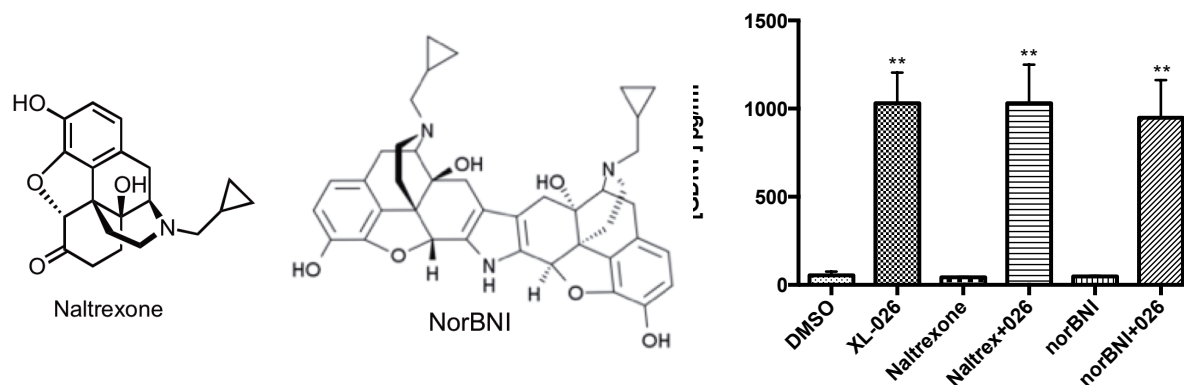


Figure 19. Structures of pan-opioid antagonist naltrexone, κ OR antagonist norBNI, and their effect on XL-026-induced GDNF release from C6 cells (passage number 41) pretreated with 1 μ M of each antagonist prior to addition of XL-026 (10 μ M, 48 hours). GDNF protein concentrations (pg/mL) in the conditioned medium were measured using ELISA after 48 hours. Data represent \pm SEM of biological replicates within one experiment, representative of 2 independent experiments. ** $p < 0.01$ indicates statistical significance compared to the control as calculated by one-way ANOVA followed by Tukey's post-hoc test.

IV.3.3 Adenosine Receptors

Adenosine receptors (A_1 , A_2 , and A_3) are present in C6 cells⁸³ and are of interest because they promote *GDNF* transcription and increase GDNF release in primary cultures of rat astrocytes through activation of A_{2B} receptors.⁸⁴ Also, FGF has been reported to act as a co-transmitter with adenosine via A_{2A} receptors to induce synergistic activation of the MAPK/ERK pathway and induce differentiation and neurite extension in PC12 cells,⁸⁵ which functionally in the CNS may occur because adenosine is increased in response to injury and induces release of other trophic factors, like NGF.²⁸ Treatment of C6 cells with adenosine (10 μ M) does not result in GDNF release in our assay (3.3 pg/mL vs. 3.2 pg/mL control in a representative experiment), nor does the small molecule CGS 21680, a pharmacological A_{2A} agonist (10 μ M, Figure 20). To confirm this result, we will use the A_{2A} antagonist ZM241385 in the presence of XL-026 to confirm that it does not attenuate GDNF release.

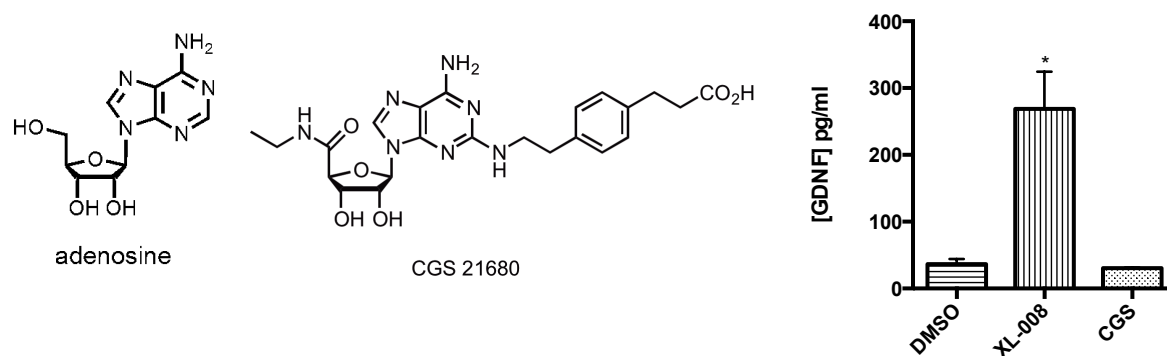


Figure 20. Structures of adenosine, the A_{2A} agonist CGS 21680, and the absence of GDNF release by CGS 21680 (10 μ M) from C6 cells (passage number 47). XL-008 (10 μ M) was used as a positive control. GDNF protein concentrations (pg/mL) in the conditioned medium were measured using ELISA after 48 hours. Data represent \pm SEM of biological replicates within one experiment, representative of 2 independent experiments. * $p < 0.05$ indicates statistical significance compared to the control as calculated by one-way ANOVA followed by Tukey's post-hoc test.

IV.3.4 Adrenergic Receptors

α_1 and β adrenergic receptors are both expressed in C6 cells, with β_1 and β_2 subtypes expressed in an approximately 7:3 ratio as determined by ligand binding experiments.⁸⁶ Interestingly, β receptor expression is down-regulated with an increasing passage number in C6 cells. As noted earlier, GDNF release also decreases with passage number. On the other hand, antidepressant treatment has also been reported to induce desensitization of β receptors in C6 cells.⁸⁷ Prazosin, an α_1 selective antagonist, was pre- and co-incubated with XL-026 and appears to induce a reproducible but variable increase in GDNF release induced by XL-026 (Figure 21). It would be worth determining the effect of agonism at this receptor on GDNF release.

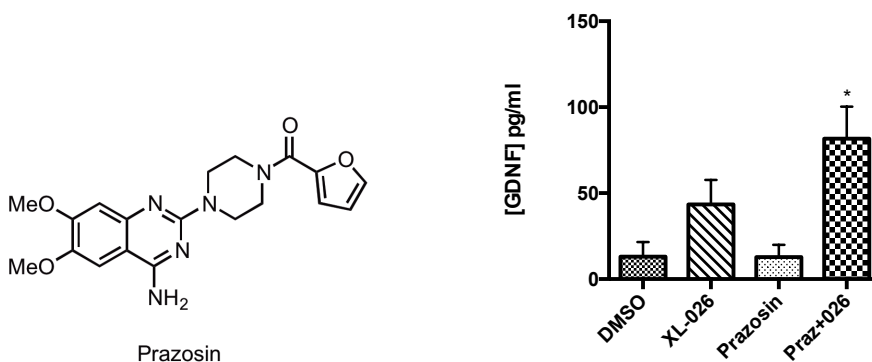


Figure 21. Structure of α_1 antagonist prazosin and potential cooperative increase in XL-026-induced GDNF release from C6 cells (passage number 41). GDNF protein concentrations (pg/mL) in the conditioned medium were measured using ELISA after 48 hours of XL-026 (10 μ M) treatment. Data represent \pm SEM of biological replicates within one experiment, representative of three independent experiments. * $p < 0.05$ indicates statistical significance compared to the control as calculated by one-way ANOVA followed by Tukey's post-hoc test.

Unexpectedly, isoproterenol (isoprenaline), a nonselective β receptor agonist, appears to reduce basal GDNF release (Figure 22). Meanwhile, pretreatment and co-incubation with the antagonist propranolol yielded conflicting results. The experiment was repeated four times; twice, the antagonist alone induced no release on its own but potentiated the release by XL-026, while twice, it induced an increase on its own as well (Figure 23). While this must be examined further before any conclusions may be drawn, the increase in XL-026-induced GDNF release in the presence of propranolol is reproducible. Since this antagonist was used at a high concentration (10 μ M), and it is known to bind to other receptors, this result should be interpreted with caution. With this caveat in mind, the results suggest that adrenergic receptors may be involved in modulating GDNF release and XL-026-induced GDNF release, either via constitutive receptor activity or via adrenergic receptor agonists secreted by C6 cells.

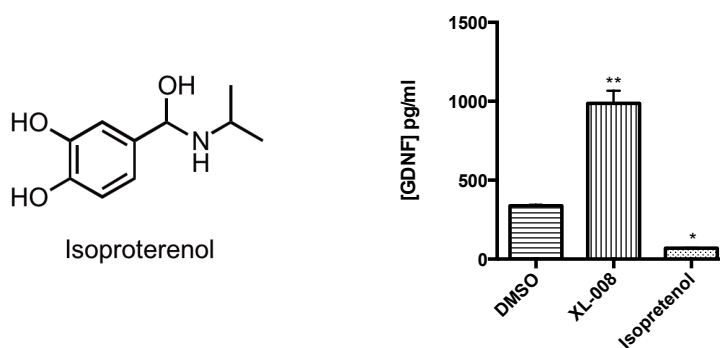


Figure 22. Structure of β -adrenoreceptor agonist isoproterenol and effect on GDNF release in C6 cells at 10 μ M (passage number 45) compared to positive control XL-008 (10 μ M). GDNF protein concentrations (pg/mL) in the conditioned medium were measured using ELISA after 48 hours. Data represent \pm SEM of biological replicates within one experiment, representative of three independent experiments. * $p < 0.05$, ** $p < 0.01$ indicates statistical significance compared to the control as calculated by one-way ANOVA followed by Tukey's post-hoc test.

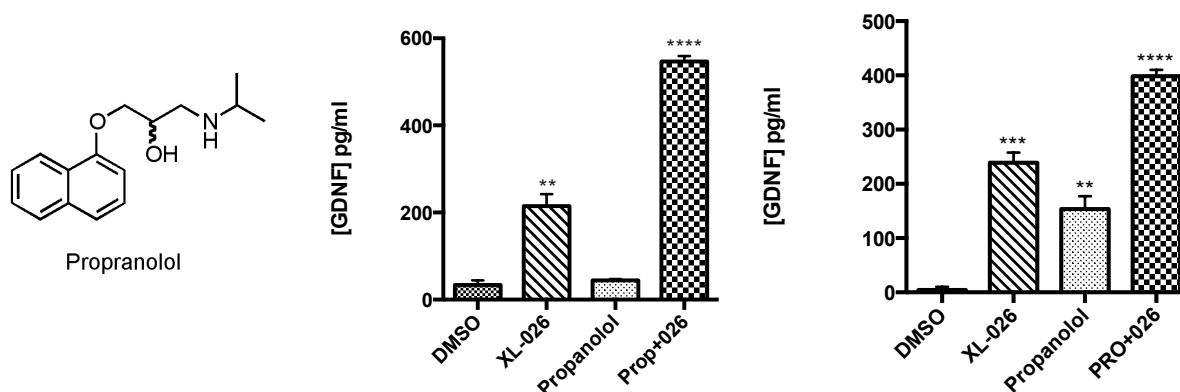


Figure 23. Structure of β -adrenoreceptor antagonist propranolol and its effect on XL-026-induced GDNF release from C6 cells in two separate experiments (passage number 42 in both experiments). GDNF protein concentrations (pg/mL) in the conditioned medium were measured using ELISA after 48 hours of treatment with XL-026 (10 μ M). Data represent \pm SEM of biological replicates within separate experiments, each representative of two independent experiments as described in the text. ** $p < 0.01$, *** $p < 0.001$, **** $p < 0.0001$ indicates statistical significance compared to the control as calculated by one-way ANOVA followed by Tukey's post-hoc test.

IV.3.5 Angiotensin Receptors

The angiotensin receptor AT₁ is a GPCR and its transcription was identified in C6 cells using RT-PCR.⁸⁸ The authors found that using losartan, an AT₁ blocker, dose-dependently

reduced implanted C6 tumor growth in rats. We chose to examine the potential role of AT₁ in the mechanism of our compounds due to its ability to induce transactivation of both EGFR and platelet-derived growth factor receptor (PDGFR) in rat astrocytes.⁸⁹ In the report, transactivation was found to occur via the canonical pathway involving reactive oxygen species (ROS), Src kinases, and Pyk2 activation, and phosphorylation of EGFR, PDGFR, and ERK1/2 was detected. As will be discussed later, the transactivation of multiple receptors is intriguing, as it is possible that multiple RTK receptors mediate GDNF release in our system. However, the use of the AT₁ antagonist losartan resulted in no significant modulation of XL-026-induced GDNF release, though there may be a slight reduction (Figure 24).

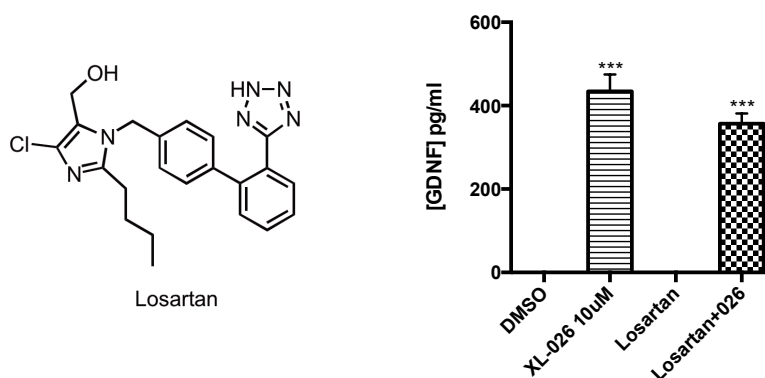


Figure 24. Structure of AT₁ antagonist losartan and its effect on XL-026-induced (10 μ M, 48 hours) GDNF release from C6 cells (passage number 41) at 10 μ M. GDNF protein concentrations (pg/mL) in the conditioned medium were measured using ELISA after 48 hours. Data represent \pm SEM of biological replicates within one experiment, representative of three independent experiments. *** $p < 0.001$ indicates statistical significance compared to the control as calculated by one-way ANOVA followed by Tukey's post-hoc test.

IV.3.6 Endothelin (ET_A & ET_B) Receptors

Endothelin-1 (ET-1) is a peptide that causes constriction of blood vessels and are strongly expressed in the heart, brain, and circulate in blood. It binds to C6 cells and stimulates inositol lipid turnover⁹⁰ and subsequently a rise in cytosolic Ca²⁺ via the GPCR ET_A and ET_B receptors

in this cell line.⁹¹ Of particular interest, ET-1 activated ERK in C6 cells via a PKC and PKA independent, but PLC, Ca^{2+} , and Src-family kinase-dependent pathway.⁹² Most importantly, ET-1 induces GDNF expression in cultured rat astrocytes.⁹³ We found, however, that ET-1 treatment (50 ng/mL) did not induce a statistically significant increase in GDNF release from C6 cells, though it did provoke a slight, reproducible increase (25.6 ± 8.8 pg/mL vs. 5.9 ± 3.1 pg/mL by the control in a representative experiment). If the receptors' cognate ligand does not elicit GDNF release, we conclude that ET_A or ET_B receptors are unlikely to be involved in isoquinuclidine-induced release.

IV.3.7 GABA_A Receptors

There is conflicting evidence in the literature for the expression of GABA_A receptors in C6 cells. One report claims that transcripts of GABA_A subunits were detected in C6 cells by RT-PCR, but functional GABA_A was not present in C6.⁹⁴ A conflicting report suggests that GABA and benzodiazepine receptors exist on C6 according to binding and functional studies on membrane preparations.⁹⁵ Despite the lack of consistent evidence for the presence of the receptor, we decided to use a pharmacological agonist and antagonist to rule out its involvement, as it can be modulated by $\sigma 1$ receptors⁹⁶ and can mediate neurogenesis in the hippocampus of adult mice.⁹⁷

Treatment with the agonist isoguvacine (10 μM) does not induce a change in basal GDNF release from C6 cells (12.6 ± 5.9 pg/mL vs. 12.4 ± 6.8 pg/mL from the control in a representative experiment). However, pretreatment and co-incubation with the antagonist bicuculline results in a small reproducible increase in release, which is statistically significant from XL-026 alone in one of the three experiments performed (Figure 25).

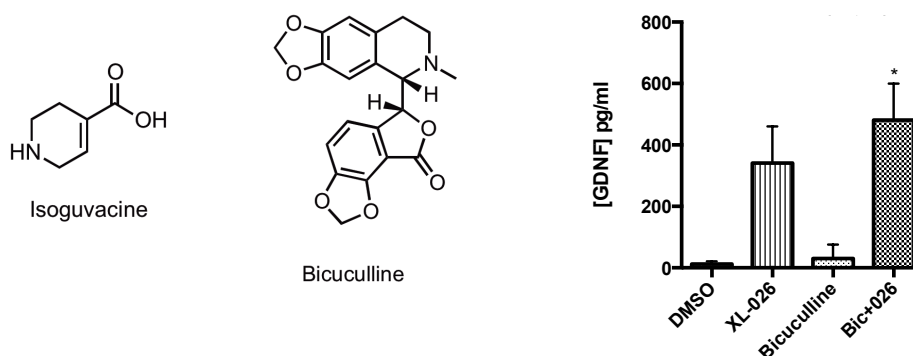


Figure 25. Structures of GABA_A agonist isoguvacine and antagonist bicuculline and the effect of the antagonist (10 μ M) on GDNF release by XL-026 (10 μ M, 48 hours) in C6 cells (passage number 41). GDNF protein concentrations (pg/mL) in the conditioned medium were measured using ELISA after 48 hours. Data represent \pm SEM of biological replicates within one experiment, representative of three independent experiments. * $p < 0.05$ indicates statistical significance compared to the control as calculated by one-way ANOVA followed by Tukey's post-hoc test.

IV.3.8 Histamine Receptors

C6 cells express H₁ histamine receptors that lead to intracellular Ca²⁺ release when activated.⁹⁸ We initially used histamine (10 μ M) to determine if H₁ receptors can induce GDNF release, and found it had no statistically significant effect compared to basal release (11.5 pg/mL vs. 2.3 pg/mL control in a representative experiment, Figure 26). In case histamine was too rapidly metabolized or carried into the cell via organic ion transporters, we also tried a pharmacological agonist, N-methylhistaprodifen (10 μ M). This H₁ agonist stimulated statistically significant GDNF release from C6 cells (Figure 26).

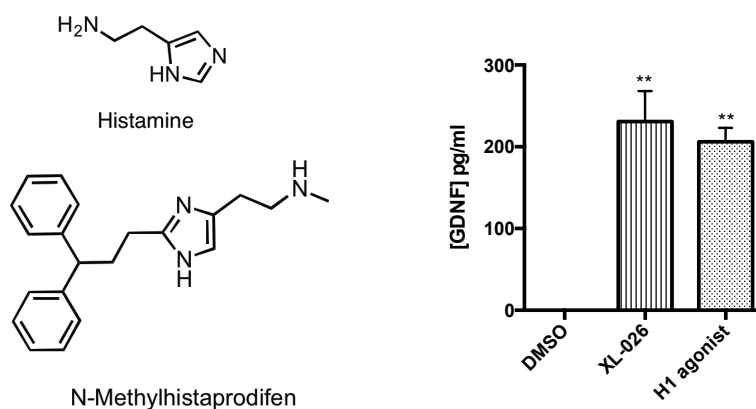


Figure 26. Chemical structures of histamine and the H₁ agonist *N*-methylhistaprodifen, and the H₁ agonist-induced (10 μM) GDNF release from C6 cells (passage number 41) showing XL-026 (10 μM, 48 hours) as a positive control. GDNF protein concentrations (pg/mL) in the conditioned medium were measured using ELISA after 48 hours. Data represent ± SEM of biological replicates within one experiment, representative of three independent experiments. ** $p < 0.01$, indicates statistical significance compared to the control as calculated by one-way ANOVA followed by Tukey's post-hoc test.

Pretreatment and co-incubation of XL-026 with the H₁ antagonist mepyramine (pyrilamine, 10 μM), which behaves as an inverse agonist, resulted in no significant difference in release (Figure 27).

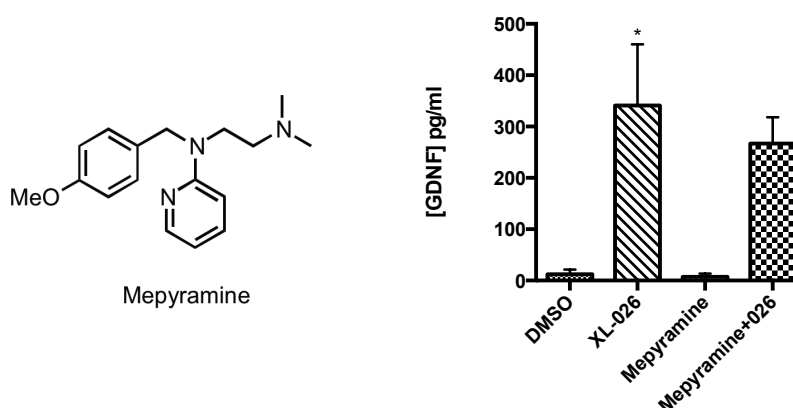


Figure 27. Chemical structure of H₁ receptor antagonist mepyramine, and its effect at 10 μM on GDNF release by XL-026 (10 μM) in C6 cells (passage number 41). GDNF protein concentrations (pg/mL) in the conditioned medium were measured using ELISA after 48 hours. Data represent ± SEM of biological replicates within one experiment, representative of three

independent experiments. * $p < 0.05$, indicates statistical significance compared to the control as calculated by one-way ANOVA followed by Tukey's post-hoc test.

IV.3.9 Glutamate Receptors

C6 cells express group I metabotropic glutamate receptors (mGluR1/5), and activation of mGluR5 leads to BDNF mRNA production.⁹⁹ Another report demonstrates expression of receptor proteins for group II mGluR2 and mGluR3, and group III mGluR4/6/7, while expressing mRNA for group II mGluR3 and group III mGluR4/6/7/8, and activation of glutamate receptors confers neuroprotection to C6 cells.¹⁰⁰ GDNF mRNA and protein is increased in response to a pharmacological mGlu2/3 agonist, LY379268, in mouse brain¹⁰¹ and GDNF as well as other neurotrophins are secreted from cultured rat Muller cells in response to glutamate treatment.¹⁰² We selected group II glutamate receptors to examine, using the agonist LY-354740 (eglumegad) and antagonist (*RS*)-APICA. LY-354740 (10 μ M) does not induce a significant increase in GDNF release from C6 cells (31.7 ± 13.5 pg/mL vs. 8.9 ± 6.3 pg/mL from the control in a representative experiment). Pre- and co-incubation with (*RS*)-APICA result in a reproducible decrease in XL-026-induced GDNF release; however, while in one experiment it completely abolished GDNF release down to basal levels, in a second experiment (Figure 28) it reduced release by approximately 50%. It is worth further examining this attenuation, possibly using mGluR2 and mGluR3 specific antagonists to determine which subtype is involved if the result with (*RS*)-APICA is indeed reproducible.

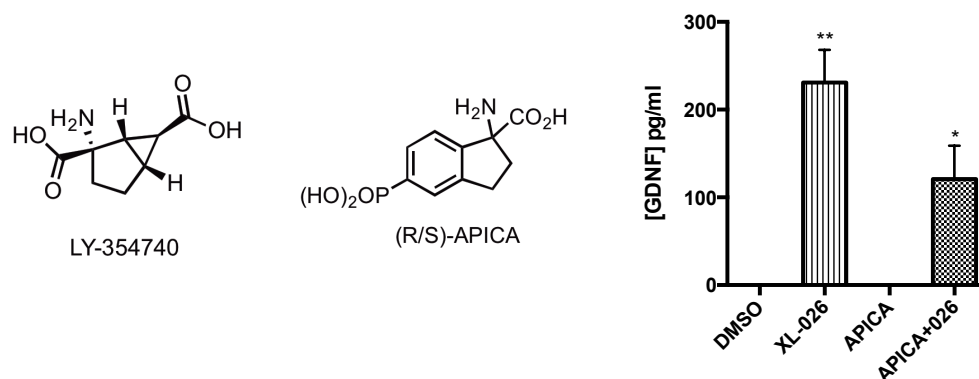


Figure 28. mGluR2/3 agonist LY-354740 and antagonist (R/S)-APICA. (R/S)-APICA (10 μ M) attenuates GDNF release by XL-026 (10 μ M, 48 hours) from C6 cells (passage number 41). GDNF protein concentrations (pg/mL) in the conditioned medium were measured using ELISA after 48 hours. Data represent \pm SEM of biological replicates within one experiment, representative of three independent experiments. * $p < 0.05$, ** $p < 0.01$, indicates statistical significance compared to the control as calculated by one-way ANOVA followed by Tukey's post-hoc test.

IV.3.10 Melatonin Receptors

MT₁ and MT₂ melatonin receptors are expressed in C6 cells, and treatment of the cells with melatonin induces GDNF mRNA expression¹⁰³ and protects them from glutamate excitotoxicity and oxidative stress.¹⁰⁴ Also, treatment of C6 cells with valproic acid, a mood stabilizer, causes an increase in MT₁ mRNA and protein expression as well as significant increases in GDNF and BDNF mRNAs,¹⁰⁵ and treatment of rat striatum with melatonin results in increased GDNF mRNA production.¹⁰⁶ This demonstrates the ability of a small molecule to induce protein expression of a receptor that also causes an increase in GDNF expression. We found that melatonin (10 μ M) does not induce GDNF release in C6 cells (2.0 ± 0.1 pg/mL vs. 2.3 ± 1.6 pg/mL from the control in a representative experiment), possibly due to rapid metabolism or transport into the cells. Further study using a pharmacological agonist and/or antagonist is necessary to draw definitive conclusions about the involvement of these receptors in XL-026-induced release.

IV.3.11 Muscarinic Receptors

M3 subtype muscarinic receptors have been detected in C6¹⁰⁷ and activation of M3 induces ERK1/2 activation in M3-transfected Chinese hamster ovary (CHO) cells^{108a} and SK-N-BE(2) human neuroblastoma cells,^{108b} which prompted us to consider their role in GDNF release from C6 cells. Carbachol (carbamylcholine), a muscarinic agonist, did not elicit a response in our assay at 10 μ M (7.7 ± 2.7 pg/mL vs. 2.4 ± 1.6 pg/mL from the control in a representative experiment). In the event that carbachol suffered the same potential fate as serotonin, which presumably is rapidly metabolized or otherwise processed by the cell, we also utilized the antagonist scopolamine (10 μ M) to probe potential M3 involvement in GDNF release. Two of three replicate experiments resulted in a slight, but non-significant increase of GDNF release by XL-026 in the presence of the antagonist; however, in the third experiment, scopolamine drastically potentiated the release by XL-026, so this experiment must be repeated at least once more to confirm the results (Figure 29).

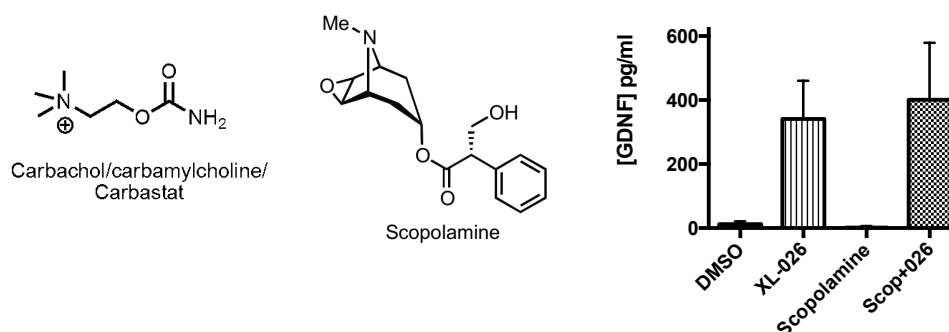


Figure 29. Structures of muscarinic receptor agonist carbachol, antagonist scopolamine, and antagonist (10 μ M) modulation of GDNF release by XL-026 (10 μ M, 48 hours) in C6 cells (passage number 41). GDNF protein concentrations (pg/mL) in the conditioned medium were measured using ELISA after 48 hours. Data represent \pm SEM of biological replicates within one experiment, representative of three independent experiments. No statistical significance compared to the control was calculated by one-way ANOVA followed by Tukey's post-hoc test in the specific experiment shown, but the other two experiments demonstrate statistically significant GDNF release induced by XL-026 and XL-026 plus scopolamine.

IV.3.12 Prostanoid Receptors

Prostaglandin E₂ (PGE₂) is a lipid hormone synthesized and released by C6 cells¹⁰⁹ in response to various stimuli, like angiotensin II,^{109a} and signal through the receptor EP₂, leading to PKA and PI3K activation.¹¹⁰ This eicosanoid molecule is interesting as it increases NGF mRNA in C6 cells,¹¹¹ though Verity found that treatment of C6 cells with PGE₂ (10 μ M) for 24 hours negatively modulated GDNF release.^{40a} Despite its negative modulation of GDNF release in the report, we chose to examine GDNF release after 48 hour treatment with PGE₂ in our assay since release after 24 hours does not necessarily reflect release after 48 hours. PGE₂ (10 μ M) did not have an effect on the basal GDNF release (2.1 ± 2.3 pg/mL vs. 0.6 ± 0.6 pg/mL from the control in a representative experiment), signifying that if PGE₂ was released in response to XL-026 (10 μ M) or if XL-026 interacted with the receptor, no signaling to activate GDNF synthesis and release occurs.

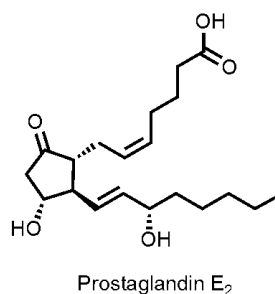


Figure 30. Structure of prostaglandin E₂ (PGE₂).

IV.3.13 Sphingosine-1-phosphate (S1P) Receptors

S1P is a bioactive phospholipid that is known to be produced in response to RTK activation and transactivate RTKs, in turn activating signal transduction.¹¹² C6 cells express S1P receptors on the cell surface and S1P activates ERK1/2¹¹³; also, TNF- α induces S1P release from C6 cells,¹¹⁴ which is intriguing, as we observe GDNF release in response to TNF- α in our assay (see Section IV.5.3). We postulated that perhaps RTK activation by XL-026 induces S1P release, which leads to further signaling to elicit GDNF synthesis and release. S1P (10 μ M), however, does not induce GDNF release on its own in C6 cells (6.3 ± 7.1 pg/mL vs. 4.1 ± 4.1 pg/mL from the control in a representative experiment).

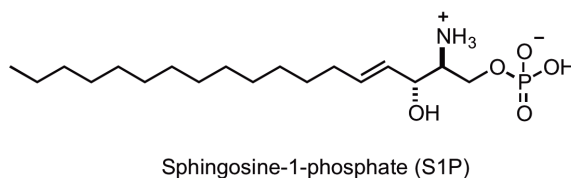


Figure 31. Structure of S1P.¹¹²

IV.3.14 PTX-sensitive receptors

Pertussis toxin (PTX), the exotoxin is produced by the bacterium *Bordetella pertussis*, is routinely used in research to sequester $G_{i/o}$ protein subunits, preventing their functional coupling to receptors. The result of this is inhibition of any GPCR that signals through $G_{i/o}$. PTX was used to show that κ OR agonist U69,593-induced ERK1/2 activation requires $G_{i/o}$ signaling, signifying that κ OR is coupled to $G_{i/o}$.^{80a} In our system, PTX (100 ng/mL) enhances GDNF release by XL-026 (10 μ M, Figure 32). Though the boost in release is reproducible between experiments, the degree of the increase varies. We may conclude that $G_{i/o}$ proteins are not coupled to the unknown target receptor of isoquinuclidines, but perhaps inactivating the proteins turns off an inhibitory pathway that dampens GDNF release under normal conditions by XL-026.

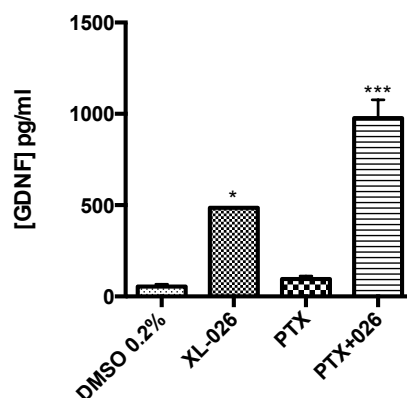


Figure 32. PTX-induced (100 ng/mL) augmentation of GDNF release by XL-026 (10 μ M) from C6 cells (passage number 44). GDNF protein concentrations (pg/mL) in the conditioned medium were measured using ELISA after 48 hours. Data represent \pm SEM of biological replicates within one experiment, representative of two independent experiments. * $p < 0.05$, *** $p < 0.001$, indicates statistical significance compared to the control as calculated by one-way ANOVA followed by Tukey's post-hoc test.

IV.3.15 Adenylate Cyclase Involvement

Another approach to probe GPCR involvement is to inhibit adenylate (adenylyl) cyclase, an enzyme responsible for converting adenosine triphosphate (ATP) to 3',5'-cyclic adenosine monophosphate (cAMP). GPCRs coupled to G_s stimulate the enzyme, leading to an increase in cAMP and subsequent PKA activation, while those coupled to G_i inhibit it. An inhibitor of adenylate cyclase, SQ 22,536, does not statistically significantly attenuate GDNF release by XL-026 (Figure 33), therefore G_s -coupled receptors and subsequent induction of cAMP are likely not involved in the mechanism of release.

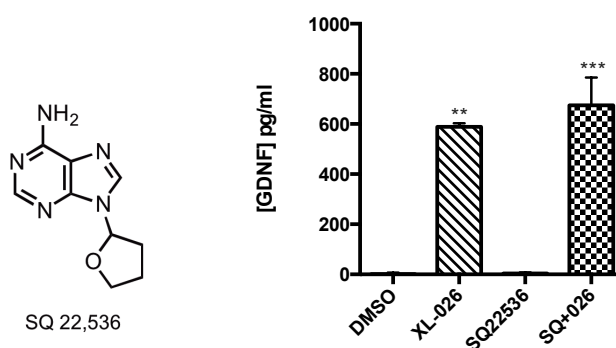


Figure 33. Structure of adenylate cyclase inhibitor SQ 22,536 and its lack of effect at 10 μ M on GDNF release by XL-026 (10 μ M) from C6 cells (passage number 42). GDNF protein concentrations (pg/mL) in the conditioned medium were measured using ELISA after 48 hours. Data represent \pm SEM of biological replicates within one experiment, representative of three independent experiments. ** $p < 0.01$, *** $p < 0.001$, indicates statistical significance compared to the control as calculated by one-way ANOVA followed by Tukey's post-hoc test.

IV.4 RTK and Other Growth Factor Receptor Involvement

While investigating Ret and/or TrkB as potential targets of isoquinuclines, we screened pharmacological inhibitors for other major RTKs expressed on C6 cells. It should be noted that true specificity of RTK inhibition is virtually impossible, as the kinase domain within RTK families is highly conserved, and commonly used inhibitors are often efficacious against more than one target since they all compete with ATP. Keeping this in mind, the implications of the

results will be discussed, and future work to narrow down the specific receptor(s) involved in GDNF release by isoquinuclidines will be discussed in Section IV.4 of this chapter.

Early on in our pharmacological inhibition studies we used the tyrosine kinase inhibitor genistein to determine if tyrosine kinases were involved in GDNF release, and not surprisingly, 50 μ M of genistein completely prevented GDNF release by XL-026 (Figure 34).

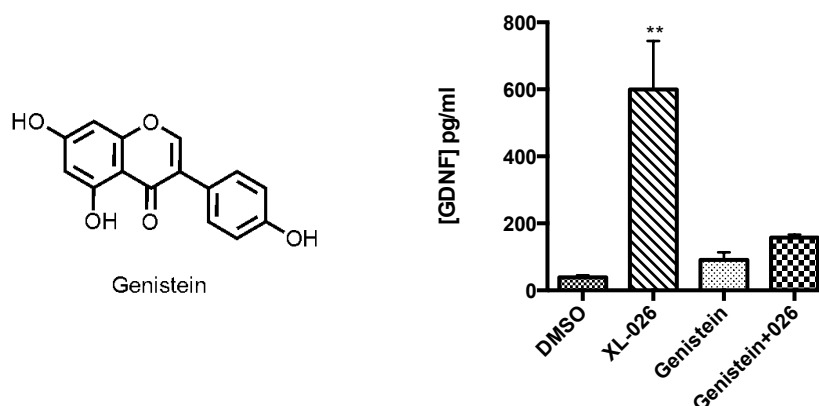


Figure 34. Structure of broad-spectrum tyrosine kinase inhibitor genistein and its reduction of GDNF release induced by XL-026 (10 μ M) at 50 μ M from C6 cells (passage number 41). GDNF protein concentrations (pg/mL) in the conditioned medium were measured using ELISA after 48 hours. Data represent \pm SEM of biological replicates within one experiment, representative of three independent experiments. ** $p < 0.01$ indicates statistical significance compared to the control as calculated by one-way ANOVA followed by Tukey's post-hoc test.

With this knowledge, we screened a small set of RTK inhibitors with various selectivities for receptors expressed in C6 cells. Also, several growth factor receptors were examined by the exogenous application of their cognate protein ligands. The most pertinent receptor targets are addressed first (see discussion above), followed by the other RTKs.

IV.4.1 Ret

Though Ret activation was not detected via western blot assays in SH-SY5Y (Section IV.1), we wanted to probe its regulation of GDNF production in the release assay in C6 cells to

rule out its potential involvement mechanism in C6 cells. Because the ELISA assay detects GDNF, we could not assess Ret/GFR α 1 involvement by treating with GDNF, so we needed other means to address this hypothesis. We considered that we might be able to take advantage of the cross-activation between GFLs and GFR α 1 co-receptors, and so tested the GFLs neurturin (NTN) and artemin (ART), with persephin (PSN) as a negative protein control, in the assay at 50 ng/mL. None of these treatments led to induction of GDNF release (Figure 35).

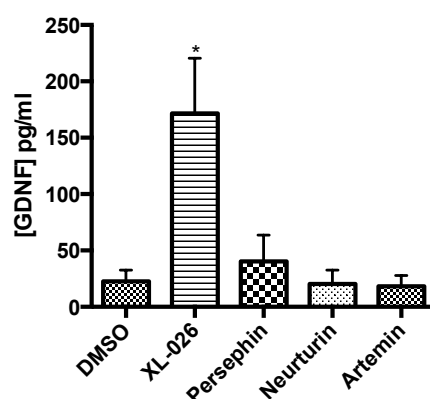


Figure 35. GDNF release from C6 cells after 48 hours (passage number 41) induced by persephin, neurturin, and artemin (all 50 ng/mL) with XL-026 (10 μ M) as a positive control. GDNF protein concentrations (pg/mL) in the conditioned medium were measured using ELISA. Data represent \pm SEM of biological replicates within one experiment, representative of three independent experiments. * $p < 0.05$ indicates statistical significance compared to the control as calculated by one-way ANOVA followed by Tukey's post-hoc test.

Unfortunately, no selective pharmacological Ret inhibitors exist, so we utilized two compounds that are known to inhibit Ret activity, SU5416 (Semaxinib)¹¹⁵ and RPI-1.¹¹⁶ SU5416 is primarily a VEGFR inhibitor,¹¹⁷ but has also been reported to be active against Ret (IC_{50} = 5 μ M),¹¹⁵ the HGF (hepatocyte growth factor) receptor c-Met (IC_{50} = 4 μ M against Met phosphorylation),¹¹⁸ Flt-3 and c-Kit receptors.¹¹⁷ We initially used the compound at 25 μ M based on literature precedent. Because it completely eliminated XL-026-dependent GDNF

release at 25 μM (Figure 36), we then performed dose-response experiments to determine potency in our assay. The experimental IC_{50} for GDNF release is approximately 63 – 116 nM (Figure 37). As it is quite potent in our system, yet not very potent against Ret and c-Met, we may tentatively conclude that we are not inhibiting Ret activity, which agrees with the lack of GDNF release by Ret ligands (Figure 35). Its activity against VEGFR and PDGFR will be discussed in Section IV.4.5.

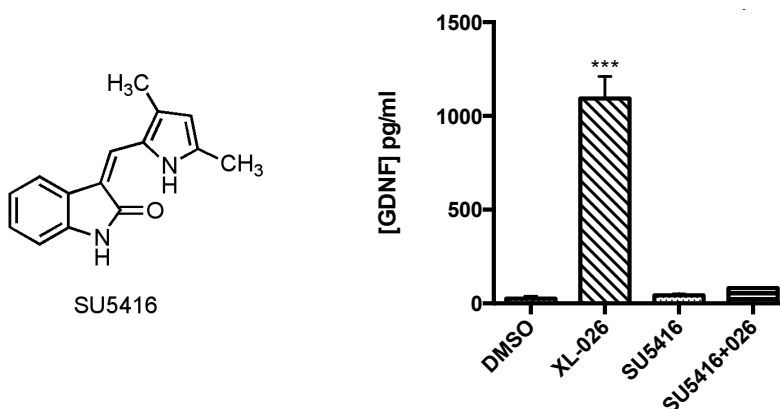


Figure 36. Structure of VEGFR/Ret inhibitor SU5416 and its prevention of GDNF release by XL-026 (10 μM) from C6 cells (passage number 41) at 25 μM . GDNF protein concentrations (pg/mL) in the conditioned medium were measured using ELISA after 48 hours. Data represent \pm SEM of biological replicates within one experiment, representative of five independent experiments. *** $p < 0.001$ indicates statistical significance compared to the control as calculated by one-way ANOVA followed by Tukey's post-hoc test.

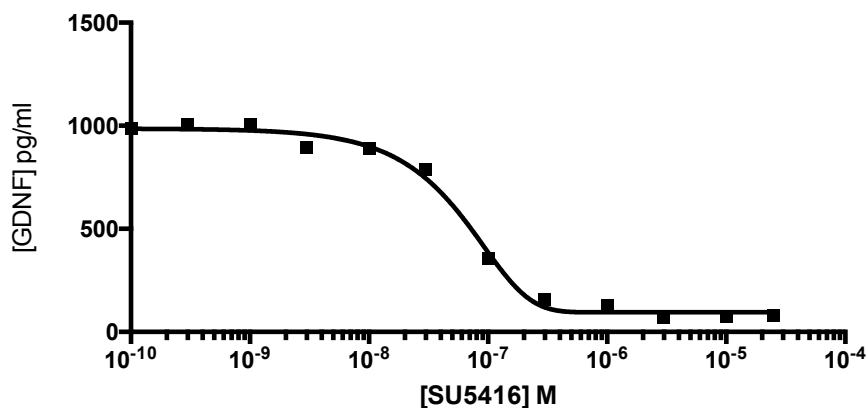


Figure 37. Representative dose-dependence of inhibition of GDNF release from C6 cells by XL-026 (10 μ M, 48 hours) (passage number 41) by SU5416 (0.1 nM – 25 μ M). GDNF protein concentrations (pg/mL) in the conditioned medium were measured using ELISA after 48 hours. Data represent \pm SEM of biological replicates within one experiment, representative of three independent experiments.

RPI-1 is structurally similar to SU5416, as both have the same indolinone core, and it inhibits purified Ret at a relatively high concentration ($IC_{50} = 104 \mu$ M) though it does inhibit phosphorylation of Ret in cells at 25 μ M in response to GDNF and inhibits growth of Ret-transfected NIH-3T3-transfected cells with $IC_{50} = 0.97 \mu$ M.¹¹⁹ 20 μ M was used in another report in cells to completely inhibit Ret phosphorylation.¹²⁰ It also inhibits c-Met phosphorylation ($IC_{50} \sim 7.5 \mu$ M).¹²¹ Further characterization of the compound's pharmacology has yet to be published, so we may not assume it is selective for Ret. We found that at 10 μ M, it inhibited GDNF release by XL-026 by $81 \pm 8\%$. The concentration-dependence of this inhibition has not been determined in our assay.

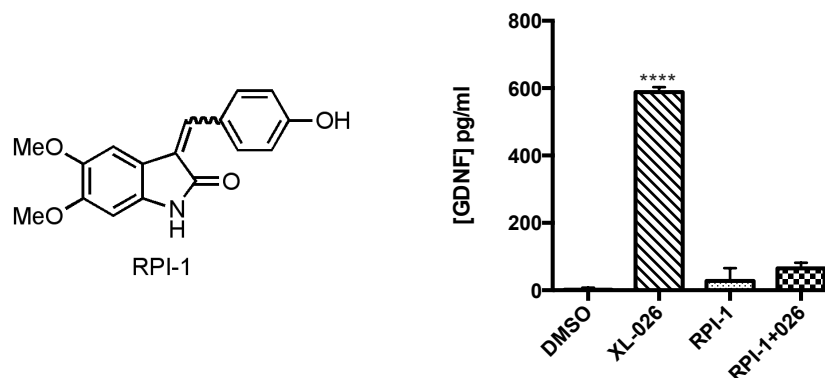


Figure 38. Structure of RTK inhibitor RPI-1 and its inhibition of XL-026 (10 μ M)-induced GDNF release in C6 cells (passage number 42) at 10 μ M. GDNF protein concentrations (pg/mL) in the conditioned medium were measured using ELISA after 48 hours. Data represent \pm SEM of biological replicates within one experiment, representative of two independent experiments. **** $p < 0.0001$ indicates statistical significance compared to the control as calculated by one-way ANOVA followed by Tukey's post-hoc test.

IV.4.2 FGFR

As mentioned previously, fibroblast growth factor receptors, specifically FGFR1 and FGFR2, are expressed in C6 cells and their activation leads to GDNF synthesis and release.^{44,40a} Riluzole, a small neuroprotective molecule used in the treatment of amyotrophic lateral sclerosis, was reported to induce GDNF mRNA synthesis and GDNF release^{122a} from C6 cells via FGFR at 25 μ M via activation of the MEK/ERK pathway and CREB.^{122b} Direct activation of the receptor by FGF- β (basic FGF, FGF-2) induces a dramatic, statistically significant increase in GDNF mRNA production¹²³ and protein release from C6 cells as well.^{40a} GDNF release from C6 cells by FGF- β was characterized, and is dependent on PI3K/Akt signaling;¹²⁴ *GDNF* gene expression is regulated not only by ERK1/2 activation, but ERK5 activation as well.^{124b} FGF receptors are important in the CNS, as they are dysregulated in major depression¹²⁵ and FGF- β has an antidepressant-like effect in rats.¹²⁶ Amitriptyline, a tricyclic antidepressant, was also reported to induce FGFR signaling in C6 cells.¹²⁷ Further, antidepressants induce an increase in FGF- β

immunoreactivity in neurons of the cerebral cortex and in astrocytes and neurons of the hippocampus,¹²⁸ making FGFRs important potential targets to consider.

To confirm the ability of FGF- β to induce GDNF release in C6 cells at 48 hours, as Verity reported release after 24 hours,^{40a} we used 50 ng/mL FGF- β and observed robust, statistically significant, reproducible GDNF release which is completely abolished by the use of the FGFR inhibitor PD173074.¹²⁹ PD173074 (Figure 39) is an ATP-competitive inhibitor of FGFR1 (IC_{50} = 25 nM in a kinase assay, and IC_{50} of FGFR1 phosphorylation in cells is 1-5 nM) and also inhibits PDGFR2 (IC_{50} = 18 μ M in a kinase assay, and IC_{50} of PDGFR2 phosphorylation in cells is 100 – 200 nM).¹³⁰ The initial concentration of PD173074 we chose to use (1 μ M) was based on literature precedent,^{44,122} and produced an approximately 50% average decrease in XL-026 and XL-008-induced GDNF release (Figure 39). We sought to establish exactly how potently it inhibited GDNF release by XL-026 by performing dose-response studies.

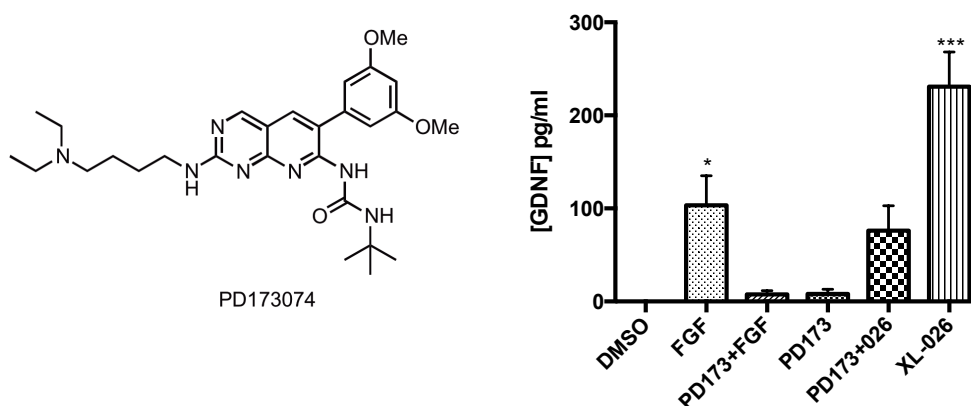


Figure 39. Structure of FGFR inhibitor PD173074 and its effect (1 μ M) on GDNF release by FGF- β (50 ng/mL, 48 hours) and XL-026 (10 μ M, 48 hours). GDNF protein concentrations (pg/mL) in the conditioned medium were measured using ELISA after 48 hours. Data represent \pm SEM of biological replicates within one experiment, representative of two independent experiments. * $p < 0.05$, *** $p < 0.001$ indicates statistical significance compared to the control as calculated by one-way ANOVA followed by Tukey's post-hoc test.

Though it was clear from inhibition of XL-026-induced GDNF release that the release was not completely dependent on FGFR action, we hoped that examining the dose-dependence of the inhibitor and comparing its IC_{50} (the concentration at which 50% inhibition of the biological response in question occurs in a specific assay) with known values from the literature would shed light on whether or not we are seeing FGFR-dependent attenuation of release or merely cross-reactivity at other RTKs. Unfortunately, due to the biological variability of GDNF release from C6 cells, we were unable to average GDNF release values across multiple repetitions of the experiment, but the IC_{50} values calculated were within the same order of magnitude across three distinct experiments. Though the IC_{50} was calculated to be approximately 100 nM, this value should be interpreted with caution since the inhibitor never completely abolishes GDNF release induced by XL-026; however, though PD173074 never inhibits release 100%, even at 10 μ M, it does achieve half-maximal inhibition at a concentration that corresponds to the published IC_{50} for PDGFR2 phosphorylation in a cell-based assay.¹³⁰ This is interesting, since functional cross talk between PDGF and FGF receptors is known.¹³¹ In one report, PDGF-BB induced the release of FGF- β and increased FGFR-1 phosphorylation in human smooth muscle cells and both these effects were found to be mediated by PDGFR, PI3K, and PKC, but not MEK or protein transcription.¹³² Interpretation of RTK inhibition studies, therefore, is made more complex as it is difficult to differentiate cross-reactivity of an inhibitor from an intrinsic interaction between receptors in a given system.

The potential involvement of FGF receptors, even if partially, raises the question of whether the receptor is directly activated by isoquinuclidines, transactivated by another receptor, or activated by induced release of FGF from C6 cells. It has been reported that C6 cells do not

release detectable FGF- β , and the authors speculate that it is possible that FGF- β does not have to be secreted in order to serve as a mitogenic factor, though they found that exogenous application of FGF- β (1 – 50 ng/mL) does not induce proliferation of C6 cells.¹³³ However, we believe that the lack of detectable FGF- β immunoreactivity in conditioned C6 cell medium may be a consequence of its sequestration by FGF-binding protein (FBP), as binding to the protein may prevent its detection by antibodies. FBP is a secreted protein that serves as a chaperone for FGF- β , reducing its affinity for heparin, thus releasing active FGF- β from extracellular matrix heparin sulfate proteoglycans and facilitating FGFR-dependent proliferation and ERK2 activation.¹³⁴ Antidepressants also increased the expression of FGF binding protein (FBP, also Hpp17).¹²⁸

IV.4.3 Trk Receptors

C6 cells transcribe TrkA, TrkB, and p75NTR mRNA,¹³⁵ and the TrkA/p75NTR system appears functional in mediating growth.¹³⁶ Though C6 cells do not express high levels of Trk receptors, we wanted to rule out their involvement due to their known interaction with Ret receptors³⁰ through utilizing putative pharmacological agonists⁴⁶ (the inefficacy of which were discussed extensively in Chapter 2 of this work), endogenous ligands, and the use of the Trk inhibitor K252a.

In our assay, BDNF, NGF, NT-3, and NT-4 were used at 50 ng/mL and none of the treatments resulted in changes of basal GDNF release (Figure 40). NT-3 was included despite the lack of evidence for TrkC receptors in the event that TrkA or TrkB ligands led to GDNF release so that it could function as a negative protein control. Our results are consistent with Verity's results for BDNF (0.76 ± 0.48 fold/control) and NGF (1.24 ± 0.37 fold/control), though

only 24-hour incubation was attempted.^{40a} Treatment with putative TrkB agonists 7,8-dihydroxyflavone (7,8-DHF),^{46b} N-acetylserotonin (NAS),^{46c} and LM224-A (triamide)^{46c} at 10 μ M result in no effect on GDNF release in our assay, in agreement with the results from the protein ligands of Trk receptors.

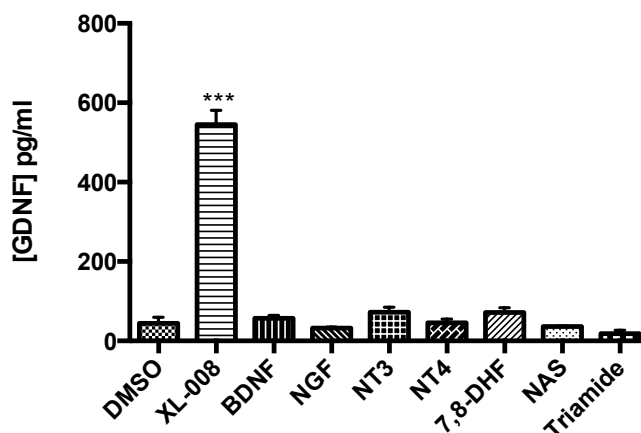


Figure 40. Effect of BDNF, NGF, NT-3, and NT-4 (all 50 ng/mL) and TrkB agonists 7,8-DHF, NAS, and LM22A-4 (triamide; all 10 μ M) on GDNF release from C6 cells (passage number 46), showing XL-008 (10 μ M) as a positive control. GDNF protein concentrations (pg/mL) in the conditioned medium were measured using ELISA after 48 hours. Data represent \pm SEM of biological replicates within one experiment, representative of three independent experiments. *** $p < 0.001$ indicates statistical significance compared to the control as calculated by one-way ANOVA followed by Tukey's post-hoc test.

IV.4.4 PDGFR

Platelet-derived growth factor (PDGF) is a monomeric secreted protein ligand for the RTK PDGFR, and functional PDGF is dimerized either in homodimers of a specific chain, like PDGF-BB, or heterodimers, like PDGF-AB. A low level of PDGFR β (PDGFR1) was detected in C6 cells by western blot, PDGF induces an autocrine loop in the cell line,¹³⁷ and a high level of autophosphorylation of PDGFR β has also been observed.¹³⁸ At least one RT-PCR study found PDGFR α (PDGFR2, but not PDGFR β) in C6 cells as well as PDGF-A but not PDGF-B

transcripts.^{135b} Thus it appears that PDGFR receptors are expressed in C6 cells, and PDGFR, as an RTK, activates ERK.¹³⁸ Autocrine signaling leading to GDNF synthesis and release could explain the amplification of GDNF release between 24- and 48-hour treatments.

PDGFR is an RTK that is commonly transactivated by GPCR receptors. For example, angiotensin II stimulates rat astrocyte mitogen-activated protein kinase activity and growth through EGF and PDGF receptor transactivation, which is interesting as more than one receptor is simultaneously transactivated.⁸⁹ Not only may transactivation occur through the canonical GPCR-RTK pathway, but also it has been shown that growth factors other than PDGF, including FGF, produce ROS that can transactivate PDGFR α .¹³⁹ On the other hand, cross-talk between PDGF and FGF receptors is known,¹³¹ and PDGF can induce FGF- β release and subsequent activation of FGFR, which is PI3K and PKC but not MEK/ERK-dependent, as demonstrated in muscle cells.¹³²

To examine the potential role of PDGFR in isoquinuclidine-mediated GDNF release, we tested PDGF-AB and PDGF-BB to determine their ability to induce release, and utilized the inhibitor AG1296. PDGF-AB and PDGF-BB (50 ng/mL) both induce a statistically significant increase in GDNF release the majority of the time either is used (Figure 41).

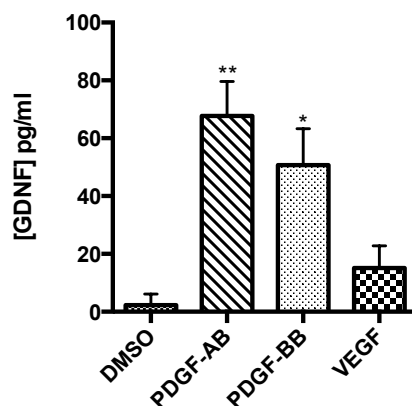


Figure 41. PDGF-AB, PDGF-BB, and VEGF-induced GDNF release from C6 cells (passage number 42) at 50 ng/mL. GDNF protein concentrations (pg/mL) in the conditioned medium were measured using ELISA after 48 hours. Data represent \pm SEM of biological replicates within one experiment, representative of at least four independent experiments. * $p < 0.05$, ** $p < 0.01$ indicates statistical significance compared to the control as calculated by one-way ANOVA followed by Tukey's post-hoc test.

AG1296 is relatively selective for PDGFR. It inhibits PDGFR phosphorylation in cells ($IC_{50} = 300 - 500$ nM), and is not active at EGFR or VEGFR ($IC_{50} > 10$ μ M).¹⁴⁰ It is also active against Flt-3 and c-Kit at concentrations similar to those active against PDGFR, yet it is not effective against Src, PKB/Akt, or IGF-IR, and the lack of activity against EGFR and VEGFR was independently confirmed.¹⁴¹ We performed dose-response studies to understand its potency and determine the lowest effective concentration to connect an experimental IC_{50} of GDNF release with IC_{50} values in the literature for the compound in functional assays as we did with SU5416 (Section IV.4.1). Using concentrations from 0.1 nM to 25 μ M, the IC_{50} for inhibition of GDNF release is calculated to be ~ 100 nM (Figure 43). This is consistent with the known potency of the compound against PDGFR.

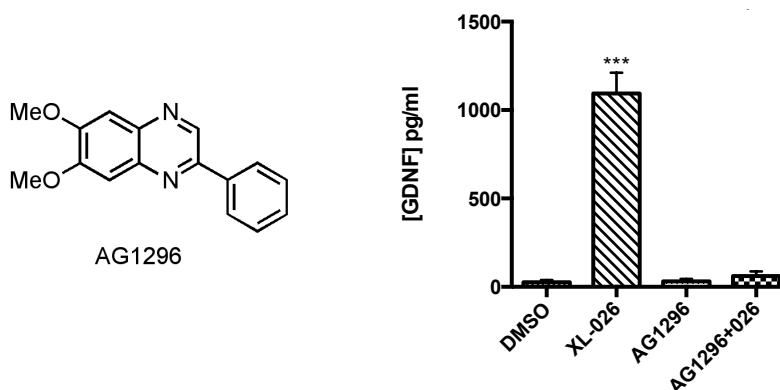


Figure 42. Structure of AG1296 and inhibition of GDNF release by XL-026 (10 μ M) by AG1296 (25 μ M) in C6 cells (passage number 41). GDNF protein concentrations (pg/mL) in the conditioned medium were measured using ELISA after 48 hours. Data represent \pm SEM of biological replicates within one experiment, representative of five independent experiments. *** $p < 0.001$ indicates statistical significance compared to the control as calculated by one-way ANOVA followed by Tukey's post-hoc test.

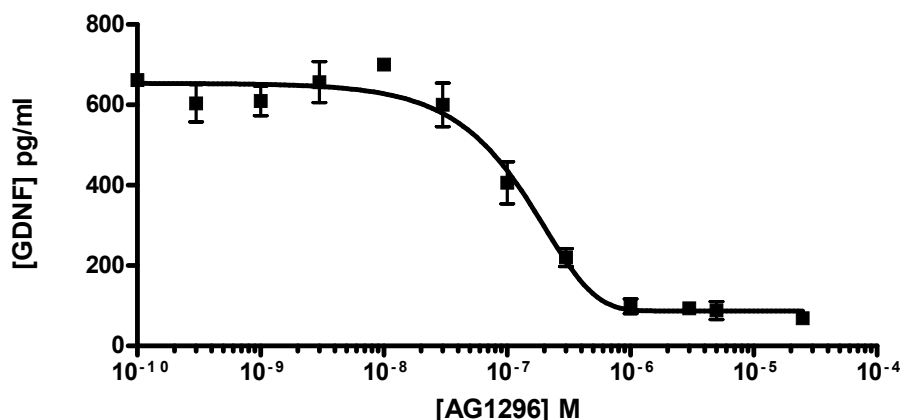


Figure 43. Dose-dependent inhibition of GDNF release induced by XL-026 (10 μ M, 48 hours) by AG1296 (0.1 nM - 25 μ M) in C6 cells (passage number 41). GDNF protein concentrations (pg/mL) in the conditioned medium were measured using ELISA after 48 hours. Data represent \pm SEM of biological replicates within one experiment, representative of three independent experiments.

As we did not know if the compound non-selectively inhibits FGFR, we sought to determine if the inhibition of isoquinuclidine-induced GDNF by AG1296 was due to off-target effects by attempting to inhibit FGF- β -induced GDNF release with the compound. The

inhibitor appears to attenuate FGF- β only slightly between experiments, whereas it inhibits PDGF-AB-induced release completely. In light of the discussion earlier in this section, it is known that FGF can activate PDGFR,¹³⁹ and PDGFR activation can lead to FGF release,^{131,132} so using a PDGFR inhibitor may reasonably affect FGF-induced release because part of the FGF-induced release could actually be due to PDGFR cross-talk with FGFR, and not because the inhibitor is non-specific.

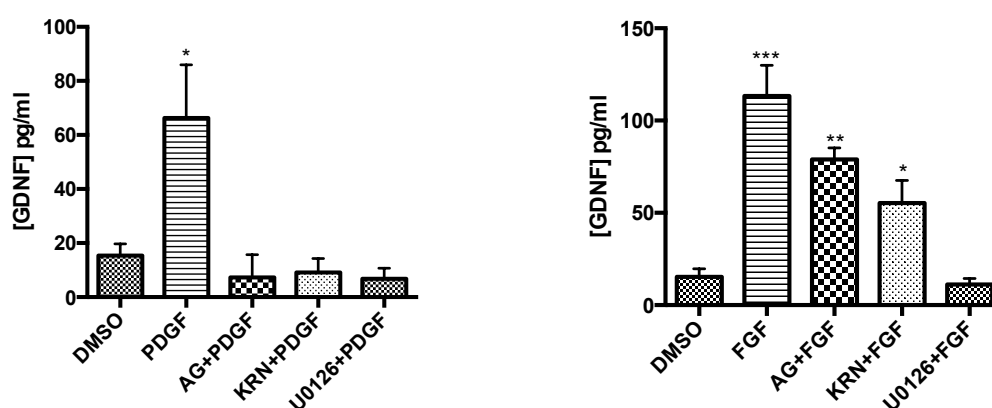


Figure 44. (Left) Inhibition of PDGF-AB (100 ng/mL)-induced GDNF release from C6 cells (passage number 42) by AG1296 (AG, 1 μ M), KRN633 (KRN, 1 μ M), and MEK inhibitor U0126 (10 μ M) and (right) inhibition of FGF- β induced GDNF release by the same treatments. GDNF protein concentrations (pg/mL) in the conditioned medium were measured using ELISA after 48 hours. Data represent \pm SEM of biological replicates within one experiment, representative of three independent experiments. * $p < 0.05$, ** $p < 0.01$, and *** $p < 0.001$ indicates statistical significance compared to the control as calculated by one-way ANOVA followed by Tukey's post-hoc test.

Overall, the results from the use of this inhibitor are very promising, as they strongly implicate PDGFR in the mechanism of GDNF release by isoquinuclidines. The only caveat is that the release by PDGF-AB and PDGF-BB on their own is relatively low compared to the release by isoquinuclidines in any given experiment, but PDGF-induced FGF- β release could explain the difference in magnitude of release.

IV.4.5 VEGFR

Vascular endothelial growth factor (VEGF) is a secreted, 46 kDa dimeric protein that acts as an angiogenic growth factor and mitogen for epithelial cells, and VEGFR2 is expressed by C6 cells.¹⁴² The receptor is relevant to our hypothesis that stress caused by our compounds may induce EOR or be involved in *Pgrmc1* signaling, since progesterone induces VEGF synthesis via *Pgrmc1*⁶⁵ and ER stress leads to upregulation of the *VEGF* gene.^{69,70} Treatment of C6 cells with VEGF (50 ng/mL) does not induce release (Figure 41). However, the inhibitor KRN633,¹⁴³ which is marketed as a selective VEGFR inhibitor, potently abolishes GDNF release by XL-026 at 1 μ M (Figure 45). To determine if this is due to non-selective inhibition of another RTK, we performed dose-response studies for this inhibitor as well (Figure 46).

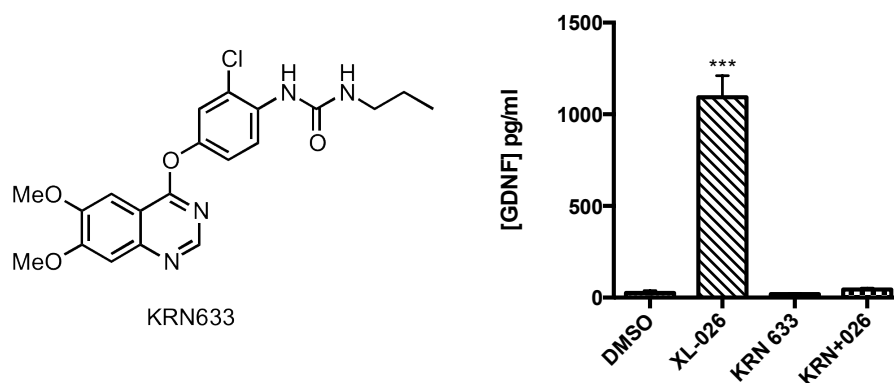


Figure 45. Structure of VEGFR inhibitor KRN633 and its complete inhibition at 1 μ M of XL-026 (10 μ M)-induced GDNF release from C6 cells (passage number 41). GDNF protein concentrations (pg/mL) in the conditioned medium were measured using ELISA after 48 hours. Data represent \pm SEM of biological replicates within one experiment, representative of at least five independent experiments. *** $p < 0.001$ indicates statistical significance compared to the control as calculated by one-way ANOVA followed by Tukey's post-hoc test.

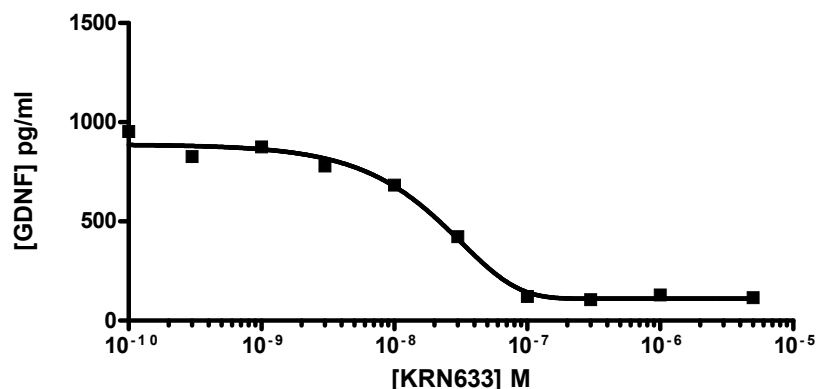


Figure 46. Dose-dependent inhibition of GDNF release by VEGFR inhibitor KRN633 (0.1 nM - 5 μ M). GDNF protein concentrations (pg/mL) in the conditioned medium were measured using ELISA after 48 hours. Data represent \pm SEM of biological replicates within one experiment, representative of three independent experiments.

IC₅₀ values for inhibition of XL-026-induced GDNF release by KRN633 were calculated to be roughly between 1 and 42 nM, demonstrating a high level of potency by this compound. It was reported to inhibit phosphorylation in cells of the following receptors: VEGFR2 (IC₅₀ = 1.16 nM), VEGFR1 (11.7 nM), c-Kit (8.01 nM), and PDGFR-1 (130 nM), while IC₅₀ values were greater than 10 μ M for FGFR-1, EGFR, and c-Met.¹⁴³ According to a kinase assay in the same report, PDGFR-2 has IC₅₀ = 965 nM, and IGFR-1, Abl, erbB4, Flt-3, INSR, Janus kinase 2, focal adhesion kinase, Wee1, and Src all were not inhibited below 10 μ M. Thus, the potency of the compound falls within the range of VEGFR, c-Kit, and PDGFR-1 activity. Since AG1296 is not active toward VEGFR, that means that both AG1296 and KRN633 are indicating potential activity against c-Kit and PDGFR and a lack of activity against INS-R1 and EGFR.

Another inhibitor we examined with activity toward PDGFR is SU5416, reported to be a VEGFR (Flk-1, VEGFR2 subtype, the most common subtype in C6 cells) inhibitor with IC₅₀ ~ 250 – 1000 nM, though it is active against other RTKs as well (Section IV.4.1). Due to the lack of specificity of the compound, we can only use these results to rule out receptors that it is

definitely not active against, mainly FGFR, EGFR, and INS-1R,¹¹⁷ or at the very least, speculate that it mediates GDNF release via a receptor target that is not one of those RTKs. As mentioned previously, it is likely not active against Ret or c-Met at the low concentrations at which we see inhibition of GDNF release.

IV.4.6 EGFR

C6 cells do not contain a functional EGFR system, as EGFR is not phosphorylated in response to 100 ng/mL EGF,⁹² but they do express the receptor.^{92,135} Treatment of C6 cells with 50 ng/mL EGF in the GDNF release assay results in no induction of GDNF (53.5 ± 3.9 pg/mL vs. 65.5 ± 16.5 pg/mL of the control in a representative experiment), which is consistent with Verity's 24-hour data (1.1 ± 0.85 fold/control).^{40a} We used AG1478 to rule out its involvement in our mechanism in the event it is transactivated via an intracellular mechanism. AG1478 has $K_i = 16$ nM¹⁴⁴ and $IC_{50} = 3$ nM, with IC_{50} values for HER2-Neu and PDGFR > 100 μ M.¹⁴⁵ Use of 10 μ M AG1478 resulted in virtually complete prevention of GDNF release by XL-026 (Figure 47). The inhibitor dose-dependently inhibits release, but is not very potent (IC_{50} values ~ between 600 and 3500 nM, not shown). The lack of potency in the low nanomolar concentrations indicates that we are likely observing off-target effects.

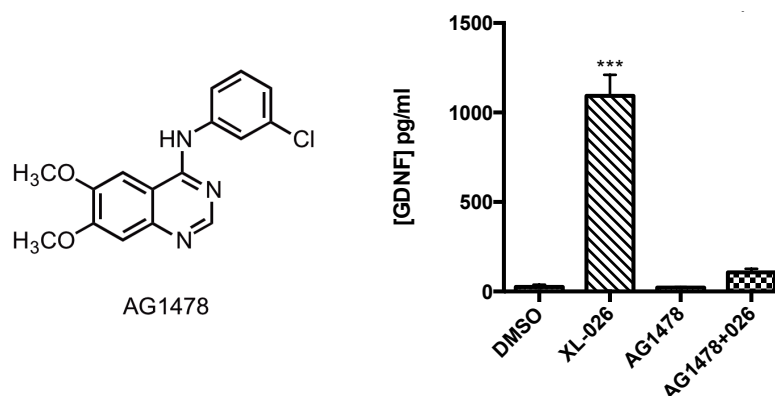


Figure 47. Structure of EGFR inhibitor AG1478 and its almost complete inhibition at 10 μ M of XL-026 (10 μ M)-induced GDNF release from C6 cells (passage number 41). GDNF protein concentrations (pg/mL) in the conditioned medium were measured using ELISA after 48 hours. Data represent \pm SEM of biological replicates within one experiment, representative of three independent experiments. *** $p < 0.001$ indicates statistical significance compared to the control as calculated by one-way ANOVA followed by Tukey's post-hoc test.

IV.4.7 TGF β -R

Transforming growth factor beta (TGF- β) is a growth factor with roles in development, differentiation, and maintenance of the immune system, and its receptor is a single-pass serine/threonine kinase.¹⁴⁶ In C6 cells, the presence of the TGF- β receptor mRNA, but not TGF- β , was detected.^{135b} This growth factor system is interesting because TGF- β is known to induce VEGF and PDGF expression¹⁴⁷ and even more so because GDNF responsiveness in neurons is increased in response to TGF- β via recruitment of GFR α 1 to the plasma membrane.¹⁴⁸ In the latter study, the authors found that pre-treatment, with TGF- β was required for GDNF-induced survival of primary chick neurons, and when incubated together, they dramatically potentiated the survival independently of Ret and GFR α 1 expression. TGF- β , however, only produced slight GDNF releases in our assay at 50 ng/mL in each of five experiments, all of which demonstrated a trend in GDNF increase by the protein but not all of which were statistically significant (Figure 48).

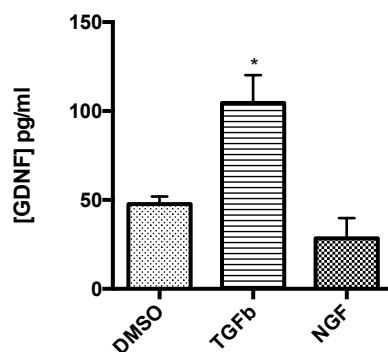


Figure 48. Increase in GDNF release by TGF- β (50 ng/mL, 48 hours) showing NGF as a negative control (50 ng/mL). GDNF protein concentrations (pg/mL) in the conditioned medium were measured using ELISA after 48 hours. Data represent \pm SEM of biological replicates within one experiment, representative of at least independent experiments. * $p < 0.05$ indicates statistical significance compared to the control as calculated by one-way ANOVA followed by Tukey's post-hoc test.

Pharmacological inhibition was performed to address the receptors' involvement in GDNF release by isoquinuclidines using the TGF- β receptor kinase inhibitor SD-208.¹⁴⁹ This compound is relatively selective for TGF- β RI, 50 times more selective over TGF- β RII in a kinase assay. At 5 μ M, it also inhibits EGFR by 68%, MEK2 by 87%, and PKD by 70%, with marginal to no effects on p38 MAPK, c-JNK, ERK2, PKA and PKC in a kinase assay.¹⁴⁹ Though the published MEK inhibition is disturbing, we observed no significant effect on GDNF release upon treatment with 10 μ M of SD-208 (Figure 49).

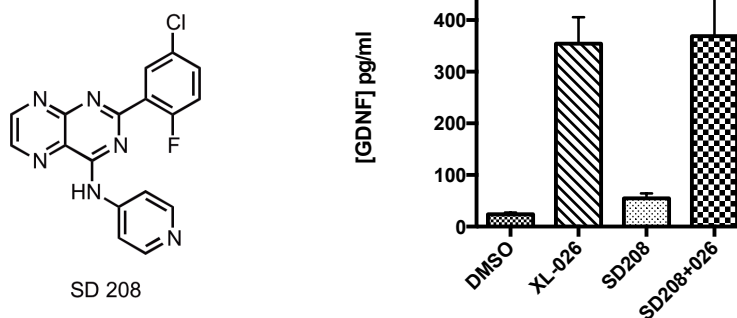


Figure 49. TGFβ-RI inhibitor SD-208 and its lack of effect at 10 μM on GDNF release by XL-026 (10 μM, 48 hours) in C6 (passage number 42). GDNF protein concentrations (pg/mL) in the conditioned medium were measured using ELISA after 48 hours. Data represent ± SEM of biological replicates within one experiment, representative of three independent experiments. ** $p < 0.01$ indicates statistical significance compared to the control as calculated by one-way ANOVA followed by Tukey's post-hoc test. XL-026 was not statistically significant in the specific experiment shown, likely a consequence of the large SEM bars shown.

Also of note is the fact that FGF-β induces TGF-β release in glioma cells.¹⁵⁰ Since it is well established that FGF-β induces GDNF release in gliomas, we thought it might be possible that FGF-β could lead to TGF-β release, which perhaps would be an intermediary on the way to GDNF synthesis and release; however, since exogenous TGF-β did not induce strong release, and no significant increases in TGF-β were detected by ELISA (not shown), we may conclude that TGF-β receptors are not a likely direct or indirect target of XL-026.

IV.4.8 Other Growth Factor and Cytokine Receptors

To rule out other growth factor receptors, and investigate various other cytokines and signaling proteins that activate ERK1/2, we assembled a panel of growth factors and cytokines based on their receptor expression in C6 cells. The proteins included ciliary neurotrophic factor (CNTF),^{139b} hepatocyte growth factor (HGF, the ligand for c-Met),^{139b} heregulin (also neuregulin-1, Her, related to EGF and a ligand for the erbB family of RTKs), insulin-like growth

factors –I and –II (IGF-I, IGF-2), and stem cell factor (SCF, ligand for the RTK c-Kit).^{139b} The GPCR agonist neuromedin B,¹⁵¹ which is a ligand for bombesin-like receptors, and the cytokines IL-6 and leukemia inhibitory factor (LIF) were also included (Figure 50). The results showed slight, irreproducible increases in some cases, but overall no treatment conditions induced robust GDNF release.

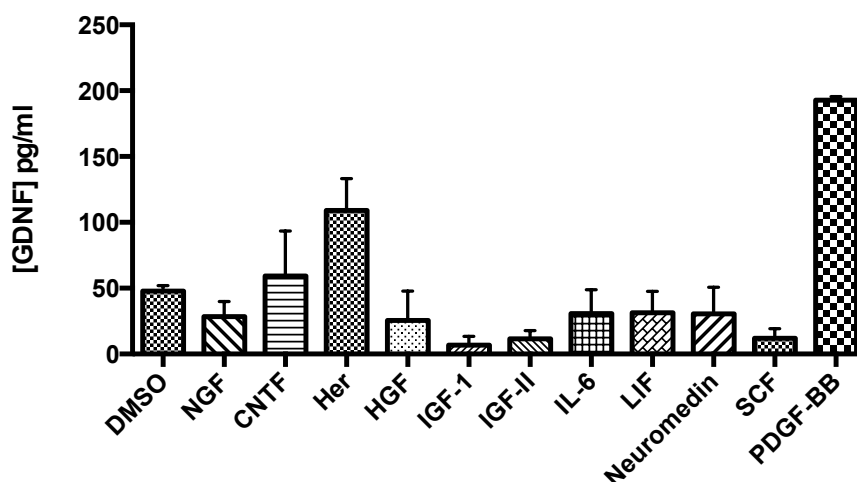


Figure 50. Ligand screen (all at 50 ng/mL) with NGF (50 ng/mL) as a negative control and PDGF-BB (50 ng/mL) as a positive control. GDNF protein concentrations (pg/mL) in the conditioned medium were measured using ELISA after 48 hours. Data represent \pm SEM of biological replicates within one experiment, representative of three independent experiments. Only PDGF-BB induced statistically significant release in this experiment. [NGF = nerve growth factor; CNTF = ciliary neurotrophic factor; Her = heregulin; HGF = hepatocyte growth factor; IGF = insulin-like growth factor; IL-6 = interleukin 6; LIF = leukemia inhibitory factor; SCF = stem cell factor; PDGF-BB = platelet-derived growth factor BB.]

IV.5 Nuclear and Cytokine Receptor Involvement

IV.5.1 Glucocorticoid (GR) Receptors

C6 cells express type I (mineralocorticoid, high affinity glucocorticoid) and type II (classical glucocorticoid) corticosteroid receptors, which are nuclear receptors.¹⁵² Mifepristone (RU486) is a glucocorticoid¹⁵³ and progesterone receptor antagonist, and its pre- and co-

incubation with XL-026 (10 μ M) results in reproducible, statistically significant potentiation of GDNF release by the isoquinuclidine (Figure 51). This is extremely intriguing considering that this compound also acts as an antagonist at the progesterone receptor. This could be a consequence of σ 1R activity, since progesterone and other neuroactive steroids bind to σ 1R.^{56,96} It should be noted that these results are preliminary, as 10 μ M is a high concentration relative to the affinity of the antagonist for the receptors (K_i = 1 nM at progesterone and glucocorticoid receptors¹⁵⁴), so it could be an off-target effect.

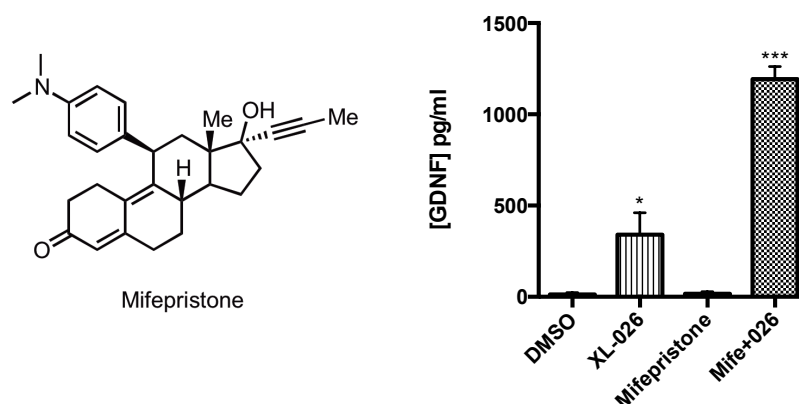


Figure 51. Structure of glucocorticoid and progesterone receptor antagonist mifepristone (RU486) and its potentiation of XL-026 (10 μ M)-induced GDNF release at 10 μ M in C6 cells (passage number 41). GDNF protein concentrations (pg/mL) in the conditioned medium were measured using ELISA after 48 hours. Data represent \pm SEM of biological replicates within one experiment, representative of three independent experiments. * $p < 0.05$ and *** $p < 0.001$ indicate statistical significance compared to the control as calculated by one-way ANOVA followed by Tukey's post-hoc test.

IV.5.2 Estrogen Receptors

Estrogen receptors are also nuclear receptors and act as transcription factors upon activation and translocation to the nucleus. We utilized the agonist β -estradiol and antagonist fulvestrant to determine if antagonism of the receptor affects GDNF release in our assay. β -

Estradiol (10 μ M) induced no significant GDNF release (3.0 ± 1.2 pg/mL vs. 1.6 ± 1.6 pg/mL from the control in a representative experiment), whereas the antagonist elicited a strong, reproducible and statistically significant increase in GDNF release in the presence of XL-026 (Figure 52). Like with mifepristone, it is possible that this potentiation is occurring through σ 1 or σ 2R receptors, but that makes it all the more interesting because on their own, the antagonists do not lead to GDNF release.

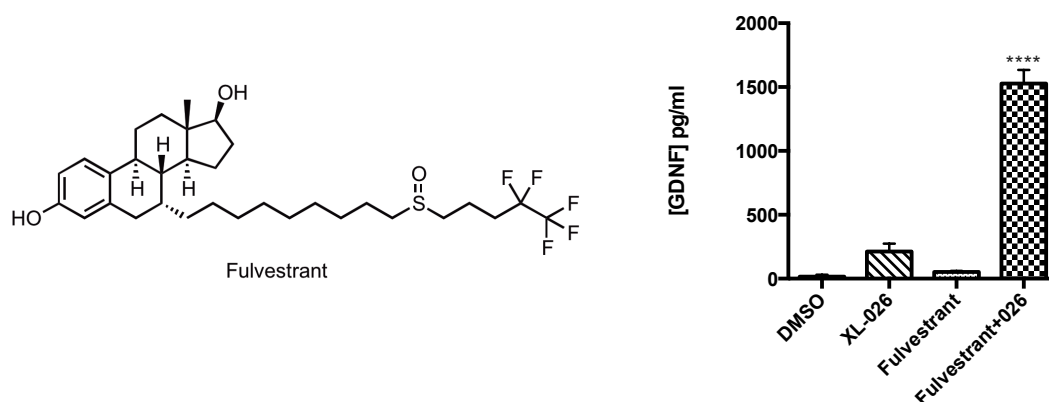


Figure 52. Structure of the ER antagonist fulvestrant and its affect on GDNF release by XL-026 (10 μ M) at 10 μ M in C6 cells (passage number 42). GDNF protein concentrations (pg/mL) in the conditioned medium were measured using ELISA after 48 hours. Data represent \pm SEM of biological replicates within one experiment, representative of three independent experiments. **** $p < 0.0001$ indicates statistical significance compared to the control as calculated by one-way ANOVA followed by Tukey's post-hoc test.

IV.5.3 TNF- α Receptors

Tumor necrosis factor alpha (TNF- α) is a inflammatory cytokine that induces signaling through its receptors TNF- α type I receptor (TNF-R1) and TNF- α type II receptor (TNF-R2), which in turn leads to activation of the JNK pathway and NF- κ B. TNF- α type I (TNF-R1) and TNF- α type II (TNF-R2) mRNA was induced in C6 cells after treatment with exogenous TNF- α .¹⁵⁵ The cytokine may have some neuroprotective effects, as it induces up-regulation of BDNF

in astrocytes.¹⁵⁶ Its connection to GDNF lies in its co-induction of expression with GDNF in response to Leu-Ile, a dipeptide investigated as a therapeutic agent for drug dependence.¹⁵⁷ Also, exogenous and endogenous TNF- α induces GDNF expression in cultured astrocytes.¹⁵⁸ Thus, it is well established that TNF- α induces GDNF production in astrocytes, and Verity reported significant release (1.69 ± 0.33 fold/control) in C6 cells in response to 10 ng/mL at 24 hours.^{40a} Therefore we treated C6 cells with TNF- α to determine if GDNF is released after 48 hours. Indeed, TNF- α (50 ng/mL) induces a statistically significant, highly reproducible release of GDNF from the cells.

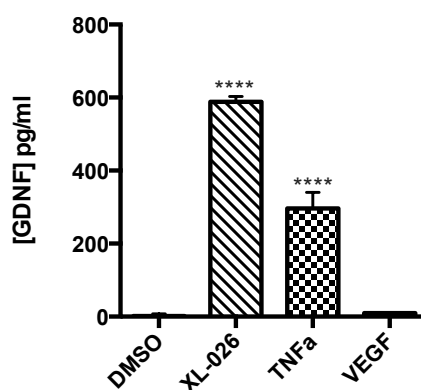


Figure 53. TNF- α (50 ng/mL, 48 hours) induces GDNF release from C6 cells (passage number 42). XL-026 (10 μ M) is included as a positive control, and VEGF (50 ng/mL) as a negative control. GDNF protein concentrations (pg/mL) in the conditioned medium were measured using ELISA after 48 hours. Data represent \pm SEM of biological replicates within one experiment, representative of three independent experiments. **** $p < 0.0001$ indicates statistical significance compared to the control as calculated by one-way ANOVA followed by Tukey's post-hoc test.

Thalidomide is known to reduce production of inflammatory cytokines, and its use (10 μ M) in conjunction with XL-026 treatment (10 μ M) in our GDNF release assay results in no attenuation or potentiation of release, suggesting that though TNF- α is capable of inducing

robust GDNF release in response to exogenous application, it likely does not play a role in the release by isoquinuclidines. Further support for this conclusion comes from the fact that the 5HT_{2A}R agonist (±)-DOI is a picomolar inhibitor of TNF- α ,¹⁵⁹ and co-incubation of DOI (albeit at 10 μ M, not shown) with XL-026 (10 μ M) results in no attenuation of signal.

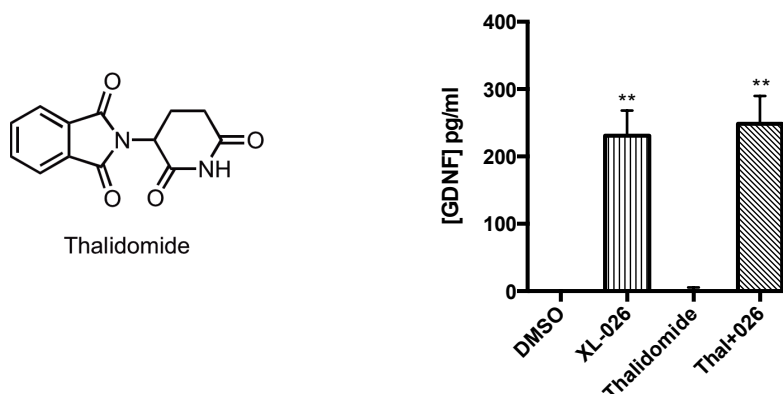


Figure 54. Structure of TNF- α production inhibitor thalidomide and its effect (10 μ M) on XL-026 (10 μ M)-induced GDNF release in C6 cells (passage number 41). GDNF protein concentrations (pg/mL) in the conditioned medium were measured using ELISA after 48 hours. Data represent \pm SEM of biological replicates within one experiment, representative of three independent experiments. ** $p < 0.01$ indicates statistical significance compared to the control as calculated by one-way ANOVA followed by Tukey's post-hoc test.

Thus far, based on treatment with small molecule, protein and cytokine ligands, we have found that treatment with (±)-DOI, a 5HT_{2A}R agonist, N-methylhistaprodifen, an H₁ agonist, FGF- β , PDGF-AB or PDGF-BB, and TNF- α lead to significant and reproducible GDNF release from the cells, and of the receptors for these ligands, pharmacological inhibition experiments implicate FGFR and PDGFR in the mechanism of release. Based on receptor antagonist work, potentiation of XL-026-induced GDNF release appears to be occurring with antagonists of nuclear receptors, and adrenergic/serotonergic antagonist propranolol, and PTX. These results reveal the complexity of the signaling pathways, in this case in the context of GDNF synthesis

and release. How our compound achieves this is not currently clear, but a more extensive discussion of isoquinuclidine-induced potentiation in of FGF- β , PDGF ligands, and TNF- α can be found later in Section V.

IV.6 Sigma Receptor Involvement

We sought to examine σ receptor involvement in our mechanism as PDSP screening data indicated that XL-026 and related isoquinuclidines bind to sigma with high potency and selectivity. A variety of ligands reported as ‘agonists’ and ‘antagonists’ of both σ 1R and σ 2R were chosen to test at the high concentration of 10 μ M. We observed that compounds defined as σ 1R agonists, namely (+)-SKF-10047 and PRE-084 (structures are shown in Figure 10) did not elicit GDNF release from C6 cells, whereas the σ 2R agonist PB28 induced a robust release. Interestingly, the non-selective σ R ligand 1,3-di-*o*-tolylguanidine (DTG), did not affect basal release. However, rimcazole, a sigma ligand that appears to act as an antagonist at low concentrations, but as a partial agonist at higher concentrations (and also shows binding affinity toward 5-HT₂ and opioid receptors),¹⁶⁰ induces a strong response in GDNF release (Figure 56).

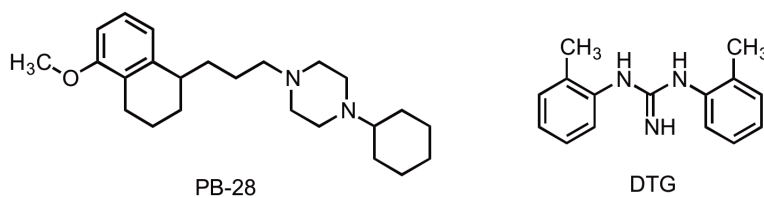


Figure 55. Chemical structures of σ 2R agonist PB28 and nonselective σ R ligand DTG (1,3-di-*o*-tolylguanidine).

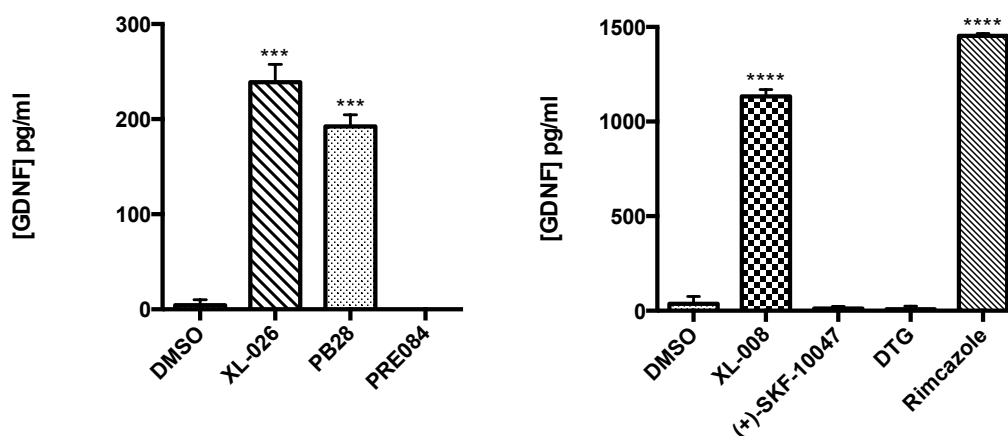


Figure 56. Effect of sigma ligands (all treatments at 10 μ M) on GDNF release from C6 cells (passage number 42). GDNF protein concentrations (pg/mL) in the conditioned medium were measured using ELISA after 48 hours. Data represent \pm SEM of biological replicates within one experiment, representative of at least three independent experiments for each treatment. *** $p < 0.001$ and **** $p < 0.0001$ indicate statistical significance compared to the control as calculated by one-way ANOVA followed by Tukey's post-hoc test.

Since it appeared that σ receptors, or a mechanism related to σ receptors, might be inducing GDNF release, we sought to modulate the release by using the σ 1R antagonist BD1047¹⁶¹ and the σ 2R antagonist SM-21.¹⁶² We were surprised to find that the antagonists induced GDNF release on their own, with apparently similar efficacy as XL-026. Also, concomitant treatment with either antagonist with XL-026 did not induce further increase in release. This implies that either the antagonists induce release by an unknown mechanism, yet also inhibit the XL-026-induced release, or that both small molecules are functioning through the same pathway, and that pathway can only reach a maximal induction leading to GDNF release. Also, it is impossible to determine if 'antagonists' are functioning through σ 1R or σ 2R exclusively, as they are not selective at the concentration we used, 10 μ M. To examine the dose-dependence of their release, we incubated XL-026 (10 μ M) and XL-008 (10 μ M, Rich

Karpowicz) with varying concentrations of BD1047 (Figure 58) and SM21 (Figure 59). We found that the antagonists are practically inactive at 1 μM , similar to our isoquinuclidines.

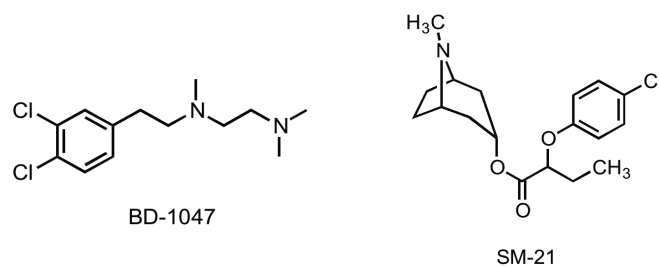


Figure 57. Structures of $\sigma_1\text{R}$ antagonist BD1047 and $\sigma_2\text{R}$ antagonist SM21.

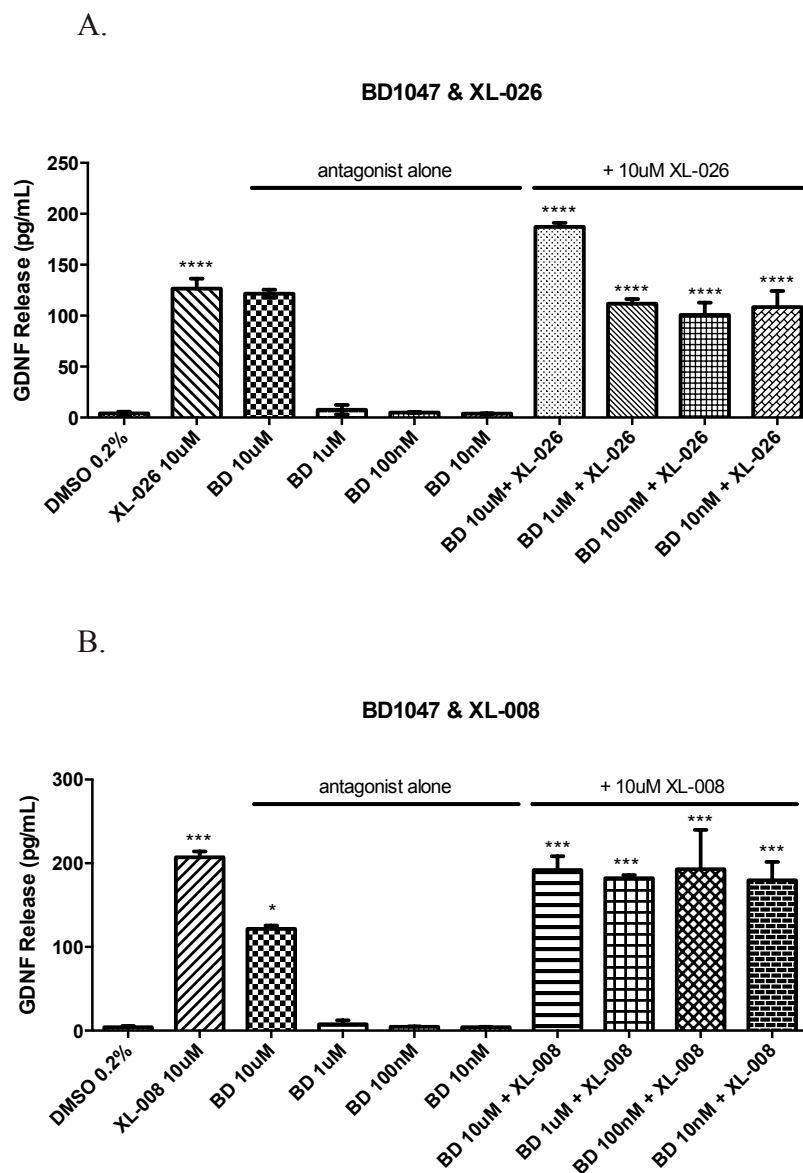


Figure 58. Modulation of XL-026 (A) and XL-008 (B) induced GDNF release in C6 cells (passage number 41) by varying concentrations of BD1047 (10 nM to 10 μ M). XL-026 and XL-008 were both used at 10 μ M. GDNF protein concentrations (pg/mL) in the conditioned medium were measured using ELISA after 48 hours. Data represent \pm SEM of biological replicates within one experiment, representative of three independent experiments for each treatment. * $p < 0.05$ and *** $p < 0.001$ indicate statistical significance compared to the control as calculated by one-way ANOVA followed by Tukey's post-hoc test. This representative experiment was performed by Rich Karpowicz.

In Figure 58, note that the magnitude of release by XL-008 is unchanged by the presence of BD1047, but in the case of XL-026, BD1047 does contribute a small, additional increase in

release. We postulate that this phenomenon is caused by maximal activation of a particular receptor or pathway, and since XL-026 is not as potent as XL-008, it alone has not reached the maximum threshold for induced release.

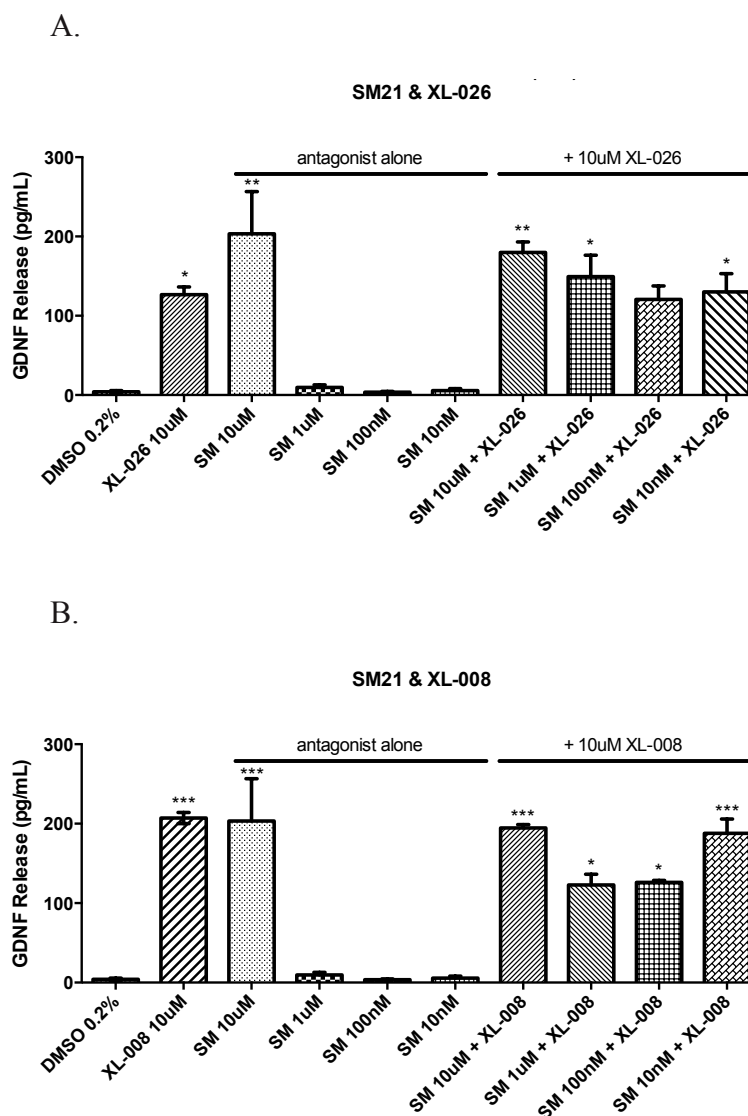


Figure 59. Modulation of XL-026 (A) and XL-008 (B) induced GDNF release in C6 cells (passage number 41) by varying concentrations of SM21 (10 nM to 10 μ M). XL-026 and XL-008 were both used at 10 μ M. GDNF protein concentrations (pg/mL) in the conditioned medium were measured using ELISA after 48 hours. Data represent \pm SEM of biological replicates within one experiment, representative of three independent experiments for each treatment. * $p < 0.05$ and *** $p < 0.001$ indicate statistical significance compared to the control as calculated by one-way ANOVA followed by Tukey's post-hoc test. This representative experiment was performed by Rich Karpowicz.

To confirm that selected sigma antagonists induce GDNF release, we examined the σ 1R antagonist NE-100 used frequently by many laboratories¹⁶³ and a structural analog of BD1047, BD1063. As expected, they induced release on their own as well, and there was a small increase in GDNF release in the presence of XL-026 (10 μ M), suggesting an additive effect up to the maximum release achievable by C6 cells (Figure 60).

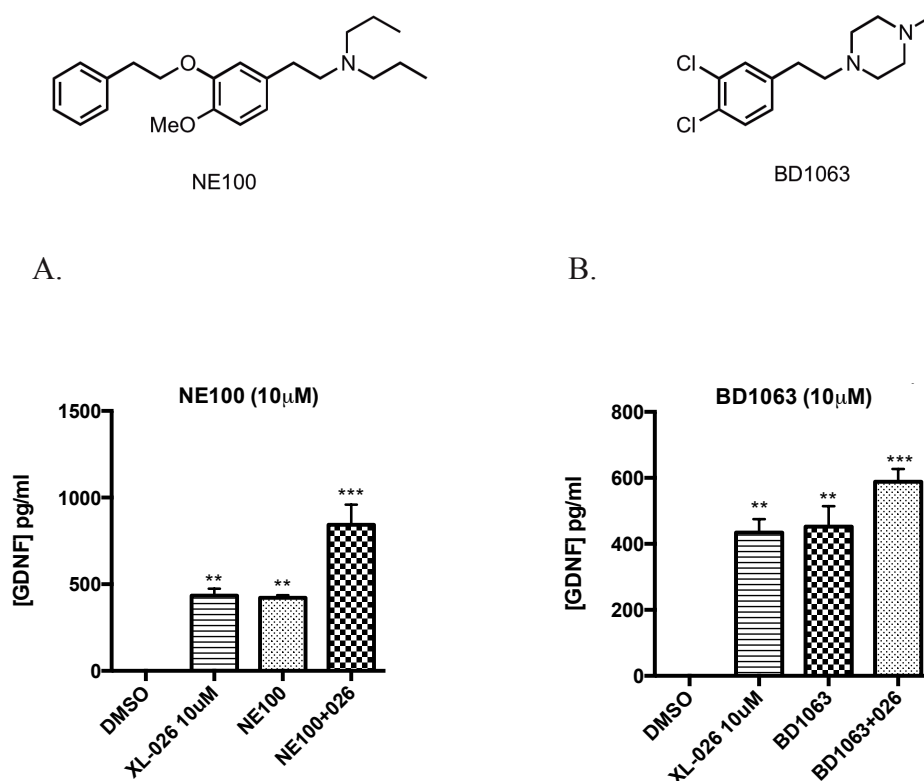


Figure 60. (A) σ 1R antagonist NE100 and its induction of GDNF release from C6 cells (passage number 41). (B) σ 1R antagonist BD1063 and its effect on GDNF release from C6 cells. All compounds were used at 10 μ M. GDNF protein concentrations (pg/mL) in the conditioned medium were measured using ELISA after 48 hours. Data represent \pm SEM of biological replicates within one experiment, representative of three independent experiments for each treatment. ** $p < 0.01$ and *** $p < 0.001$ indicate statistical significance compared to the control as calculated by one-way ANOVA followed by Tukey's post-hoc test.

When considering why a compound like PB28, which is supposedly a σ 2R agonist, would induce release, but nonselective sigma antagonists do as well, we need to keep in mind that the definition of sigma agonist versus antagonist is tentative and unclear and the assignment of agonist versus antagonist may be different when determined by different assays.¹⁶⁴ For example, BD1047 has even been reported as either an antagonist or a partial agonist of σ 1R.¹⁶⁵ Furthermore, the concentrations at which these σ R ligands induce GDNF release are much higher than the reported binding affinities and functional potencies ($< 1 \mu\text{M}$). It is highly possible that PB28 behaves like rimcazole, which is why they are both such strong releasers.

As mentioned earlier in this chapter, Prgmc1 is the putative σ 2R, so we were curious what the effect of Prgmc1 modulation would be in our assay. Progesterone, neither at $10 \mu\text{M}$ or 10 nM , does not result in GDNF release, though it was reported to lead to BDNF release from C6 cells.⁶⁶

On the other hand, the molecule AG205, a Prgmc1 antagonist,¹⁶⁶ induces release on its own at $10 \mu\text{M}$. The results of pre- and then co-incubation of AG205 with XL-026 does not block or attenuate XL-026-induced GDNF release (Figure 61).

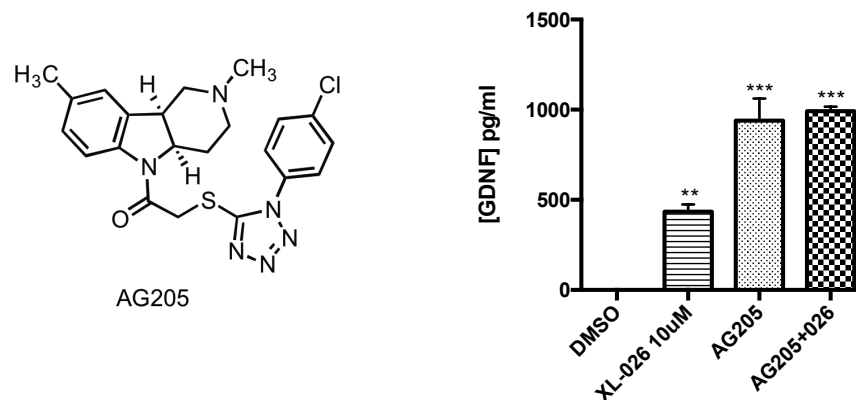


Figure 61. Structure of Pgrmc1 inhibitor AG205 and its effect at 10 μ M on GDNF release by XL-026 (10 μ M, 48 hours) in C6 cells (passage number 41). GDNF protein concentrations (pg/mL) in the conditioned medium were measured using ELISA after 48 hours. Data represent \pm SEM of biological replicates within one experiment, representative of three independent experiments for each treatment. ** $p < 0.01$ and *** $p < 0.001$ indicate statistical significance compared to the control as calculated by one-way ANOVA followed by Tukey's post-hoc test

V. Potentiation of Growth Factor-Induced GDNF Release

The hypothesis that XL-026 can act as a direct agonist at the RTKs suggested by the inhibition experiments or as a potentiator of growth factors (that may be secreted) prompted us to examine the effect of co-incubation XL-026 with FGF- β and PDGF. Surprisingly, we found that GDNF release was enhanced by co-incubation, which called for a more detailed investigation.

V.1 FGFR-Induced GDNF Release is Potentiated by XL-026

Co-treatment of C6 cells with highly active concentrations of both XL-026 (10 μ M) and FGF- β (50 ng/mL) resulted in a statistically significant increase in GDNF release, and we discovered that this potentiation is concentration-dependent, where as low as 1 μ M XL-026 produced statistically significant release (Figure 62). Comparing the release for FGF- β alone

with that co-incubated with 1 μM XL-026, the release is more than doubled, whereas there is only a trace of an increase in XL-026-induced GDNF release at this concentration. This effect is magnified at 5 and 10 μM XL-026. At each of these concentrations (1, 5 and 10 μM XL-026) the magnitude of release induced by coincubation of XL-026 and FGF- β is greater than the sum of those induced by individual treatment.

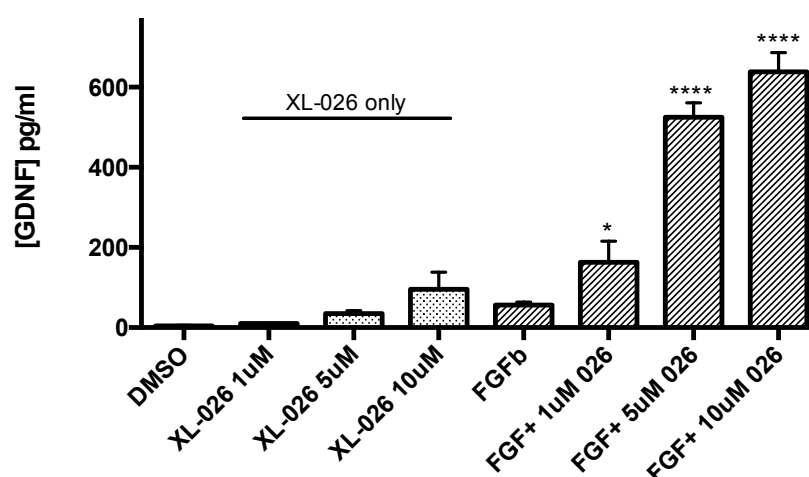


Figure 62. XL-026-induced potentiation of FGF- β -induced GDNF release is dose-dependent. Various concentrations of XL-026 and FGF- β were incubated with C6 cells (passage number 41) and GDNF protein concentrations (pg/mL) in the conditioned medium were measured using ELISA after 48 hours. Data represent \pm SEM of biological replicates within one experiment, representative of three independent experiments for each treatment. * $p < 0.05$ and **** $p < 0.0001$ indicate statistical significance compared to the control as calculated by one-way ANOVA followed by Tukey's post-hoc test.

Knowing that the potentiation is dependent on the concentration of XL-026, we next performed a dose-response study to determine the affect of varying the concentration of FGF- β . Using concentrations from 0.1 ng/mL to 100 ng/mL FGF- β , we found XL-026-induced GDNF release is potentiated with FGF- β with $\text{EC}_{50} \sim 2$ ng/mL (Figure 63, preliminary results).

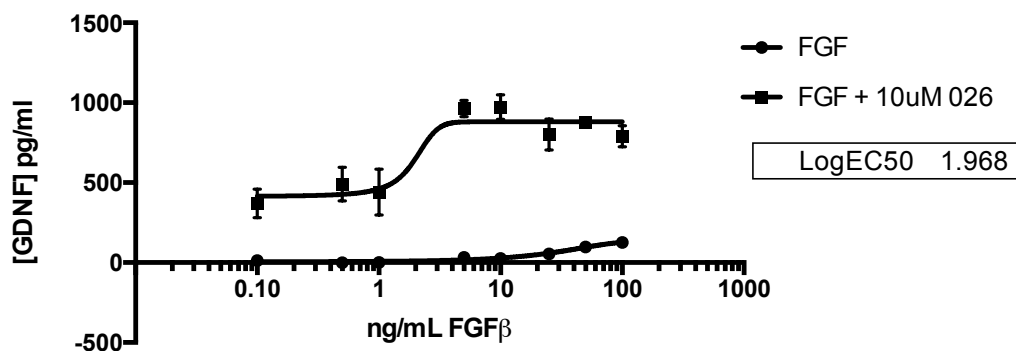


Figure 63. XL-026 induces potentiation of FGF- β -induced GDNF release potently. Various concentrations of XL-026 with and without FGF- β were incubated with C6 cells (passage number 41) and GDNF protein concentrations (pg/mL) in the conditioned medium were measured using ELISA after 48 hours. Data represent \pm SEM of biological replicates within one experiment, preliminary results.

The concept of potentiating an FGF- β -induced response has been noted in the literature, as a small molecule pyrimidine compound MS-818 is known to enhance the neurotrophic effects of FGF- β .¹⁶⁷

V.2 PDGFR-Induced GDNF Release is Potentiated by XL-026

Concomitant treatment of C6 cells with PDGF-AB and XL-026 results in a potentiation in PDGF-AB-induced release, albeit to a lesser extent than that for FGF- β , and the potentiation is dose-dependent on XL-026 as well. As the release is lower for PDGF-treated cells (causing us to use 100 ng/mL in this experiment), error bars are at times larger, but the SEM in the representative experiment shown does not obscure the fact that the release caused by PDGF-AB and XL-026 (10 μ M) together is more than double the release due to XL-026 alone and more than addition of the values obtained with each agent. Though the error in this particular experiment is large and interferes with statistical analyses, it is clear that potentiation begins at 5

μM XL-026 (whereas in the case of FGF- β , potentiation was observable at 1 μM XL-026; Figure 64).

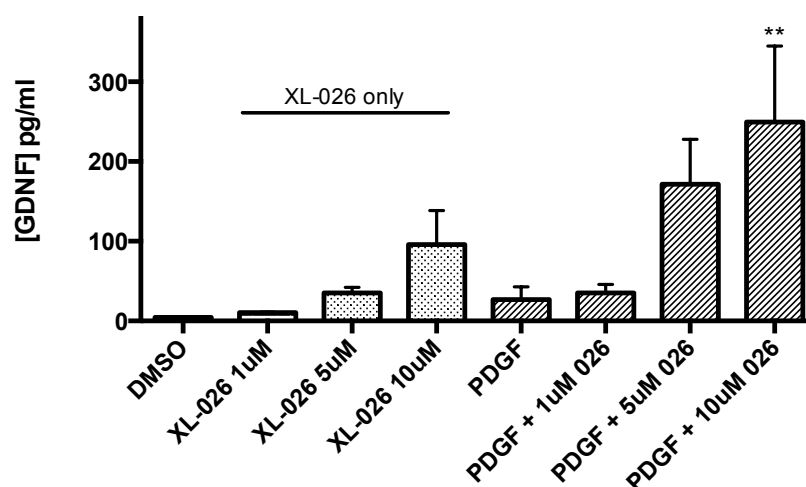


Figure 64. PDGF-AB-induced GDNF release is potentiated in a dose-dependent manner by XL-026. Various concentrations of XL-026 and PDGF-AB were incubated with C6 cells (passage number 41) and GDNF protein concentrations (pg/mL) in the conditioned medium were measured using ELISA after 48 hours. Data represent \pm SEM of biological replicates within one experiment, representative of three independent experiments for each treatment. ** $p < 0.05$, indicates statistical significance compared to the control as calculated by one-way ANOVA followed by Tukey's post-hoc test.

V.3 TNF- α -R-Induced GDNF Release is Potentiated by XL-026

The potentiation of GDNF release by TNF- α is strongly potentiated by XL-026 at 5 and 10 μM ; no potentiation on GDNF release is observed at 1 μM (Figure 65).

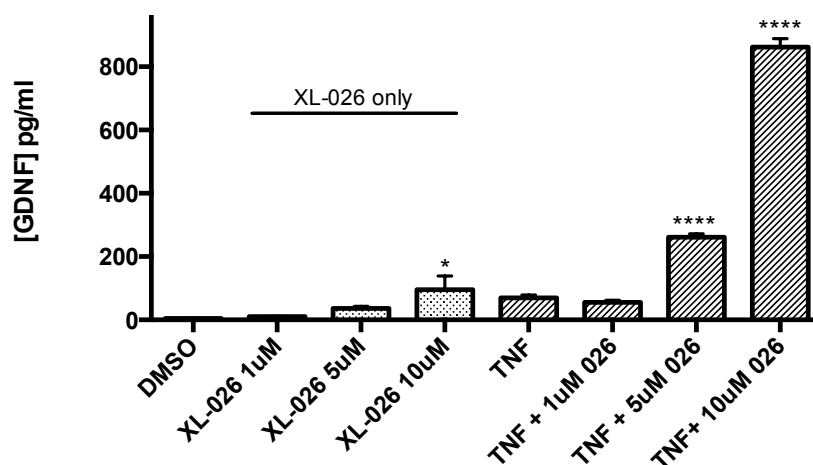


Figure 65. XL-026-induced potentiation of TNF- α -induced GDNF release is dose-dependent. Various concentrations of XL-026 and TNF- α were incubated with C6 cells (passage number 41) and GDNF protein concentrations (pg/mL) in the conditioned medium were measured using ELISA after 48 hours. Data represent \pm SEM of biological replicates within one experiment, representative of three independent experiments for each treatment. * $p < 0.05$ and **** $p < 0.0001$ indicate statistical significance compared to the control as calculated by one-way ANOVA followed by Tukey's post-hoc test.

V.4 Other RTKs Are Not Potentiated by Co-treatment With XL-026

Once the potentiation of GDNF release by XL-026 and FGF- β was discovered, we immediately screened the major growth factors in our ligand panel to determine if the phenomenon was applicable to other growth factors. The results below suggest that potentiation does not occur if the growth factor itself does not induce release, though we intend to continue testing other cytokines to confirm this conclusion. Potentiation in a similar scenario has been observed with Trk receptors, as small molecules have been reported that potentiate the activity of NT-3.¹⁶⁸ BDNF, EGF, NGF, TGF- β , and VEGF had no effect on XL-026-induced GDNF release (Figure 66).

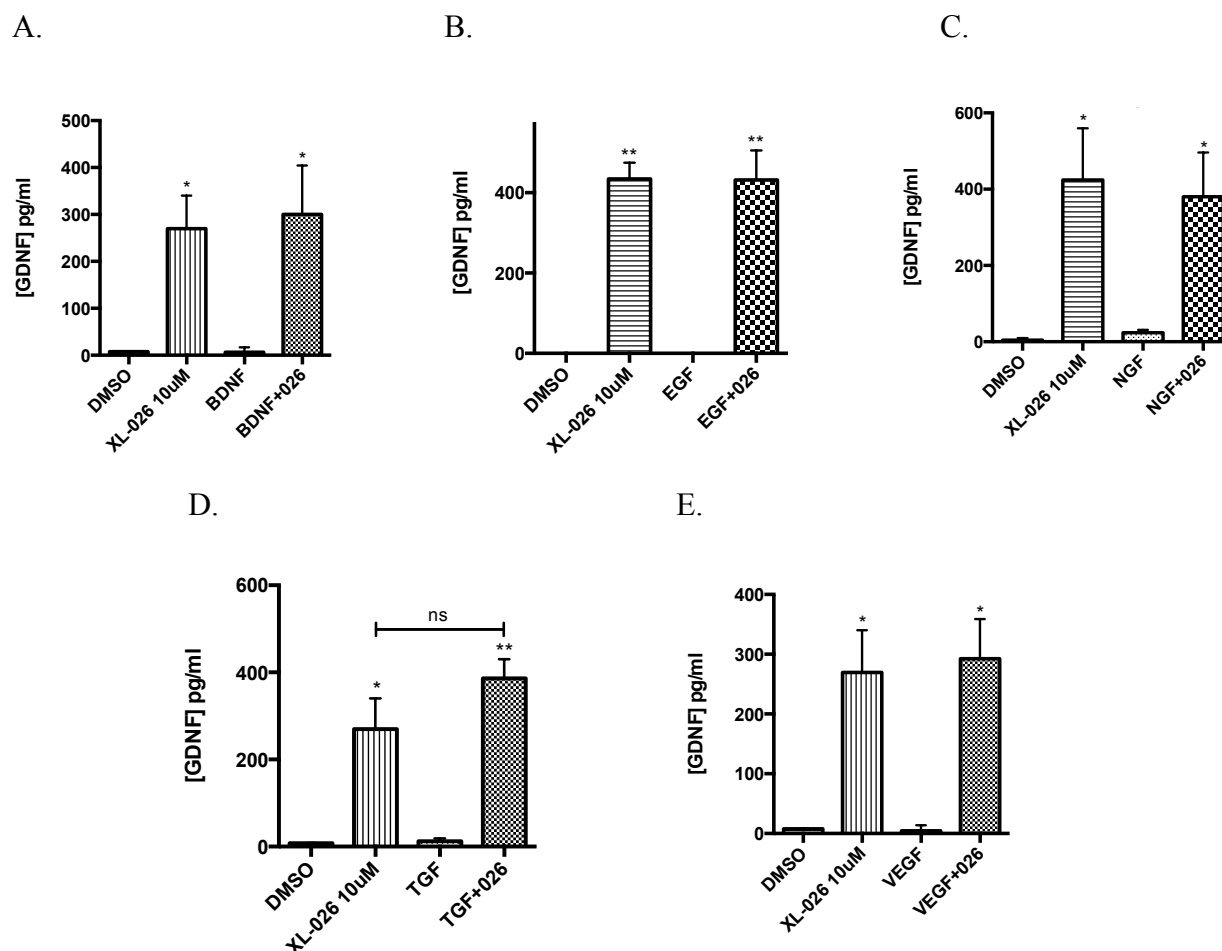


Figure 66. (A) BDNF, (B) EGF, (C) NGF, (D) TGF- β , and (E) VEGF do not potentiate GDNF release in the presence of XL-026. XL-026 (10 μ M) was incubated with C6 cells (passage number 42) in the presence and absence of a growth factor and GDNF protein concentrations (pg/mL) in the conditioned medium were measured using ELISA after 48 hours. Data represent \pm SEM of biological replicates within one experiment, representative of three independent experiments for each treatment. * $p < 0.05$ and ** $p < 0.01$ indicate statistical significance compared to the control as calculated by one-way ANOVA followed by Tukey's post-hoc test.

V.5 RTK Signaling Potentiation: Precedent

As discussed previously, sigma receptors have been reported to lead to expression of neurotrophins and growth factors, and potentiate NGF-induced neurite outgrowth from PC12 cells. Several sigma ligands are capable of doing so, including donepezil (but not an acetylcholinesterase (AChE) inhibitor that does not bind to σ 1R),¹⁶⁹ SA4503 and other σ 1R

agonists such as fluvoxamine,¹⁷⁰ ifenprodil,¹⁷¹ and papaverine.¹⁷² In each case, the authors demonstrated σ 1R-dependence by using NE100, the σ 1R antagonist, and since upon activation, σ 1R separates from IP₃R on the ER that induces its activation, they used the IP₃ receptor inhibitor Xestospongine C. The cells were incubated with the treatments for 4-5 days, so the treatment may be considered chronic, as in our 48-hour assay. Ketamine also potentiates NGF-induced neurite outgrowth in a σ 1R-dependent manner.¹⁷³ Another study utilizing chronic treatment discovered that fluoxetine and olanzapine increase FGF- β mRNA and protein expression in rat prefrontal cortex, hippocampus, and striatum when co-administered, but independently do not lead to an increase in expression.¹⁷⁴ This phenomenon also occurred in a study where alone, (+)-PTZ has no effect on neurite sprouting, but in the presence of NGF, it potentiates sprouting and shifts the dose curve to the left, but only until the maximum induction at 20 ng/mL NGF is reached.⁶⁷ It appears in the study that there is a maximal effect that any combination of σ 1R ligand and NGF may have; this maximal effect on neurite sprouting also manifests itself the presence of 15% serum in the experimental medium, as opposed to 0.5% serum used in their other experiments. This is intriguing for us, as we also see what appears to be a maximal threshold for GDNF release by our compounds with/without σ 1R antagonist ligands. It would be interesting to see if GDNF release is dependent on serum proteins, as we use 0.5% serum in our experimental medium. σ 2R ligands are also capable of various processes; for example, they potentiate conventional chemotherapies and improve survival in models of pancreatic adenocarcinoma.¹⁷⁵

Other examples include σ R-mediated potentiation of the PLC- γ pathway by antidepressants. BDNF is known to activate the PLC- γ /IP₃/Ca²⁺ signaling pathway (Chapter 2) and chronic 48 hour pretreatment with the antidepressants imipramine and fluvoxamine

potentiate activation of PLC- γ and glutamate release by BDNF.¹⁷⁶ Both of these effects were PLC- γ and IP₃-dependent, while Akt and ERK1/2 were not potentiated and the protein expression of PLC- γ , TrkB, or BDNF was not changed by pretreatment with imipramine. Imipramine also enhanced the interaction of TrkB and PLC- γ . Thus, there is a significant literature precedent for σ receptors inducing potentiation of signaling.

VI. Conclusions and Mechanistic Models

GDNF is an important neurotrophic factor and therefore its induction and release by small molecules may represent a promising experimental approach to treating a number of brain disorders. On the basis of the natural product ibogaine that shows remarkable effects in animals and in humans, we generated several derivatives that show high efficacy of GDNF release and modest potency ($\sim 5 \mu\text{M}$), such as compounds XL-026, which was the focus of the present investigation.

We have systematically mapped the C6 glioma cell line, the frequently used cell model of glia cells, with respect to potential molecular targets and their signaling involved in XL-026-induced release of GDNF, including an exhaustive list of GPCR receptors, RTK receptors, cytokine receptors and nuclear receptors. We selected these molecular targets on the basis of the following criteria: 1) Precedent for involvement in induction of GDNF expression and/or release; 2) evidence for expression in C6 cells; and 3) ability to activate ERK1/2; and used pharmacological approaches to assess their potential involvement. In parallel, we submitted XL-026 (as well as other related analogs) to a broad CNS receptor screen (PDSP, 50 common CNS targets). On the basis of extensive data acquired by this study and the literature precedent, there

are four key molecular targets that are likely involved directly in the mechanism of XL-026 action: σ receptors (σ 1R or σ 2R), PDGFR (1 or 2), FGFR (1 or 2), and ERK1/2/5.

VI.1 Mechanistic Model for Potentiation of FGF- β and PDGF-Induced GDNF Release

We propose that XL-026 binds to σ 1R and/or σ 2R, which then potentiates the MAPK signaling pathway turned on by the corresponding RTK receptor, which in turn activates ERK1/2/5 and leads to GDNF expression, synthesis and release (Figure 67). The exact mechanism is not known, but σ Rs are protein chaperones that may interact and thus modulate the RTK receptor complex or any downstream signaling proteins. The use of several inhibitors of different structures confirm the ERK kinases as the signaling hub and the central target that regulates GDNF induction in C6 cells.

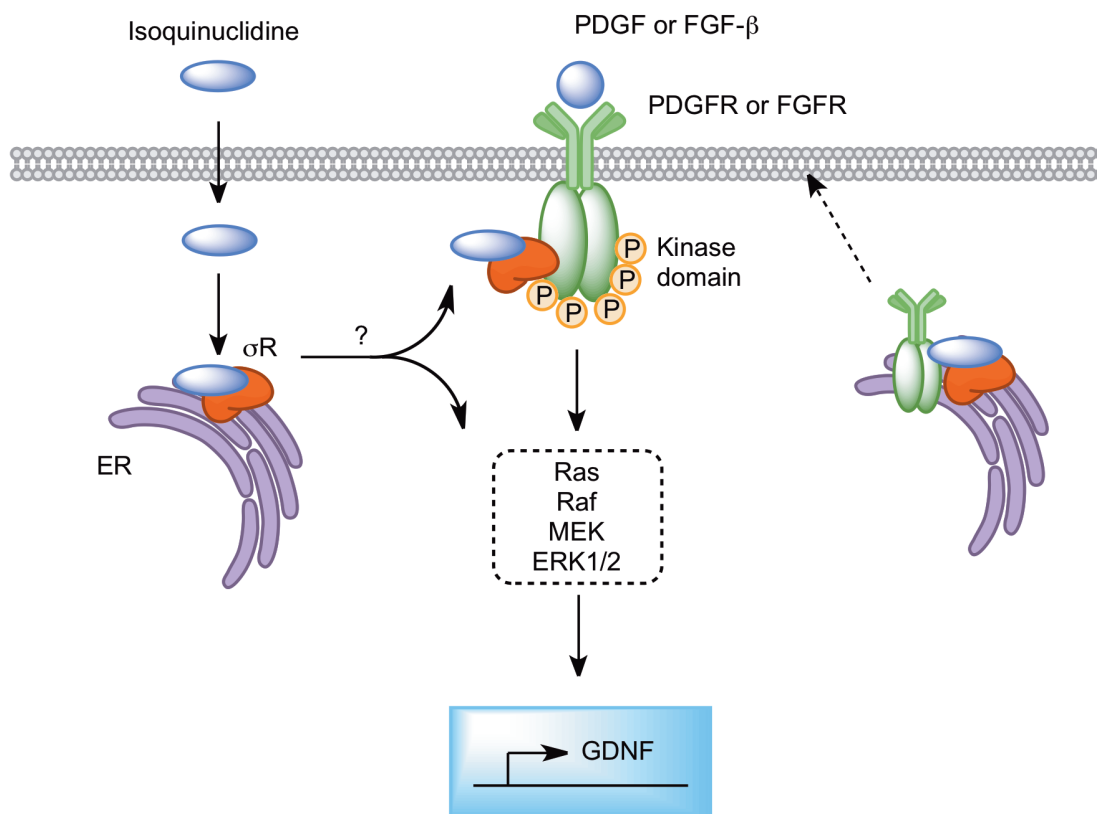


Figure 67. Proposed mechanism for isoquinuclidine-induced GDNF synthesis and release. Isoquinuclidine enters the cell and binds to σR (either $\sigma 1R$ or $\sigma 2R$) in ER and/or in the plasma membrane, possibly inducing its translocation from the ER. σR s either directly associate and modulate the RTK or they associate and modulate the downstream signaling proteins. Isoquinuclidines either potentiate RTK-induced signaling or activates MAPK signaling directly from σR s.

VI.2 Mechanistic Model for XL-026-Induced GDNF Release: σR s as Key Players

We also propose that $\sigma 1R$ or $\sigma 2R$ (*Pgrmc1*) is the primary molecular target for XL-026 as supported by the binding assays (K_i ($\sigma 1R$) = 2.3 nM, K_i ($\sigma 2R$) = 2.1 nM). Interaction of XL-026 with a σR induces activation of the MAPK signaling pathway, most likely via PDGFR (or a related RTK), ultimately leading to ERK1/2/5 activation and GDNF up-regulation. As a variation of this model, XL-026 through its interaction with σR s induces release of growth factors that in an autocrine manner induce subsequent up-regulation and release of GDNF. For

example, XL-026 may induce FGF- β release, which would then lead to FGFR activation, activation of the MAPK signaling pathway, and finally synthesis and release of GDNF.

VI.3 Alternate Mechanistic Models: Stress-Induced GDNF Release

Cellular stress, as described earlier, leads to activation of protective signaling, including generation of ROS. ER stress may be a consequence of isoquinuclidine penetration into the cell, which could then either induce ROS or other second messenger signaling to activate RTKs, which then induce the MAPK pathway to turn on GDNF synthesis and release.

VII. Future studies

To confirm the involvement of the selected targets, most notably the $\sigma 1$ and $\sigma 2$ Rs, we will perform the knock-down experiments with silencing RNA. If induction of release by XL-026, XL-008, and possibly even σ ligands we have been working with is dampened or eradicated by receptor knockdown, then we will have confirmation that the σ receptor is involved in the induction mechanism. We could also attempt to support these experiments by trying progesterone as a sigma inhibitor,¹⁷⁷ since progesterone on its own does not induce release whereas the sigma antagonists do.

To determine if our compounds, like siramesine and other sigma ligands, are lysosomal detergents, our compounds will be compared to the published compounds in the same lysosomal pH detection assay using LysoTracker Red that the authors use,⁷² as well as possibly amiodarone and imipramine.¹⁷⁸ GDNF release in response to this stress would be an appropriate protective response by the cell.

To determine if ER stress is the culprit of triggering GDNF release in response to stress, we may be able to identify up-regulation of ER stress proteins, like GRP78 (BiP),⁷⁰ GRP94, and calreticulin,¹⁷⁹ as well as COX-2, another protein induced by ER stress.¹⁸⁰ Western blotting should detect increased expression of these ER proteins. We can also use pharmacology to induce or probe ER stress, like using the Ca^{2+} ionophore A23187 to release calcium from ER stores, brefeldin A to inhibit ER-to-Golgi vesicle transport, and tunicamycin to prevent protein glycosylation at the ER, which induces stress.

If receptor up-regulation is leading to the potentiation of GDNF release, we can easily probe for the expression of the protein of interest. In the near future, we would like to consider the possibility that FGFR, PDGFR, and $\text{TNF}\alpha$ -R are induced by isoquinuclidine treatment, since the synthesis-dependent release could be a direct product of the up-regulation of these three receptors. Since the receptors are already known to induce GDNF release following activation by their cognate ligands, increasing receptor expression could further sensitize them to their ligand and produce a non-linear increase in GDNF release.

Also, we need to know if the potentiation is dependent on endogenous ligand secretion. If, for example, treatment with XL-026 induces FGF- β release from C6 cells, the ligand will go on to induce GDNF synthesis and release in an autocrine or paracrine manner; further increasing the concentration of the growth factor by exogenous application could provide the boost in GDNF synthesis and release that we observe.

An alternate mechanism for a potentiation of GDNF release could be from two distinct signaling pathways; if the isoquinuclidines induce a particular signaling cascade that leads to GDNF synthesis and release, whereas the protein ligands FGF- β , PDGF-AB, or $\text{TNF-}\alpha$ induce a separate pathways that converges with the first at a specific point, the consequence is

coincidence detection by the protein(s) that function as the convergence point and modulate the input from the two separate pathways.¹⁸¹ In this case, that modulation might be synergistic, since the result is greater than if the two separate GDNF releases were added together.

VIII. Experimental

Materials

C6 cells were purchased from American Type Culture Collection (#CCL-107; Rockville, MD) at passage 37 and routinely grown in a 5% CO₂ atmosphere at 37°C, in DMEM (high glucose with GlutaMax, #10569; Life Technologies Corp., Grand Island, NY) supplemented with 5% FBS (Premium Select, Atlanta Biologicals; Atlanta, GA), 100 U/mL penicillin, and 100 µg/mL streptomycin (#15140, Life Technologies). SH-SY5Y cells (CRL-2266) were obtained from ATCC and grown in DMEM supplemented with 10% FBS, 100 U/mL penicillin and 100 µg/mL streptomycin. 100 mm polystyrene tissue culture plates were purchased from Corning (#430169; Corning, NY), and 6-well (#657165) and 12-well plates (#665180) were purchased from Greiner Bio-One (Monroe, NC). For ELISA assays, Nunc Immulon 4 HBX flat well plates were used (#3855; Thermo Scientific, Pittsburgh, PA), and other assays were performed using Costar 96-well plates (#3370, Corning).

Protein ligands, cytokines and small molecules were obtained from the following: Recombinant artemin (540-17), BDNF (450-02), CNTF (450-50), EGF (400-25), FGF-β (100-18B), GDNF (450-10), HGF (100-39), heregulin-β1 (100-03), IGF-I (100-11), IGF-II (100-12), β-NGF (450-01), neurturin (450-11), persephin (450-12), PDGF-AB (100-00AB), PDGF-BB (100-14B), SCF (400-22), TGF-β1 (100-21), TNF-α (400-14), VEGF₁₆₅ (400-31) were purchased from Peprotech (Rocky Hill, NJ). Recombinant rat LIF (LIF3005) was purchased from Millipore (Temecula, CA). Neuromedin B was obtained from American Peptide Company (Sunnyvale, CA). NT-3, NT-4, N-acetyl-5-hydroxytryptamine (N-acetylserotonin, NAS), adenosine, BD1047 hydrochloride, (±)-DOI hydrochloride, β-estradiol, endothelin-1, fulvestrant, histamine hydrochloride, (-)-isoproterenol hydrochloride, K252a, LY-354740, N-

dimethylhisaprodifen dioxalate, melatonin, mifepristone, naltrexone hydrochloride, *nor*-binaltorphimine dihydrochloride (norBNI), PB28 dihydrochloride, PD184352, PRE-084, (\pm) propranolol hydrochloride, and RPI-1 were purchased from Sigma-Aldrich (Saint Louis, MO). DTG and U0126 were purchased from Alfa Aesar (Ward Hall, MA), AG1478 was purchased from Alexis Biochemicals (San Diego, CA), scopolamine was purchased from TCI (Portland, OR), and PD 173074 was purchased from TSZ Chem (Framingham, MA). Ibogaine (I-001) was purchased from Cerilliant Corporation (Round Rock, TX). (*RS*)-APICA, endomorphin-1, mepyramine maleate, NE 100 hydrochloride, rimcazole dihydrochloride, (+)-SKF-10047 hydrochloride, SM-21 maleate, CGS 21680 hydrochloride, and (-)-U50488 hydrochloride, were purchased from Tocris (Minneapolis, MN). (+)-Bicuculline, genistein, isoguvacine, prostaglandin E₂, and SQ 22536 were purchased from Enzo Life Sciences (Farmingdale, NY). BIX02189, KRN633, and PD98059 were acquired from Selleck Chemicals (Houston, TX). Losartan, LY294002, sphingosine-1-phosphate, and Tyrphostin AG1296 were purchased from Cayman Chemicals (Ann Arbor, MI). KN-93 (water-soluble) and pertussis toxin were from Calbiochem/EMD Biosciences (San Diego, CA). Carbachol and cycloheximide were purchased from Acros Organics (via Fisher Scientific, Pittsburgh, PA), and cyproheptadine hydrochloride, prazosin hydrochloride, and thalidomide were purchased from MP Biomedicals (Santa Ana, CA).

Materials for western blotting experiments were obtained from the following: Protease inhibitor cocktail (P8340), phosphatase inhibitor cocktails 2 (P5726) and 3 (P0044), and bovine serum albumin (BSA) were from Sigma-Aldrich. ERK1/2 rabbit polyclonal antibody (#9102), phospho-ERK1/2 (Thr202/Tyr204) XP™ rabbit monoclonal antibody (#4370), phospho-Ret (Tyr905) polyclonal rabbit (#3221), anti-mouse HRP-linked (#7076) and anti-rabbit HRP-linked

(#7074) antibodies were purchased from Cell Signaling Technology (Beverly, MA). Ret (H-300) rabbit polyclonal antibody (#sc-13104) was purchased from Santa Cruz Biotechnology (Santa Cruz, CA). Pierce RIPA buffer, Pierce ECL 2 Western Blotting Substrate, and Pierce BCA Protein Assay kit were purchased from Thermo Scientific (Rockford, IL).

GDNF ELISA

C6 cells were thawed into two 100 mm culture plates in complete growth medium, grown to 95% confluency, and sub-cultured into 100 mm culture dishes and grown to confluency before cryopreserving at passage 39. Before most experiments, one vial was thawed into two 100 mm culture dishes and grown to confluency before plating into 12-well plates at 300,000 cells/well. 24 hours later, the cells were washed in PBS and the medium replaced with 0.5 mL/well of low serum (0.5% FBS) DMEM. 24 hours later, the experiment was started by adding 0.5 mL/well of 2x concentrated treatment medium to each well. Each treatment was performed in duplicate. 48 hours after addition of agonists or experimental compounds, the experiment was stopped by transferring the culture medium into microcentrifuge tubes, washing the cells twice with cold PBS, and storing the monolayers and supernatants at -80°C until assaying.

To measure GDNF release from C6 cells, the GDNF Emax ImmunoAssay kit from Promega (Madison, WI) was used according to the manufacturer's instructions. Briefly, a 96-well ELISA plate was coated overnight with 100 uL/well of 1:1000 monoclonal GDNF antibody in carbonate coating buffer at 4°C. The next day, the plate was blocked with 200 µL/well of 1X Block & Sample Buffer for 1 hour at room temperature while the samples thawed. The samples were homogenized before distributing into the assay plate. The standard curve was generated according to the instructions in the kit and the samples were assayed in triplicate wells, 100

uL/well, and incubated for 6 hours at room temperature while shaking. The plate was washed 5 times with TBST with a manual plate washer and incubated with 100 μ L/well of 1:500 polyclonal GDNF antibody in 1X Block & Sample Buffer overnight at 4°C. On the following day the plate was washed as before and incubated for two hours with 1:200 secondary antibody in 1X Block & Sample Buffer at room temperature with shaking, while the TMB One development solution was equilibrated to room temperature. After washing the plate, 100 μ L/well TMB One was added per well and incubated for several minutes until the aqua blue color in the standard curve was prominent. The reaction was stopped by 100 μ L/well of 1N aqueous HCl and the absorbance was measured at 450 nm in a Bio-Tek H1MF plate reader (Burlington, VT). LDH release into the medium was detected using the CytoTox 96 NonRadioactive Cytotoxicity assay (Promega) according to the manufacturer's instructions.

Ret and ERK1/2 activation

SH-SY5Y or C6 cells were grown until confluence and subcultured into 6-well plates at 1 million cells/well and grown for 24 hours in 2 to 3 mL of medium. For C6 experiments, cells were washed with sterile PBS and the medium replaced with 0.5% FBS low serum medium; for SH-SY5Y experiments, cells were washed and the medium was replaced with 1% FBS low serum medium. On the day of the experiment, a small volume was removed from the well (100 μ L) and replaced with an equal volume of a concentrated solution of experimental compound or control at the appropriate time. Compounds were diluted from 1000x concentrated stock solutions in DMSO or sterile water. For time course experiments, a control well was run for every time point, since basal ERK1/2 phosphorylation rises approximately 10 – 15 minutes after a treatment is added. To stop the experiment, the medium was removed and the plates rinsed

twice with cold PBS while on ice. 150 to 200 μ L of lysis buffer (Pierce RIPA buffer + 1:100 protease inhibitor cocktail, phosphatase 2 and 3 inhibitor cocktails, and 0.5M EDTA solution) was immediately added to the wells and incubated over ice for 15 minutes to an hour, after which cells were scraped and the lysate transferred into microcentrifuge tubes. After homogenizing the samples with a sonicator, the tubes were centrifuged at 14,000 rpm for 10 minutes, the supernatant was transferred to fresh tubes, and the protein content was measured using the Pierce BCA assay. Equal quantities of protein (\sim 10 μ g for ERK blots, > 20 μ g for Ret blots) were added to each well of a 10% bis-tris acrylamide gel and were blotted onto Immobilon P PVDF transfer membranes. Blots were blocked in 3% BSA in TBS for at least 1 hour, followed by overnight incubation with the primary antibody with rocking at 4°C. The next day, the blots were washed 3 x 5 minutes with TBST (0.05% Tween 20), incubated for 1 hour with secondary antibody (typically 1:1000) in the buffer indicated on the antibody's corresponding data sheet, then washed again for 3 x 5 minutes prior to development with the ECL kit. Chemiluminescence was visualized with a Kodak Image Station 440CF imager.

Data Analysis

Bands from Western blots were routinely quantified using densitometry by the gel analysis tools in ImageJ (NIH, Bethesda, MD). For GDNF release experiments, data were initially processed in Microsoft Excel to calculate GDNF concentrations using a standard curve, then transferred into GraphPad Prism (6) to create graphs and perform statistical analyses. Multiple comparisons were analyzed by one-way ANOVA followed by Tukey's post-test, and statistical significance was considered $p > 0.05$.

IX. References

- ¹ Lin, L. F.; Doherty, D. H.; Lile, J. D.; Bektesh, S.; Collins, F. GDNF: a glial cell line- derived neurotrophic factor for midbrain dopaminergic neurons. *Science* **1993**, *260*, 1130–1132.
- ² (a) Enomoto, H. Regulation of neural development by glial cell line-derived neurotrophic factor family ligands. *Anat. Sci. Int.* **2005**, *80*, 42–52. (b) de Graaff, E.; Srinivas, S.; Kilkenny, C.; D’Agati, V.; Mankoo, B. S.; Costantini, F.; Pachnis, V. Differential activities of the RET tyrosine kinase receptor isoforms during mammalian embryogenesis. *Genes Dev.* **2001**, *15*, 2433–2444.
- ³ (a) Carnicella, S.; Ron, D. GDNF—A potential target to treat addiction. *Pharmacol. Ther.* **2009**, *122*, 9–18. (b) Carnicella, S.; Ahmadiantehrani, S.; Janak, P. H.; Ron, D. GDNF is an endogenous negative regulator of ethanol-mediated reward and of ethanol consumption after a period of abstinence. *Alcohol. Clin. Exp. Res.* **2009**, *33*, 1012–1024. (c) Carnicella, S.; Amamoto, R.; Ron, D. Excessive alcohol consumption is blocked by glial cell line-derived neurotrophic factor. *Alcohol* **2009**, *43*, 35–43. (d) Leggio, L.; Cardone, S.; Ferrulli, A.; Kenna, G. A.; Diana, M.; Swift, R. M.; Addolorato, G. Turning the clock ahead: potential preclinical and clinical neuropharmacological targets for alcohol dependence. *Curr. Pharm. Des.* **2010**, *16*(19), 2159–2218. (e) Ghitza, U. E.; Zhai, H.; Wu, P.; Airavaara, M.; Shaham, Y.; Lu, L. Role of BDNF and GDNF in drug reward and relapse: A review. *Neurosci. Biobehav. Rev.* **2010**, *35*, 157–171.
- ⁴ Airaksinen, M. S.; Saarma, M. The GDNF family: Signalling, biological functions and therapeutic value. *Nature Rev. Neurosci.* **2002**, *3*, 383–394.
- ⁵ Arighi, E.; Borrello, M. G.; Sariola, H. RET tyrosine kinase signaling in development and cancer. *Cytokine Growth Factor Rev.* **2005**, *16*, 441–467.
- ⁶ Nanobashvili, A.; Airaksinen, M. S.; Kokaia, M.; Rossi, J.; Asztély, F.; Olofsdotter, K.; Mohapel, P.; Saarma, M.; Lindvall, O.; Kokaia, Z. Development and persistence of kindling epilepsy are impaired in mice lacking glial cell line-derived neurotrophic factor family receptor $\alpha 2$. *Proc. Natl. Acad. Sci. U.S.A.* **2000**, *97*, 12312–12317.
- ⁷ Asai, N.; Jijiwa, M.; Enomoto, A.; Kawai, K.; Maeda, K.; Ichihara, M.; Murakumo, Y.; Takahashi, M. RET receptor signaling: Dysfunction in thyroid cancer and Hirschsprung’s disease. *Pathol. Int.* **2006**, *56*, 164–172.
- ⁸ Messer, C. J.; Eisch, A. J.; Carlezon, W. A.; Whisler, K.; Shen, L.; Wolf, D. H.; Westphal, H.; Collins, F.; Russell, D. S.; Nestler, E. J. Role for GDNF in biochemical and behavioral adaptations to drugs of abuse. *Neuron* **2000**, *26*, 247–257.

- ⁹ (a) Kitagawa, H.; Hayashi, T.; Mitsumoto, Y.; Koga, N.; Itoyama, Y.; Abe, K. Reduction of ischemic brain injury by topical application of glial cell line derived neurotrophic factor after permanent middle cerebral artery occlusion. *Stroke* **1998**, *29*, 1417–1422. (b) Wang, Y.; Lin, S.-Z.; Chiou, A.-L.; Williams, L. R.; Hoffer, B. J. Glial cell line-derived neurotrophic factor protects against ischemia-induced injury in the cerebral cortex. *J. Neurosci.* **1997**, *17*, 4341–4348. (c) Arvidsson, A.; Kokaia, Z.; Airaksinen, M. S.; Saarma, M.; Lindvall, O. Stroke induces widespread changes of gene expression for glial cell line-derived neurotrophic factor family receptors in the adult rat brain. *Neurosci.* **2001**, *106*, 27–41.
- ¹⁰ (a) Åkerud, P.; Canals, J. M.; Snyder, E. Y.; Arenas, E. Neuroprotection through delivery of glial cell line-derived neurotrophic factor by neural stem cells in a mouse model of Parkinson's disease. *J. Neurosci.* **2001**, *21*, 8108–8118. (b) Zurn, A. D.; Widmer, H. R.; Aebischer, P. Sustained delivery of GDNF: towards a treatment for Parkinson's disease. *Brain Res. Rev.* **2001**, *36*, 222–229. (c) Rangasamy, S. B.; Soderstrom, K.; Bakay, R. A.E.; Kordower, J. H. Neurotrophic factor therapy for Parkinson's disease. *Prog. Brain Res.* **2010**, *184*, 237–264.
- ¹¹ Kotzbauer, P. T.; Lampe, P. A.; Heuckeroth, R. O.; Golden, J. P.; Creedon, D. J.; Johnson Jr., E. M.; Milbrandt, J. Neurturin, a relative of glial-cell-line-derived neurotrophic factor. *Nature* **1996**, *384*, 467–470.
- ¹² Milbrandt, J.; de Sauvage, F. J.; Fahrner, T. J.; Baloh, R. H.; Leitner, M. L.; Tansey, M. G.; Lampe, P. A.; Heuckeroth, R. O.; Kotzbauer, P. T.; Simburger, K. S.; Golden, J. P.; Davies, J. A.; Vejsada, R.; Kato, A. C.; Hynes, M.; Sherman, D.; Nishimura, M.; Wang, L.-C.; Vandlen, R.; Moffat, B.; Klein, R. D.; Poulsen, K.; Gray, C.; Garces, A.; Johnson Jr., E. M. Persephin, a novel neurotrophic factor related to GDNF and neurturin. *Neuron* **1998**, *20*, 245–253.
- ¹³ Baloh, R. H.; Tansey, M. G.; Lampe, P. A.; Fahrner, T. J.; Enomoto, H.; Simburger, K. S.; Leitner, M. L.; Araki, T.; Johnson Jr., E. M.; Milbrandt, J. Artemin, a novel member of the GDNF ligand family, supports peripheral and central neurons and signals through the GFR α 3-RET receptor complex. *Neuron* **1998**, *21*, 1291–1302.
- ¹⁴ Paratcha, G.; Ledda, F.; Baars, L.; Couplier, M.; Besset, V.; Anders, J.; Scott, R.; Ibáñez, C. F. Released GFR α 1 potentiates downstream signaling, neuronal survival, and differentiation via a novel mechanism of recruitment of c-Ret to lipid rafts. *Neuron* **2001**, *29*, 171–184.
- ¹⁵ Jing, S.; Wen, D.; Yu, Y.; Holst, P. L.; Luo, Y.; Fang, M.; Tamir, R.; Antonio, L.; Hu, Z.; Cupples, R.; Louis, J.-C.; Hu, S.; Altrock, B. W.; Fox, G. M. GDNF-induced activation of the Ret protein tyrosine kinase is mediated by GDNFR- α , a novel receptor for GDNF. *Cell* **1996**, *85*, 1113–1124.
- ¹⁶ Sariola, H.; Saarma, M. Novel functions and signalling pathways for GDNF. *J. Cell Sci.* **2003**, *116*, 3855–3862.
- ¹⁷ Paratcha, G.; Ledda, F.; Ibáñez, C. F. The neural cell adhesion molecule NCAM is an alternative signaling receptor for GDNF family ligands. *Cell* **2003**, *113*, 867–879.

-
- ¹⁸ Santoro, M.; Melillo, R. M.; Carlomagno, F.; Vecchio, G.; Fusco, A. Minireview: RET: normal and abnormal functions. *Endocrinology* **2004**, *145*, 5448–5451.
- ¹⁹ Glick, S. D.; Maisonneuve, I. M.; Szumlinski, K. K. 18-Methoxycoronaridine (18-MC) and ibogaine: Comparison of antiaddictive efficacy, toxicity, and mechanisms of action. *Ann. N.Y. Acad. Sci.* **2000**, *914*, 369–386.
- ²⁰ (a) Popik, P.; Layer, R. T.; Skolnick, P. 100 Years of ibogaine: Neurochemical and pharmacological actions of a putative anti-addictive drug. *Pharm. Rev.* **1995**, *47*(2), 235–253. (b) Sershen, H.; Hashim, A.; Lajtha, A. Chapter 6. Characterization of multiple sites of action of ibogaine. In *The Alkaloids: Chemistry and Biology* **2001**, *56*, 115–133. (c) Alper, K. R. Chapter 1. Ibogaine: A review. In *The Alkaloids: Chemistry and Biology* **2001**, *56*, 1–38.
- ²¹ (a) Bowen, W. D.; Vilner, B. J.; Williams, W.; Bertha, C. M.; Kuehne, M. E.; Jacobson, A. E. Ibogaine and its congeners are sigma 2 receptor-selective ligands with moderate affinity. *Eur. J. Pharmacol.* **1995**, *279*, R1–R3. (b) Bowden, W. D. Chapter 9. Sigma Receptors And Iboga Alkaloids. *The Alkaloids: Chemistry and Biology*. **2001**, *56*, 173–191.
- ²² Obach, R. S.; Pablo, J.; Mash, D. C. Cytochrome P4502D6 catalyzes the O-demethylation of the psychoactive alkaloid ibogaine to 12-hydroxyibogamine. *Drug. Metab. Dispos.* **1998**, *26*, 764–768.
- ²³ (a) Glick, S. D.; Maisonneuve, I. M.; Hough, L. B.; Kuehne, M. E.; Bandarage, U. K. (±)-18-Methoxycoronaridine: A novel *Iboga* alkaloid congener having potential anti-addictive efficacy. *CNS Drug Rev.* **1999**, *5*(1), 27–42. (b) Maisonneuve, I. M.; Glick, S. D. Anti-addictive actions of an *iboga* alkaloid congener: a novel mechanism for a novel treatment. *Pharmacol. Biochem. Behav.* **2003**, *75*(3), 607–618. (c) Glick, S. D.; Kuehne, M. E.; Maisonneuve, I. M.; Bandarage, U. K.; Molinari, H. H. 18-Methoxycoronaridine, a non-toxic *iboga* alkaloid congener: effects on morphine and cocaine self-administration and on mesolimbic dopamine release in rats. *Brain Res.* **1996**, *719*(1-2), 29–35.
- ²⁴ Carnicella, S.; He, D.-Y.; Yowell, Q. V.; Glick, S. D.; Ron, D. Noribogaine, but not 18-MC, exhibits similar actions as ibogaine on GDNF expression and ethanol self-administration. *Addict. Biol.* **2010**, *15*, 424–433.
- ²⁵ He, D.-Y.; McGough, N. N. H.; Ravindranathan, A.; Jeanblanc, J.; Logrip, M. L.; Phamluong, K.; Janak, P. H.; Ron, D. Glial cell line-derived neurotrophic factor mediates the desirable actions of the anti-addiction drug ibogaine against alcohol consumption. *J. Neurosci.* **2005**, *25*, 619–628.
- ²⁶ He, D.-Y.; Ron, D. Autoregulation of glial cell line-derived neurotrophic factor expression: implications for the long-lasting actions of the anti-addiction drug, Ibogaine. *FASEB J.* **2006**, *20*, E1820–E1827.

-
- ²⁷ Sherer, T. B.; Fiske, B. K.; Svendsen, C. N.; Lang, A. E.; Langston, J. W. Crossroads in GDNF therapy for Parkinson's disease. *Mov. Disord.* **2006**, *21*, 136–141.
- ²⁸ Saavedra, A.; Baltazar, G.; Duarte, E. P. Driving GDNF expression: The green and the red traffic lights. *Prog. Neurobio.* **2008**, *86*, 186–215.
- ²⁹ Tokugawa, K.; Yamamoto, K.; Nishiguchi, M.; Sekine, T.; Sakai, M.; Ueki, T.; Chaki, S.; Okuyama, S. XIB4035, a novel nonpeptidyl small molecule agonist for GFR α -1. *Neurochem. Int.* **2003**, *42*, 81–86.
- ³⁰ Esposito, C. L.; D'Alessio, A.; de Franciscis, V.; Cerchia, L. A cross-talk between TrkB and Ret tyrosine kinases receptors mediates neuroblastoma cells differentiation. *PloS One* **2008**, *3*, e1643.
- ³¹ Maruyama, W.; Nitta, A.; Shamoto-Nagai, M.; Hirata, Y.; Akao, Y.; Yodim, M.; Furukawa, S.; Nabeshima, T.; Naoi, M. *N*-Propargyl-1 (R)-aminoindane, rasagiline, increases glial cell line-derived neurotrophic factor (GDNF) in neuroblastoma SH-SY5Y cells through activation of NF- κ B transcription factor. *Neurochem. Int.*, **2004**, *44*, 393–400.
- ³² Wiesenhofer, B.; Stockhammer, G.; Kostron, H.; Maier, H.; Hinterhuber, H.; Humpel, C. Glial cell line-derived neurotrophic factor (GDNF) and its receptor (GFR- α 1) are strongly expressed in human gliomas. *Acta Neuropathol.* **2000**, *99*, 131–137.
- ³³ Nishiguchi, M.; Tokugawa, K.; Yamamoto, K.; Akama, T.; Nozawa, Y.; Chaki, S.; Ueki, T.; Kameo, K.; Okuyama, S. Increase in secretion of glial cell line-derived neurotrophic factor from glial cell lines by inhibitors of vacuolar ATPase. *Neurochem. Int.* **2003**, *42*, 493–498.
- ³⁴ Grobбен, B.; De Deyn, P. P.; Slegers, H. Rat C6 glioma as experimental model system for the study of glioblastoma growth and invasion. *Cell Tissue Res.* **2002**, *310*, 257–270.
- ³⁵ Caumont, A.-S.; Octave, J.-N.; Hermans, E. Amantadine and memantine induce the expression of the glial cell line-derived neurotrophic factor in C6 glioma cells. *Neurosci. Lett.* **2006**, *394*, 196–201.
- ³⁶ Caumont, A.-S.; Octave, J.-N.; Hermans, E. Specific regulation of rat glial cell line-derived neurotrophic factor gene expression by riluzole in C6 glioma cells. *J. Neurochem.* **2006**, *97*, 128–139.
- ³⁷ Shao, Z.; Dyck, L. E.; Wang, H.; Li, X.-M. Antipsychotic drugs cause glial cell line-derived neurotrophic factor secretion from C6 glioma cells. *J. Psychiatry Neurosci.* **2006**, *31*, 32–37.
- ³⁸ Hisaoka, K.; Nishida, A.; Koda, T.; Miyata, M.; Zensho, H.; Morinobu, S.; Ohta, M.; Yamawaki, S. Antidepressant drug treatments induce glial cell line-derived neurotrophic factor (GDNF) synthesis and release in rat C6 glioblastoma cells. *J. Neurochem.* **2001**, *79*, 25–34.

- ³⁹ Golan, M.; Schreiber, G.; Avissar, S. Antidepressants elevate GDNF expression and release from C6 glioma cells in a β -arrestin1-dependent, CREB interactive pathway. *Int. J. Neuropsychopharmacol.* **2011**, *14*, 1289–1300.
- ⁴⁰ (a) Verity, A. N.; Wyatt, T. L.; Hajos, B.; Eglen, R. M.; Baecker, P. A.; Johnson, R. M. Regulation of glial cell line-derived neurotrophic factor release from rat C6 glioblastoma cells. *J. Neurochem.* **1998**, *70*, 531–539. (b) Verity, A. N.; Wyatt, T. L.; Lee, W.; Hajos, B.; Baecker, P. A.; Eglen, R. M.; Johnson, R. M. Differential regulation of glial cell line-derived neurotrophic factor (GDNF) expression in human neuroblastoma and glioblastoma cell lines. *J. Neurosci. Res.* **1999**, *55*, 187–197.
- ⁴¹ (a) Daub, H.; Wallasch, C.; Lankenau, A.; Herrlich, A.; Ullrich, A. Signal characteristics of G protein-transactivated EGF receptor. *EMBO J.* **1997**, *16*, 7032–7044. (b) Fisher, O. M.; Hart, S.; Ullrich, A. Dissecting the epidermal growth factor receptor signal transactivation pathway. *Methods Mol. Biol.* **2006**, *327*, 85–97.
- ⁴² Malarkey, K.; Belham, C. M.; Paul, A.; Graham, A.; McLees, A.; Scott, P. H.; Plevin, R. The regulation of tyrosine kinase signalling pathways by growth factor and G-protein-coupled receptors. *Biochem. J.* **1995**, *309*, 361–375. (b) Lee, F. S.; Rajagopal, R.; Chao, M. V. Distinctive features of Trk neurotrophin receptor transactivation by G protein-coupled receptors. *Cytokine Growth Factor Rev.* **2002**, *13*, 11–17. (c) Shah, B. H.; Catt, K. J. GPCR-mediated transactivation of RTKs in the CNS: mechanisms and consequences. *Trends Neurosci.* **2004**, *27*, 48–53. (d) Piiper, A.; Zeuzem, S. Receptor tyrosine kinases are signaling intermediates of G protein-coupled receptors. *Curr. Pharm. Des.* **2004**, *10*, 3539–3545.
- ⁴³ (a) Wetzker, R.; Böhmer, F.-D. Transactivation joins multiple tracks to the ERK/MAPK cascade. *Nat. Rev. Mol. Cell. Biol.* **2003**, *4*, 651–657. (b) Werry, T. D.; Sexton, P. M.; Christopoulos, A. ‘Ins and outs’ of seven-transmembrane receptor signalling to ERK. *Trends Endocrin. Met.* **2005**, *16*, 26–33.
- ⁴⁴ (a) Hisoaka, K.; Nishida, A.; Takebayashi, M.; Koda, T.; Yamawaki, S.; Nakata, Y. Serotonin increases glial cell line-derived neurotrophic factor release in rat C6 glioblastoma cells. *Brain Res.* **2004**, *1002*, 167–170. (b) Tsuchioka, M.; Takebayashi, M.; Hisoaka, K.; Maeda, N.; Nakata, Y. Serotonin (5-HT) induces glial cell line-derived neurotrophic factor (GDNF) mRNA expression via the transactivation of fibroblast growth factor receptor 2 (FGFR2) in rat C6 glioma cells. *J. Neurochem.* **2008**, *106*, 244–257.
- ⁴⁵ Whitty, A.; Borysenko, C. W. Small molecule cytokine mimetics. *Chem. Biol.* **1999**, *6*, R107–R118.
- ⁴⁶ (a) Jang, S.-W.; Liu, X.; Chan, C.-B.; Weinshenker, D.; Hall, R. A.; Xiao, G.; Ye, K. Amitriptyline is a TrkA and TrkB receptor agonist that promotes TrkA/TrkB heterodimerization and has potent neurotrophic activity. *Chem. Biol.* **2009**, *16*, 644–656. (b) Jang, S.-W.; Liu, X.; Yepes, M.; Shepherd, K. R.; Miller, G. W.; Liu, Y.; Wilson, W. D.; Xiao, G.; Blanchi, B.; Sun, Y. E.; Ye, K. A selective TrkB agonist with potent neurotrophic activities

- by 7,8-dihydroxyflavone. *Proc. Nat. Acad. Sci. U.S.A.* **2010**, *107*, 2687–2692. (c) Massa, S. M.; Yang, T.; Xie, Y.; Shi, J.; Bilgen, M.; Joyce, J. N.; Nehama, D.; Rajadas, J.; Longo, F. M. Small molecule BDNF mimetics activate TrkB signaling and prevent neuronal degeneration in rodents. *J. Clin. Invest.* **2010**, *120*(5), 1774–1785. (d) Jang, S.-W.; Liu, X.; Chan, C. B.; France, S. A.; Sayeed, I.; Tang, W.; Lin, X.; Xiao, G.; Andero, R.; Chang, Q.; Ressler, K. J.; Ye, K. Deoxygedunin, a natural product with potent neurotrophic activity in mice. *PloS One* **2010**, *5*, e11528. (e) Jang, S.-W.; Liu, X.; Pradoldej, S.; Tosini, G.; Chang, Q.; Iuvone, P. M.; Ye, K. *N*-acetylserotonin activates TrkB receptor in a circadian rhythm. *Proc. Nat. Acad. Sci. U.S.A* **2010**, *107*, 3876–3881.
- ⁴⁷ (a) Pirrung, M. C.; Deng, L.; Lin, B.; Webster, N. J. G. Quinone replacements for small molecule insulin mimics. *ChemBioChem* **2008**, *9*, 360–362. (b) Lin, B.; Li, Z.; Park, K.; Deng, L.; Pai, A.; Zhong, L.; Pirrung, M. C.; Webster, N. J. G. Identification of novel orally available small molecule insulin mimetics. *J. Pharmacol. Exp. Ther.* **2007**, *323*(2), 579–585.
- ⁴⁸ (a) Tian, S.-S.; Lamb, P.; King, A. G.; Miller, S. G.; Kessler, L.; Luengo, J. I.; Averill, L.; Johnson, R. K.; Gleason, J. G.; Pelus, L. M.; Dillon, S. B.; Rosen, J. A small, nonpeptidyl mimic of granulocyte-colony-stimulating factor. *Science* **1998**, *281*, 257–259. (b) Kusano, K.; Ebara, S.; Tachibana, K.; Nishimura, T.; Sato, S.; Kuwaki, T.; Taniyama, T. A potential therapeutic role for small nonpeptidyl compounds that mimic human granulocyte colony-stimulating factor. *Blood* **2004**, *103*, 836–842.
- ⁴⁹ Massa, S. M.; Xie, Y.; Yang, T.; Harrington, A. W.; Kim, M. L.; Yoon, S. O.; Kraemer, R.; Moore, L. A.; Hempstead, B. L.; Longo, F. M. Small, nonpeptide p75NTR ligands induce survival signaling and inhibit proNGF-induced death. *J. Neurosci.* **2006**, *26*, 5288–5300.
- ⁵⁰ Lin, B.; Pirrung, M.; Deng, L.; Li, Z. Neuroprotection by small molecule activators of the nerve growth factor receptor. *J. Pharmacol. Exp. Ther.* **2007**, *322*, 59–69.
- ⁵¹ Freidinger, R. M. Nonpeptidic ligands for peptide and protein receptors. *Curr. Opin. Chem. Biol.* **1999**, *3*, 395–406.
- ⁵² Vilner, B. J.; John, C. S.; Bowen, W. D. Sigma-1 and sigma-2 receptors are expressed in a wide variety of human and rodent tumor cell lines. *Cancer Res.* **1995**, *55*, 408–413.
- ⁵³ Barg, J.; Thomas, G. E.; Bem, W. T.; Parnes, M. D.; Ho, A. M.; Belcheva, M. M.; McHale, R. J.; McLachlan, J. A.; Tolman, K. C.; Johnson, F. E. In vitro and in vivo expression of opioid and sigma receptors in rat C6 glioma and mouse N18TG2 neuroblastoma cells. *J. Neurochem.* **1994**, *63*, 570–574.
- ⁵⁴ Guitart, X.; Codony, X.; Monroy, X. Sigma receptors: biology and therapeutic potential. *Psychopharmacology* **2004**, *174*, 301–319.
- ⁵⁵ Hayashi, T.; Su, T.-P. Sigma-1 receptor chaperones at the ER-mitochondrion interface regulate Ca(2+) signaling and cell survival. *Cell* **2007**, *131*, 596–610.

- ⁵⁶ (a) Snyder, S. H.; Largent, B. L. Receptor mechanisms in antipsychotic drug action: focus on σ receptors. *J Neuropsychiatry* **1989**, *1*, 7–15. (b) Ishikawa, M.; Hashimoto, K. The role of sigma-1 receptors in the pathophysiology of neuropsychiatric diseases. *J. Receptor Ligand Channel Res.* **2010**, *3*, 25–36. (b) Kourrich, S.; Su, T.-P.; Fujimoto, M.; Bonci, A. The sigma-1 receptor: roles in neuronal plasticity and disease. *Trends Neurosci.* **2012**, 1–10.
- ⁵⁷ Morin-Surun, M. P.; Collin, T.; Denavit-Saubié, M.; Baulieu, E. E.; Monnet, F. P. Intracellular sigma1 receptor modulates phospholipase C and protein kinase C activities in the brainstem. *Proc. Nat. Acad. Sci. U.S.A* **1999**, *96*, 8196–8199.
- ⁵⁸ Tan, F.; Guio-Aguilar, P. L.; Downes, C.; Zhang, M.; O'Donovan, L.; Callaway, J. K.; Crack, P. J. The σ 1 receptor agonist 4-PPBP elicits ERK1/2 phosphorylation in primary neurons: a possible mechanism of neuroprotective action. *Neuropharmacology* **2010**, *59*, 416–424.
- ⁵⁹ Penas, C.; Pascual-Font, A.; Mancuso, R.; Forés, J.; Casas, C.; Navarro, X. Sigma receptor agonist 2-(4-morpholinethyl)1 phenylcyclohexanecarboxylate (Pre084) increases GDNF and BiP expression and promotes neuroprotection after root avulsion injury. *J. Neurotrauma* **2011**, *28*, 831–840.
- ⁶⁰ Fujimoto, M.; Hayashi, T.; Urfer, R.; Mita, S.; Su, T.-P. Sigma-1 receptor chaperones regulate the secretion of brain-derived neurotrophic factor. *Synapse* **2012**, *66*, 630–639.
- ⁶¹ Kikuchi-Utsumi, K.; Nakaki, T. Chronic treatment with a selective ligand for the sigma-1 receptor chaperone, SA4503, up-regulates BDNF protein levels in the rat hippocampus. *Neurosci. Lett.* **2008**, *440*, 19–22.
- ⁶² (a) Vilner, B. J.; Bowen, W. D. Sigma receptor-active neuroleptics are cytotoxic to C6 glioma cells in culture. *Eur. J. Pharm.* **1993**, *244*, 199–201. (b) Vilner, B. J.; de Costa, B. R.; Bowen, W. D. Cytotoxic effects of sigma ligands: sigma receptor-mediated alterations in cellular morphology and viability. *J. Neurosci.* **1995**, *15*, 117–134. (c) Colabufo, N. A.; Berardi, F.; Contino, M.; Niso, M.; Abate, C.; Perrone, R.; Tortorella, V. Antiproliferative and cytotoxic effects of some sigma2 agonists and sigma1 antagonists in tumour cell lines. *Naunyn-Schmiedeberg's Arch. Pharmacol.* **2004**, *370*, 106–113. (d) Zeng, C.; Rothfuss, J.; Zhang, J.; Chu, W.; Vangveravong, S.; Tu, Z.; Pan, F.; Chang, K. C.; Hotchkiss, R.; Mach, R. H. Sigma-2 ligands induce tumour cell death by multiple signalling pathways. *Br. J. Cancer* **2012**, *106*, 693–701.
- ⁶³ Xu, J.; Zeng, C.; Chu, W.; Pan, F.; Rothfuss, J. M.; Zhang, F.; Tu, Z.; Zhou, D.; Zeng, D.; Vangveravong, S.; Johnston, F.; Spitzer, D.; Chang, K. C.; Hotchkiss, R. S.; Hawkins, W. G.; Wheeler, K. T.; Mach, R. H. Identification of the PGRMC1 protein complex as the putative sigma-2 receptor binding site. *Nature Comm.* **2011**, *2*, 380.
- ⁶⁴ Ahmed, I. S.; Rohe, H. J.; Twist, K. E.; Craven, R. J. Pgrmc1 (progesterone receptor membrane component 1) associates with epidermal growth factor receptor and regulates erlotinib sensitivity. *J. Biol. Chem.* **2010**, *285*, 24775–24782.

-
- ⁶⁵ Lange, M. S.; Stampfl, A.; Hauck, S. M.; Zischka, H.; Gloeckner, C. J.; Deeg, C. A.; Ueffing, M. Membrane-initiated effects of progesterone on calcium dependent signaling and activation of VEGF gene expression in retinal glial cells. *Glia* **2007**, *1073*, 1061–1073.
- ⁶⁶ Su, C.; Cunningham, R. L.; Rybalchenko, N.; Singh, M. Progesterone increases the release of brain-derived neurotrophic factor from glia via progesterone receptor membrane component 1 (Pgrmc1)-dependent ERK5 signaling. *Endocrinology* **2012**, *153*, 4389–4400.
- ⁶⁷ Takebayashi, M.; Hayashi, T.; Su, T.; Unit, C. P.; Neurobiology, C. Nerve Growth Factor-Induced Neurite Sprouting in PC12 Cells Involves Sigma-1 Receptors : Implications for Antidepressants. *J. Pharmacol. Exp. Ther.* **2002**, *303*, 1227–1237.
- ⁶⁸ Hung, J.-H.; Su, I.-J.; Lei, H.-Y.; Wang, H.-C.; Lin, W.-C.; Chang, W.-T.; Huang, W.; Chang, W.-C.; Chang, Y.-S.; Chen, C.-C.; Lai, M.-D. Endoplasmic reticulum stress stimulates the expression of cyclooxygenase-2 through activation of NF-kappaB and pp38 mitogen-activated protein kinase. *J. Biol. Chem.* **2004**, *279*, 46384–46392.
- ⁶⁹ Shweiki, D.; Neeman, M.; Itin, A.; Keshhet, E. Induction of vascular endothelial growth factor expression by hypoxia and by glucose deficiency in multicell spheroids: Implications for tumor angiogenesis. *Proc. Natl. Acad. Sci. U.S.A.* **1995**, *92*, 768–772.
- ⁷⁰ Marjon, P. L.; Bobrovnikova-Marjon, V.; Abcouwer, S. F. Expression of the pro-angiogenic factors vascular endothelial growth factor and interleukin-8/CXCL8 by human breast carcinomas is responsive to nutrient deprivation and endoplasmic reticulum stress. *Mol. Cancer* **2004**, *3*, 4–16.
- ⁷¹ Ostensfeld, M. S.; Fehrenbacher, N.; Høyer-Hansen, M. et. al. Effective tumor cell death by s-2 receptor ligand siramesine involves lysosomal leakage and oxidative stress. *Cancer Res.* **2005**, *65*, 8975–8983.
- ⁷² Ostensfeld, M. S.; Høyer-Hansen, M.; Bastholm, L.; Fehrenbacher, N.; Olsen, O. D.; Groth, L.; Puustinen, P.; Kirkegaard-Sørensen, T.; Nylandsted, J.; Farkas, T.; Jäättelä, M. Anti-cancer agent siramesine is a lysosomotropic detergent that induces cytoprotective autophagosome accumulation. *Autophagy* **2008**, *4*, 487–499.
- ⁷³ Hornick, J. R.; Vangveravong, S.; Spitzer, D.; Abate, C.; Berardi, F.; Goedegebuure, P.; Mach, R. H.; Hawkins, W. G. Lysosomal membrane permeabilization is an early event in sigma-2 receptor ligand mediated cell death in pancreatic cancer. *J. Exp. Clin. Canc. Res.* **2012**, *31*, 41.
- ⁷⁴ (a) Song, H.; Moon, A. Glial cell-derived neurotrophic factor (GDNF) promotes low-grade Hs683 glioma cell migration through JNK, ERK-1/2 and p38 MAPK signaling pathways. *Neurosci. Res.* **2006**, *56(1)*, 29–38. (b) Wan, G.; Too, H.-P. A specific isoform of glial cell line-derived neurotrophic factor family receptor alpha 1 regulates RhoA expression and glioma cell migration. *J. Neurochem.* **2010**, *115*, 759–770.

-
- ⁷⁵ Paratcha, G.; Ledda, F.; Ibáñez, C. F. The neural cell adhesion molecule NCAM is an alternative signaling receptor for GDNF family ligands. *Cell* **2003**, *113*, 867–869.
- ⁷⁶ Nishimoto, S.; Nishida, E. MAPK signaling: ERK5 versus ERK1/2. *EMBO reports* **2006**, *7*, 782–786.
- ⁷⁷ Mody, N.; Leitch, J.; Armstrong, C.; Dixon, J.; Cohen, P. Effects of MAP kinase cascade inhibitors on the MKK5/ERK5 pathway. *FEBS Lett.* **2001**, *502*, 21–24.
- ⁷⁸ Bain, J.; Plater, L.; Elliott, M.; Shpiro, N.; Hastie, J.; McLauchlan, H.; Klevernic, I.; Arthur, J. S. C.; Alessi, D. R.; Cohen, P. The selectivity of protein kinase inhibitors: a further update. *Biochem. J.* **2007**, *408*, 297–315.
- ⁷⁹ Wei, J.-W.; Yeh, S.-R.; Cheng, C.-L. Characterization of 3H-serotonin (5-HT) binding and effects on the phosphoinositides (PI) turnover in cultured C6 glioma and N2 neuroblastoma cells from rodents. *Chin. J. Physiol.* **1992**, *35*(3), 227–239.
- ⁸⁰ (a) Bohn, L. M.; Belcheva, M. M.; Coscia, C. J. Mitogenic signaling via endogenous κ -opioid receptors in C6 glioma cells. *J. Neurochem.* **2000**, *74*, 564–573. (b) Bohn, L. M.; Belcheva, M. M.; Coscia, C. J. μ -Opioid agonist inhibition of κ -opioid receptor-stimulated extracellular signal-regulated kinase phosphorylation is dynamin-dependent in C6 glioma cells. *J. Neurochem.* **2000**, *74*, 574–581.
- ⁸¹ Belcheva, M. M.; Haas, P. D.; Tan, Y.; Heaton, V. M.; Coscia, C. J. The fibroblast growth factor receptor is at the site of convergence between μ -opioid receptor and growth factor signaling pathways in rat C6 glioma cells. *J. Pharmacol. Exp. Ther.* **2002**, *303*, 909–918.
- ⁸² Chien, C.-C.; Pasternak, G. W. Sigma antagonists potentiate opioid analgesia in rats. *Neurosci. Lett.* **1995**, *190*, 137–139.
- ⁸³ Castillo, C. A.; Albasanz, J. L.; Fernández, M.; Martín, M. Endogenous expression of adenosine A₁, A₂ and A₃ receptors in rat C6 glioma cells. *Neurochem. Res.* **2007**, *32*, 1056–1070.
- ⁸⁴ Yamagata, K.; Hakata, K.; Maeda, A.; Mochizuki, C.; Matsufuji, H.; Chino, M.; Yamori, Y. Adenosine induces expression of glial cell line-derived neurotrophic factor (GDNF) in primary rat astrocytes. *Neurosci. Res.* **2007**, *59*, 467–474.
- ⁸⁵ Flajolet, M.; Wang, Z.; Futter, M.; Shen, W.; Nuangchamnong, N.; Bendor, J.; Wallach, I.; Nairn, A. C.; Surmeier, D. J.; Greengard, P. FGF acts as a co-transmitter through adenosine A_{2A} receptor to regulate synaptic plasticity. *Nat. Neurosci.* **2008**, *11*(12), 1402–1409.
- ⁸⁶ (a) Ikesue, H.; Kataoka, Y.; Kawachi, R.; Dohgu, S.; Shuto, H.; Oishi, R. Cyclosporine enhances α 1-adrenoceptor mediated nitric oxide production in C6 glioma cells. *Eur. J. Pharm.* **2000**, *407*, 221–226. (b) Fishman, P. H.; Miller, T.; Curran, P. K.; Feussner, G. K.

- Independent and coordinate regulation of $\beta 1$ and $\beta 2$ -adrenergic receptors in rat C6 glioma cells. *J. Rec. Res.* **1994**, *14*(5), 281–296.
- ⁸⁷ Chen, J.; Rasenick, M. M. Chronic treatment of C6 glioma cells with antidepressant drugs increases functional coupling between a G protein (G_s) and adenylyl cyclase. *J. Neurochem.* **1995**, *64*, 724–732.
- ⁸⁸ Rivera, E. et. al. AT1 receptor is present in glioma cells; its blockage reduces the growth of rat glioma cells. *Br J Cancer* **2001**, *85*(9), 1396–1399.
- ⁸⁹ Clark, M. A.; Gonzalez, N. Angiotensin II stimulates rat astrocyte mitogen-activated protein kinase activity and growth through EGF and PDGF receptor transactivation. *Reg. Pept.* **2007**, *144*, 115–122.
- ⁹⁰ Couraud, P.-O.; Durieu-Trautmann, O.; Nguyen, D. L.; Marin, P.; Gilbert, F.; Strosberg, A. D. Functional endothelin-1 receptors in rat astrocytoma C6. *Eur. J. Pharmacol.* **1991**, *206*(3), 191–198.
- ⁹¹ (a) Wan-Wan, L.; Kiang, J. G.; Chuang, D.-M. Pharmacological characterization of endothelin-stimulated phosphoinositide breakdown and cytosolic free Ca^{2+} rise in rat C6 glioma cells. *J. Neurosci.* **1992**, *12*(3), 1077–1085. (b) Sedo, A.; Malík, R.; Vlášicová K, Rovero P. Calcium-mediated endothelin signaling in C6 rat glioma cells. *Neuropeptides* **1993**, *33*(1), 13–17.
- ⁹² Cramer, H.; Schmenger, K.; Heinrich, K.; Horstmeyer, A.; Böning, H.; Breit, A.; Piiper, A.; Lundstrom, K.; Müller-Esterl, W.; Schroeder, C. Coupling of endothelial receptors to ERK/MAP kinase pathway. Roles of palmitoylation and $G\alpha_q$. *Eur. J. Biochem.* **2001**, *268*(20), 5449–5459.
- ⁹³ Koyama, Y.; Tsujikawa, K.; Matsuda, T.; Baba, A. Endothelin-1 stimulates glial cell line-derived neurotrophic factor expression in cultured rat astrocytes. *Biochem. Biophys. Res. Comm.* **2003**, *303*, 1101–1105.
- ⁹⁴ (a) Tyndale, R. F.; Hales, T. G.; Olsen, R. W.; Tobin, A. J. Distinctive patterns of GABA_A receptor subunit mRNAs in 13 cell lines. *J. Neurosci.* **1994**, *14*(9), 5417–5428. (b) Hales, T. G.; Tyndale, R. F. Few cell lines with GABA_A mRNAs have functional receptors. *J. Neurosci.* **1994**, *14*(9), 5429–5436.
- ⁹⁵ Baraldi, M.; Guidotti, A.; Schwartz, J. P.; Costa, E. GABA receptors in clonal cell lines: A model for study of benzodiazepine action at a molecular level. *Science* **1979**, *205*, 821–823.
- ⁹⁶ Maurice, T.; Phan, V.-L.; Urani, A.; Kamei, H.; Noda, Y.; Nabeshima, T. Neuroactive neurosteroids as endogenous effectors for the sigma1 ($\sigma 1$) receptor: Pharmacological evidence and therapeutic opportunities. *Jpn. J. Pharmacol.* **1999**, *81*, 125–155.

-
- ⁹⁷ Duveau, V.; Laustela, S.; Barth, L.; Gianolini, F.; Vogt, K. E.; Keist, R.; Chandra, D.; Homanics, G. E.; Rudolph, U.; Fritschy, J.-M. Spatiotemporal specificity of GABA_A receptor-mediated regulation of adult hippocampal neurogenesis. *Eur. J. Neurosci.* **2011**, *34*(3), 362–373.
- ⁹⁸ (a) Peakman, M.-C.; Hill, S. J. Endogenous expression of histamine H1 receptors functionally coupled to phosphoinositide hydrolysis in C6 glioma cells: regulation by cyclic AMP. *Br. J. Pharmacol.* **1994**, *113*, 1554–1560. (b) Tseng, C.-L.; Wei, J.-W. Investigation on signal transduction pathways after H1 receptor activated by histamine in C6 glioma cells: Involvement of phosphatidylinositol and arachidonic acid metabolisms. *J. Chin. Med. Assoc.* **2012**, *75*, 143–150.
- ⁹⁹ Viwatpinyo, K.; Chongthammakun, S. Activation of group I metabotropic glutamate receptors leads to brain-derived neurotrophic factor expression in rat C6 cells. *Neurosci. Lett.* **2009**, *467*, 127–130.
- ¹⁰⁰ Yao, H. H.; Ding, J. H.; Zhou, F.; Wang, F.; Hu, L. F.; Sun, T.; Hu, G. Enhancement of glutamate uptake mediates the neuroprotection exerted by activating group II or III metabotropic glutamate receptors on astrocytes. *J. Neurochem.* **2005**, *92*, 948–961.
- ¹⁰¹ Battaglia, G.; Molinaro, G.; Rizzo, B.; Storto, M.; Busceti, C. L.; Spinsanti, P.; Bucci, D.; Di Liberto, V.; Mudo, G.; Corti, C.; Corsi, M.; Nicoletti, F.; Belluardo, N.; Bruno, V. Activation of mGlu3 receptors stimulates the production of GDNF in striatal neurons. *PLoS One* **2009**, *4*(8), e6591.
- ¹⁰² Taylor, S.; Srinivasan, B.; Wordinger, R. J.; Roque, R. S. Glutamate stimulates neurotrophin expression in cultured Muller cells. *Brain Res.* **2003**, *111*(1-2), 189–197.
- ¹⁰³ Armstrong, K. J.; Niles, L. P. Induction of GDNF mRNA expression by melatonin in rat C6 glioma cells. *Neuroreport* **2002**, *13*, 473–475.
- ¹⁰⁴ Das, A.; Belagodu, A.; Reiter, R. J.; Ray, S. K.; Banik, N. L. Cytoprotective effects of melatonin on C6 astroglial cells exposed to glutamate toxicity and oxidative stress. *J. Pineal Res.* **2008**, *45*, 117–124.
- ¹⁰⁵ Rincón Castro, L. M.; Gallant, M.; Niles, L. P. Novel targets for valproic acid: up-regulation of melatonin receptors and neurotrophic factors in C6 glioma cells. *J. Neurochem.* **2005**, *95*, 1227–1236.
- ¹⁰⁶ Tang, Y. P.; Mia, Y. L.; Chao, C. C.; Chen, K. Y.; Lee, E. H. Y. Enhanced glial cell line-derived neurotrophic factor mRNA expression upon (-)-deprenyl and melatonin treatments. *J. Neurosci. Res.* **1998**, *53*, 593–604.
- ¹⁰⁷ Pinkas-Kramarski, R.; Edelman, R.; Stein, R. Indications for selective coupling to phosphoinositide hydrolysis or to adenylate cyclase inhibition by endogenous muscarinic

-
- receptor subtypes M3 and M4 but not by M2 in tumor cell lines. *Neurosci. Lett.* **1990**, *108*(3), 335–340.
- ¹⁰⁸ (a) Budd, D. C.; Willars, G. B.; McDonald, J. E.; Tobin, A. B. Phosphorylation of the Gq/11-coupled M3-muscarinic receptor is involved in receptor activation of the ERK-1/2 mitogen-activated protein kinase pathway. *J. Biol. Chem.* **2001**, *276*, 4581–4587. (b) Kim, J. Y.; Yang, M. S.; Oh, C. D.; Kim, K. T.; Ha, M. J.; Kang, S. S.; Chun, J. S. Signalling pathway leading to an activation of mitogen-activated protein kinase by stimulating M3 muscarinic receptor. *Biochem. J.* **1999**, *337*(Pt2), 275–280.
- ¹⁰⁹ (a) Jaiswal, N.; Diz, D. I.; Tallant, E. A.; Khosla, M. C.; Ferrario, C. M. Characterization of angiotensin receptors mediating prostaglandin synthesis and release in C6 glioma cells. *Am. J. Physiol. Regul. Integr. Comp. Physiol.* **1991**, *260*, R1000–R1006. (b) Kitanaka, J.; Hashimoto, H.; Gotoh, M.; Kondo, K.; Sakata, K.; Hirasawa, Y.; Sawada, M.; Suzumura, A.; Marunouchi, T.; Matsuda, T.; Baba, A. Expression pattern of messenger RNAs for prostanoid receptors in glial cell cultures. *Brain Res.* **1996**, *707*(2), 282–287.
- ¹¹⁰ Park, M. K.; Kang, Y. J.; Ha, Y. M.; Jeong, J. J.; Kim, H. J.; Seo, H. G.; Lee, J. H.; Chang, K. C. EP₂ receptor activation by prostaglandin E₂ leads to induction of HO-1 via PKA and PI3K pathways in C6 cells. *Biochem. Biophys. Res. Commun.* **2009**, *379*(4), 1043–1047.
- ¹¹¹ Dal Toso, R.; De Bernardi, M. A.; Brooker, G.; Costa, E.; Mocchetti, I. Beta adrenergic and prostaglandin receptor activation increases nerve growth factor mRNA content in C6-2B rat astrocytoma cells. *J. Pharmacol. Exp. Ther.* **1988**, *246*, 1190–1193.
- ¹¹² Lebman, D. A.; Spiegel, S. Cross-talk at the crossroads of sphingosine-1-phosphate, growth factors, and cytokine signaling. *J. Lipid Res.* **2008**, *49*, 1388–1394.
- ¹¹³ Sato, K.; Tomura, H.; Igarashi, Y.; Ui, M.; Okajima, F. Possible involvement of cell surface receptors in sphingosine 1-phosphate-induced activation of extracellular signal-regulated kinase in C6 glioma cells. *Mol. Pharmacol.* **1999**, *55*, 126–133.
- ¹¹⁴ Vann, L. R.; Payne, S. G.; Edsall, L. C.; Twitty, S.; Spiegel, S.; Milstien, S. Involvement of sphingosine kinase in TNF- α -stimulated tetrahydrobiopterin biosynthesis in C6 glioma cells. *J. Biol. Chem.* **2002**, *277*(15), 12649–12656.
- ¹¹⁵ Mologni, L.; Sala, E.; Cazzaniga, S.; Rostagno, R.; Kuoni, T.; Puttini, M.; Bain, J.; Cleris, L.; Redaelli, S.; Riva, B.; Formelli, F.; Scapozza, L.; Gambacarti-Passerini, C. Inhibition of RET tyrosine kinase by SU5416. *J. Mol. Endocrin.* **2006**, *37*, 199–212.
- ¹¹⁶ Lanzi, C.; Cassinelli, G.; Cuccuru, G.; Zaffaroni, N.; Supino, R.; Vignati, S.; Zanchi, C.; Yamamoto, M.; Zunino, F. Inactivation of Ret/Ptc1 oncoprotein and inhibition of papillary thyroid carcinoma cell proliferation by indolinone RPI-1. *Cell. Mol. Life Sci.* **2003**, *60*, 1449–1459.

-
- ¹¹⁷ Fong, T. A. T.; Shawver, L. K.; Sun, L.; Tang, C.; App, H.; Powell, T. J.; Kim, Y. H.; Schreck, R.; Wang, X.; Risau, W.; Ullrich, A.; Hirth, K. P.; McMahon, G. SU5416 is a potent and selective inhibitor of the vascular endothelial growth factor receptor (Flk-1/KDR) that inhibits tyrosine kinase catalysis, tumor vascularization, and growth of multiple tumor types. *Cancer Res.* **1999**, *59*, 99–106.
- ¹¹⁸ Wang, S. Y.; Chen, B.; Zhan, Y. Q.; Xu, W. X.; Li, C. Y.; Yang, R. F.; Zheng, H.; Yue, P. B.; Larsen, S. H.; Sun, H. B.; Yang, X. SU5416 is a potent inhibitor of hepatocyte growth factor receptor (c-Met) and blocks HGF-induced invasiveness of human HepG2 hepatoma cells. *J. Hepatol.* **2004**, *41*, 267–273.
- ¹¹⁹ Lanzi, C.; Cassinelli, G.; Pensa, T.; Cassinis, M.; Gambetta, R. A.; Borrello, M. G.; Menta, E.; Pierotti, M. A.; Zunino, F. Inhibition of transforming activity of the ret/ptc1 oncoprotein by 2-indolinone derivative. *Int. J. Cancer* **2000**, *85*, 384–390.
- ¹²⁰ Cuccuru, G.; Lanzi, C.; Cassinelli, G.; Pratesi, G.; Tortoreto, M.; Petrangolini, G.; Serengni, E.; Martinetti, A.; Laccabue, D.; Zanchi, C.; Zunino, F. Cellular effects and antitumor activity of RET inhibitor RPI-1 on MEN2A-associated medullary thyroid carcinoma. *J. Natl. Cancer Inst.* **2004**, *96*, 1006–1014.
- ¹²¹ Cassinelli, G.; Lanzi, C.; Petrangolini, G.; Tortoreto, M.; Pratesi, G.; Cuccuru, G.; Laccabue, D.; Supino, R.; Belluco, S.; Favini, E.; Poletti, A.; Zunino, F. Inhibition of c-Met and prevention of spontaneous metastatic spreading by the 2-indolinone RPI-1. *Mol. Cancer Ther.* **2006**, *5*, 2388–2397.
- ¹²² (a) Caumont, A.-S.; Octave, J.-N.; Hermans, E. Specific regulation of rat glial cell line-derived neurotrophic factor gene expression by riluzole in C6 glioma cells. *J. Neurochem.* **2006**, *97*, 128–139. (b) Tsuchioka, M.; Hisoaka, K.; Yano, R.; Shibasaki, C.; Kajitani, Takebayashi, M. Riluzole-induced glial cell line-derived neurotrophic factor production is regulated through fibroblast growth factor receptor signaling in rat C6 glioma cells. *Brain Res.* **2011**, *1384*, 1–8.
- ¹²³ Suter-Crazzolara, C.; Unsicker, K. GDNF mRNA levels are induced by FGF-2 in rat C6 glioblastoma cells. *Mol. Brain Res.* **1996**, *41*, 175–182.
- ¹²⁴ (a) Tanabe, K.; Matsushima-Nishiwaki, R.; Iida, M.; Kozawa, O.; Iida, H. Involvement of phosphatidylinositol 3-kinase/Akt on basic fibroblast growth factor-induced glial cell line-derived neurotrophic factor release from rat glioma cells. *Brain Res.* **2012**, *1463*, 21–29. (b) Obara, Y.; Nemoto, W.; Kohno, S.; Murata, T.; Kaneda, N.; Nakahata, N. Basic fibroblast growth factor promotes glial cell-derived neurotrophic factor gene expression mediated by activation of ERK5 in rat C6 glioma cells. *Cell. Signal.* **2011**, *23*, 666–672.
- ¹²⁵ Evans, S. J.; Choudary, P. V.; Neal, C. R.; Li, J. Z.; Vawter, M. P.; Tomita, H.; Lopez, J. F.; Thompson, R. C.; Meng, F.; Stead, J. D.; Walsh, D. M.; Myers, R. M.; Bunney, W. E.; Watson, S. J.; Jones, E. G.; Akil, H. Dysregulation of the fibroblast growth factor system in major depression. *Proc. Nat. Acad. Sci.* **2004**, *101*(43), 15506–15511.

-
- ¹²⁶ Turner, C. A.; Gula, E. L.; Taylor, L. P.; Watson, S. J.; Akil, H. Antidepressant-like effects of intracerebroventricular FGF2 in rats. *Brain Res.* **2008**, *1224*, 63–68.
- ¹²⁷ Hisoaka, K.; Tsuchioka, M.; Yano, R.; Maeda, N.; Kajitani, N.; Morioka, N.; Nakata, Y.; Takebayashi, M. Tricyclic antidepressant amitriptyline activates fibroblast growth factor receptor signaling in glial cells. *J. Biol. Chem.* **2011**, *286*(24), 21118–21128.
- ¹²⁸ Bachis, A.; Mallei, A.; Cruz, M. I.; Wellstein, A.; Mocchetti, I. Chronic antidepressant treatments increase basic fibroblast growth factor and fibroblast growth factor-binding protein in neurons. *Neuropharmacology* **2008**, *55*, 1114–1120.
- ¹²⁹ Skaper, S. D.; Kee, W. J.; Facci, L.; Macdonald, G.; Doherty, P.; Walsh, F. S. The FGFR1 inhibitor PD 173074 selectively and potently antagonizes FGF-2 neurotrophic and neurotropic effects. *J. Neurochem.* **2000**, *75*, 1520–1527.
- ¹³⁰ Mohammadi, M.; Froum, S.; Hamby, J. M.; Schroeder, M. C.; Panek, R. L.; Lu, G. H.; Eliseenkova, A. V.; Green, D.; Schlessinger, J.; Hubbard, S. R. Crystal structure of an angiogenesis inhibitor bound to the FGF receptor tyrosine kinase domain. *EMBO J.* **1998**, *17*(20), 5896–5904.
- ¹³¹ Millette, E.; Rauch, B. H.; Kenagy, R. D.; Daum, G.; Clowes, A. W. Platelet-derived growth factor-BB transactivates the fibroblast growth factor receptor to induce proliferation in human smooth muscle cells. *Tr. Cardio. Med.* **2006**, *16*(1), 25–28.
- ¹³² Millette, E.; Rauch, B. H.; Defawe, O.; Kenagy, R. D.; Daum, G.; Clowes, A. W. Platelet-derived growth factor-BB-induced human smooth muscle cell proliferation depends on basic FGF release and FGFR-1 activation. *Circ. Res.* **2005**, *96*, 172–179.
- ¹³³ Westermann, R.; Unsicker, K. Basic fibroblast growth factor (bFGF) and rat C6 glioma cells: Regulation of expression, absence of release, and response to exogenous bFGF. *Glia* **1990**, *3*, 510–521.
- ¹³⁴ Tassi, E.; Al-Attar, A.; Aigner, A.; Swift, M. R.; McDonnell, K.; Karavanov, A.; Wellstein, A. Enhancement of fibroblast growth factor (FGF) activity by an FGF-binding protein. *J. Biol. Chem.* **2001**, *276*(43), 40247–40253.
- ¹³⁵ (a) Hutton, L. A.; deVellis, J.; Perez-Polo, J. R. Expression of p75^{NTR} TrkA, and TrkB mRNA in rat C6 glioma and type I astrocyte cultures. *J. Neurosci. Res.* **1992**, *32*, 375–383. (b) Zaheer, A. Expression of mRNAs of multiple growth factors and receptors by astrocytes and glioma cells: Detection with reverse transcription-polymerase chain reaction. *Cell. Mol. Neurobio.* **1995**, *15*(2), 221–237.

-
- ¹³⁶ Weis, C.; Wiesenhofer, B.; Humpel, C. Nerve growth factor plays a divergent role in mediating growth of rat C6 cells via binding to the p75 neurotrophin receptor. *J. Neurooncol.* **2002**, *56*, 59–67.
- ¹³⁷ Strawn, L. M.; Mann, E.; Elliger, S. S.; Chu, L. M.; Germain, L. L.; Niederfellner, G.; Ullrich, A.; Shawver, L. K. Inhibition of glioma cell growth by a truncated platelet-derived growth factor-b receptor. *J. Biol. Chem.* **1994**, *269*(33), 21215–21222.
- ¹³⁸ Lokker, N. A.; Sullivan, C. M.; Hollenbach, S. J.; Israel, M. A.; Giese, N. A. Platelet-derived growth factor (PDGF) autocrine signaling regulates survival and mitogenic pathways in glioblastoma cells: Evidence that the novel PDGF-C and PDGF-D ligands may play a role in the development of brain tumors. *Cancer Res.* **2002**, *62*, 3729–3735.
- ¹³⁹ (a) Lei, H.; Kazlauskas, A. Growth factors outside of the platelet-derived growth factor (PDGF) family employ reactive oxygen species/Src family kinases to activate PDGF receptor α and thereby promote proliferation and survival of cells. *J. Biol. Chem.* **2009**, *284*(10), 6329–6336. (b) Lei, H.; Velez, G.; Kazlauskas, A. Pathological signaling via platelet-derived growth factor receptor α involves chronic activation of Akt and suppression of p53. *Mol. Cell. Biol.* **2011**, *31*(9), 1788–1799.
- ¹⁴⁰ Kovalenko, M.; Gazit, A.; Böhmer, A.; Rorsman, C.; Rönnstrand, L.; Heldin, C.-H.; Waltenberger, J.; Böhmer, F.-D.; Levitzki. Selective platelet-derived growth factor receptor kinase blockers reverse sis-transformation. *Cancer Res.* **1994**, *54*, 6106–6114.
- ¹⁴¹ Gazit, A.; Yee, K.; Uecker, A.; Böhmer, F.-D.; Sjöblom, T.; Östman, A.; Waltenberger, J.; Golomb, G.; Banai, S.; Heinrich, M. C.; Levitzski, A. Tricyclic quinoxalines as potent kinase inhibitors of PDGFR kinase, Flt3 and Kit. *Bioorg. Med. Chem.* **2003**, *11*, 2007–2018.
- ¹⁴² Blásquez, C.; González-Feria, L.; Álvarez, L.; Haro, A.; Casanova, L.; Guzmán, M. Cannabinoids inhibit the vascular endothelial growth factor pathway in gliomas. *Cancer Res.* **2004**, *64*, 5617–5623.
- ¹⁴³ Nakamura, K.; Yamamoto, A.; Kamishohara, M.; Takahashi, K.; Taguchi, E.; Miura, T.; Kubo, K.; Shibuya, M.; Isoe, T. KRN633: A selective inhibitor of vascular endothelial growth factor receptor-2 tyrosine kinase that suppresses tumor angiogenesis and growth. *Mol. Cancer Ther.* **2004**, *3*, 1639–1649.
- ¹⁴⁴ Ward, W. H. J.; Cook, P. N.; Slater, A. M.; Davies, D. H.; Holdgate, G. A.; Green, L. R. Epidermal growth factor receptor tyrosine kinase: Investigation of the catalytic mechanism, structure-based searching and discovery of a potent inhibitor. *Biochem. Pharmacol.* **1994**, *48*(4), 659–666.
- ¹⁴⁵ Levitzki, A.; Gazit, A. Tyrosine kinase inhibition: An approach to drug development. *Science* **1995**, *267*, 1782–1788.

-
- ¹⁴⁶ Yingling, J. M.; Blanchard, K. L.; Sawyer, J. S. Development of TGF- β signaling inhibitors for cancer therapy. *Nat. Rev.* **2004**, *3*, 1011–1022.
- ¹⁴⁷ Dunn, I. F.; Heese, O.; Black, P. McL. Growth factors in glioma angiogenesis: FGFs, PDGF, EGF, and TGFs. *J. Neurooncol.* **2000**, *50*, 121–137.
- ¹⁴⁸ Peterziel, H.; Unsicker, K.; Krieglstein, K. TGF β induces GDNF responsiveness in neurons by recruitment of GFR α 1 to the plasma membrane. *J. Cell Biol.* **2002**, *159*(1), 157–167.
- ¹⁴⁹ Uhl, M.; Aulwurm, S.; Wischhusen, J.; Weiler, M.; Ma, J. Y.; Almirez, R.; Mangadu, R.; Liu, Y.-W.; Platten, M.; Herrlinger, U.; Murphy, A.; Wong, D. H.; Wick, W.; Higgins, L. S.; Weller, M. SD-208, a novel transforming growth factor b receptor I kinase inhibitor, inhibits growth and invasiveness and enhances immunogenicity of murine and human glioma cells *in vitro* and *in vivo*. *Cancer Res.* **2004**, *64*, 7954–7961.
- ¹⁵⁰ Dhandapani, K. M.; Wade, M. F.; Mahesh, V. B.; Brann, D. W. Basic fibroblast growth factor induces TGF- β release in an isoform and glioma-specific manner. *NeuroReport* **2002**, *13*, 239–241.
- ¹⁵¹ (a) Wang, L.-H.; Battey, J. F.; Wada, E.; Lin, J.-T.; Mantey, S.; Coy, D. H.; Jensen, R. T. Activation of neuromedin B-preferring bombesin receptors on rat glioblastoma C6 cells increases cellular Ca²⁺ and phosphoinositides. *Biochem. J.* **1992**, *286*, 641–648. (b) Charlesworth, A.; Rozengurt, E. Bombesin and neuromedin B stimulate the activation of p42(mapk) and p74(raf-1) via a protein kinase C-independent pathway in Rat-1 cells. *Oncogene* **1997**, *14*(19), 2323–2329.
- ¹⁵² Beaumont, K. Rat C6 glioma cells contain type I as well as type II corticosteroid receptors. *Brain Res.* **1985**, *342*(2), 252–258.
- ¹⁵³ Agarwal, M. K. The antigluco-corticoid action of mifepristone. *Pharmacol. Ther.* **1996**, *70*(3), 183–213.
- ¹⁵⁴ Cadepond, F.; Ulmann, A.; Baulieu, E.-E. RU486 (Mifepristone): Mechanisms of action and clinical uses. *Annu. Rev. Med.* **1997**, *48*, 129–156.
- ¹⁵⁵ Huang, H.; Lung, H. L.; Leung, K. N.; Tsang, D. Selective induction of tumor necrosis factor receptor type II gene expression by tumor necrosis factor- α in C6 glioma cells. *Life Sci.* **1998**, *62*(10), 889–896.
- ¹⁵⁶ Saha, R. N.; Liu, X.; Pahan, K. Up-regulation of BDNF in astrocytes by TNF- α : A case for the neuroprotective role of cytokine. *J. Neuroimmune Pharmacol.* **2006**, *1*, 212–222.
- ¹⁵⁷ Niwa, M.; Nitta, A.; Yamada, K.; Nabeshima, T. The roles of glial cell line-derived neurotrophic factor, tumor necrosis factor- α , and an inducer of these factors in drug dependence. *J. Pharmacol. Sci.* **2007**, *104*, 116–121.

-
- ¹⁵⁸ Kuno, R.; Yoshida, Y.; Nitta, A.; Nabeshima, T.; Wang, J.; Sonobe, Y.; Kawanokuchi, J.; Takeuchi, H.; Mizuno, T.; Suzumura, A. The role of TNF- α and its receptors in the production of NGF and GDNF by astrocytes. *Brain Res.* **2006**, *1116*, 12–18.
- ¹⁵⁹ Yu, B.; Becnel, J.; Zerfaoui, M.; Rohatgi, R.; Boulares, A. H.; Nichols, C. D. Serotonin 5-hydroxytryptamine_{2A} receptor activation suppresses tumor necrosis factor- α -induced inflammation with extraordinary potency. *J. Pharmacol. Exp. Ther.* **2008**, *327*, 316–323.
- ¹⁶⁰ Gilmore, D. L.; Liu, Y.; Matsumoto, R. R. Review of the pharmacological and clinical profile of rimcazole. *CNS Drug Rev.* **2004**, *10*(1), 1–22.
- ¹⁶¹ Matsumoto, R. R.; Bowen, W. D.; Tom, M. A.; Vo, V. N.; Truong, D. D.; DeCosta, B. R. Characterization of two novel sigma receptor ligands: antidystonic effects in rats suggest sigma receptor antagonism. *Eur. J. Pharmacol.* **1995**, *280*(3), 301–310.
- ¹⁶² Ghelardini, C.; Galeotti, N.; Bartolini, A. Pharmacological identification of SM-21, the novel sigma(2) antagonist. *Pharmacol. Biochem. Behav.* **2000**, *67*, 659–662.
- ¹⁶³ Chaki, S.; Tanaka, M.; Muramatsu, M.; Otomo, S. NE-100, a novel potent sigma ligand preferentially binds to sigma 1 binding sites in guinea pig brain. *Eur. J. Pharmacol.* **1994**, *251*, R1–R2.
- ¹⁶⁴ Skuza, G.; Rogoz, Z. Effect of BD1047, a sigma1 receptor antagonist, in the animal models predictive of antipsychotic activity. *Pharmacol. Rep.* **2006**, *58*(5), 626–635.
- ¹⁶⁵ Zambon, A. C.; De Costa, B. R.; Kanthasamy, A. G.; Nguyen, B. Q.; Matsumoto, R. R. Subchronic administration of N-[2-(3,4-dichlorophenyl)ethyl]-N-methyl-2-(dimethylamino)ethylamine (BD1047) alters sigma 1 receptor binding. *Eur. J. Pharmacol.* **1997**, *324*(1), 39–47.
- ¹⁶⁶ (a) Luetke, N. C.; Phillips, H. K.; Qiu, T. H.; Copeland, N. G.; Earp, H. S.; Jenkins, N. A.; Lee, D. C. The mouse waved-2 phenotype results from a point mutation in the EGF receptor tyrosine kinase. *Genes Dev.* **1994**, *8*, 399–413. (b) Ahmed, I. S.; Rohe, H. J.; Twist, K. E.; Mattingly, M. N.; Craven, R. J. Progesterone receptor membrane component 1 (Pgrmc1): A heme-1 domain protein that promotes tumorigenesis and is inhibited by a small molecule. *J. Pharmacol. Exp. Ther.* **2010**, *333*, 564–573.
- ¹⁶⁷ Sanjo, N.; Owada, K.; Kobayashi, T.; Mizusawa, H.; Awaya, A.; Michikawa, M. A novel neurotrophic pyrimidine compound MS-818 enhances neurotrophic effects of basic fibroblast growth factor. *J. Neurosci. Res.* **1998**, *54*(5), 604–612.
- ¹⁶⁸ Lewis, M. A.; Hunihan, L.; Franco, D.; Robertson, B.; Palmer, J.; Laurent, D. R. S.; Balasubramanian, B. N.; Li, Y.; Westphal, R. S. Identification and characterization of

-
- compounds that potentiate NT-3-mediated Trk receptor activity. *Mol. Pharmacol.* **2006**, *69*, 1396–1404.
- ¹⁶⁹ Ishima, T.; Nishimura, T.; Iyo, M.; Hashimoto, K. Potentiation of nerve growth factor-induced neurite outgrowth in PC12 cells by donepezil: Role of sigma-1 receptors and IP₃ receptors. *Prog. Neuro-Psychopharmacol. Biol. Psychiatry* **2008**, *32*, 1656–1659.
- ¹⁷⁰ Nishimura, T.; Ishima, T.; Iyo, M.; Hashimoto, K. Potentiation of nerve growth factor-induced neurite outgrowth by fluvoxamine: Role of sigma-1 receptors, IP₃ receptors and cellular signaling pathways. *PLoS One* **2008**, *3*(7), e2558.
- ¹⁷¹ Ishima, T.; Hashimoto, K. Potentiation of nerve growth factor-induced neurite outgrowth in PC12 cells by ifenprodil: The role of sigma-1 and IP₃ receptors. *PLoS One* **2012**, *7*(5), e37989.
- ¹⁷² Itoh, K.; Ishima, T.; Kehler, J.; Hashimoto, K. Potentiation of NGF-induced neurite outgrowth in PC12 cells by papaverine: Role played by PLC- γ , IP₃ receptors. *Brain Res.* **2011**, *1377*, 32–40.
- ¹⁷³ Robson, M. J.; Elliott, M.; Seminerio, M. J.; Matsumoto, R. R. Evaluation of sigma (σ) receptors in the antidepressant-like effects of ketamine in vitro and in vivo. *Eur. Neuropsychopharm.* **2012**, *22*, 308–317.
- ¹⁷⁴ Maragnoli, M. E.; Fumagalli, F.; Gennarelli, M.; Racagni, G.; Riva, M. A. Fluoxetine and olanzapine have synergistic effects in the modulation of fibroblast growth factor 2 expression within the rat brain. *Biol. Psych.* **2004**, *55*, 1095–1102.
- ¹⁷⁵ Kashiwagi, H.; McDunn, J. E.; Simon, Jr., P. O.; Goedegebuure, P. S.; Vangveravong, S.; Chang, K.; Hotchkiss, R. S.; Mach, R. H.; Hawkins, W. G. Sigma-2 receptor ligands potentiate conventional chemotherapies and improve survival in models of pancreatic adenocarcinoma. *J. Transl. Med.* **2009**, *7*, 24.
- ¹⁷⁶ Yagasaki, Y.; Numakawa, T.; Kamamaru, E.; Hayashi, T.; Tsung-Ping, S.; Kunugi, H. Chronic antidepressants potentiate via sigma-1 receptors the brain-derived neurotrophic factor-induced signaling for glutamate release. *J. Biol. Chem.* **2006**, *281*(18), 12941–12949.
- ¹⁷⁷ Johannessen, M.; Fontanilla, D.; Mavlyutov, T.; Ruoho, A. E.; Jackson, M. B. Antagonist action of progesterone at σ -receptors in the modulation of voltage-gated sodium channels. *Am. J. Physiol. Cell. Physiol.* **2011**, *300*(2), C328–C337.
- ¹⁷⁸ Piccotti, J. R.; LaGattuta, M. S.; Knight, S. A.; Gonzales, A. J.; Bleavins, M. R. Induction of apoptosis by cationic amphiphilic drugs amiodarone and imipramine. *Drug Chem. Toxicol.* **2005**, *28*, 117–133.

-
- ¹⁷⁹ Bown, C. D.; Wang, J.-F.; Young, T. Increased expression of endoplasmic reticulum stress proteins following chronic valproate treatment of rat C6 glioma cells. *Neuropharmacology* **2000**, *39*, 2162–2169.
- ¹⁸⁰ Hung, J.-H.; Su, I.-J.; Lei, H.-Y.; Wang, H.-C.; Lin, W.-C.; Chang, W.-T.; Huang, W.; Chang, W.-C.; Chang, Y.-S.; Chen, C.-C.; Lai, M.-D. Endoplasmic reticulum stress stimulates the expression of cyclooxygenase-2 through activation of NF- κ B and pp38 mitogen-activated protein kinase. *J. Biol. Chem.* **2004**, *279*(45), 46384–46392.
- ¹⁸¹ Krauss, G. *Biochemistry of Signal Transduction and Regulation*, 4th ed.; Wiley-VCH Verlag: Weinheim, 2008.